RELIABILITY ANALYSIS: APPLICATIONS TO STRUCTURAL CONNECTIONS AND DEFECT ASSESSMENT IN OFFSHORE STRUCTURES

by

C.A. PLANE

submitted to
The University of Glasgow
for the degree of
Doctor of Philosophy

Department of Mechanical Engineering
The University of Glasgow
Glasgow G12 8QQ
Scotland

ProQuest LLC.
789 East Eisenhower Parkway
P.O. Box 1346
Ann Arbor, MI 48106 – 1346

SUMMARY

The work described in this thesis concerns the application of proven Advanced Level II reliability methods to specific problems related to the structural integrity of offshore structures. The two major components of the work are

i) Connections (welded and bolted)

ii) Assessment of crack-like defects found by inspection.

Connections

Safety requirements for the static strength of welded and High Strength-Friction Grip bolted connections on offshore structures are established for the first time. Target reliabilities are proposed by basing them on the values used for bridge structures and making allowances for the difference in design life and greater acceptable risk. Statistical models for resistance are established by analysing data on the slip of bolted connections and rupture of welded joints. Loading statistical models are selected to represent dead, live, and environmental loads. Partial factors on static strength are then established to ensure a minimum spread of reliabilities about the target. On the basis of the data analysed, a revision to the strength formulation is proposed for fillet welded joints and partial safety factors are re-calculated. As a result of the revision the scatter in the reliabilities of welded joints with different weld orientations is shown to be significantly reduced.

Defect Assessment

The assessment of crack-like defects has been approached from an entirely new perspective and constitutes a major development in the understanding of the safety of flawed structures. The work described is the first application of reliability analysis to embrace all the relevant uncertainties relating to a known defect, viz: material toughness, applied stress and defect size. From this arise significant insights into the relative importance of the variables which in turn will enable operators of offshore structures to make more rational decisions on the allocation of resources. Reliability levels in existing and revised defect assessment procedures are quantified and target reliability levels are appraised. By a process of calibration, partial safety factors are, for the first time, established for the inputs into such assessments. A choice of methods is provided for making assessments with uniform reliability at the target level. The first is more complex and requires the user to make subjective assessment of the quality of the information on defect size and stress level. Using tabulated results, a global factor of safety on defect size may then be established. A separate calculation of safety factor is required for each new defect but the resulting scatter of reliabilities is small. The second method provides blanket values of partial safety factors to be applied for all assessments and the user is only required to distinguish between 'accurate' or 'uncertain' estimates of defect size and stress. The scatter in reliabilities for the revised procedure is shown to be significantly less than the assessment methods used hitherto.

ACKNOWLEDGEMENTS

I am deeply grateful to my supervisor Dr. Mike Cowling for his help and encouragement as well as the latitude he has given me to develop my own ideas.

The fracture work was funded through the Methodology Working Group of the Defect Assessment of Offshore Structures programme. I am indebted to the Group for the opportunity to discuss aspects of the work. Particular thanks are due to Professor Mike Burdekin and Victor Nwegbu of UMIST and Dr. Steve Garwood and Dr. Tarsam Jutla of the Welding Institute.

The static strength work was undertaken whilst I was a member of the Department of Naval Architecture and Ocean Engineering under funding from the U.K. Department of Energy. I am most grateful to my former supervisor Dr. Paul Frieze, to Dr. Purnendu Das and Professor Douglas Faulkner for their erstwhile support.

I would like to express my thanks to David Fildes and Paul Rosenburg of the Computing Services Department for their expert assistance in handling problems with the computer systems and the NAG mathematical library respectively.

I would like to express my appreciation to Professor Titterington and his staff of the consultancy service of the Department of Statistics for their help with statistical theory.

Especial thanks to Lynn Cullen of Marine Technology for her speedy and accurate typing as well as her intelligent interpretation of dubious handwriting.

Finally, thanks to Miriam who believed in me.

CONTENTS

To Ma-ayan and Liell

RELIABILITY ANALYSIS: APPLICATIONS TO STRUCTURAL CONNECTIONS AND DEFECT ASSESSMENT IN OFFSHORE STRUCTURES

INTRODUCTION

This thesis is in two distinct but complementary parts. The first part, Sections 2 to 4, deals with the static strength of offshore structural components and the use of reliability theory to determine partial safety factors for inclusion in future design guidelines for offshore structures. Such use is well established in the UK and elsewhere for land based concrete and steel structures. As a review of the procedures involved Section 2 examines the reliability based evaluation of partial safety factors for steel highway bridges in the U.K. Section 3 presents an account of the evaluation of partial safety factors for offshore structural members. Section 4 presents a detailed account of the evaluation of partial safety factors for the rupture strength of welded joints and the slip resistance of high strength - friction grip bolted connections on offshore structures.

The second part of this thesis, Sections 5 to 8, considers failure by fracture initiating from weld defects or fatigue cracks in 'hot spot' regions of tubular joints. Reliability analysis is used to calculate suitable factors of safety to be used with standardised defect assessment procedures. The approach aims to embrace all relevant uncertainties in defect assessment and is original in this respect. Section 5 introduces fracture mechanics concepts and considers the various failure models which relate remote stress, material toughness and defect size. Section 6 draws on the experience of component strength reliability to formulate a failure function for defect assessment. An anomaly is discovered regarding the level of stress and its effect on the safety index. In Section 7 a study of the sensitivity of safety index to different amounts of uncertainty in the basic variables is presented. The stress anomaly makes the study particularly convoluted. In Section 8 a solution to the stress anomaly is proposed, and, on the basis of this, partial factors are evaluated.

Section 1 is a general introduction to the terms, concepts and methods used in the text.

SECTION 1

INTRODUCTION TO LEVEL II RELIABILITY

This Section introduces the basic concepts in Level II reliability and shows how they are applied to the calibration of design codes. The final sub-section, Prognosis, presents an overview of the standing of Level II reliability analysis in the engineering profession and forecasts future applications and developments.

1.1 Basic Concepts in Level II Reliability Analysis

1.1.1 Levels of Reliability

In 1975 the Joint Committee on Structural Safety, whose recommendations are summarised in Reference 1, sought to classify the various means of ensuring reliability in structural design. Three reliability levels were described and their terminology has now become widely accepted. In the lowest of these, Level I, reliability is ensured by using safety checking equations with a number of partial factors typically on load and resistance variables. These partial factors would have been previously calibrated to the appropriate reliability using one of the higher levels of reliability analysis. The fact that most structural design codes developed in the last decade are Level 1 codes demonstrates the engineers' performance. Their predilection for safety factors over the more realistic concept of reliability (complement to unity of 'failure probability') was fully appreciated by Freudenthal[2] two decades prior to the Joint Committee on Structural Safety . He seemed to pre-empt the concept of

Level 1 codes by writing:

> "... because the concept of safety is deeply rooted in engineering design whereas the notion of a finite (no matter how small) probability of failure or at least of unserviceability is repulsive to a majority of engineers, it appears desirable to retain the concept of 'safety' rather than to replace it by that of 'probability of failure' and to reformulate the former in terms of the latter. The safety factor is thus transformed into a parameter that is a function of the random variation of all design characteristics..."

Levels II and III are bone fide applications of reliability analysis to design. The major distinction between them is in the accuracy they achieve. Monte Carlo simulation is one Level III method which calculates the "exact" probability that the load on a structure/member will exceed the resistance of that structure or member. It does so by generating artificial values of load and resistance whose probabilities of occurrence are automatically selected according to a specified probability law. Depending upon relative values of the load and resistance generated in each simulation the simulated event can be classified as failure (i.e. load greater than resistance) or non-failure. As the number of simulations becomes infinite so the 'true' failure probability can be evaluated as the ratio of the number of failures to the total number of simulated events. This method is described here because it gives a clear intuitive picture of the reliability problem and the nature of its solution. It has two significant drawbacks: firstly the computed reliability is only accurate in so far as the probability laws describing load and resistance are realistic; secondly it is computationally inefficient, taking a considerable amount of computer time to

produce an acceptable solution. Other Level III methods have similar drawbacks. Level II methods, by making certain approximations, are able to increase the computational efficiency to a level where computer time becomes almost negligible whilst accuracy is maintained at a value approaching that of Level III. The first drawback still applies however. Furthermore the apparent increased level of complexity of the Level II calculation makes the results seem more suspect to some engineers.

1.1.2 Uncertainty in Engineering

Uncertainty manifests itself in engineering in two distinct forms: random and systematic. Random uncertainty is usually associated with scatter of values about some central point. Examples are variations in the thickness of a reinforcing bar or the cube strength of concrete from the same batch. Systematic uncertainty on the other hand affects all values to a similar degree. This could arise as a result of a defective measuring device but more commonly, in applications where reliability is used, it describes the amount by which the nominal value differs from the mean of actual values. Examples are the topside weight of an offshore structure (the actual weight often differs from the design weight as more equipment is brought aboard) or the nominal or guaranteed minimum yield stress of a material. The difference in strain rate occuring from service loading and that used in material tests is similarly accounted for in terms of systematic error.

Systematic error is measured by bias ξ and is related to the statistical parameter of location m_X (e.g. the mean) by

$$m_X = x_{nom}(1+\xi) \qquad (1.1)$$

where x_{nom} is the nominal value of variable x. Bias is usually quoted as a percentage, i.e. ξ x 100%, but sometimes the term 'bias' is used for the quantity $(1+\xi)$. Altering the bias results in the probability density function (pdf) being shifted bodily along the variable (horizontal) axis.

Random error is measured by standard deviation or coefficient of variation (COV=standard deviation/mean). The effect on the pdf of a change in standard deviation depends on the type of distribution. For normally distributed variables the result of an increase in standard deviation is a flattening of the familiar bell-shape. For skewed distributions remote from the f(x) axis the result is also a flattened profile. For non-negative skewed distributions with long right hand tails, close to the f(x) axis, however, the result of increasing the standard deviation is a more peaked mode further towards the left i.e. closer to the f(x) axis. The two-parameter Weibull distribution used to model fracture toughness in Section 6 of this thesis is of this type.

Uncertainty in strength (or load) modelling is treated in the same way as other uncertainties. Systematic error in strength modelling is determined from the mean value of

$$\frac{\text{actual resistance}}{\text{predicted resistance}}$$

where the actual resistance is determined from a number of test results. When the number of such results is reasonably large the random modelling error may be evaluated as the standard deviation of this expression. The random variable of model uncertainty, X_m, is used in reliability analysis to 'correct' any bias in the strength formulation. In this way the simplifying assumptions made in deriving the strength model are quantified and the resulting conservatism (or non-conservatism) corrected.

1.1.3 Definitions of Safety Index and the Development of the First Order-Second Moment (FOSM) Methods

To formulate the reliability problem it is necessary to consider a mapping g of n independent variables x_i, i=1 to n, to a single dependent variable M.

$$M = g(\underline{x}) \qquad (1.2)$$

$$(\underline{x}) = (x_1, \ldots, x_n) \qquad (1.3)$$

g is a failure function if it maps design parameters (loads, strengths and dimensions) such that combinations giving rise to failure result in M<0 and combinations giving rise to non-failure result in M>0. The surface M=0 in the n-dimensional design space of $\underline{x} = (x_1,\ldots,x_n)$ is called a failure surface. The region of the design space for which M < 0 is termed the failure domain, M > 0 corresponds to the safe domain.

A fundamental example of a failure function is

$$M = f(\text{Load}(L), \text{Resistance}(R)) = R-L$$

M may be termed the safety margin. In Level III methods the joint distribution of the n basic variables is required. In Level II methods the approximate reliability is calculated using only the first and second moments of the pdf of each design variable treated as a random variable. Generally these are the mean m_i and the standard deviation s_i though the coefficient of variation COV (= s_i/m_i) is used interchangeably with standard deviation.

Although the concept of reliability index or safety index is generally attributed to Cornell[3] in 1969 it was Freudenthal[2] in 1954 who showed that probabilistic safety corresponded to a distance measured in the normalised design space. He showed that for independent normally distributed action, L, and capacity, R, normalised by

$$x = (R - M_R)/S_R$$

$$y = (L - M_L)/S_L$$

the lines of constant probability density $p(x,y) = p_0$ in the (x,y) plane are circles:

$$x^2 + y^2 = (-2\ln(2\pi p_0))$$

with radii:

$$\rho = \sqrt{(-2\ln(2\pi p_0))}$$

and centres at the origin.

If the line

$$r = R - L = 0$$

(the failure surface) is tangential to the circle corresponding to density p_0 then the failure probability p_f is given as that part of the volume under the surface of rotation p(x,y) which is cut off by the plane along the line r = 0 and perpendicular to the (x,y) plane. Since this is also the area under the normal curve beyond the ordinate p_0 (i.e. area = $1 - \Phi^{-1}(p_0)$) the link was

established between p_f and the radius of the largest circle, centred at the origin, existing entirely within the safe domain. Freudenthal showed comparable results for R and L having lognormal and extreme valued distributions but did not at that time extend the geometric interpretation to account for R and L being, themselves, functions of other independent random variables. Cornell[3] in 1969 defined the safety index, β, as

$$\beta = m_M / s_M \tag{1.4}$$

For the fundamental example where R and L are uncorrelated

$$M = L - R \tag{1.5}$$

$$m_M = m_L - m_R \tag{1.6}$$

$$s_M^2 = s_L^2 + s_R^2 \tag{1.7}$$

$$\beta = \frac{m_R - m_L}{(s_R^2 + s_L^2)^{\frac{1}{2}}} \tag{1.8}$$

If R and L were correlated with correlation coefficient ρ_{RL} the denominator in Equation 1.8 would be replaced by

$$(s_R^2 + s_L^2 + 2\rho_{RL}\, s_R\, s_L)^{\frac{1}{2}}$$

If the failure surface were to be non-linear in the basic variables (often the case when resistance depends on the square of a linear dimension) m_M and s_M can be obtained by expanding f about $(x_1,\ldots,x_n) = (m_1,\ldots,m_n)$ and ignoring non-linear terms:

$$M = f(x_1, \ldots, x_n)$$

$$\simeq f(m_1, \ldots, m_n) + \sum_{i=1}^{n} \frac{\partial f}{\partial x_i} (x_i - m_i) \tag{1.9}$$

where $\frac{\partial f}{\partial x_i}$ is evaluated at $(m_1, \ldots, m_n)$.

The following approximations are obtained:

$$m_M = f(m_1, \ldots, m_n) \qquad (1.10)$$

$$s_M^2 = \sum_{i=1}^{n} \sum_{j=1}^{n} \frac{\partial f}{\partial x_i} \frac{\partial f}{\partial x_j} \mathrm{Cov}[x_i, x_j] \qquad (1.11)$$

or $s_M^2 = \sum_{i=1}^{n} (\frac{\partial f}{\partial x_i})^2$ if none of the x_i are correlated.

where Cov[.] is the covariance.

First order-second moment (FOSM) methods are so called because the failure function is expanded to a first order approximation and the probability density functions are described by their first two moments. The above definition is described as a mean FOSM method because expansion is made about the mean point $(x_1,\ldots,x_n) = (m_1,\ldots,m_n)$.

Clearly for non-linear functions the first order approximation depends on the choice of linearisation point. In advanced FOSM methods expansion is made about a point on the failure surface. This is a far more reasonable choice of expansion point as will be made clear in the following discussion.

The safety index defined as in Equation 1.4 depends on the way in which the failure function is written down. Different but equivalent expressions of the failure function result in slightly different safety indices. For example, if resistance and load are expressed as stresses σ_R and σ_L rather than loads R and L the mapping is

$$M = f(\sigma_R, \sigma_L) = \sigma_R - \sigma_L \qquad (1.12)$$

and M=0 describes the failure surface. The failure equations are equivalent but numerical calculation of the safety index by Equation 1.8 gives rise to different safety indices. This is termed lack of invariance.

The safety index defined above cannot in general be related to the failure probability p_f

$$p_f = p(M<O)$$

$$= \int_F f_{\underline{X}}(\underline{x})\, d_{\underline{X}} \qquad (1.13)$$

where $f_{\underline{X}}$ is the joint probability density function and F is the failure domain. For the special case where the mapping f is linear in the basic variables x_i and these basic variables are normally distributed then:

$$p_f = \Phi(-\beta) \qquad (1.14)$$

and $$\beta = -\Phi^{-1}(p_f) \qquad (1.15)$$

where Φ is the standard normal distribution function.

For the 2-dimensional case where M=R-L with R and L independent, with means m_R and m_L and standard deviations s_R and s_R respectively, the shortest distance OA (see Figure 1.1) from the origin of the normalised space

$$\underline{z} = \left[\frac{x_i - m_i}{s_i},\ i=1,\ldots,n\right] \qquad (1.16)$$

to the failure surface is β.

Firstly the normalised R^1 and L^1 are given by

$$R^1 = (R-m_R)/s_R \qquad (1.17)$$

$$L^1 = (L-m_L)/s_L \qquad (1.18)$$

The failure surface in the normalised $\underline{z}$-space becomes

$$s_R R^1 + m_R - L^1 s_L - m_L = 0 \qquad (1.19)$$

$$s_R R^1 - s_L L^1 + (m_R - m_L) = 0 \qquad (1.20)$$

which is a straight line whose perpendicular distance to the origin is

$$\frac{m_R - m_L}{\sqrt{s_R^2 + s_L^2}}$$

which equals the β of Equation 1.8. This same property can be shown to exist for the n-dimensional case.

The Hasofer-Lind[4] reliability index is defined as the shortest distance from the origin to the failure surface in the normalised space. This defintion has been shown to be equivalent to the earlier definition of safety index for linear failure surfaces. It thus bears the same relationship to the failure probability as Equations 1.14 and 1.15. Since it is no longer dependent on the choice of failure function it is invariant, unlike the former definition. Non-linear failure surfaces can be treated in a similar way as before but rather than expanding the failure function about the mean point the expansion is made about the design point (see Figure 1.1). When expansion is taken to first order terms only this is equivalent to linearising the failure surface at the design point. This approximation of the failure surface means Level III 'exact' reliability solutions will diverge from advanced FOSM solutions for non-linear failure surfaces, even when all the design variables are distributed normally. In practice the degree of non-linearity in engineering problems is small and the approximation is a good one. This is due to the fact that most

of the probability mass is concentrated in a circle (hypersphere in n-dimensions) centred at the origin of the normalised space.

The Hasofer-Lind reliability index may be formulated as

$$\beta = \min\left(\sum_{i=1}^{n} (z_i))^2\right)^{\frac{1}{2}} \qquad (1.21)$$

This is not however a useful expression from which to solve the problem of finding the minimum distance. The expressions used to solve for β relate directly to the geometry of the design space. The direction cosine α_i is the cosine of the angle between the z_i axis and OA (see Figure 1.1). In triangle OAB

$$\alpha_1 = z_1^*/\beta$$

where * superscript denotes the design point value. In the original coordinates

$$\alpha_1 = \frac{x_1^* - m_1}{s_1 \beta} \qquad (1.22)$$

$$\text{or } x_1^* = m_1 + \alpha_1 \beta s_1$$

and in general

$$x_i^* = m_i + \alpha_i \beta s_i \qquad i=1,n \qquad (1.23)$$

The direction cosine can also be expressed in terms of the partial derivatives of the failure surface at the design point (provided these exist). They are

$$\alpha_i = - \frac{\frac{\partial f}{\partial z_i}}{\sum_{j=1}^{n} \left[\frac{\partial f}{\partial z_i}\right]^2\Big]^{\frac{1}{2}}} \qquad i=1,n \qquad (1.24)$$

in the transformed space and

$$\alpha_i = - \frac{\frac{\partial f}{\partial x_i} s_i}{\left[\sum_{j=1}^{n} \left[\frac{\partial f}{\partial x_i}\right]^2\right]^{\frac{1}{2}}} \qquad i=1,n \qquad (1.25)$$

in the original space.

Tallying up unknowns and equations there are n unknown direction cosines (Equation 1.24), n unknown design point coordinates (Equation 1.23) and unknown β giving a total of 2n+1 unknowns. There are n equations for the direction cosines and n equations for the design point coordinates. The final equation needed in order to solve the problem results from the fact that the design point must lie on the failure surface so that

$$f(x_1^*, \ldots, x_n^*) = 0 \qquad (1.26)$$

Any scheme of solving simultaneously these 2n+1 equations will give the correct advanced Level II β value.

The Hasofer-Lind safety index problem has been reduced to solving a small number of simultaneous equations. Refinements to the solution exist for cases were correlation exists between two or more of the variables. In practice it is often possible to formulate the problem so that the basic variables are mutually independent and so avoid the problem of correlation. When non-normal variables arise in the failure function corrections to m_i and s_i can be made so that the non-normal distribution is approximated by an equivalent normal distribution at the design point. This improves the accuracy of the Hasofer Lind approach to reliability vis-a-vis Level III methods. The corrections are due to Rackwitz and Fiessler[5] and these are presented in Section 6.

The process of determining reliability, given the failure surface and the distribution parameters of the basic variables, has been shown to be straightforward and relatively simple. Indeed software packages are beginning to appear on the market for this calculation. The most difficult aspect of reliability analysis is to obtain a form of the failure function which will give intelligible and unambiguous results.

Educated guesswork is often used to obtain distribution parameters and probability models, especially on the loading side of the failure equation. Although much effort is made to arrive at a reasonable set of parameters it is often found in calibration exercises that the resulting partial safety factors are insensitive to small changes in these assumptions.

Section 3 deals with reliability of the strength of structural components - (columns, beams, stiffened flanges and webs) on offshore structures. The design space thus comprises loads, yield stresses, member dimensions, and model uncertainties. In Section 4, dealing with bolted and welded connections, bolt preload and coefficients of friction are added to the design space. In Sections 5 and 6 the uncertainties associated with assessment of a cracked member make up the design space. These are fracture toughness, local stress and defect size. Each of the design or assessment problems investigated commences with choosing suitable distribution functions and estimating distribution parameters for each of these basic variables. Secondly the failure function is written down and the nature of the expected results using it are discussed. The third and most straightforward part is the reliability analysis. The final part, calibration is discussed in Section 1.2.

1.1.4 Significant Limitations

That Level II reliability methods are an approximation to Level III has already been mentioned. The approximation can be illustrated by reference to the geometry of the normalised design space obtained by using the normal transformation

$$z = \frac{x - m_x}{s_x} \qquad (1.27)$$

on each basic variable x. The origin of this space thus corresponds to the mean of the untransformed variables and each unit travelled along any axis represents a one standard deviation move away from the mean. If the basic variables are jointly normal then hyperspheres centred at the origin will have shells of equal probability density and a hypersphere of radius β (tangential to the failure surface) will contain most of the joint probability mass. (In the same way as the probability mass of a single normal random variable is concentrated in an interval centred on the mean).

The failure probability is the joint probability mass lying in the failure domain and for a linear failure surface has been shown to be

$$p_f = 1 - \Phi(\beta)$$

exactly. The degree of approximation thus depends on the joint probability mass lying between the linearised and actual failure surfaces. If the safe domain is convex (thicker through the origin than elsewhere) Equation 1.14 will underestimate the failure probability as determined by exact (Level III) methods. The converse would be true for concave safety domains. This aspect is investigated further in Reference 6. Frequently though the shape of the

safety domain (being either convex or concave) is different for each 2-dimensional section (for example consider the "saddle" shape in 3-dimensions) and generalisations cannot be made. To a lesser extent the distribution type affects the approximation although the use of Rackwitz-Fiesler transformations for non-normal distributions goes a long way to rectifying this.

The same illustration also highlights the fact that it is the tail of the joint distributions which make up the joint probability mass in the failure domain. As such the calculated probability of failure is extremely sensitive to the tail shape of the individual variables. Since this is exactly the part of the distribution where data is usually absent, the calculated failure probabilities are little better than the educated guesswork employed to model the basic variables. Of the two limitations described it is this latter one which is significant since it far outweighs the computational differences between Level II and III.

A single time-varying parameter is permissible in the method described. If all other variables are time-independent the value they have at the beginning of the service life is unchanged throughout the design life. If one variable is time dependent then it need only acquire a value at the design point once for failure to ensue. It can thus be treated in the same manner as the time-independent variables when the probability of failure <u>in the design life</u> is of interest. When two time-dependent variables are present in the design space however a single occurrence of one of them at the design point is not sufficient to cause failure. Treating them both as time-independent variables hence leads to pessimistic predictions of failure probability.

Although solutions to the time-dependence problem exist[7] the data needed for individual time-dependent variables is seldom available. The tendency is for the solutions not to be used in code calibration work. The resulting errors are significant in the design of offshore structures as well as defect assessment. Wind, current and waves in the North Sea seldom if ever reach maximum values simultaneously. Moreover the maximum load effect is also dependent on the direction of the three environmental forces. For defect assessment loading, temperature (which affects toughness) and crack size are all time dependent although for instantaneous assessment crack growth can be ignored.

1.2 Calibration

Calibration is the process by which reliability is preserved and regulated in code revisions. Consider a design code covering a range of member types which is in the process of being replaced by a new code which is to adopt the results of recent research in its strength formulations. The process of calibration may be as follows:

1. determine the reliabilities of a set of components designed to the rules contained in the original code.
2. calculate the average of these reliabilities - called the target reliability.
3. determine the reliabilities of the same components designed to the new code using an assumed trial set of partial safety factors.
4. adjust the values of partial factors to achieve two objectives simultaneously:
   - i the new average reliability equals the target reliability
   - ii the spread of new reliabilities about the average is a minimum.

This is the procedure recommended in CIRIA 63[8] and followed with some deviations by code developers. The deviation commonly used[9] is to calibrate component by component rather than using a blanket target reliability as an average of all components. The justification for this is often made on grounds of the consequences of failure or where a particular component taken as a group shows consistently different reliability when designed to the old code.

A second common deviation is when evaluating target reliability to omit categories of components whose strength formulation in the old code is generally regarded as being inadequate. The target reliability is then the average reliability of components designed to the old code where the strength formulations for these is satisfactory. Such omissions have been made for stiffened flanges designed to BS153 (see Section 3) and defects in bending assessed by PD6493 (see Section 6).

The need for target reliability based on economic criteria, rather than previous experience has been gaining recognition in recent years. The total expected cost, E(CT), is assumed to be the sum of the initial cost, CI, and the expected cost of failure, E(CF).

$$E(CT) = CI + E(CF) \qquad (1.28)$$

The expected cost of failure is proportional to the cost of failure times the failure probability and therefore is a function which increases with failure probability. The initial cost, on the other hand, is a decreasing function of failure probability. The sum therefore has a minimum point and the value of the failure probability at the minimum is taken as the target. Reference 10 gives a full description of economic optimisation.

Calibration as described raises some questions for reliability analysis in general. Firstly the arbitrary choice of preserving average reliability rather than some lower value is often questioned[11]. Advances of knowledge into physical behaviour of components under load should result in a lower safety margin than that previously employed to offset ignorance. Not to take advantage of the possible reduction in safety, and therefore cost, is tantamount to negating the research effort put into winning the improved understanding.

The following considerations would seem to add weight to this proposition. If calibration was to be carried out purely on a componet by component basis the components designed to the new code would be exactly the same as components designed to the old code. This is a verifiable fact and comes about purely as a result of the way reliabilities of components designed to code provisions are calculated. The advantage in calibration only comes if the reliability of distinct components are levelled out at some target value. Preserving average failure probability gives a lower reliability than any of the other obvious choices, e.g. average safety index, average logarithm of failure probability. Table 1.1 illustrates this for the failure probabilities 10^{-3}, 10^{-6} and 10^{-9}.

Table 1.1 Comparisons of averaging failure probabilities

				ave.	pf
p_f	10^{-3}	10^{-6}	10^{-9}	0.3×10^{-3}	0.3×10^{-3}
β	3.09	4.75	6.00	4.61	2.01×10^{-6}
$-\log_{10} p_f$	3.0	6.0	9.0	6.0	1×10^{-6}

Comparison of the orders of magnitude of the final column in Table 1.1 show that averaging failure probabilities gives a value similar to the order of magnitude of the least reliable. In the example shown the average failure probability is three times as safe as the least reliable but three hundred times less safe than the second least reliable.

On the basis of this comparison it would seem that the choice of average failure probability gives a reasonable lower bound reliability without any undue conservatism.

The second question concerns what meaning, if any, should be attached to the value of failure probability. This aspect is obviously interesting to certifying authorities but should be equally important to personnel living on board any offshore platform.

The short answer is that there is no meaning outside the immediate sphere of the calibration exercise. The omissions in the analysis of accurate modelling of tails has already been mentioned. Human error is mentioned in the following sub-section. The list of omissions can be extended almost indefinitely. The most significant of these, redundancy, has been estimated[11] to give a two to three fold global factor of safety against system failure beyond first component failure. The affect on failure probability of this reserve would be several orders of magnitude. Reference 12 considers the relative importance of member and system reliabilities.

Reliability analysis in the form used for code calibration is analagous to a measuring stick. Such a stick is a useful practical means of marking off

equal lengths of timber, and for all but the most exacting joinery purposes, sufficiently accurate. When the length is communicated to other builders (failure probabilities to analysts in other fields) the measure is useless unless there is some universal system of units (unless probability means the same thing to reliability analysts as it does to insurers). At present there is no such universal language.

1.3 Prognosis

Since the 1950's when probabilisitc approaches to structural safety were beginning to be recognised by the various learned engineering bodies there has been a growing number of engineers who have accepted the need to deal rationally with variability. Simultaneously there has been a growing lobby of engineers who are opposed to the measures put forward by the reliability camp on the grounds that

1. the fundamental object being dealt with i.e. "failure probability" does not concord with the ordinary sense of the word and does not have any readily identifiable meaning (unlike "load", "stress" and "deflection").

2. the resulting increased complexity of design codes is not justified.

Both these criticisms must be carefully considered by code drafting bodies if they are not to alienate potential code users. As a starting point for such consideration a simple expedient such as a change in terminology may help to offset the first criticism.

The phrase "probability that load exceeds resistance" is a more precise (if less optimistic) description than "failure probability" especially when modes of failure other than static overload govern design.

The second criticism is a perennial one which researchers and code draughters are used to dealing with. The standard response is "if a new expression for strength (say) predicts behaviour with better consistency than the old one then it is justified". Belief in this maxim has resulted over the years in a seemingly boundless increase in the complexity of some design codes.

There is a strong case for a lower limit on variability in model prediction and a coefficient of variation of 10% is often suggested for this. Once a strength model can be shown to predict strengths with this degree of consistency then the use of more complex models in design codes should be restricted. As the study reported in Section 3 will show this leaves room for further improvement of many of the strength formulations for buckling components. For fracture and fatigue, where prediction is fraught with much larger uncertainties, it seems unlikely that such consistency will ever be approached unless massive advances in material production are made.

Away from component reliability, human error and system reliability are areas with limited but ongoing support. Although studies of the relative importance of making errors in one design variable or another[13,14] are interesting the idea that anything can be done to offset the effects of human error seems misplaced. If a system of design and construction was developed such that the effects of commonly made errors were minimised would there not be a knock-on effect whereby less vigilance is paid by supervising engineers which in turn would breed more serious errors?

System reliability is a term needing careful definition. What is not meant is the duplication of systems and other common sense precautions taken to guarantee safety in electrical, chemical and nuclear plants, avionics, telecommuncations, etc.. What is meant is the reliability of structural systems such as offshore jacket structures calculated by enumeration of possible failure paths of a series of individual structural components. The Beta-Unzipping method[15] is an example but similar approaches to the problem have attracted research funding worldwide[16,17]. One of the more tenable results is the application to optimisation of structural configuration.

Typically in these methods the system reliability of a framed structure is determined by applying a load to the structure and computing, by a Level II method, the least reliable component. This is then removed and the next least reliable component is determined and so on until final collapse is predicted. The system reliability is then given as a function of the individual reliabilities of the components removed. By comparing system reliabilities of structures with different configurations (K-braced, X-braced, number of bays etc.) the optimum configuration can be obtained. Comparisons of steel weight and fabrication costs with reliability can then be made. Reference 18 contains a detailed account.

Having focussed on the negative aspects of reliability analysis it is appropriate to spell out the genuine benefits it is bringing to the engineering profession. These are that uncertainty is at last being treated rationally and through Level I design codes increased consistency in reliability is being achieved.

The focus for Level II reliability analysis has in recent years (86/87) moved away from static strength towards in-service assessment. As early North Sea structures are reaching the end of their design lives and as design faults of many highway bridges are coming to light it is to be expected that research effort and funding will stay in this area for some time to come.

In addition to this activity a broadening of applications of Level II reliability is anticipated in the following areas, all of which would benefit from rational treatment of associated diverse uncertainties:

i) foundation and slope engineering with associated uncertainties in soil properties, moisture content and loads;

ii) reservoir design which is governed by the probabilitistic nature of rainfall, seepage and demand;

iii) ship design with its uncertainties in strength and resistance;

iv) sea defences where tidal height, land subsidence, wind effect and structural resistance are all probabilistic by nature and

v) fatigue analysis in which the available models are subject to very large uncertainties.

1.4 References

1. Thoft-Christiansen, P. and Baker, M.J., 'Structural Reliability Theory and its Applications', Springer-Verlag, 1982.
2. Freudenthal, A.M., 'Safety and the Probability of Structural Failure', Trans. ASCE, Vol. 121 1956, pp1337-1375.
3. Cornell, C.A.; 'A Probability Based Structural Code', ACI-Journ., Vol 66, 1969, pp974-985.

4. Hasofer, A.M. and Lind, N.C.; 'An Exact Invariant First Order Reliability Format'. Proc. ASCE, J. Eng. Mech. Div., 1974, pp111-121.

5. Rackwitz, R. and Fiessler, B.; 'Note on Discrete Safety Checking when using Non-normal Stochastic Models for Basic Variables'. Berichte zur Sicherheitstheorie der Bauwerke, Lab. für Konstr. Ingb., Munchen, H. 14 (1976).

6. Leporati, E.; 'The Assessment of Structural Safety', Series in Cement and Concrete Research edited by A. Short, Research Studies, Press, 1979, pp1-95.

7. Rackwitz, R. and Fiessler, B.; 'Structural Reliability under Combined Random Load Sequences'. Computers and Structures, Vol. 9, 1978, pp489-494.

8. CIRIA; Rationalisation of Safety and Serviceability Factors in Structural Codes. Construction Industry Research and Information Association, Report No. 63, 1977.

9. Moses, F.; 'Recent Applications'. Paper 4 at Seminar on Probabilistic Methods in Structural Design, Construction and Assessment. June 16 and 17, 1987, Imperial College, London.

10. Stahl, Bernhard, 'Reliability Engineering and Risk Analysis', Ch. 5 in Planning and Design of Fixed Offshore Platforms, Ed. by B. McClelland and M.D. Reifel, Van Nostrand Reinhold Co., New York, 1986.

11. Faulkner, D.; 'On Selecting a Target Reliability for Deep Water Tension Leg Platforms', 11th IFIP Conference on System Modelling and Optimisation. (Modelling of Offshore Structures), Copenhagen, July 1983.

12. Moses, F., 'System Reliability Developments in Structural Engineering', Structural Safety, 1, 1982, pp3-13.

13. Lind, N.C.; 'Models of Human Error in Structural Reliability'. Structural Safety 1, 1983, pp167-175.

14. Nowak, A.S.; 'Modelling Human Errors'. Paper 7 at Imperial College and The City University on Probabilistic Methods in Structural Design, Construction and Assessment, 16th and 17th June, 1987.

15. Thoft-Christensen, P.; 'Reliability Analysis of Structural Systems by the β-Unzipping Method', Institute of Building Technology and Structural Engineering, Aalborg Universitetscenter, Aalborg, Danmark, March, 1984.

16. Murotsu, Y.; 'Combinatorial Properties of Indentifying Dominant Failure Paths in Structural Systems', Bulletin of the University of Osaka Prefecture, Series A, Vol. 32, No. 2, 1983.

17. Crohas, H. and Tai, A-A.; 'Reliability Analysis of Offshore Structurs Under Extreme Environmental Loading', 16th Annual OTC in Houston, Texas, May 7th-9th, 1984, Offshore Technology Conference OTC 4826.

18. Thoft-Christensen, P.; 'Application of Structural Systems Reliability Theory in Offshore Engineering, State-of-the-Art,' In Integrity of Offshore Structures 3, edited by D. Faulkner, M.J. Cowling and A. Incecik, Elsevier Applied Science, 1987.

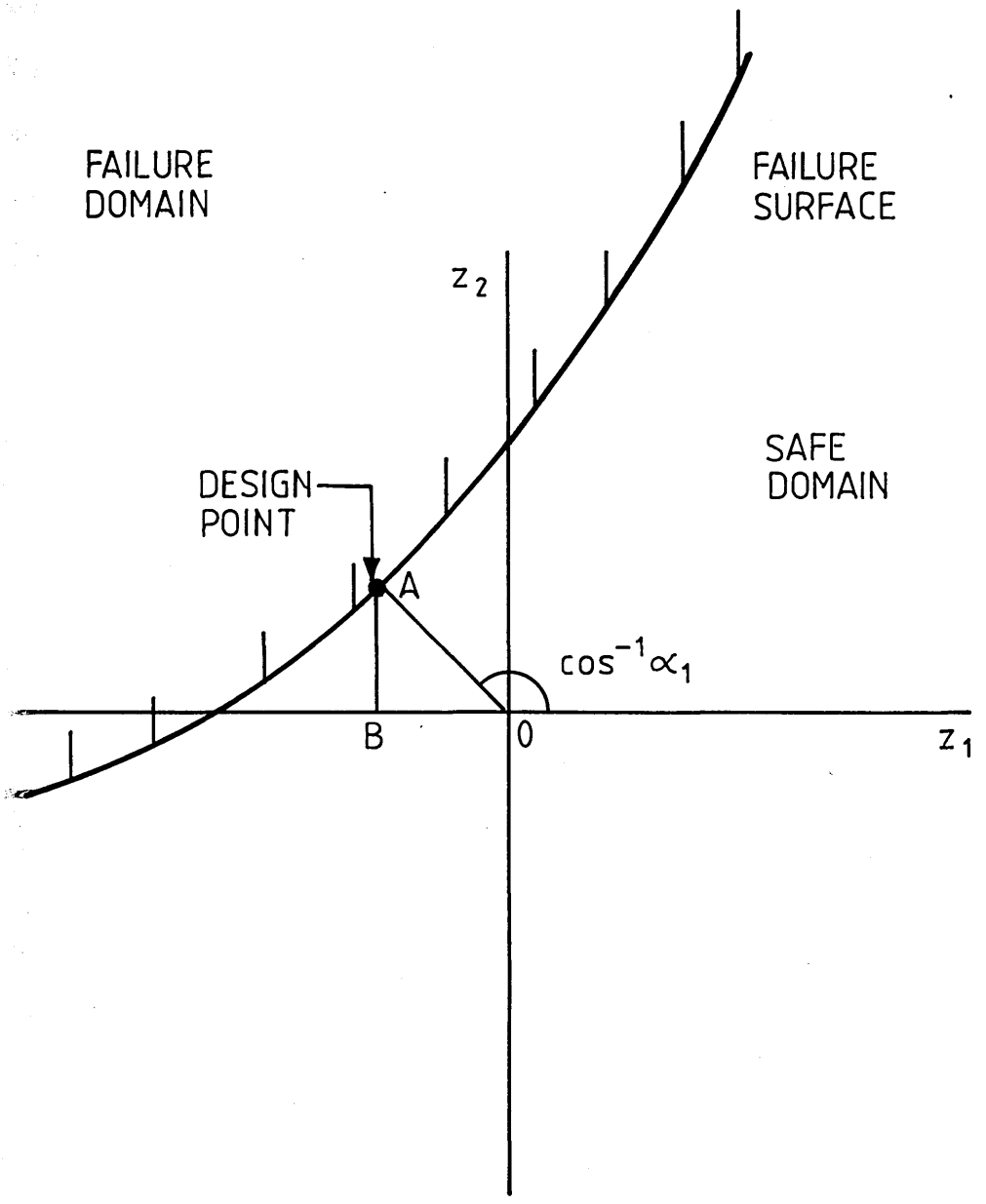

Fig. 1·1 TWO DIMENSIONAL SECTION of DESIGN SPACE THROUGH the ORIGIN.

SECTION 2

REVIEW OF THE ORIGINAL CALIBRATION OF BS5400: PART 3

2.1 Introduction

This section reviews the calibration of the new bridge code BS5400[1] from its predecessor BS153[2]. The study was undertaken at Imperial College and completed in August 1980. The new code was developed mainly for the purposes of incorporating technical improvements to many design clauses; but at the same time the opportunity was taken to rationalise the safety provisions and to change from a permissible stress to a limit state format. The aim of the calibration was to evaluate partial safety factors so that the average reliability of components designed to the original code would be preserved in the new code and that the scatter of reliabilities about this mean would be a minimum.

Sections 2.2 to 2.6 below present a summary of the study. Firstly in Section 2.2 the code format is described. Section 2.3 outlines the calibration procedure and presents the form of the failure function for struts. Section 2.4 describes the optimisation procedure and the way in which a potentially complex problem with many degrees of freedom was reduced to a relatively simple calculation. In Section 2.5 the bridge types (construction and span) and ranges of components used in the calibration study are described. The components not included and the reasons for their exclusion are also mentioned. In Section 2.6 the statistical models used for loading and strength, including model uncertainties, are presented with reasons for their choice. Section 2.7 discusses results of the study with reference to the choice of target reliability.

The overall study is then discussed as a model for subsequent reliability and code calibration work. In particular the form of the failure function is discussed and a recommendation is made regarding the manner in which failure functions are reported. Then some general properties of failure functions are described. Finally the claim that calculated reliability is only as good as the strength model is discussed.

2.2 Partial Factor Format

The partial factor or code format is intended to show, using general design expressions, the partial factors used in the code, which uncertainties they are deemed to cover and the position they take in the design equations. The format used in BS5400[1] Part 1 for collapse and serviceability is:

$$R^* > S^* \qquad (2.1)$$

$$\text{where} \quad R^* = \text{function}\left[\frac{f_k}{\gamma_m}\right] \text{ or } \frac{\text{function } (f_k)}{\gamma_m} \qquad (2.2)$$

$$S^* = \gamma_{f3} \text{ (effects of } \gamma_{fL} Q_k) \qquad (2.3)$$

in which

Q_k is the nominal load defined in Part 2 of the code

f_k is the characteristic material strength

γ_{fL} = function $(\gamma_{f1}, \gamma_{f2})$

γ_{f1} and γ_{f2} take into account the probability of unfavourable deviation of the loads from their nominal values and that various loading acting together will not all reach their nominal values simultaneously. Values for these factors are already fixed and given in Part 2 of the code.

γ_{f3} takes into account inaccurate assessment of the effects of loading

γ_m is a reduction factor on resistance = γ_{m1}, γ_{m2}

γ_{m1} is intended to cover the possible reductions in strength of material below the characteristic value

γ_{m2} is intended to cover possible weaknesses of the structure arising from any cause other than reduction in the strength of the material.

This format follows the recommendations of ISO standard 2394[3] with the exception that factors γ_{n1} and γ_{n2} on resistance are omitted. These factors are intended to cover the extent to which prior warning of impending failure is given and the consequences of failure. The factors were omitted because

a) the onset of extreme vehicular live load effect will be rapid and even ductile distortion is unlikely to be noticed in time for traffic to be stopped;

b) "catastrophic" failure such as local buckling is 'designed out' by imposing limits on the dimensions of outstands etc..

Although the format used in Part 3 complies with these general intentions the distinction between γ_{m1} and γ_{m2} was not made on the above lines. They were instead calculated to satisfy optimising criterion. For the purposes of partial factor evaluation γ_{m1} and γ_{m2} were separated so that

$$R^* = \frac{1}{\gamma_{m2}} \text{ function } \left(\frac{f_k}{\gamma_{m1}}, \text{ other parameters}\right) \qquad (2.4)$$

Thus when R^* is proportional to f_k the effective factor is $\gamma_{m1}\gamma_{m2}$; whereas when R^* is independent of f_k (e.g. pure elastic buckling) the effective factor is γ_{m2}. With this format the distinction between γ_{m2} and γ_{f3} is arbitrary since they will always be multiplied together. Consequently for calibration γ_{f3} was absorbed into γ_{m2}. The calibration proceeded by evaluating a single value of γ_{m1} applied to steel yield stress and separate values of γ_{m2} to apply to each component type.

2.3 Calibration Procedure

Calibration was carried out using a data set of a range of components whose dimensions and steel grades were specified and which were of the type covered by the old (BS153) code and its replacement (BS5400). The weighting factors applied to each member of the set were estimates of the relative occurrence of different structural components designed to BS153.

The procedure followed closely that described in CIRIA report 63[4]:

1) Define a set of n structural components with weighting factors w_i based on frequency of use such that

$$\Sigma w_i = 1.0 \qquad (2.5)$$

Only components for which experimental data relative to actual predicted strengths was available were selected.

2) Design the components to the limits set in BS153 on the assumption that component sizes are unaffected by rounding up, fatigue considerations or any other constraints other than static strength.

3) Calculate the probabilities of failure for these designs; $p_f(153)_i$.

4) Calculate the target failure probability

$$p_{fT} = \Sigma w_i p_f(153)_i \qquad (2.6)$$

Stiffened compression flanges and unwelded plate panels were excluded in this calculation since the strength modelling in BS153 was generally considered to be unsound.

5) Design the components to BS5400 Part 3 using an assumed set of values for the partial factors γ_{m1} and γ_{m2}.

6) Calculate the failure probabilities for these designs.

7) Calculate the weighted average failure probability

$$\Sigma w_i p_f(5400)_i$$

8) Calculate the magnitude of the objective function

$$S = \Sigma w_i (\log_{10} p_f(5400)_i - \log_{10} p_{fT})^2 \qquad (2.7)$$

9) Repeat steps (5) to (8) using a systematic procedure to modify γ_{m1} and γ_{m2} until

$$\Sigma w_i p_f(5400)_i = p_{fT} \qquad (2.8)$$

and the objective function is a minimum.

For struts the failure equation used to determine reliabilities was

$$M = \underline{f}_{116} \cdot \frac{f_{test}}{f_{116(des)}} \cdot \frac{1}{\theta} ((1-\lambda) f_{153} \underline{V}_{DL} + \lambda f_{153} \underline{V}_{LL}) \qquad (2.9)$$

where $\underline{f}_{116}$ is a random variable whose mean value is the deterministic limiting sectional stress to B/1116 rules. (These rules were the best available for struts which do not resort to numerical simulation. They were subsequently used in BS5400.) The standard deviation of $\underline{f}_{116}$ depends on the statistical parameters chosen for yield stress, dimensions and initial imperfections.

$\frac{f_{test}}{f_{116(des)}}$ is the mean value of this ratio when f_{test} is the limiting stress determined from test data and $f_{116(des)}$ is the deterministic value of the limiting stress to B/116 rules using design values of the input variables i.e. yield stress, dimensions and initial imperfections.

This first term gives the ultimate capacity of the strut. Similar descriptions might be critical resistance or true resistance. The second term represents the load where:

λ is the proportion of live load to total load.

f_{153} is the capacity or allowable resistance to BS153 rules.

$\underline{V}_{DL}$ is a random variable of mean 1.0 and COV 3%. Its function in the equation is to randomise the dead load.

$\underline{V}_{LL}$ is a random variable which randomises the vehicular live load. Its statistical parameters were determined from studies of actual sequences of heavy vehicles subsequently analysed to give predictions of the 120 year live load.

θ = 1 when reliability of BS153 designs are being calculated.

= (sectional area of designs to BS5400)/(sectional area of designs to BS153) when BS5400 designs are being analysed.

When θ=1 it will be seen that the mean value of the load term is numerically equal to the deterministic allowable resistance to BS153. When θ is the ratio of sectional areas the mean value of the load term is equal to the deterministic allowable resistance to BS5400.

2.4 Partial Factor Evaluation

The criterion adopted was to select values of γ_{m1} and γ_{m2} that minimise the scatter of failure probabilities of components designed to the new code about the target failure probability. The objective function used was

$$S = \min \Sigma w_i \ (\log_{10} p_f(5400)_i - \log_{10} p_{fT})^2 \qquad (2.10)$$

subject to the constraint

$$\Sigma w_i p_f(5400)_i = p_{fT} \qquad (2.11)$$

where p_{fT} is the target reliability and $p_f(5400)_i$ is the notional failure probability of the i^{th} component designed to BS5400 Part 3. Logarithms were used in the objective function to obtain a value more linearly related to the initial cost of the structure. Various other forms of the function were investigated but they showed no significant changes in the results.

The optimisation was organised as follows:

1) Choose a value of γ_{m1}
2) For each component type in turn, find the value of γ_{m2} which satisfies the constraint $\Sigma w_i p_f(5400)_i = p_{fT}$
3) Using the values of $p_f(5400)_i$ calculated above calculate the objective function S.
4) Choose another value of γ_{m1} and repeat steps 2 and 3 to find which γ_{m1} gives the minimum value of S.

The problem was reduced in complexity in this way to an unconstrained minimisation of a function of a single variable.

A futher simplification was made as a result of the fact that four of the component types (beam, flanges, ties, fillet welds and friction grip bolts) have strengths directly proportional to the characteristic material strengths. Hence R^* defined above was proportional to

$$\frac{f_k}{\gamma_{m1}\gamma_{m2}}$$

In these cases once the constraint had been satisfied no further freedom existed to reduce the spread of reliabilities. Of course γ_{m1} had to be first obtained from optimisation of the other four components in the manner described.

Step 2 in the above algorithm, the determination of γ_{m2}, requires the solution of

$$f(\gamma_{m2}) = \Sigma w_i p_f(5400)_i - p_{fT} = 0 \qquad (2.12)$$

This was solved by using an adaptation of the Newton-Raphson method.

The fourth step in which γ_{m1} must be re-estimated the scheme used was to increase γ_{m1} in steps of 0.1 until the minimum value of S was passed. The next guess was obtained by quadratic interpolation between the value of γ_{m1} which produced the minimum S to date and the two adjacent values. A more localised search then ensued with a reduced step length of 0.01. The search stopped when the step length was 0.001.

2.5 Bridge Types and Components Considered

In order to cover the likely range of the various structural elements reference was made to a survey of existing plate girder (spans 27m to 64m) and box girder (spans 18m to 213m) designs. Also typical ranges of dead load to live load ratio were obtained for bridges with spans from 2.0m to 100m.

Before selecting components for inclusion in the calibration the authors ensured

a) each could be deemed satisfactorily designed by existing practice and

b) that sufficient reliable test data relating predicted to observed strength were available. The components were:

1. Compression members: Rolled and welded sections in mild and high yield steel with slenderness ratios (L/r) between 55 to 130. Plate panels of various length/breadth and breadth/thickness ratios.
2. Tension members.
3. Beams: Tension and compression flanges and webs of composite plate girders. The strength formulation in BS153 was considered inadequate for webs in continuous girders with high coincidence of bending and shear and longitudinally stiffened webs. The web components used in calibration were therefore limited to plate panels forming parts of simply-supported girders. The loading on the panels was confined to shear alone.

The design of stiffened compression flanges were considered to be inadequately covered in BS153 and consequently they were omitted in the calculation of target reliability. To enable partial factors to be derived 8 examples of stiffened compression flanges in box girder bridges in service were used.

4. Connections: Fillet welds and high strength friction grip (HSFG) bolts were studied but were not included in the evaluation of target reliability. Fillet welds had a very high notional reliability which is desirable in view of the severe consequences of failure. Conversely HSFG bolts had a low notional reliability when considering slip. Since slip may be regarded as a serviceability, and not collapse, limit state the low reliability was not a matter for concern. Reliability against collapse by bolt shearing or plate bearing was not considered. These two connection types were calibrated to target reliabilities determined independently from the other components. Throat thickness, bolt preload and coefficient of friction were treated as random variables.

2.6 Loading and Strength Models

Part 2 of BS5400 contains guidance of all loading including the partial factors to be applied on dead and live loads. These were not based however on knowledge of the statistics of the various load types. For the purposes of evaluating partial factors on strength it was necessary to select appropriate probabilistic loading models for vehicular live and dead loads equivalent to combination (1) loading. (Permanent and primary live loads.) Wind and temperature loads were not considered. Despite this the optimised partial factors γ_{m_1} and γ_{m_2} are recommended for use with all load combinations.

2.6.1 Loads

Dead Load: Variation in dead load covered variation in steel weight arising from departures from nominal thickness, variation in thickness and

density of concrete deck slabs and variation in thickness of surfacing. For the first two of these, data was obtained from literature on steel and concrete variations. For surfacing, however, no statistical data was available and neither is there any standard controlling the build up of surface thickness. It was decided to combine all dead load uncertainties together and model them as a single random variable with mean 1.05 times the calculated nominal value and a coefficient of variation of 5%.

Vehicular Live Loads: Probabilistic models of vehicular live load were derived from surveys of lengths, axle weights and impact effects on certain trunk roads. The information from the survey was combined with data obtained from a study of the frequency of occurrence of vehicles of different types in the slow lane of a motorway. The result was a load effect frequency distribution for bridges of different span. The prediction based on these models differed markedly from the loading specification given in Part 2 of BS5400. The difference was thought to be due to the former having been derived from limited records and from objective judgement as to the percentage of heavy goods vehicles and the occurrence of jam situations. Various alternative loading models were examined. Finally it was decided to adopt a model in which the statistical parameters were chosen as proportions of the HA design value, and hence the model was independent of loaded length. The final choice was:

Distribution type	Extreme I
120 yr return load	1.0
5% characteristic	1.2
Mean	1.0385
Standard deviation	0.0855
(COV	≈ 8%)

2.6.2 Strength

Whilst estimates of mean and standard deviation of strength variables may be guessed or obtained from the literature there is little information available regarding the tails of the distributions. Since the shape of these is all important for calculation of reliability resort has to be made to rationally based guesswork. Accordingly resisting variables which in general cannot be negative are modelled using lognormal distributions.

Steel Thickness: For commonly used thicknesses the available data suggested standard deviation of average thickness to be 1.9% of nominal, i.e. a COV of 1.9%. Since this is negligible compared to other uncertainties thickness was treated deterministically.

Yield Stress: A large amount of data was studied in which statistics varied from one mill to another. Most representative estimates were standard deviation of 25N/mm^2 for Grade 50 and 20N/mm^2 for Grade 43 steel. The mean strength was typically 2 standard deviations above the nominal value. It is widely known however that straining rates in commerical tests are high resulting in high yield stresses. It was decided to reduce the mean values by 15N/mm^2 to give a value appropriate to service loading. The resulting characteristics for yield stress in N/mm^2 were:

	Mild	High Yield
Mean	270	390
Standard deviation	20	25
COV	7.4%	6.4%
Distribution	Lognormal	Lognormal

Model Uncertainties:

1) Struts: Values of the ratio of test strength to predicted strength were used from European data. These did not however include welded sections. The results were grouped in two slenderness ratios as follows:

	Distribution	Mean	Std Devn	COV
1/r = 55	Lognormal	1.30	0.117	9%
1/r = 130	Lognormal	1.22	0.067	5.5%

2) Tension and Compression Flanges: Data was supplied from the Department of Transport. Certain test results were eliminated because of inadequate reporting of test configurations. For compression flanges a lognormal distribution with mean 1.00 and standard deviation 0.119 (COV=11%) was used.

3) Webs, Plate Panels and Ties: Results of the data surveyed were:

	Distribution	Mean	Std Devn	COV
Webs	Lognormal	1.09	0.122	11%
Plate Panels	Lognormal	1.22	0.122	10%
Ties	Lognormal	1.30	0.160	12%

2.6.3 Connections

1) Fillet Welds

Statistical characteristics of the strengths of fillet welds in simple shear were based on data from the International Test Series[5]. Material and weld

metal ultimate tensile stresses, the root thickness and penetration were treated as random variables. Model uncertainties were obtained from test results on transverse and longitudinal welds. The results of the study are presented in Reference 6.

2) High Strength Friction Grip Bolts

Bolt preload and coefficient of friction were treated as random variables. Comprehensive details of the study may be found in Reference 6.

2.7 Discussion and Lessons

2.7.1 Summary of Relevant Results

The overall range of notional reliabilities of BS153 designs covered many orders of magnitude. Large differences were apparent between both the mean reliability of different component types and the reliabilities within any specific type. The most reliable, a slender strut, had a notional failure probability of the order of 10^{-63} whilst the least reliable, an unwelded plate panel, had a notional failure probability the order of 10^{-3}. Values of failure probability below 10^{-15} are meaningless since, as the authors point out, smaller values are subject to machine accuracy.

The differences between component types show that the BS153 design rules as drafted have different amounts of inherrent conservatism.

The calculation of average reliability is heavily influenced by the least reliable. Excluding compression flanges and unwelded plate panels the average failure probability was 0.63×10^{-6} ($-\log_{10} p_f = 6.2$). Making the same exclusions the highest failure probability was 5.01×10^{-5} ($-\log_{10} p_f = 4.3$). The average is seen to be only slightly lower than the highest failure probability.

In order to carry out the calibration of resisting partial factors a typical average value of the partial factor on dead load was used. viz. γ_{fLD} = 1.13. The live load factor used was the value specified in Part 2 of BS5400[1] viz. γ_{fLL} = 1.50. As part of a wider sensitivity study one calibration exercise was carried out by allowing the dead and live load factors to be optimised along with the resistance factors γ_{m1} and γ_{m2}. Despite this freedom the optimised load factors were very close to the factors prescribed in Part 2 of BS5400 (cf γ_{fLD} = 1.16 and γ_{fLL} = 1.47). Considering that the Part 2 load factors were suggested by a loading committee without the help of statistical methods their estimates were surprisingly accurate.

The saving in steel weight when using the BS5400 design rules with the proposed set of partial factors was also estimated. A saving of 28% was claimed for tension flanges against an increase of 14% for stiffened compression flanges. An overall saving of 6% was claimed.

2.7.2 Discussion

That notional reliabilities are subject to wide variation for designs within the same code is a common finding where the code in question has not been the subject of probabilistic calibration. This is hardly surprising and reflects the different levels of confidence in designing different components. It is interesting to note that the most reliable component in the study was a slender strut: intuitively a difficult component to design. The safety margin employed to offset the uncertainty in design is shown in this case to be overconservative. Opposed to this the least reliable was a plate panel which like the slender struts has a strength determined by buckling considerations. That these two buckling components are at the extreme ends of the reliability order is consistent with the idea that design to resist buckling has a large associated uncertainty.

In Section 1 the arguments for setting target reliabilities in line with the least reliable design as opposed to the average reliability of designs to former rules were presented. In the current case such a choice would mean a target failure probability of 5.01×10^{-5} instead of 0.63×10^{-6} (ignoring the design rules with well acknowledged shortcomings). The effect on partial safety factors for this small reduction in target reliability would be very small, however, any reduction is readily accommodated without any additional complexity into the limit state format and would result in cost benefits.

With a view to carrying out and reporting subsequent reliability work the following discussion focusses on three topics: the choice of statistical models to represent the various basic uncertainties; formulating and reporting of failure functions, including a recommendation for notation; the general mathematical properties of failure functions.

Estimation of statistical models in the work described is by a mixture of intuition, guesswork and hard data. A complete statistical model comprises the type of distribution (Normal, Lognormal, Weibull etc.) and the parameters which define it. For any distribution the n^{th} moment is given by

$$m_n = \int_{-\infty}^{\infty} x^n \, f_X(x) \, dx \qquad (2.13)$$

where $f_X(x)$ is the pdf of the random variable x. For the normal distribution, defined by

$$f_X(x) = \frac{1}{s_X \sqrt{2\pi}} \exp\left\{ - \tfrac{1}{2} [(x - m_X) / s_X]^2 \right\} \qquad (2.14)$$

the first and second moments are simply the mean m_X and the variance s_X^2 respectively. For the normal distribution the first and second moments are easily identified as the parameters defining the distribution. For the lognormal distribution, given by

$$f_y(y) = \frac{1}{y\sqrt{2\pi}\, s_{lny}} \exp\left\{ - \tfrac{1}{2}\left[\frac{1}{s_{lny}} \ln\left[\frac{y}{m_y}\right]\right]^2\right\} \qquad (2.15)$$

the moments are

$$m_y = \breve{m}_y \exp(\tfrac{1}{2} s_{lny}) \qquad (2.16)$$

and

$$s_y^2 = \breve{m}_y^2 [\exp(s_{lny}^2) - 1] \exp(s_{lny}^2) \qquad (2.17)$$

and

$$s_y^2/m_y^2 = V_y^2 = \exp(s_{lny}^2) - 1 \qquad (2.18)$$

The final expression gives the ratio of second to first moment squared and is the square of the coefficient of variation (COV) mentioned previously. The parameters of the lognormal distibution are s_{lny} - the standard deviation of the logarithms of the lognormally distributed variable and $\breve{m}_y$ - termed the median since it is the value of the random variable which devides the pdf into equal areas (unlike the mean which corresponds to the centre of gravity of the pdf). Estimates from data of s_{lny} and $\breve{m}_y$ have not been made in this study. Rather the sample mean and sample COV have been calculated in the usual way and Equations 2.16 to 2.18 solved to obtain s_{lny} and $\breve{m}_y$. The decision to model a variable using the Normal, Lognormal or other distribution can of course be taken after performing various methods of hypothesis testing. However more intuitive means seem to have been employed here. It is often the case that several different statistical models can be made to fit the same

data with high levels of confidence. Recourse to intuition thus often seems more valid. A variable which cannot sensibly be negative will often exclude the use of the Normal distribution. This applies to modelling uncertainty and material properties. The Central Limit Theorum can often point the way towards using either the Normal or Lognormal distribution: A variable whose values are the sum of a large number of contributing factors tends towards being Normally distributed whilst a variable whose values are the product of a large number of contributing factors tends towards being Lognormally distributed. Thus, in the absense of data, loads, being the sum of many smaller contributing loads, are often considered to be Normally distributed. Fatigue life is considered to be Lognormally distributed because the damage after n cycles is a factor of the stress state resulting from the n^{th} load application.

The failure function for struts, Equation 2.9, together with the code format Equations 2.1 to 2.3 do not give sufficient detail to enable the calculation of margin M to be repeated. Furthermore since Equation 2.9 contains a mixture of deterministic quantities and random variables it would improve clarity if a notation were adopted which would immediately identify the random variable with its mean value and COV or standard deviation. For example $f_{116}[150, 0.3]$ meaning a random variable f_{116} with mean 150 and COV 30%. In the case reported f_{116} is a function of other random quantities yield stress, σ_y, and dimension, φ. The notation can be adapted and used alongside functional notation so that for example:

$$\underline{f}_{116} = f_{116}(\sigma_y[243 \ , \ 0.08] \ , \ \varphi[30.0 \ , \ 0.02])$$

When the mean value of any random variable is itself the result of some

deterministic calculation the same notation can be employed e.g. for centrally loaded slender strut of length l the random Euler buckling load might be:

$$\underline{P}_E = P_E \left[\frac{\pi^2 EI}{4l^2} \ , \ 0.15\right]$$

Note that in this notation:

$$\underline{P}_E = P_E \left[\frac{\pi^2 EI}{4l^2} \ , \ 0.15\right] / \gamma = P_E \left[\frac{\pi^2 EI}{4l^2 \gamma} \ , \ 0.15\right]$$

Finally to completely specify the failure function the detail should extend to include the partial factors. The idea that safety factors are functions of reliability is central to Level 1 code philosophy (see Section 1). The results of calibration studies should preferably be illustrated with tables and graphs showing reliability as a function of safety factor. For the benefit of the inquirer the mathematical expressions defining these graphs should be reported, this would enable the reader to see the mathematical link between (partial) safety factor and reliability. In the present case the results for the designs to BS5400 might be expressed as:

$$\bar{p}_f(\gamma_m, \gamma_{fLD}, \gamma_{fLL}) = \frac{1}{n} \sum_{i=1}^{n} p_{fi}$$

where $p_{fi} = P(M_i < 0)$

where

$$M_i = \underline{f}_{116i} X_m - \left\{ (1 - \lambda) f_{5400i}(\gamma_m) \frac{\underline{V}_{DL}}{\gamma_{fDL}} + \lambda f_{5400i}(\gamma_m) \frac{\underline{V}_{LL}}{\gamma_{fLL}} \right\}$$

giving an expression for X_m and typical expressions for f_{116i} and $f_{5400i}(\gamma_m)$.

The properties of failure functons give indications of the behaviour of the function M = 0 and the probability P(M < 0).

The first property is that M and 1 - P(M < 0) are monotonic increasing with any partial factor. This assumes that material properties or strengths ('resisting variables') will be divided by a partial factor and loads or stresses ('loading variables') will be multiplied by one.

The second property is that P(M < 0) (i.e. the probability of failure) increases as the COV of any variable increases.

A resistance variable is one which, if increased in value, leads to an increase in M. A loading variable has the converse property i.e. an increase leads to a reduction in M. In the current application, therefore, the length of a slender strut is a loading variable. Bias is defined as the value of

$$\frac{\text{actual value}}{\text{assumed value}}$$

and could apply to loads, material properties or resistances. The third property of failure functions can now be stated. For a resisting variable P(M < 0) increases as the bias of any resisting variable increases but decreases as the bias of any loading variable increases.

The fourth and final property only applies for the special case where the mean value of the second term of the failure function is equal to the mean value of the first term. In such a case when all partial factors are set equal to 1.0 then M=0, P(M < 0) $\simeq$ 0.5 and $\beta \simeq 0$. The approximation becomes exact if the distribution of M is symmetrical about M=0 as would be the case when all the random variables are normal.

Having described the properties a general observation can be made:
The reliability calculated in this way is only as good as the strength

formulation from which R, the critical resistance is calculated. Any change to the strength formulation will affect R, thus the same component under any given load will have different reliabilities if different strength formulations are used in the failure function. This highlights the subjectivity of reliability calculations and backs the case against comparing reliabilities without reference to the formulation (and model uncertainty parameters) used in their calculation. However a qualification is necessary here. The historical process by which strength formulations came about is evolutionary, i.e. by a process of gradual changes the end product becomes ideally suited to the application. The prerequisite of an accurate strength formulation is that it has been developing over a long period of time. This process is illustrated by the development of the buckling strength formulation from Euler to the present day. The formulation Euler made in the mid-19th century was non-conservative except for very slender struts. The first modification came with the cut-off point at yield strength for stocky struts. The compound Euler/yield stress curve still was non-conservative for the wide mid-range slendernesses. Ayrton and Perry[7] in 1886 proposed modifications to the Euler/yield stress curve which provided the basis for present day strut design. They essentially smoothed out the compound Euler/yield stress curve giving a mean value curve for the entire range of slendernesses. The changes since then have been minor and directed at modifications to the value assumed for initial imperfections (e.g. Robertson in 1925[8]).

The qualification to the warning given regarding comparison of reliabilities without reference to the strength formulations is that any formulation which has undergone a sustained period of development will have sufficient accuracy to impart meaningful calculated reliabilities.

A further point bourne out in the BS5400 study is the opportunity to rationalise and simplify the optimisation procedure. It has been seen in this context to diminish in complexity from a constrained minimization of several variables to an unconstrained minimization of a single variable viz γ_{m2}. Such simplifications render the problem orders of magnitude less complex and less costly. In conclusion it can be said that so long as the outward objective of optimisation is not lost, i.e. the reduction of the spread of reliabilities about the target, then any scheme, method or short cut is acceptable.

2.8 References

1. BS5400: Steel, Concrete and Composite Bridges. British Standards Institution, London, 1982.
2. BS153: Specification for Steel Girder Bridges. British Standards Institution.
3. International Standards Organisation General Principals for the Verification of the Safety of Structures. I.S.O. 2394, February, 1973.
4. Construction and Industry Research and Information Association, 'The Rationalisation of Safety and Serviceability Factors in Structural Codes', CIRIA Report 63, July, 1977.
5. Lightenberg, F.K., 'International Test Series', Final Report, International Institute of Welding Document XV-242-68, 1968.
6. Flint and Neill Partnership - Imperial College, 'Derivation of Safety Factors for BS5400: Part 3', Final Report, August, 1980.
7. Ayerton, W.E. and Perry, J., 'On Struts', The Engineer, Vol. 62, pp464-513, 1886.
8. Robertson, A., 'The Strength of Struts', The Institution of Civil Engineers, No. 28, pp3-55, 1925.

SECTION 3

COMPONENTS: A RE-EVALUATION OF BS5400 PARTIAL FACTORS FOR OFFSHORE USE

3.1 Introduction

This section describes part of the pilot study, sponsored by the U.K. Department of Energy on revisions to their Guidance Notes[1] for the design of offshore installations. The current Guidance Notes refer designers to either BS153 Parts 3B and 4 or BS449 for permissible stresses for structural components. BS449, however, is in the process of being superseded by a limit state code and BS153 has been superseded by BS5400[2] whose limit state formulation was the subject of Section 2. For various reasons the new codes cannot simply replace their permissible stress counterparts. Consequently a study was initiated to consider how the Guidance Notes on structural steel design need to be altered to allow limit state codes to be used and to consider the changes to the codes needed to make them suitable for offshore installations. The part of the study relevant to this thesis is the re-calibration of the partial factors contained in BS5400: Part 3 for use offshore.

International agreement exists[3] on recommended partial safety factors and these include two resistance factors, one to account for material variability and the other to account for all other resistance uncertainties including modelling. In the BS5400: Part 3 evaluation little increase in the spread of reliabilities arose as a result of amalgamating the factors into a single partial factor. The same course was followed for the present re-evaluation. The material factor and all other partial factors are presented in Section 3.2 in the Code Format. Section 3.3 summarises the principal requirement for 'optimising' partial safety factors.

Unlike bridge structures there is not a long history of experience with offshore structures. Consequently a value of target reliability was chosen not from previous codes of practice but rather after considering Norwegian and North American experience. Section 3.4 presents the deliberations on target reliability. Since this value is the single most influential affecting the resulting partial safety factors the choice is critically examined in the discussion in Section 3.14.

The major difference between structural design of bridges and offshore installations is in the environmental loading. For bridges, wind loading was not considered[4] to be significant enough for the purposes of evaluation of partial factors. For offshore structures, however, the loads imposed by waves, wind and currents dominate the final design. The statistical models for environmental and other loads are discussed in Section 3.5 together with models for resistance. Following this, in Section 3.6, the factor which accounts for inaccuracies in structural analysis, the 'analysis factor', is discussed and a value is chosen appropriate for offshore structures. The final choice was based on engineering judgement rather than probabilistic optimisation.

Section 3.7 describes the BS5400: Part 3 strength models for the four main structural components considered viz: columns, beams, stiffened flanges and stiffened webs. This is followed by descriptions of data banks (Section 3.8) of test data on offshore component strengths compiled in part by J.F. Kenny and Partners[5] for the Department of Energy. These were used to establish strength model uncertainty factors for discrete slenderness ranges of each of the four components (Section 3.9). Section 3.10 presents typical Level II reliability solutions for each component type on the assumption of a trial set of partial factors. The salient points of the solution are discussed. The work in Sections 3.7 to 3.10 is described in greater detail in References 6 to 10.

Sections 3.11 and 3.12 describe the manner in which the seven partial factors (four resistance and three loading) were obtained to ensure a minimum spread of reliabilities at an average value equal to the target. In Section 3.13 the results of partial factor evaluation are compared with other codes by plotting non-dimensional allowable stress versus slenderness for each of the four components.

The discussion in Section 3.14 focusses independently upon target reliability, load modelling and general considerations. Conclusions, recommendations for improvements and extensions are summarised in Section 3.15.

3.2 Code Format

The safety factor format in BS5400 requires that $R \geqslant S$

where $R = \text{function}\left[\frac{f_k}{\gamma_m}\right]$ is the design resistance,

$S = \gamma_{f3}[\text{effects of } \gamma_{fL} Q_k]$ are the design load effects,

f_k is the characteristic value of component strength or resistance,

γ_m is the partial factor on resistance,

γ_{f3} is the factor to take account of the inaccurate assessment of load effects, i.e. the analysis factor,

γ_{fL} are the partial factors on loading, and

Q_k are the nominal loads.

f_k is the value of strength as predicted by the Part 3 formulations. It is defined as a 'characteristic value' although nowhere in BS5400 is it indicated

just which 'characteristic' it represents. As will be seen later, the strength formulations appear to predict mean values, i.e. f_k is not strictly a characteristic value.

γ_m normally[3] consists of two components γ_{m1} and γ_{m2}. The first of these, γ_{m1}, is introduced to account for the uncertainties associated with material only while the second, γ_{m2}, covers all other uncertainties associated with strength other than material. This would normally cover geometry variables and the elastic modulus. As indicated in the introduction, the original Part 3 derivation found that very little loss of accuracy arose from amalgamating the two and it also had the particular advantage of simplifying the format. This same approach was adopted in the present work.

The loading components γ_{fL} and Q_k are determined for each load type and for each combination of loads considered. In BS5400, seven different basic load types are defined in up to five different combinations. Not all load types are considered in every combination and, of the load types, one refers to temporary erection loads and another to secondary live loading associated with the primary live loading.

3.3 Partial Factor Evaluation Procedure

The basic objective of partial factor evaluation is to select a set of partial factors such that the spread of the resulting set of failure probabilities of a range of structures is minimised. In the present context, it is intended to use test data to represent the range of structures considered.

The process of selecting partial factors is therefore one of optimisation which can be expressed as follows. The objective function to be minimised is:

$$\left[\sum_{i}^{n} \omega_i (p_{fi} - p_{ft})^2\right]^{\frac{1}{2}} \qquad (3.1)$$

where p_{fi} is the probability of failure of the i^{th} element designed in accordance with the Part 3 strength formulations using the trial values of partial factors,

p_{ft} is the target probability of failure (target reliability),

ω_i is the frequency of occurrence of element i, and

n is the total number of elements in the design space.

During the investigation, each component was examined alone when subjected to each of the main load categories with the objective of identifying the appropriate γ_m and γ_{fL} product to minimise the spread of failure probabilities. The results are presented in Section 3.12.

3.4 Target Reliability

For the purpose of establishing an upper limit for failure probabilities studies[11,12] of actual failures expressed as annual failure frequencies were reviewed. Figures ranged from losses of semi-submersibles at 2.0×10^{-3} to losses of jack-ups at 1.2×10^{-2}. Comparisons were then made with the values of annual failure probabilities between Norwegian and North American studies. The values published by Det norske Veritas (DnV)[13] of structures designed to their 1977 Rules[14] ranged from 5×10^{-7} to 1×10^{-4} per annum with steel structures generally lying in the range of higher failure probabilities. Objections were raised[15,16], however, concerning the rationale behind these values. The

annual failure probabilities for steel structures designed to the API RP2A recommendations[17] for fixed offshore structures were reported to have ranged from 6×10^{-5} for dead load dominated structures to 1.5×10^{-3} for environmental load dominated structures. The reported recommendations of the Rule Case Committee (RCC) of the joint Conoco-American Bureau of Shipping (ABS) project for a reliability based design code of tension leg platforms (TLP) whose work is summarised in Reference 18 were, after surveying safety levels in other related codes, for a target annual failure probability of 4×10^{-6}. The same committee also reommended a less conservative annual failure probability of 3.0×10^{-5} when designs were performed using reliability analysis directly.

Comparisons of annual failure probabilities are summarised as follows:

actual failure	2.0×10^{-3} to 1.2×10^{-2}
DnV 1977 Rules	5.0×10^{-7} to 1.0×10^{-4}
API 2RPA	6.0×10^{-5} to 1.5×10^{-3}
RCC for TLPs	4.0×10^{-6} or 3.0×10^{-5}

A value of 1×10^{-4} per annum was adopted for the re-evaluation. Two bracketing values were also adopted to demonstrate the effect on the partial factors.

3.5 Statistical Definitions

3.5.1 Geometry

Departures from nominal dimensions occur as a result of the rolling of large plates. The material in the centre portion of a rolled plate has greater

thickness than at the edges due to small but measureable deflections of the rollers. The original BS5400: Part 3 calibration study in Reference 4 assumed dimensions were deterministic. It was felt that some allowance had to be made for corrosion expected in offshore structures and References 19 to 25 were consulted. These gave values of COV between 0.2% for diameters of circular sections and 3.1% on areas of column test specimens. A value of 2% was finally selected.

The same COV was selected for lengths even though it was appreciated that in general tolerances are likely to be smaller than for sectional dimensions. Dimensions were assumed to be represented by a normal distribution with mean equal to nominal or measured value, i.e. zero bias.

3.5.2 Material Properties

Reference 26 contains results of a large statistical survey on the yield stress of material leaving steel mills. They concluded that for mild steel the weight and average COV was 4.8% and a weighted average bias of 10.6%. Bias being calculated from

$$\frac{m}{m_{nom}} - 1$$

where m is the mean measured value and m_{nom} the nominal value. For high strength steel the corresponding results were 4.9% and 10.1% respectively.

The authors of Reference 4 noted that this survey related to pre-nationalisation days in the industry and undertook a small survey on high strength steel. Their findings were an increase of COV to 6.7% and an

increased bias to 15.6%. There was concern that the proportion of material falling below the minimum specified level showed a marked increase. These results however were from a mill which was under the threat of closure. Also the sample size was only 6.

All the above data were subject to strain rate effects.

The experience of DnV[13] indicates a COV of 5% and a bias of 5% but the values are not fully substantiated.

In References 24 and 25 a COV of 4.7% was used for high strength steel. The bias was 10%. Japanese data[20] indicated the following values

Section and Grade		Bias(%)	COV(%)
Plate	- mild steel	38	6.0
	- high strength	24	5.2
Angle	- mild steel	31	3.3
Stiffeners	- high strength	21	2.7

The COVs are consistent with UK values. The biases however are higher and the main reason is thought to be the high strain rates used. Also the high bias reflects the thickness of sections used being 9mm to 19mm. Another Japanese author[21] reported a bias of 17% and COV of 11.1%. The thickness in this case was less than 10mm which would account for the large bias. The tests were for static yield stress. The reason for the high COV was most likely to be the large range of sections and plating in the data.

The model eventually used for the original partial factor derivation[4] accounted for strain rate by reducing the mean by 15 N/mm^2. The standard deviations were, for mild steel (Grade 43) 20 N/mm^2, and for high strength (Grade 50), 25 N/mm^2. The design value of yield stress within each grade was taken to be constant i.e. independent of thickness. On this basis the COVs were

mild steel	20/(245+2x20-15) = 20/270 = 7.4%
high strength	25/(355+2x25-15) = 25/390 = 6.4%

The corresponding biases were

mild steel	270/245 - 1 = 10.2%
high strength	390/355 - 1 = 9.9%

The COVs for steel thicknesses pertinent to offshore structures were, according to tabulated data in References 4 and 26, as high as 8%. On this basis and considering the possibility of overseas' steel being used in UK offshore construction a COV of 8% was assumed for the re-evaluation.

The effect on the bias of an increased strain rate is an increased apparent bias. In order to obtain the bias for strain rates which would better reflect the rate of service loading the mean yield stress must be reduced. The correction for strain rate used in the original calibration was 15 N/mm^2. This is applicable to UK mills only. Information presented in Reference 21 indicates the correction amounts to 50 N/mm^2 for mild steel and up to 80 N/mm^2 for high strength steel. This is based on data relating mainly to Japanese steels but also includes those from Europe. Limited evidence from the U.S. suggested the correction there is 35 N/mm^2[27].

The reason for higher strain corrections being applicable to Japanese and US steels is that a faster rate of straining is specified by them when conducting tensile tests. It is 625000 μstrain/minute compared with the UK standard of 7000 to 8000 μstrain/minute.

The proportion of below strength material expected according to the BS5400 models when strain rate correction has been made is approximately 5%.

Having adopted a COV of 8% for the re-evaluation the bias consistent with below average material of 5% is an expectation of 12½%. This value was adopted for the study although it is apparent that hard data from offshore yards is lacking. This value of bias was adopted together with a recommendation that a survey of steels from offshore yards should be undertaken.

A lognormal distribution was assumed since negative yield stresses are excluded. This was also the model used in the original evaluation.

Variation in elastic modulus is sometimes apparent but usually can be explained in terms of the method of measurement. It was treated deterministically.

3.5.3 Load Effects

The load categories in the DEn guidance notes[1] were amended so that loads having a similar amount of variability were categorised together. This resulted in hydrostatic forces being categorised with dead load and dynamic forces (those arising from a structures momentum in response to imposed loads) were categorised with environmental loads.

The resulting categories were

1. dead plus hydrostatic: i.e. weight of structure and fixed equipment and machinery, hydrostatic forces, buoyancy.
2. live: i.e. operation loads, stores, portable equipment, crew, berthing and landing load, motion loads for mobile platforms, thermal stresses, construction forces.
3. environmental plus dynamic: i.e. wind, wave, slamming, vortex shedding, marine growth effects, snow, ice, currents and dynamic forces.

The unamended DEn load categories differed only from the API RP2A[27] definitions in that buoyancy was included as a live load while in the API specification it was included under dead loads. This reflects possibly the greater uncertainty associated in the North Sea environment compared with the Gulf of Mexico.

The load categories in the proposed TLP code[18] are derived according to the influence they have on the structure and in this they reflect the special need of the structure. The categories were

1. static: time invariant loads such as weight, all movable and fixed fittings and stores, buoyancy and static tendon tension.
2. quasi static: forces changing slowly with time such as offset and vertical set-down caused by winds.
3. dynamic: i.e. wave induced.

The models for TLP and fixed platform load categories are summarised below.

TLPs	Bias	COV%	Distribution
static	1.0 (0%)	10	Normal
quasi-static	1.0 (0%)	20	Normal
dynamic	0.9 (-10%)	26	Normal

Fixed	Bias	COV%	Distribution
Dead & hydrostatic	1.075 (7.5%)	5	Normal
Live	1.15 (15%)	10	Normal
Environmental & dynamic	1.0 (0%)	30	Normal

The static loads for TLPs correspond approximately to dead and hydrostatic and live load categories combined and they can be seen to have similar statistical models. Likewise the quasi-static and dynamic TLP categories correspond in the kinds of load and statistical modelling parameters to the environmental and dynamic category.

The increased bias for the first two categories for fixed structures was adopted in recognition of the weight growth problem which affects dead loading and live loading - the latter to a greater extent.

The bias for the third load category followed closely the bias for the TLP dynamic category which in turn was decided upon after consulting various

experts. These opinions varied widely from -50% (0.5) to 10% (1.1)[18]. It was further recognised that the common practise of linear addition of wave and current velocities (rather than a more realistic vectorial combination) is significantly conservative.

The COV for dead load of 5% was adopted on the grounds that future platforms would be subjected to strict weight audits. The values are the same as that used for dead load in the original bridge calibration.

The live load COV followed the TLP value for static loads viz 10%.

3.5.4 Summary

The following table summarises the bias, COV's and distributions assumed for each of the resistance variables and load types to be considered in the final partial safety factor optimisation:

Design Variable	Bias (%)	COV (%)	Distribution
Geometry	0	2	normal
Yield Stress	12.5	8	log-normal
Dead load effect	7.5	5	normal
Live load effect	15	10	normal
Environmental load effect	0	30	normal

3.6 Analysis Factor

The analysis factor, γ_{f3} in the Code Format, is intended to reduce the effects of inaccuracies in structural analysis. The value recommended for BS5400: Part 3 was 1.1, based on engineering judgement. The same value was recommended for fixed offshore structures which, like bridges, can be successfully analysed statistically. For components responding dynamically e.g. components in the splash zone and deep water platforms, dynamic analysis is required. Being more complex these introduce greater inaccuracies which need to be reflected in γ_{f3}. The recommended values depend upon the type of structural analysis as follows

Method	
Static solution	1.1
Linear frequency-domain solution (Random waves)	1.2
Non-linear time-domain solution (Regular or random large waves, plus current)	1.15
Non-linear design wave	1.15

The recommended figures reflect largely the degree of confidence held in the procedure for fixed offshore structures. This is less for linear frequency domain solutions than for either non-linear time-domain or non-linear design wave methods.

Finally it was recognised that to a small extent the level of accuracy achieved with any of the dynamic methods depends on the experience of the user. Designers were encouraged to make subjective judgements: reducing the factor for well-experienced personnel and increasing it for the less experienced.

3.7 Part 3 Strength Models

For each of the components to be examined, the Part 3 strength model (or formulation) will only be described in outline below. Details, however, are presented with 'hand calculations' representing the sequence of calculations in References 6 to 10.

3.7.1 Columns

The column strength formulation in Part 3 is identical to the 'European Column Curves'. These curves were derived after an extensive experimental and numerical programme involving over 1000 tests on pin-ended columns[22]. The strength curves were evaluated as the mean minus two standard deviations of the experimental results which would be accurately reproduced by the numerical procedure adopted.

3.7.2 Beams

Two strength models are provided in Part 3 for the design of beams. Both seek to establish a value for the slenderness of the beam, denoted λ_{LT}, which reflects the type of loading, its position of application on the cross-section, the boundary conditions and the unsupported length of the beam.

Once the slenderness has been determined, the maximum permitted stress is determined from a Perry-type formula. From this stress, the moment capacity can be determined for comparison with the moment arising from loading. In both approaches, λ_{LT} is not used directly but after factoring by $\sqrt{\sigma_{YC}/355}$ where σ_{YC} is the nominal yield stress for the compression flange. This was introduced primarily to generate slenderness values more or less identical with the ℓ/r_y (length ÷ radius of gyration about the weaker axis) values used in the previous code. It was hoped that this would help make the new formulations more accessible to designers.

In both methods, the cross-section has to be checked to identify whether local buckling is a possibility or not. If not, it is described as compact and can be designed up to its full plastic moment capacity. Otherwise the section is non-compact, and its properties may have to be calculated on an effective width basis.

In the first or simplified approach, the so-called 'slenderness parameter' $\lambda_{LT}\sqrt{\sigma_{YC}/355}$ is calculated from:

$$SP = k_1 k_2 (L/r_y) k_4 \eta V\sqrt{(\sigma_{YC}/355)} \qquad (3.2)$$

where k_1 is an effective length parameter determined by the type of end fixity,

k_2 is an effective length parameter determined by the level of the applied load with respect to the beam's neutral axis,

L is the span between points of lateral restraint,

k_4 is determined according to whether the beam is rolled or welded and by the web to flange thickness ratio,

η is a parmeter determined by the type of applied load, and

V is dependent on the shape of the beam.

In the second or exact method, the slenderness parameter is found from

$$ESP = \surd(\Pi^2 E\ S/\sigma_{ci})\ \surd(\sigma_{YC}/355) \qquad (3.3)$$

where S $= z_{pe}/z_{xc}$ for compact sections,

$= D/2y_t$ for non-compact sections,

z_{pe} is the plastic section modulus,

z_{xc} is the elastic section modulus,

D is the overall section depth,

y_t is the distance from the neutral axis to the extreme tension fibre,

E is Young's modulus, and

σ_{ci} is the maximum compressive bending stress as determined by an elastic analysis at the theoretical lateral torsional buckling load.

In the code, values for all the variables are either calculated from given expressions, given as constants, or can be found from tables or charts.

The slenderness parameters 'SP' and 'ESP' can also be used as a means of presenting results. A similar but non-dimensional parameter is $\surd(M_p/M_{cr})$ where M_p is the plastic moment capacity of the section and M_{cr} its elastic critical moment at lateral torsional buckling. Both parameters are directly related and when the elastic critical moment is equal to the plastic capacity so $\surd(M_p/M_{cr}) = 1$, SP = ESP = 75.

Note that although the latter relationship holds, M_{cr} will generally be different as determined by the two methods.

3.7.3 Stiffened Flanges

The Part 3 design approach for stiffened flanges is to replace the stiffened plate by a series of independent longitudinal struts consisting of a longitudinal stiffener and a piece of attached plating of width equal to the stiffener spacing. The strength of the stiffened plate is then equated to that of the strut calculated using simple bending theory on the basis of a fully effective stiffener but only partly effective plating, the reduction in effectiveness accounting for the effect on strength of plate buckling.

Strut section properties are thus based on this plating effective width and are then used in a Perry formula to determine strength based on the onset of yield in one of two places, either the stiffener tip ('stiffener induced failure') or at mid-plane of the plate ('plate induced failure'). The lower of the applied stresses necessary to generate either of these two failure modes is taken as the strength of the strut.

3.7.4 Webs

The Part 3 formulation for webs is dependent on whether longitudinal stiffeners are present or not. Even for transversely stiffened webs with longitudinally stiffened flanges, the girder must be treated as being longitudinally stiffened. Otherwise it is transversely stiffened. Even though web strength is dictated by considerations of its shear capacity, it is also necessary to calculate its flexural capacity. Thus, web design involves the determination of two ultimate limit states and the use of an appropriate interaction equation.

3.7.4.1 Transversely Stiffened Webs: The rules for transversely stiffened webs derive drom the acknowledged fact that web panels can support shear loads greater than their elastic critical buckling load by the development of a diagonal tension field. The nature of this field and how it is affected by the stiffness of boundary members has been the subject of research for many years[30]. The rules, representing the synthesis of this research, provide the choice of a numerical solution or a graphical one. The former requires evaluation of the ultimate shear stress in terms of the elastic critical shear stress and the tensile field stress. The angle that the tension field makes with the neutral axis is unknown, and iterations involving increasing values of this angle are required until a maximum is obtained. The latter method uses seven graphs of ultimate shear stress plotted against slenderness for discrete values of aspect ratio and the ratio flange stiffness/web stiffness. Interpolation for aspect ratio and stiffness ratio is required. The ease with which the numerical method can be programmed makes it the preferred one of the two.

The limiting bending stress is found as described above for beams. Premature failure by buckling in the compression zone of the web is taken into account by using an effective (reduced) web thickness.

Interaction between bending moment and shear is handled by a pair of equations which approximate a parabola. Because of this, in contrast to the rules for columns, beams and stiffened flanges, the formulation does not provide a direct value of ultimate strength. In order to arrive at a limiting load value, iterations involving increasing loads must be carried out until one of the interaction expressions equals unity. Fast and accurate convergence was obtained using the Newton-Raphson technique with the experimental collapse load providing the first guess value.

3.7.4.2 Longitudinally Stiffened Webs: The rules for longitudinally stiffened beams require two separate checks to be made for each web panel. Firstly yielding must not occur and secondly its buckling strength must not be exceeded. The Mises-Hencky criteria is used for the yielding check. A reduction of the bending stress component by 0.77 allows for partial plastic redistribution.

The buckling check is conducted by evaluating the buckling coefficients for pure compression, pure bending and shear and using them in an interaction equation. When the checks are applied to each web panel, any trapezoidal stress distribution which exists in a panel, for example, because its axis does not coincide with the beam's neutral axis, must be decomposed into a direct stress element and a pure bending element. As for transversely stiffened webs, the ultimate collapse load cannot be found directly but must be determined by iteration.

3.8 Data Banks

All data used to establish the accuracy of the Part 3 strength formulations were taken from the public literature. In three cases, the data had been collated and reportedly assessed by others. This was then used as the source of results without any further additions.

In all cases, the data were critically examined in an effort to ensure they were firstly complete in all details and secondly did not suffer from weaknesses in the testing procedure. The latter were not always easy to identify and if it could not be confirmed that errors had been introduced, the results were retained although clearly doubts still existed concerning their accuracy.

In References 6 to 10 lists of all the data collected for the study are presented. Where possible sufficient details are given to allow independent assessment to be performed.

3.8.1 Columns

Data relating to 303 cylindrical columns were presented in Ref. 5. They had been collated from a number of sources. Following a preliminary evaluation of the model uncertainty parameter, 280 were selected for final analysis.

3.8.2 Beams

The beam data originally used to substantiate the Part 3 formulation was summarised in Ref. 31. It related to 360 lateral torsional buckling tests taken from Refs. 30 to 36.

3.8.3 Stiffened Flanges

Test results referring to 186 isolated stiffened flanges plus ten on stiffened compression flanges of box girders or similar were presented in Ref. 5. They were taken from Refs. 37 to 51. However, following a re-assessment of several features of the strength modelling and of the test models[52], a number of the data were deleted from the data base. This left a working base of 97 models.

3.8.4 Webs

The data on webs have been taken from Refs. 53 to 56 although the results presented in Ref. 55 itself represents a collection of a number of sources. Unfortunately, in many of the cases reported, the beam or girder length was not quoted. This did not affect the assessment of shear strength but rendered the calculation of flexural strength problematical. Thus although 93 models had been reported, only 61 could be confidently used in the analysis.

3.9 Model Uncertainty Parameter X_m

Section 1.1.3 indicates the limit state strength of an element is given by:

$$M = g(x_1, x_2, \ldots x_n) \qquad (3.4)$$

where x_i are the n independent random design variables such as dimensions, material properties, imperfections and empirical constants. Unless g(.) accurately reflects the physical behaviour of the model under consideration, it will not accurately predict its strength.

In codified design, it is not usually possible, or indeed desirable, to adopt accurate models as it would generally involve complex procedures. Consequently, code models represent a simplification of true models arrived at by the omission of particular variables and the introduction of empirical relationships and constants. For example, residual stresses in columns are accounted for by the lowering of a column curve rather than any explicit reference to residual

stress. Consequently, the functional relationship g(.) is generally not exact and may indeed have a deliberate bias in order to be conservative. The true strength of the element may be expressed as:

$$M = X_m \, g(x_1, x_2, \ldots x_n) \qquad (3.5)$$

where X_m is the random model uncertainty parameter being the statistical distribution of the ratio defined by:

$$X_m = \frac{\text{actual strength}}{\text{predicted strength}}$$

In this study, the strength functions g(.) are of course the Part 3 design formulations. X_m is thus evaluated by comparing the test result with the Part 3 prediction, using the measured value of yield stress in the formula, not the nominal one. The range of X_m values thus obtained is assessed statistically either for the complete range of models or, more frequently, for a number of divisions of the slenderness range for which the data are available. The latter was adopted because X_m sometimes varied significantly with slenderness.

3.9.1 Columns

Figures 3.1 and 3.2 present scatter plots of model uncertainty parameter, X_m, against slenderness parameters and diameter/thickness ratio respectively. Figures 3.3 and 3.4 present, in histogram form, discretised slenderness range versus mean and COV of model uncertainty factor. Two features of Figs. 3.3 and 3.4 are worth noting. Firstly, the maximum mean and COV occur in the same slenderness range, viz. 125 to 150, when it would be expected to occur at

about 75 because that is the slenderness at which yield stress and elastic critical buckling stress coincide, and it thus represents the slenderness most sensitive to imperfections. This result suggests that some of the specimens may not have had the simply supported end conditions with which they were attributed.

Secondly, the COV in the range 150 to 175 is extremely small. This is somewhat surprising in view of the small number of tests falling into this range, four in all, but which nevertheless show a remarkable degree of consistency. Although this value appears inconsistent especially when compared with the COV found in the slenderness range 125 to 150, it was initially used in the study. Later, a linear variation of COV between the values found for the ranges 125-150 and 200-225 was adopted to examine the consequences of this on the partial factors.

3.9.2 Beams

Figure 3.5 presents X_m versus both the Part 3 slenderness parameter - SP in Equation 2.15 - and the non-dimensional parameter $\sqrt{(M_p/M_{cr})}$. The numbers of the plot correspond to the sources as identified in the report on beams produced during the course of the work - Ref. 8.

Up to an SP of about 70, the results are generally reasonably evenly disposed either side of the predicted value. Beyond this slenderness, however, two distinct trends are apparent with models from series 9, 11 and 13 continuing to straddle the X_m = 1.0 line while those of group 2, 29 and 30 rise rapidly to X_m values greater than 3.0.

These two distinct groups have been examined in an attempt to identify the variable(s) which causes the difference. Any differences between rolled and welded sections are excluded as groups 1 to 19 related to rolled members and 20 to 30 to welded ones. Compactness of section was also examined as shown in Figure 3.6 but again does not appear to be the basic cause.

Using the more exact approach to calculate strength - Equation 3.3 - leads to the results presented in Figure 3.7. Again the same trend is apparent although the overall variation is considerably reduced. Below an ESP of about 75, the results are very similar to those calculated using the simpler approach.

Since using the 'exact SP' gives a better estimate of beam strength and is no more difficult to use for doubly-symmetric beams than the simpler method, it is to be preferred of the two design approaches. However, since the simpler approach is the one likely to be used in practice, the remainder of the analysis will concentrate on this procedure.

Figures 3.8 and 3.9 present the variation of the mean and COV of X_m for each increment of 25 in the slenderness range SP. Gaps in the results indicate no data are available in this particular slenderness range. As was noted in the case of columns, both the mean and COV tend to reach a maximum at a slenderness corresponding to a non-dimensional value of 2.0. In this case, however, the maximum values of both the mean and the COV are significantly greater than the corresponding values calculated for columns.

3.9.3 Stiffened Flanges

Figure 3.10 presents X_m versus both the Part 3 slenderness parameter and

the non-dimensional parameter $\sqrt{(\sigma_Y/\sigma_{cr})}$ for the range of stiffened flange models considered. A number of groups of the data originally examined[9] was deleted, one because the value of yield stress had been assumed (Group 13), several others because separate yield stresses for the plating and stiffener comprising the flange were not reported (Groups 2, 5-7, 9, 10 and 15), and one because although the yield stress was reportedly measured, only three different values were quoted to cover 27 models (Group 8). Several results from the remaining groups were also discarded because they related to fixed ended tests whose effective lengths were not possible to define. Reference 52 gives further details on these aspects.

The bulk of the data can be seen in Figure 10 to lie between 0.5 and 1.3 with one point in excess of the latter. This relates to a group 17 model which is similar to a flange of a box girder. In the BS5400 calculation, this requires an extra initial distortion term be taken into account: this has been done. A factor which could contribute to the higher than average strength demonstrated by this and similar specimens is that the webs to which they are welded exercise longitudinal in-plane strain control. This can help restrain the effects of buckling although this is generally understood to only be of importance in the post-buckling range. That is, post-peak response is controlled but the maximum load is probably not affected. On average, however, the results are seen to be clearly less than 1.0.

The variation of the mean and COV for X_m for each group of data considered has been summarised in Table 3.2. The generally high mean value of X_m for stiffened flanges tested as components of box girders or similar is obvious. Amongst the isolated flanges, the high COV associated with group 12

would suggest these data need checking, although the models within this group, and group 11, having been manufactured using methods typical of naval construction, are more likely to be representative of offshore construction procedures than the models in most of the other data groups.

Figure 3.11 shows the variation of the mean of X_m for each slenderness parameter interval of 25 within the range of slenderness examined. The Part 3 strength formulation appears to be nearly 20% optimistic at the stocky end of the range where, in general, strengths are normally expected to be greater than yield which coincides with $X_m = 1.0$.

As the slenderness increases, X_m remains ostensibly constant until the non-dimensional slenderness exceeds unity. From here it increases to a maximum in the largest slenderness range considered of nearly 1.4. This part of the range tends to be dominated by the 'built-in' flanges and so may not be typical for isolated stiffened plates.

It is possible that within this range the Part 3 strength is in fact a slight overestimation since it ignores the possibility of tensile yield in the stiffener being the limiting factor rather than compressive yield of the effective plate as currently governs in plate-induced failures.

In Figure 3.12, the COV of X_m is presented as a function of slenderness. Apart from the slenderness range 100-125 which relates to built-in flanges, the COV fluctuates between about 15 and 20% seemingly independent of slenderness. In the range 100-125 the COV is small ($\simeq$1.4%), the two results in this interval demonstrating remarkable consistency.

3.9.4 Webs

Table 3.3 summarises the different sources of data used for webs indicating, as noted above, the number of models for which length was not specified. Where it seemed appropriate to assume the beam length was twice the quoted web panel length, this has been done as indicated in the Table.

Groups 2 and 3 originally consisted of 7 tests each, but 5 models from group 2 and 2 from group 3 had slenderness values greater than 300. This is beyond the scope of the Part 3 formulations so the size of the data base was reduced accordingly.

X_m has been calculated for each acceptable model. In Table 2.3, a statistical assessment of X_m for each group is given. From this it can be seen that, provided the girder length is known, the transversely stiffened web results are reasonably well predicted and do not demonstrate a large scatter - worst mean = 1.19 and worst COV = 15.4%. The pure bending tests - group 5 - show little scatter, COV = 7.4%, but are significantly over-predicted by the Part 3 strength formulation - mean of X_m = 0.68. The longitudinally stiffened webs demonstrate much greater inconsistency with the worst mean being 1.73 and the worst COV 24%.

If all the results for girders for which the lengths are unknown are included, Table 3.3 indicates that the scatter on X_m will increase dramatically. For this reason, all girders not completely documented were omitted from further consideration. This had the obvious effect of reducing the data source considerably. However, even so, because of the different strength formulations

for longitudinally and transversely stiffened webs and because pure moment test results seemed to be significantly different from combined load test results, it was decided that the models would be grouped and treated as follows:

a) transversely stiffened girders with separate X_m means and COVs derived for slenderness ranges of 25 covering the available data;
b) pure moment tests with one X_m mean and COV determined from the data; and
c) longitudnally stiffened girders with one X_m mean and COV.

The resulting average X_m's and their scatter are indicated in Table 3.4. These values confirm that the groups as now selected appear to be non-correlated.

3.10 Typical Reliability Analysis Results

Using the advanced Level II procedure described in Section 1, reliability analyses were performed on a selection of models of each component type. The load effect selected represented 'design' dead loading in that it had the same bias and degree of uncertainty as adopted herein for this type of action. The load level was generally determined assuming $\gamma_m = \gamma_{fL} = 1.15$ so that the design effect for which the component was analysed was determined as follows:

$$\gamma_{f3}\gamma_{fL}Q_k = \frac{f_k}{\gamma_m}$$

where f_k are the Part 3 predictions assumed as means, $\gamma_{f3}=1.0$ as no structural analysis is involved, and the design stress $S_d=1.075\ Q_k$.

The purpose of these typical analyses was to identify the important design variables for each of the components, particularly in their variation with slenderness, and to obtain a measure of the variability of reliability with slenderness. For each interval of the slenderness range for which X_m was evaluated, one member was selected at random for analysis. A selection of these are presented in the following sections. They were identified mainly on the basis of what they highlight in terms of influential variables.

The format for all tables is similar. The first column lists the variables and their dimensions. Next the type of distribution assumed is generally indicated as well as the means (from the test data) and COVs. The latter are all as discussed in Section 3.5 except for that of X_m which was derived as described in Section 3.9. The failure (design) point x^* is then defined, while in the next column, the value of the sensitivity factor is given. The magnitude of these factors reflects how dependent failure is to a particular variable - the larger the factor the greater the influence - while their sign reflects whether the variable is stabilising or destabilising as indicated by a +ve or -ve sign respectively. The 'partial factor' is the ratio of the design to the mean value of the variable. These are the central factors and are normally greater than unity for destabilising variables and less than unity for stabilising ones. However, as resistance partial factors are normally expressed as the reciprocal of the values as calculated by the reliability analysis, the value of the reciprocal is also given.

Values of the safety index and corresponding probabilities of failure are given at the bottom of the tables.

The identity of the models analysed is given on the table so that their details can be traced to the appropriate location in References 6 to 10.

3.10.1 Columns

Results for columns are presented in Tables 3.5 to 3.8, listed in order of increasing slenderness. The notation used is:

L : length	D : diameter
T : thickness	S_d: design stress
S_y: yield stress	E : elastic modulus

Apart from the results shown in Table 3.7, all the columns demonstrated a reasonable degree of consistency from the viewpoint of failure probability. Clearly, the very small COV on X_m for the model examined in Table 3.7 can be expected to affect this significantly and here an order of magnitude is demonstrated. The size of this COV will also affect the trend in other areas such as sensitivity and partial factors so will be ignored in generalising upon these in the following paragraphs.

In general the magnitude of the COV can be used as a guide as to which parameter will be most influential. This can be seen in the variation of the sensitivity factor X_m which dominates completely when its COV reached a maximum of 16.7% (Table 3.6).

Yield stress is seen to be important when slenderness is small (Table 3.5) but negligible when slenderness is high (Table 3.8): this of course is expected. Loading is quite influential across the complete range of slendernesses while the geometry variables of length and diameter become important when the slenderness is high (Table 3.8). This reflects the fact that elastic buckling rather than material limits are now dictating behaviour.

3.10.2 Beams

The reliability analysis results for beams are presented in Tables 3.9 to 3.12. The notation used is:

L	: length	D	: overall depth of section
B	: flange width	TW	: web thickness
TF	: flange thickness	MDGN	: design moment

For slenderness less than 75, the sensitivity to yield stress is significant while for slendernesses greater than 75 it is relatively insignificant (cf Tables 3.9 and 3.10). The sensitivity to geometry is generally small except for the higher slenderness range when the flange dimensions become important (Table 3.12) although this does coincide with the COV on X_m being very small. Interstingly enough, length also only appears influential when the COV on X_m is very small (cf Tables 3.11 and 3.12). Loading is influential across the entire slenderness range as is X_m except when its COV falls below that of the loading (cf Tables 3.11 and 3.12).

The range of reliabilities obtained is large, β varying from 1.45 to 6.67. This large variation is probably due to the disparity between the means and the COVs of X_m for each slenderness interval.

3.10.3 Stiffened Flanges

Reliability analysis results for flanges are presented in Tables 3.13 to 3.16.

The notation adopted is:

LX : overall flange length

T : plate thickness

DWX : longitudinal stiffener depth

DFX : longitudinal stiffener flange width

BX : transverse stiffener spacing

TWY : transverse stiffener web thickness

TFY : transverse stiffener flange thickness

YSS : stiffener yield stress

LY : overall width

BY : longitudinal stiffener spacing

TWX : longitudinal stiffener web thickness

TFX : longitudinal stiffener flange thickness

DWY : transverse stiffener depth

DFY : transverse stiffener flange width

YSP : plate yield stress

Although the results presented in Tables 3.13 to 3.16 are in terms of all the basic stiffened flange variables, some of these play little direct part in the strength calculation but they are necessary for other checks. For example, LX is the overall flange length, while BX is the transverse frame spacing. For flanges with no transverse frames, BX and the four subsequent variables are zero and LX is the 'length' variable. When transverse frames are present, BX becomes the length variable. The sensitivity factors and partial safety factor have to be judged accordingly.

It can be seen from the tables that because of the generally relatively high COV on X_m, this variable usually dominates the sensitivity factors. The corresponding partial factor, however, is not significant until the slenderness lies in the range of 60 to 70 and greater (cf Tables 3.14 and 3.15). The sensitivity to yield stress is seen generally to decrease with slenderness but note it equals zero for the non-governing failure mode. However, it is only in the highest slenderness range (Table 3.16) that the corresponding partial safety factor is of any significance. The sensitivity to loading and the corresponding partial safety factors are generally smaller than those of yield stress, except, again when the slenderness is high. However, loading is really the only other variable which is influential except for length and stiffener depth (DWX) in the highest slenderness range considered (Table 3.16) although, even here the corresponding partial safety factors are small.

The probability of failure for all models examined is reasonably consistent until the highest slenderness interval when a six orders of magnitude reduction is recorded. This is a direct result of the high strength demonstrated by models in this slenderness interval.

3.10.4 Webs

As indicated in Section 3.9.4, webs were treated in three separate groups. The reliability analyses performed on webs reflected this. Thus, one transversely stiffened model selected at random from each interval of 25 of the slenderness range covering the range of available data was examined together with one to represent pure bending and three to represent a spread of slenderness of the longitudinally stiffened beams. Results selected for presentation are given in

Tables 3.17 to 3.21 where:

L : length between supports

BW : panel length

TF : flange thickness

ETA1 : distance of 1st longitudinal web stiffener from compression edge of web

ETA12: distance of 2nd longitudinal web stiffener from compression edge of web

WDGN : design load

SYF : flange yield stress

SYW : web yield stress

TW : web thickness

DW : panel depth

BF : flange width

When no longitudinal web stiffener is present corresponding to ETA1 and ETA12, these variables are set to zero.

For this particular structural member it was found necessary to increase γ_m and γ_{fL} in order to avoid negative β values being obtained. A value of 1.5 was used in each case which had the effect of lowering the general level of failure probabilities obtained on top of the wide spread that was calculated: 3.7×10^{-3} to 2.1×10^{-20} (β = 2.7 to 9.2).

Tables 3.17 to 3.19 relate to transversely stiffened webs. Sensitivity is dominated by X_m followed by loading. Flange yield stress is relatively

important in relation to stocky members (Table 3.17) because of the importance of the flange in supporting the web diagonal tension field. Web thickness is also relatively influential in this range of geometries although its corresponding partial factor is always small. The role of web shear stress is seen to increase as web slenderness increases (cf Tables 3.17 and 3.19).

In Table 3.20, results pertaining to a pure moment load case with one longitudinal stiffener are presented. The sensitivity is seen to be dominated by the modelling parameter and web yield stress, followed by loading and panel depth.

The results for a longitudinally stiffened web are presented in Table 3.21. Again X_m dominates the sensitivity. The associated partial factor is also large. The influence of loading and web yield stress are similar although the partial factor associated with yield stress is the larger of the two. Flange yield stress is of little importance since tension field behaviour is not recognised by the Part 3 formulation.

3.11 $\gamma_m\gamma_{fL}$ Evaluation

For each component studied the value of the product of γ_m and γ_{fL} was determined for each load category. The value of $\gamma_m\gamma_{fL}$ was found such that

$$\sum_{i=1}^{N} \omega_i p_{fi} = p_{fT} \qquad (3.6)$$

In all cases the design equation can be rearranged such that γ_m and γ_{fL} occur as a product hence distinctions between them at this stage is of no

consequence. As a result once the condition of Equation 3.6 has been satisfied no further freedom exists to minimise the spread of reliabilities. Put another way once Equation 3.6 has been satisfied the spread of reliabilities is by necessity a minimum. γ_{fL} values corresponding to γ_m's of 1.2 and 1.3 were then calculated. Note that the values of γ_m given here are not the final values since the bias in yield stress still has to be taken into account. That is, any γ_m value derived from the analysis must be reduced by the factor 1.125.

The results are presented in Tables 3.22 to 3.25. First the target reliability (β_t) is indicated followed by the load type as defined in terms of its statistical parameters. The product $\gamma_m\gamma_{fL}$ is then given followed by the values of γ_{fL} corresponding to γ_m's of 1.2 and 1.3. The average target probability of failure achieved p_{fi} is indicated and then the corresponding spread of reliabilities β_{min} - β_{max}. Discussion will concentrate on the middle range of results as this corresponds to the selected target reliability. For the lower and higher reliability levels (β = 2.326 and 3.719), partial factors will be smaller and larger respectively.

From the tables, it can be seen that as the COV on load increases, so do the values of the partial factors whiie the corresponding spread of reliabilities decreases. It is also clear that as the general level of COV on X_m increases, a similar effect is produced on the partial factors. It may be recalled that the variability in X_m is smallest for columns and largest for stiffened flanges and webs. In all cases, the differences between the two environmental specifications is small so that, because it is slightly easier to handle the normal rather than the log-normal case, the former only will be considered in the final partial factor optimisation.

3.12 Optimised Partial Factors

Having derived the products $\gamma_m\gamma_{fL}$ which satisfy the constraint (Eqn. 3.6) the individual values of γ_m and γ_{fL} which give rise to the same products will necessarily ensure a minimum spread of reliabilities about the target. Hence a solution is required to the twelve simultaneous equations in γ_m and γ_{fL}. The four γ_m's are the material/component partial factor for columns γ_{mC}, beams γ_{mB}, stiffened flanges γ_{mF} and webs γ_{mW}. The three γ_{fL}'s are the load partial factors for dead plus hydrostatic load γ_{fLD}, 'live' load γ_{fLL} and environmental loads γ_{fLE}.

By taking logarithms, the twelve equations can be expressed in matrix form by Ax=B where x is the vector of logarithms of unknown load and component partial factors (seven in all, three load and four component factors), B is the vector of logarithms of γ_m γ_{fL} products and A is the matrix of (unit) coefficients representing the twelve γ_m γ_{fL} relationships.

Initial attempts to solve the relationship were only partially successful since the matrix A was singular. The largest non-singular submatrix of A was of order six indicating that another relationship between the seven unknown partial factors was required for a complete solution.

The additional relationship was obtained by requiring that the live load partial factor with its bias omitted and the column partial factor, after the yield stress bias had been removed, should be equal. This was decided on the basis that the COV's on live load and on the overal X_m of column data were approximately equal. (The COV on X_m of the complete set of column data is 10.5% compared with the live load value of 10%).

With this extra relationship the set of equations was solved by minimising $\sum_i |r_i|$ where r_i are the elements of R and R = Ax - B.

Minimising R for the target probability of failure of 2.5×10^{-3} (β=2.807) leads to the first set of values listed in the table below. If these are adjusted slightly to generate 'round' numbers, the second set of values are obtained.

Component/Load	Optimised Factors	Rounded Factors
Columns γ_{mC}	1.14	1.12
Beams γ_{mB}	1.29	1.25
Stiffened Flanges γ_{mF}	1.76	1.70
Stiffened Webs γ_{mW}	1.55	1.50
Dead Load γ_{fLD}	1.18	1.20
Live Load γ_{fLL}	1.32	1.35
Environmental Load γ_{fLE}	1.46	1.50

The penalty for adopting the rounded set of factors instead of the optimised ones is to increase the sum of the absolute values of the differences between the calculated and achieved values of the $\gamma_m\gamma_{fL}$ products from 0.146 to 0.235, while the maximum difference between the two is -3.2%: the penalty for rounding is small.

For comparison, the current Part 3 component partial factors are 1.05 for all 'stable' components plus columns and 1.20 for beams and stiffeners dictated by buckling considerations. These are a considerable simplification and modification of the factors originally derived[4] which were columns 0.98, beams 1.08, stiffened flanges 1.28 and webs 1.25 - the justification for the changes has not been published.

It is believed the main reason for the increase in the γ_m factors as derived here is that the modelling uncertainties calculated in the present study are somewhat larger than those used in the original partial factor derivation. For example, the stiffened compression flange model uncertainty factor used in Ref. 2 had a mean of 1.08 and a COV of 11% constant across the full range of slendernesses while, in the present work, the mean ranged from 0.813 to 1.19 with COV's up to 21%.

The effect of using these partial factors on the design of members is considered in the following section.

In deriving the above factors, it was not found possible through computer-time requirements to evaluate the reliability indices using the Level II procedure. Instead, for each model, a least squares procedure was used to evaluate the coefficients of a parabola representing the relationship between design load and β. Such relationships had previously been shown to be unique[57] so that once the design load was known, β could be rapidly evaluated.

3.13 Design Comparisons

Comparisons of designs using the evaluated partial safety factors with designs to both the DnV 1977[14] rules and API RP2A rules[17] were carried out to show the degrees on relative conservatism. Of course it must be borne in mind that the API rules are more appropriate to the experience in the Gulf of Mexico and the DnV rules to the North Sea. The comparisons were performed on the basis of deriving allowable characteristic or nominal stresses

since they are equivalent to the 'permissible working stresses' in API RP2A and comparing them across the practical range of slendernesses. This method of presentation effectively reflects the 'global' safety factors inherent in the designs. The results are presented in Figures 3.13 to 3.18 for columns, beams and stiffened flanges respectively. Webs were excluded because of significant differences which exist in strength modelling.

For the purpose of the study 'operating' and 'extreme' load combinations were defined as follows:

	Dead	Live	Environmental
Operating	O.333	O.333	O.333
Extreme	O.16	O.12	O.72

To find the total design load effects these figures were mutliplied by their corresponding partial load factors. Thus for the operating condition the total load factor is

$$1.20 \times 0.333 + 1.35 \times 0.333 + 1.50 \times 0.333 = 1.350$$

and for the extreme condition

$$1.20 \times 0.16 + 1.35 \times 0.12 + 1.50 \times 0.72 = 1.434$$

From the Code Format (Section 3.2)

$$S = R$$

when

$$\gamma_{f3}\ \gamma_{fL}\ Q_K = \frac{f_K}{\gamma_m}$$

$$\text{so}\quad Q_K = \frac{f_K}{\gamma_f\ \gamma_{f3}\ \gamma_m}$$

and the denominator is the global factor i.e. ratio of characteristic strength to nominal load.

The corresponding load factors for designs to DnV rules are:

operating 1.3 x 0.333 + 1.3 x 0.333 + 0.7 x 0.333 = 1.10

extreme 1.0 x 0.16 + 1.0 x 0.12 + 1.3 x 0.72 = 1.216

For API RP2A designs the operating and extreme global safety factors ignoring slenderness effects are 1.667 and 1.250 respectively.

The comparisons were carried out for two cases of γ_{f3} i.e. γ_{f3} = 1.1 and γ_{f3} excluded (= 1.0). The most common characteristic in the results, see Figures 3.13 to 3.18, is that BS5400: Pt 3 designs with partial factors evaluated in this study tend to be more conservative for small slendernesses though of similar conservatism at higher slendernesses when compared with designs to DnV and API rules. The exceptions are columns under operating conditions were the API rules are more conservative at small slendernesses and beams under operating conditions where the API rules are more conservative at large slendernesses. Designs using γ_{f3} = 1.1 gave rise to a significant amount of additional conservatism and lead to the conclusion that this value was perhaps too pessimistic.

The operational/extreme division highlighted additional differences between the API and BS5400:Pt 3 rules for stocky columns and stocky beams under extreme loading. The API rules were respectively 40% and 50% more conservative for these components.

The DnV designs were more in line with BS5400:Pt 3 designs for both columns and stiffened flanges. A second conclusion was that the failure probability for designs to API RP2A rules was in excess of 1×10^{-4} per annum.

Finally the differences between designs to BS54OO:Pt 3 with re-evaluated partial factors and those to DnV and API RP2A rules were attributed to the large COVs for model uncertainty for the Part 3 models.

3.14 Discussion

3.14.1 Target Reliability

In the re-evaluation study a target reliability level was set independently from previous successful designs. This is in contrast to the bridge code calibration study and was necessitated by the relatively short history of deeper marine structures. As such, the re-evaluation and others like it can be seen as a testing ground for some of the claims made for modern reliability analysis. It is natural, in this respect, to focus attention on the choices of target reliabilities for this study and the TLP study of ABS[18]. The discussion starts by highlighting the difficulty of associating target reliability for static strength with time and goes on to show that if failure probability were to be expressed as a function of time a reduction in partial factors would result.

If the model adopted for environmental load accounts, as reported, only for uncertainties in the hydrodynamic constants C_D and C_m used in Morrison's equation, then the probability determined in the study, p_f, is independent of the extreme wave used in the design. If L_n is the load effect of the n-year wave and R_n is the capacity of a component designed to resist the n-year wave then

$$p_f = P(M_n = R_n - L_n < 0)$$

L_n will be affected by the choice of n but R_n will be affected proportionately since the same global safety factor must be maintained. The probability as calculated will thus be the same whichever return period is chosen to define the design wave. In this sense there is no mathematical justification for the claim that the probability calculated is a probability 'per annum'. It is more accurately described as the failure probability assuming a design wave occurs.

M_n is a function of yield stress, model uncertainty, dimensions and design loads, none of which change with time. If a 100-year design wave is used, the probability of encountering one in the first year of service is the same as the probability of encounter in the 25th year of service and equal to 1/100. The probability of not encountering a 100-year wave in 25 years is $(1 - 1/100)^{25}$. The probability of encounter in 25 years is $1 - (1 - 1/100)^{25} = 0.222 = (4.5)^{-1}$.

The true probability of failure in the service life p_{fs}^{+} can then be

expressed as

$$p_{fs}^{+} = P(M_n < 0) \times \text{probability of encountering design wave in the service life}$$

which for the 100-year wave and a 25 year service life is

$$P(M_n < 0) \times 1/4.5$$

The true probability of failure in one year, p_{fa}^{+}, is

$$p_{fa}^{+} = P(M_n < 0) \times \text{probability of encountering design wave in 1 year}$$
$$= P(M_n < 0) \times 1/100$$

For the optimised partial factors $P(M_n < 0) = 2.5 \times 10^{-3}$. Thus the true annual failure probability p_{fa}^{+} is $2.5 \times 10^{-3} \times 1/100 = 2.5 \times 10^{-5}$. The optimised partial factors thus provide greater safety than the adopted target annual failure probability of 1×10^{-4}. A reduction in $\gamma_m \gamma_f$ of between 0.1 and 0.2 could be realised.

3.14.2 Loading Model

The single most influential factor on calculated 'failure probability' is the choice of bias and COV for environmental loading. The choice of the loading model in the re-evaluation study has similarities to, and was probably influenced by, a decision of a committee of the American Bureau of Shipping

(ABS) and Conoco who, in 1981, jointly initiated a project to develop reliability-based limit state design standards for the main structural components of tension leg platforms. The Rule Case Committee, RCC, as it was called, had the responsibility for developing a code format, loading and resistance models, reliability and calibration. The RCC acknowledged the complexity of the problem of environmental loading and identified the factors which affected the motions and fluid loadings on TLPs. These were

barometric pressure field
windfield
swell from distant storms
general oceanic circulation
astronomical tide

all of which have a direct or indirect effect on waves, currents and tides. Statistical properties of waves and currents can be obtained from 'scatter diagrams' and it is known that correlations and co-linearity exist between wind and waves as well as current and waves. Once the contributing factors have been used to describe the fluid field i.e. the water elevations at a particular site, there are three further steps, all of which introduce statistical uncertainties, before load effects can be determined.

These are:

calculation of wave kinematics (i.e. water particle velocites and accelerations)
computation of forces on the structure e.g. by Morrison's equation or diffraction theory
structural analysis to obtain axial forces, bending moments and shears i.e. the load effects.

The RCC concluded that such a comprehensive analysis was not practicable given the limitations on time at their disposal so they opted for what has since become known as the 'Interim Loading Model' - so called because, presumably, a better one will be forthcoming. In this the uncertanties in load effects arising from prediction of extreme wave heights, as characterised by significant wave height and zero-crossing period, together with uncertainties in wave kinematics and fluid-structure forces were treated by regarding them as dynamic forces with a COV of 26%. The effects of wind, current, tidal level, mean wave, drift, etc. were considered as quasi-static (vary slowly with time) and modelled with a COV of 20% and the static load effects arising from platform weight, buoyancy, static tendon tension were modelled with COV of 10%.

There is clearly scope for improving the Interim Loading Model especially as more accurate modelling of world climate becomes available. Any reduction in the COV of the (especially environmental) loading model would mean lower partial factors and more economic designs for the same target reliability.

3.14.3 General Discussion

The work was carried out and completed as proposed i.e. target reliabilities identified, load and resistance models adopted and partial factors evaluated to meet the requirements of minimum spread of reliabilities about the target. Unlike most engineering research projects there is no experiment one can devise to validate the results of the study. Naturally one could compare reliabilities as calculated by the Level II method with those calculated using 'exact' methods such as Monte Carlo simulation. Such a course of action is

redundant however, since the question of validation of the Level II method has been established by several authors, most notably Chang[58] and found to be within acceptable margins of error for a wide range of failure functions. The only option, as far as validation is concerned, is to compare designs with those from other codes for North Sea structures - as was done in the previous subsection with the DnV code. Even with this it is difficult to pin down differences in final designs to any single shortcoming of the code or the way in which it has been developed. For any code whose safety margins have been derived along reliability lines the final design safety margins are affected (in declining order of importance) by:

I choice of target reliability

II choice of load model

III choice of resistance model

IV choice of failure function

V component set

VI the number of partial factors

VII optimisation criteria

VIII reliability analysis method.

In this study the first three in this list have received attention. The differences in design acknowledged in Section 3.13 could be due to any number of the above effects.

It is clear that deliberation on the choice of target reliability, being the single most influential factor on partial safety factors, could be extended to cover factors other than the DnV and ABS codes. The most promising course

of investigation seems to be optimising the expected total cost of failure as outlined in Section 1. In order to facilitate such an investigation the results would be better presented as relationships between partial factors and mean failure probability.

3.15 Conclusions

1) When true partial factors are

$\gamma_{fLD} = 1.20$

$\gamma_{fLL} = 1.35$

$\gamma_{fLE} = 1.50$

$\gamma_{mC} = 1.12$

$\gamma_{mB} = 1.25$

$\gamma_{mF} = 1.70$

$\gamma_{mW} = 1.50$

the average probability that design load effect exceeds resistance is 2.5×10^{-3}. The range of safety indices for these factors is approximately from 2.04 to 16.4

2) The 'failure probability' calculated is unaffected by choice of design wave, neither does it relate to any time period.

3) If the true annual failure probability is defined as the probability that design load effect exceeds resistance times the probability that a design wave occurs in any year then lower partial factors than those reported would result for the same selected target.

4) The study should be extended to present reliability as a function of the partial factors. In this way other criteria, such as economics, could be considered before finalising a choice of target reliability.

3.16 References

1. 'Offshore Installations, Guidance on Design and Construction', Dept. of Energy, HMSO, July 1977.
2. BS5400: Steel, Concrete and Composite Bridges. British Standards Institution, London, 1982.
3. ISO 2394, 'General Principles for Verification of the Safety of Structures', International Organisation for Standardisation, Switzerland, 1973.
4. Flint & Neill Partnership - Imperial College, 'Derivation of Safety Factors for BS5400: Part 3', Final Report, August, 1980.
5. Kenny, J.P. & Partners Ltd., 'Buckling of Offshore Structures. Background Reports Nos I and IV', Job No. 1087, London, 1982/83.
6. Frieze, P.A., Das, P.K. and Plane, C., 'BS5400: Part 3. Partial Safety Factor Evaluation for Offshore Application. Columns - Interim Report', Department of Naval Architecture & Ocean Engineering, University of Glasgow, Report No. NAOE-83-72, December, 1983.
7. Frieze, P.A., Das, P.K. and Plane, C., 'BS5400: Part 3. Partial Safety Factor Evaluation for Offshore Application. Columns - Final Report', Department of Naval Architecture & Ocean Engineering, University of Glasgow, Report No. NAOE-84-04, February, 1984.
8. Frieze, P.A., Das, P.K. and Plane, C.A., 'BS5400: Part 3. Partial Safety Factor Evaluation for Offshore Application. Beams - Final Report', Department of Naval Architecture & Ocean Engineering, University of Glasgow, Report No. NAOE-84-43, August, 1984.
9. Frieze, P.A. and Plane, C.A., 'BS5400: Part 3. Partial Safety Factors for Offshore Application. Stiffened Flanges', Department of Naval Architecture & Ocean Engineering, University of Glasgow, Report No. NAOE-84-48, September, 1984.

10. Frieze, P.A. and Plane, C.A., 'BS5400: Part 3. Partial Safety Factor Evaluation for Offshore Application. Webs', Department of Naval Architecture & Ocean Engineering, University of Glasgow, Report No. NAOE-84-64, December, 1984.

11. Stiansen, S.G., 'Development of Reliability-Based Structural Criteria for Tension Leg Platforms', in Marine and Offshore Safety, ed. Frieze, McGregor and Winkle, Elsevier Science Publ., Amsterdam, 1984.

12. Furnes, O. and Kohler, P.E., 'Safety of Offshore Platforms - Classification Rules and Lessons Learned', in Marine and Offshore Safety, ed. Frieze, McGregor and Winkle, Elsevier Science Publ., Amsterdam, 1984.

13. Fjeld, S., 'Reliability of Offshore Structures', Jnl. Pet. Tech., 1978, October, pp1486-1496.

14. Det norske Veritas. 'Rules for the Design, Construction and Inspection of Offshore Structures', DnV, Oslo, 1977.

15. Frieze, P.A., 'Critical Assessment of the DnV Rules Limit State Safety Factor Format', Department of Naval Architecture & Ocean Engineering, University of Glasgow, Report No. NAOE-82-04, February, 1982.

16. Frieze, P.A., Cho, S-R and Faulkner, D., 'Strength of Ring-Stiffened Cylinders under Combined Loads', Offshore Technology Conference, Paper OTC 4714, 1984.

17. API RP2A. API Recommended Practice for Planning, Designing and Construction Fixed Offshore Platforms', American Petroleum Inst., Dallas, 1977.

18. Faulkner, D., Birrell, N.D. and Stiansen, S.G., 'Development of a Reliability Based Code for the Structure of Tension Leg Platforms', Offshore Technology Conference, Paper OTC4648, 1983.

19. Flint, et al. 'The Derivation of Safety Factors for Design of Highway Bridges', in The Design of Steel Bridges, ed. Rockey and Evans, Granada, London, 1981, pp11-36.

20. Yoshida, K. Submission to International Ship Structures Congress (ISCC) Committee v-2, 30 September, 1983.

21. Fukumoto, Y., 'Numerical Data Bank for the Ultimate Strength of Steel Structures', US-Japan Seminar on Inelastic Stability of Steel Structures and Elements, Tokyo, May, 1981.

22. Sfintesco, D., 'Fondement experimental des Courbes Europeennes de Flambement', Construction Metallique No. 3, September, 1970, pp5-12.

23. Bouma, A.L., et al., 'Probabilistic Reliability Analyses', proc. 2nd Int. Conf. BOSS, London, 1979.

24. Baker, M.J. and Wyatt, T.A., 'Methods of Reliability Analysis for Jacket Platforms', Proc. 2nd Int. Conf. BOSS, London, 1979.

25. Baker, M.J. and Ramachandran, K., 'Reliability Analysis as a Tool in the Design of Fixed Offshore Platforms', Integrity of Offshore Structures, ed. Faulkner, et al. Applied Sciences Publishers, London, 1981, pp135-153.

26. Baker, M.J., 'Variability on the Strength of Structural Steels - A Study in Structural Safety - Part 1: Material Variability', CIRIA Tech. Note 44, September, 1972.

27. API RP2A. API Recommended Practice for Planning, Designing and Construction Fixed Offshore Platforms', American Petroleum Inst., Dallas, 1981.

28. Rockey, K.C., Evans, H.R. and Porter, D.M., 'The Design of Stiffened Web Plates - A State-of-the-Art Report', in the Design of Steel Bridges, Granada, London, 1981.

29. Nethercot, D.A., 'Comparison of Proposed Beam Design Curves with Cost Data', Report BE/2/0129/1 to Dept. of Transport, September, 1979.

30. Fukuomoto, Y. and Kubo, M., 'An Experimental Review of Lateral Buckling of Beams and Girders', SSRC Colloquium in Stability of Structures under Static and Dynamic Loading, Washington, 1977.

31. Dibley, J.E., 'Lateral Torsional Buckling of I-Sections in Grade 55 Steel', Proc. Instn. Civ. Engrs., 43, August, 1969, pp599-627.

32. Hecktman, R.A., Hatrup, J.S., Styer, E.F., and Tredman, J.L., 'Lateral Buckling of Rolled Steel Beams', Trans. ASCE, 122, November 1957, pp823-843.

33. Singh, K.P., 'Ultimate Behaviour of Laterally Loaded Beams', PhD. Thesis, University of Manchester, 1969.

34. Linder, J., 'Development on Lateral Torsional Buckling', SSRC Colloquium on Stability of Structures under Static and Dynamic Loads, Washington, 1977.

35. Fukumoto, Y., Yoshito, I. and Kubo, M., 'Strength Variation of Laterally Unsupported Beams', J. Struct. Div. ASCE, 106, No. ST 1, January, 1980, pp165-181.

36. Kitipornchai, S. and Trahair, M.S., 'Inelastic Buckling of Simply Supported Steel I-Beams', J. Struct. Div. ASCE, 107, No. ST 7 , July, 1975.

37. Smith, C.S., 'Compressive Strength of Welded Steel Ship Grillages', Trans RINA, Vol. 117, pp325-359, 1975.

38. Kondo, J. and Ostapenko, A., 'Tests on Longitudinally Stiffened Plate Panels and Fixed Ends. Effect of Lateral Loading', Lehigh University, Fritz Engg Laboratory, Report No. 248.12, 1964.

39. Horne, M.R., et al., 'Ultimate Capacity of Axially Loaded Stiffened Plates Collapsing by Outstand Failure', University of Manchester, Simon Engg Laboratory, January, 1976.

40. Horne, M.R., et al., 'The Influence of Stiffener Spacing and Weld/Gap Ratio on the Ultimate Capacity of Axial Loaded Stiffened Plates', University of Manchester, Simon Engg Laboratory, February, 1976.

41. Horne, M.R. and Narayanan, R., 'The Influence of Rectification Procedures on the Strength of Welded Steel Stiffened Plates', University of Manchester, Simon Engg Laboratory, March, 1976.

42. Horne, M.R. and Narayanan, R., 'Influence on the Weld Size and Spacing on the Strength of Stiffened Panels', University of Manchester, Simon Engg Laboratory, December, 1974.

43. Murray, N.W., 'Buckling of Stiffend Panels Loaded Axially and in Bending', Structural Engineer, Vol. 51, 1973, pp285-301.

44. Fukomoto, Y., et al., 'Inelastic Buckling Strength of Stiffened Plates in Compression', IABSE Proceedings, 1977, pp8-77.

45. Walker, A.C. and Elsharkawai, K., 'Parametric Study on Stiffened Plate Panels in Compression', University College, London, Dept. of Civil Engg., 1978.

46. Faulkner, D., 'Compression Tests on Welded Eccentrically Stiffened Plate Panels', in Steel Plated Structures, ed. by P.J. Dowling, et al., Crosby Lockwood Staples, London, 1967, pp581-617.

47. Bell, A.O., et al., 'Beam and Column Strength of Stiffend Plates', Trans RINA, Vol. 105, 1963, pp435-466.

48. Horne, M.R. and Narayanan, R., 'Ultimate Capacity of Longitudinally Stiffend Plates used in Box Girders', Proc. Instn. Civ. Engrs., part 2, Vol. 61, June, 1976, p253.

49. Dorman, A.P. and Dwight, J.B., 'Tests on Stiffened Compression Plates and Plate Panels', in Steel Box Girder Bridges, Instn. Civl. Engrs, London, 1974, pp63-76.

50. Dowling, P.J. et al., 'Experimental and Predicted Collapse Behaviour of Rectangular Steel Box Girders', in Steel Box Girder Bridges, Instn. Civ. Engrs, London, 1973, pp77-94.

51. Massonnet, C. and Maquoi, R., 'New Theory and Tests on the Ultimate Strength of Stiffened Box Girders', in Steel Box Girder Bridges, Instn. Civ. Engrs, London, 1973, pp131-144.

52. Plane, C.A. and Frieze, P.A., 'BS5400: Part 3. Partial Safety Factor Evalauation for Offshore Application. Stiffened Flanges - Final Report', Department of Naval Architecture & Ocean Engineering, University of Glasgow, Report No. NAOE-85-37, January, 1985.

53. Rockey, K.C., Evans, H.R. and Porter, D.M., 'Ultimate Load Capacity of Stiffened Webs subjected to Shear and Bending', in Steel Box Girder Bridges, Instn. Civ. Engrs., London, 1973, pp45-61.

54. Owen, D.R.J. and Rockey, K.C., 'The Ultimate Load Behaviour of Longitudinally Reinforced Web Plates subjected to Pure Bending', IABSE, 1970, pp113-148.

55. Rockey, K.C. and Skaloud, 'The Ultimate Load Behaviour of Plate Girders Loaded in Shear', Structural Engineer, Vol. 50, 1972, pp29-47.

56. Ostapenko, A. and Chern, C., 'Strength of Longitudinally Stiffened Plate Girders under Combined Loads', Fritz Engineering Laboratory, Report No. 328.10, December, 1970.

57. Das, P.K., Frieze, P.A. and Faulkner, D., 'Structural Reliability Modelling of Stiffened Components of Floating Structures', Structural Safety, 2, 1984, pp3-16.

58. Chang, J.T.L, 'Investigation of the Wu Algorithm for Computing Structural Reliability', Engineering Experiment Station, College of Engineering, The University of Arizona, October 1985.

Table 3.1

Comparison of Measured and Assumed Yield Stress Bias and COV

Source and Steel Grade	COV(%)	Bias (%)	
		Strain Rate Uncorrected	Strain Rate Corrected
Measured:			
Ref. 28 - mild steel	4.8	10.6	4.3
- high strength	4.9	10.1	5.8
Ref. 3 - high strength	6.7	15.6	11.2
Assumed:			
BS5400 - mild steel	7.4	NA	10.2
- high strength	6.4	NA	9.9
BS5400 - re-evaluation	8.0	NA	12.5

Table 3.2

Comparison of Statistical Definitions of Load Effects

Load Type and Statistic	Refs			
	4(bridges)	13(DNV)	18(TLP)	Present
Bias(%)				
Dead	5 used	5 used	-	7.5
Live	-2 to 17(meas)	-30		15
	5 used	5 used	-	
Environmental	-	-50 to 10		0
		-10 used	-	
COV(%)				
Dead	5 used	7 to 11 (land based)	-	5
Live	8(meas)	7 to 80	10(dead and live)	10
Environmental	-	14 to 28(+refs 23,24) drag and inertia 10 to 35(+ref 24) wave	25-30	30
Distribution				
Dead	N	N	-	N
Live	-	-	-	N
Environmental	-	-	-	N

A dash indicates values not considered.

N - Normal.

meas - derived from measured data.

used - value used, other values were noted in that reference.

Table 3.3

Stiffened Flanges - Summary of X_m Results

Group No.	No. of Tests	Mean of X_m	COV of X_m	Author	Remarks
1	7	0.818	13.8	Smith[37]	
3	10	0.849	11.5	Horne, et al.[39]	
4	7	0.916	5.3	Horne, et al.[40]	
11	18	0.816	16.6	Faulkner[46]	
12	24	0.819	23.9	Faulkner[46]	
14	24	0.789	12.0	Horne & Narayanan[48]	
16	4	0.968	15.6	Dowling, et al.[49]	Box sections
17	3	1.200	15.9	Massonnet & Marquoi[51]	Box-type section

Table 3.4

Web Test Data Statistics

Group No.	Typical Model Designation	Construction and Loading	Slenderness Range	N/L	X_m		Author and Source Reference
					Mean	COV (%)	
1	1AS1.0	3C	145-158	13/2	1.34*	24.3	Rockey[53]
2†	SH1	1C	57-72	2/2	1.69	24.1	Rockey[53]
3†	LS1-T2	2C	50-126	5/5	1.39	17.0	Cooper[56]
4	3 test 1	1C	62-83	5/5	1.73	17.0	Rockey[53]
5	TG1-1	1M	11-13	8/8	0.675	7.41	Owen & Rockey[54]
6	Series I	0C	180-212	23/23	1.07	15.4	Rockey & Skaloud[55]
7	Series II	0C	120-248	12/12	1.19	6.85	Rockey & Skaloud[55]
8	Series III	0C	118-273	6/6	1.19	15.4	Rockey & Skaloud[55]
9	G1	0C	60-99	8/0	1.11*	9.53	Sakai, et al.[55]
10	G1	0C	61-78	4/0	0.48*	11.1	Nishino & Okumwa[55]
11	A1	0C	72-79	3/0	0.75*	29.4	Longbottom & Heyman[55]
12	H1T1	0C	184-187	4/0	0.67*	22.2	Cooper,Lew & Yen[55]

*Where girder length is unknown, it is assumed to be twice the panel length.

†Originally contained tests on webs with slenderness > 300.

Construction and Loading
0 - Transverse stiffeners only
1 - Transverse plus one longitudinal stiffener
2 - Transverse plus two longitudinal stiffeners
3 - Battle deck flange and transverse web stiffeners
C - Central point load and simple supports
M - Pure moment
N - Number of tests for which X_m mean and COV calculated
L - Number of tests for which length is known

Table 3.5

Web Modelling Factor

Category	Group	No. of Tests	X_m Mean	X_m COV
Transversely Stiffened:				
slenderness range				
100 - 125	all from	7	1.19	6.56
125 - 150	6, 7 & 8	1	1.01	-
150 - 175	"	1	1.40	-
175 - 200	"	11	1.06	14.6
200 - 225	"	14	1.11	16.8
225 - 250	"	6	1.17	8.33
250 - 275	"	1	1.01	-
Longitudinally Stiffened:	1, 3 & 4	12	1.55	18.9
Pure Moment	5	8	0.675	7.41

Table 3.6

Reliability Analysis of Column

Model No. 1

Basic Variables	Distribution Type	Mean	COV	Design Point	Sensitivity Factor	Partial Factor
L mm	Normal	145.4	2%	145.4	-0.0074	1.000
D mm	Normal	31.75	2%	31.74	+0.0074	1.000
T mm	Normal	1.32	2%	1.32	-0.0004	1.000
S_d N/mm^2	Normal	405.3	5%	421.2	-0.4350	1.039
S_y N/mm^2	Log-normal	500.0	8.0%	450.3	+0.7135	0.901(1.110)
E kN/mm^2	Log-normal	197.0	3.0%	196.9	0.0000	1.000
X_m	Log-normal	0.994	6.0%	0.936	+0.5464	0.942(1.062)

$\beta = 1.78$
$p_f = 3.75 \times 10^{-2}$

Ref: Appendix Table 1.10 Model No. 5

Table 3.7

Reliability Analysis of Column

Model No. 6

Basic Variables	Distribution Type	Mean	COV	Design Point	Sensitivity Factor	Partial Factor
L mm	Normal	1273.0	2%	1283.0	-0.197	1.008
D mm	Normal	31.75	2%	31.48	+0.212	0.992(1.009)
T mm	Normal	1.32	2%	1.32	-0.008	1.000
S_d N/mm^2	Normal	103.8	5%	106.27	-0.270	1.027
S_y N/mm^2	Log-normal	444.0	8%	493.7	+0.040	0.990(1.010)
E kN/mm^2	Log-normal	206.0	3%	205.9	0.0000	1.000
X_m	Log-normal	1.181	16.7%	0.859	+0.918	0.727(1.375)

$\beta = 2.000$

$p_f = 2.3 \times 10^{-2}$

Ref: Appendix Table 1.12 Model No. 10

Table 3.8

Reliability Analysis of Column

Model No. 7

Basic Variables	Distribution Type	Mean	COV	Design Point	Sensitivity Factor	Partial Factor
L mm	Normal	2133.6	2%	2195.5	-0.509	1.029
D mm	Normal	34.93	2%	33.79	+0.573	0.967(1.034)
T mm	Normal	1.30	2%	1.30	-0.020	1.001
S_d N/mm^2	Normal	46.8	5%	51.10	-0.639	1.091
S_y N/mm^2	Log-normal	324.3	8%	319.2	+0.056	0.984(1.016)
E kN/mm^2	Log-normal	198.0	3%	197.9	0.0000	1.000
X_m	Log-normal	1.004	0.3%	1.004	+0.041	1.000

$\beta = 2.85$
$p_f = 2.2 \times 10^{-3}$

Ref: Appendix Table 1.1 Model No. 42

Table 3.9

Reliability Analysis of Column

Model No. 9

Basic Variables	Distribution Type	Mean	COV	Design Point	Sensitivity Factor	Partial Factor
L mm	Normal	2438.4	2%	2470.4	-0.380	1.013
D mm	Normal	33.34	2%	32.86	+0.417	0.986(1.015)
T mm	Normal	1.63	2%	1.63	-0.019	1.001
S_d N/mm^2	Normal	32.57	5%	33.9	-0.484	1.042
S_y N/mm^2	Log-normal	338.4	8%	335.9	+0.030	0.993(1.007)
E kN/mm^2	Log-normal	196.0	3%	195.9	0.0000	1.000
X_m	Log-normal	0.973	6.6%	0.900	+0.668	0.925(1.082)

$\beta = 1.73$
$p_f = 4.2 \times 10^{-2}$

Ref: Appendix Table 1.1. Model No. 68

Table 3.10

Basic Variables and Statistical Assumptions in Analysis of Beams

Model No. 2. Slenderness Range 25-50 Slenderness = 30.95
Group 1 No. 3. (Simple method)

Basic Variables	Distribution Type	Mean	COV	Design Point	Sensitivity Factor	Partial Factor	1/Partial Factor
L mm	N	1100.0	2%	1100.0	0.000	1.000	
D mm	N	200.0	2%	199.2	0.169	0.996	(1.004)
B mm	N	100.0	2%	99.8	0.099	0.998	(1.002)
TW mm	N	5.50	2%	5.50	0.030	0.999	(1.001)
TF mm	N	8.00	2%	7.98	0.090	0.998	(1.002)
M_{dgn} KNm	N	42.61	5%	43.38	-0.316	1.018	
$_{y}$ Nmm^{-2}	LN	261.9	8%	249.1	0.515	0.951	(1.52)
X_m	LN	0.981	11.93%	0.878	0.766	0.895	(1.118)

$\beta = 1.45$

$p_f = 1.26 \times 10^{-1}$

Table 3.11

Basic Variables and Statistical Assumptions in Analysis of Beams

Model No. 4. Slenderness Range 75-100 Slenderness = 96.4
Group 2 No. 24. (Simple method)

Basic Variables	Distribution Type	Mean	COV	Design Point	Sensitivity Factor	Partial Factor	1/Partial Factor
L mm	N	6030.0	2%	6045.1	-0.074	1.002	
D mm	N	158.0	2%	157.8	0.035	0.999	(1.001)
B mm	N	153.0	2%	152.2	0.152	0.995	(1.005)
TW mm	N	6.60	2%	6.6	-0.003	1.000	
TF mm	N	9.30	2%	9.26	0.113	0.996	(1.004)
M_{dgn} KNm	N	38.72	5%	39.3	-0.181	1.015	
y Nmm^{-2}	LN	462.0	8%	457.2	0.053	0.990	(1.010)
X_m	LN	1.34	26.58%	0.843	0.960	0.631	(1.584)

$\beta = 1.70$
$p_f = 4.48 \times 10^{-1}$

Table 3.12

Basic Variables and Statistical Assumptions in Analysis of Beams

Model No. 7. Slenderness Range 150-175 Slenderness = 173.1
Group 13 No. 29. (Simple method)

Basic Variables	Distribution Type	Mean	COV	Design Point	Sensitivity Factor	Partial Factor	1/Partial Factor
L mm	N	15240	2%	15260	-0.042	1.001	
D mm	N	457	2%	456.8	+0.011	1.000	
B mm	N	191	2%	190.5	+0.081	0.997	(1.003)
TW mm	N	9.5	2%	9.50	+0.002	1.000	
TF mm	N	14.3	2%	14.27	+0.069	0.998	(1.002)
M_{dgn} KNm	N	60.04	5%	60.52	-0.099	1.008	
y Nmm^{-2}	LN	270.5	8%	269.3	+0.010	0.995	(1.005)
X_m	LN	2.051	52.8%	0.824	+0.988	0.402	(2.488)

$\beta = 1.60$
$p_f = 5.37 \times 10^{-2}$

Table 3.13

Basic Variables and Statistical Assumptions in Analysis of Beams

Model No. 8. Slenderness Range 200-225 Slenderness = 208.2
Group 11 No. 4. (Simple method)

Basic Variables	Distribution Type	Mean	COV	Design Point	Sensitivity Factor	Partial Factor	1/Partial Factor
L mm	N	6080	2%	6295	-0.266	1.035	
D mm	N	203	2%	201.42	+0.058	0.992	(1.008)
B mm	N	58.0	2%	53.44	+0.589	0.921	(1.085)
TW mm	N	3.4	2%	3.40	-0.004	1.001	
TF mm	N	5.8	2%	5.42	+0.489	0.935	(1.070)
M_{dgn} KNm	N	2.98	5%	3.52	-0.543	1.181	
$_{y}$ Nmm^{-2}	LN	372.6	8%	361.89	+0.049	0.971	(1.030)
X_m	LN	1.37	1.59%	1.340	+0.204	0.978	(1.022)

$\beta = 6.67$

$p_f = 1.3 \times 10^{-11}$

Table 3.14

Reliability Analysis Results
Stiffened Flanges

Group 1 No. 2 Slenderness = 29.818

Parameter	Mean	COV	Design Point	Sensitivity Factor	Partial Factor	1/Partial Factor
LX (mm)	6100.000	2.000	6100.000	0.000	1.000	1.000
LY (mm)	3202.000	2.000	3202.000	0.000	1.000	1.000
T (mm)	7.370	2.000	7.369	0.011	1.000	1.000
BY (mm)	305.000	2.000	305.020	-0.007	1.000	1.000
DWX (mm)	104.700	2.000	104.700	0.000	1.000	1.000
TWX (mm)	5.380	2.000	5.380	-0.001	1.000	1.000
DFX (mm)	44.700	2.000	44.700	-0.001	1.000	1.000
TFX (mm)	9.530	2.000	9.530	-0.001	1.000	1.000
BX (mm)	1524.00	2.000	1524.016	-0.001	1.000	1.000
DWY (mm)	287.700	2.000	187.700	0.000	1.000	1.000
TWY (mm)	8.330	2.000	8.330	0.000	1.000	1.000
DFY (mm)	102.600	2.000	102.600	0.000	1.000	1.000
TFY (mm)	16.300	2.000	16.300	0.000	1.000	1.000
SDGN (N/mm^2)	198.891	5.000	200.183	-0.297	1.006	0.994
YSP (N/mm^2)	264.000	8.000	258.998	0.456	0.981	1.019
YSS (N/mm^2)	279.500	8.000	278.610	0.000	0.997	1.003
X_m	0.846	14.130	0.795	0.839	0.940	1.064

BETA = 0.438

p_f = 0.33068E+00

Table 3.15

Reliability Analysis Results
Stiffened Flanges

Group 3 No. 3 Slenderness = 59.130

Parameter	Mean	COV	Design Point	Sensitivity Factor	Partial Factor	1/Partial Factor
LX (mm)	3000.000	2.000	3000.000	0.000	1.000	1.000
LY (mm)	700.000	2.000	700.000	0.000	1.000	1.000
T (mm)	10.000	2.000	10.000	0.000	1.000	1.000
BY (mm)	140.000	2.000	140.000	0.000	1.000	1.000
DWX (mm)	148.500	2.000	148.500	0.000	1.000	1.000
TWX (mm)	9.850	2.000	9.850	0.000	1.000	1.000
DFX (mm)	0.000	0.000	0.000	0.000	0.000	0.000
TFX (mm)	0.000	0.000	0.000	0.000	0.000	0.000
BX (mm)	0.000	0.000	0.000	0.000	0.000	0.000
DWY (mm)	0.000	0.000	0.000	0.000	0.000	0.000
TWY (mm)	0.000	0.000	0.000	0.000	0.000	0.000
DFY (mm)	0.000	0.000	0.000	0.000	0.000	0.000
TFY (mm)	0.000	0.000	0.000	0.000	0.000	0.000
SDGN (N/mm^2)	254.136	5.000	255.061	-0.216	1.004	0.996
YSP (N/mm^2)	346.500	8.000	342.192	0.347	0.998	1.013
YSS (N/mm^2)	420.100	8.000	418.762	0.000	0.997	1.003
X_m	0.813	21.275	0.745	0.913	0.917	1.091

BETA = 0.337

p_f = 0.36816E+00

Table 3.16

Reliability Analysis Results
Stiffened Flanges

Group 14 No. 23 Slenderness = 74.565

Parameter	Mean	COV	Design Point	Sensitivity Factor	Partial Factor	1/Partial Factor
LX (mm)	1830.000	2.000	1832.814	-0.070	1.002	0.998
LY (mm)	1523.000	2.000	1523.000	0.000	1.000	1.000
T (mm)	6.500	2.000	6.497	0.018	1.000	1.000
BY (mm)	457.000	2.000	457.182	-0.018	1.000	1.000
DWX (mm)	76.000	2.000	75.889	0.066	0.999	1.001
TWX (mm)	12.500	2.000	12.500	0.002	1.000	1.000
DFX (mm)	0.000	0.000	0.000	0.000	0.000	0.000
TFX (mm)	0.000	0.000	0.000	0.000	0.000	0.000
BX (mm)	0.000	0.000	0.000	0.000	0.000	0.000
DWY (mm)	0.000	0.000	0.000	0.000	0.000	0.000
TWY (mm)	0.000	0.000	0.000	0.000	0.000	0.000
DFY (mm)	0.000	0.000	0.000	0.000	0.000	0.000
TFY (mm)	0.000	0.000	0.000	0.000	0.000	0.000
SDGN (N/mm^2)	147.389	5.000	149.201	-0.223	1.012	0.988
YSP (N/mm^2)	342.200	8.000	335.504	0.188	0.980	1.020
YSS (N/mm^2)	389.600	8.000	388.359	0.000	0.997	1.003
X_m	0.813	21.275	0.638	0.951	0.785	1.274

BETA = 1.101
p_f = 0.13540E+00

Table 3.17

Reliability Analysis Results
Stiffened Flanges

Group 16 No. 4 Slenderness = 107.697

Parameter	Mean	COV	Design Point	Sensitivity Factor	Partial Factor	1/Partial Factor
LX (mm)	3962.400	2.000	3962.400	0.000	1.000	1.000
LY (mm)	1219.000	2.000	1219.000	0.000	1.000	1.000
T (mm)	4.720	2.000	4.759	-0.084	1.008	0.992
BY (mm)	122.000	2.000	123.585	-0.131	1.013	0.987
DWX (mm)	38.000	2.000	35.731	0.600	0.940	1.064
TWX (mm)	6.370	2.000	6.285	0.134	0.987	1.013
DFX (mm)	0.000	0.000	0.000	0.000	0.000	0.000
TFX (mm)	0.000	0.000	0.000	0.000	0.000	0.000
BX (mm)	1320.000	2.000	1378.605	-0.446	1.044	0.957
DWY (mm)	76.200	2.000	76.200	0.000	1.000	1.000
TWY (mm)	6.350	2.000	6.350	0.000	1.000	1.000
DFY (mm)	0.000	0.000	0.000	0.000	0.000	0.000
TFY (mm)	0.000	0.000	0.000	0.000	0.000	0.000
SDGN (N/mm^2)	109.036	5.000	124.706	-0.578	1.144	0.874
YSP (N/mm^2)	276.000	8.000	275.121	0.000	0.997	1.003
YSS (N/mm^2)	311.900	8.000	289.490	0.180	0.928	1.077
X_m	1.191	1.377	1.176	0.182	0.988	1.013

BETA = 4.976

Table 3.18

Reliability Analysis Results
Stiffened Webs

Group 7 No. 30 Slenderness = 120.6

Parameter	Mean	COV	Design Point	Sensitivity Factor	Partial Factor	1/Partial Factor
L (mm)	1245.000	2.000	1271.939	-0.118	1.022	0.979
TW (mm)	2.030	2.000	1.942	0.236	0.957	1.045
BW (mm)	305.000	2.000	308.348	-0.060	1.011	0.989
DW (mm)	305.000	2.000	299.213	0.103	0.981	1.019
TF (mm)	3.250	2.000	3.215	0.059	0.989	1.011
BF (mm)	76.200	2.000	75.385	0.058	0.989	1.011
ETA1 (mm)	0.000	0.000	0.000	0.000	0.000	0.000
ETA12 (mm)	0.000	0.000	0.000	0.000	0.000	0.000
WDGN (kn)	47.687	5.000	58.240	-0.482	1.221	0.819
SYW (N/mm^2)	229.000	8.000	201.265	0.172	0.879	1.138
SYF (N/mm^2)	305.000	8.000	256.827	0.230	0.842	1.188
X_m	1.190	6.560	0.746	0.771	0.627	1.594

BETA = 9.185
p_f = 0.20619E-19

Table 3.19

Reliability Analysis Results
Stiffened Webs

Group 6 No. 1 Slenderness = 189.3

Parameter	Mean	COV	Design Point	Sensitivity Factor	Partial Factor	1/Partial Factor
L (mm)	1295.000	2.000	1298.378	-0.027	1.003	0.997
TW (mm)	2.720	2.000	2.683	0.143	0.986	1.014
BW (mm)	610.000	2.000	613.712	-0.064	1.006	0.994
DW (mm)	610.000	2.000	602.841	0.123	0.988	1.012
TF (mm)	4.700	2.000	4.691	0.020	0.998	1.002
BF (mm)	102.000	2.000	101.819	0.019	0.998	1.002
ETA1 (mm)	0.000	0.000	0.000	0.000	0.000	0.000
ETA12 (mm)	0.000	0.000	0.000	0.000	0.000	0.000
WDGN (kn)	108.624	5.000	116.055	-0.288	1.068	0.936
SYW (N/mm^2)	253.000	8.000	228.129	0.264	0.902	1.109
SYF (N/mm^2)	253.000	8.000	245.184	0.074	0.969	1.032
X_m	1.056	14.628	0.563	0.895	0.633	1.877

BETA = 4.754

p_f = 0.99686E-06

Table 3.20

Reliability Analysis Results
Stiffened Webs

Group 7 No. 24 Slenderness = 248.6

Parameter	Mean	COV	Design Point	Sensitivity Factor	Partial Factor	1/Partial Factor
L (mm)	1245.000	2.000	1251.328	-0.032	1.005	0.995
TW (mm)	0.965	2.000	0.934	0.199	0.968	1.033
BW (mm)	305.000	2.000	309.355	-0.090	1.014	0.986
DW (mm)	305.000	2.000	295.704	0.192	0.970	1.031
TF (mm)	3.120	2.000	3.074	0.092	0.985	1.015
BF (mm)	76.200	2.000	75.832	0.030	0.995	1.005
ETA1 (mm)	0.000	0.000	0.000	0.000	0.000	0.000
ETA12 (mm)	0.000	0.000	0.000	0.000	0.000	0.000
WDGN (kn)	18.073	5.000	20.892	-0.392	1.056	0.865
SYW (N/mm^2)	219.000	8.000	169.568	0.397	0.774	1.292
SYF (N/mm^2)	305.000	8.000	274.419	0.161	0.900	1.111
X_m	1.173	8.325	0.710	0.753	0.606	1.652

BETA = 7.958
p_f = 0.87697E-15

Table 3.21

Reliability Analysis Results
Stiffened Webs

Group 5 No. 1 Slenderness = 13.6

Parameter	Mean	COV	Design Point	Sensitivity Factor	Partial Factor	1/Partial Factor
L (mm)	0.000	0.000	0.000	0.000	0.000	0.000
TW (mm)	14.402	2.000	14.334	0.087	0.995	1.005
BW (mm)	1270.000	2.000	1270.000	0.000	1.000	1.000
DW (mm)	1270.000	2.000	1252.641	0.250	0.986	1.014
TF (mm)	12.700	2.000	12.646	0.077	0.996	1.004
BF (mm)	203.200	2.000	202.360	0.076	0.996	1.004
ETA1 (mm)	254.000	2.000	253.890	0.008	1.000	1.000
ETA12 (mm)	0.000	0.000	0.000	0.000	0.000	0.000
WDGN (kn)	764.274	5.000	804.343	-0.383	1.052	0.950
SYW (N/mm^2)	211.528	8.000	183.163	0.644	0.866	1.155
SYF (N/mm^2)	242.408	8.000	241.636	0.000	0.997	1.003
X_m	0.675	7.410	0.597	0.597	0.884	1.132

BETA = 2.736
p_f = 0.31096E-02

Table 3.22

Reliability Analysis Results
Stiffened Webs

Group 3 No. 7 Slenderness = 126.4

Parameter	Mean	COV	Design Point	Sensitivity Factor	Partial Factor	1/Partial Factor
L (mm)	3810.000	2.000	3817.126	-0.016	1.002	0.998
TW (mm)	4.880	2.000	4.792	0.159	0.982	1.018
BW (mm)	1270.000	2.000	1274.227	-0.029	1.003	0.997
DW (mm)	1270.000	2.000	1257.863	0.084	0.990	1.010
TF (mm)	38.400	2.000	38.334	0.015	0.998	1.002
BF (mm)	359.000	2.000	358.414	0.014	0.998	1.002
ETA1 (mm)	635.000	2.000	636.234	-0.017	1.002	0.998
ETA12 (mm)	0.000	0.000	0.000	0.000	0.000	0.000
WDGN (kn)	497.932	5.000	530.606	-0.231	1.066	0.938
SYW (N/mm^2)	335.000	8.000	298.173	0.250	0.890	1.124
SYF (N/mm^2)	210.000	8.000	209.331	0.000	0.997	1.003
X_m	1.550	18.900	0.571	0.922	0.368	2.716

BETA = 5.683
p_f = 0.66097E-08

Table 3.23

Column Optimised Partial Factors

β_t	Load COV	Load Bias	Dist Type	$\gamma_m \gamma_f$	γ_f ($\gamma_m = 1.2$)	γ_f ($\gamma_m = 1.3$)	$\bar{p}_{fi}$	β_{min} - β_{max}
2.326	5	1.075	N	1.38	1.15	1.06	1.0×10^{-2}	2.04 - 3.54
	10	1.15	N	1.57	1.31	1.21	1.0×10^{-2}	2.14 - 2.99
	25	1.0	LN	1.77	1.48	1.36	1.0×10^{-2}	2.20 - 2.51
	30	1.0	N	1.78	1.48	1.37	1.0×10^{-2}	2.19 - 2.50
2.807	5	1.075	N	1.47	1.23	1.13	2.5×10^{-3}	2.44 - 4.41
	10	1.15	N	1.68	1.40	1.29	2.5×10^{-3}	2.51 - 3.71
	25	1.0	LN	2.02	1.68	1.55	2.5×10^{-3}	2.69 - 2.94
	30	1.0	N	1.97	1.64	1.52	2.5×10^{-3}	2.69 - 3.07
3.719	5	1.075	N	1.69	1.41	1.30	1.0×10^{-4}	3.23 - 6.34
	10	1.15	N	1.94	1.62	1.49	1.0×10^{-4}	3.29 - 5.26
	25	1.0	LN	2.58	2.15	1.98	1.0×10^{-4}	3.64 - 3.90
	30	1.0	N	2.37	1.98	1.82	1.0×10^{-4}	3.49 - 4.24

Table 3.24

Beam Optimised Partial Factors

(Simple Method)

β_t	Load COV	Load Bias	Dist Type	$\gamma_m\gamma_f$	γ_f $\gamma_m = 1.2$	γ_f $\gamma_m = 1.3$	$-p_{fi}$	β max-	β_{min}
2.326	5	1.075	N	1.5490	1.29	1.19	1.0×10^{-2}	8.70	1.91
	10	1.15	N	1.7243	1.44	1.33	1.0×10^{-2}	7.04	1.96
	25	1.0	LN	1.8426	1.54	1.42	1.0×10^{-2}	3.76	2.13
	30	1.0	N	1.8782	1.57	1.44	1.0×10^{-2}	4.68	2.13
2.807	5	1.075	N	1.7050	1.42	1.31	2.5×10^{-3}	9.93	2.10
	10	1.15	N	1.9106	1.59	1.47	2.5×10^{-3}	8.16	2.16
	25	1.0	LN	2.1401	1.78	1.65	2.5×10^{-3}	4.35	2.48
	30	1.0	N	2.1370	1.78	1.64	2.5×10^{-3}	5.60	2.40
3.719	5	1.075	N	2.2690	1.89	1.75	1.0×10^{-4}	13.56	2.67
	10	1.15	N	2.5094	2.09	1.93	1.0×10^{-4}	11.20	2.69
	25	1.0	LN	2.8820	2.40	2.22	1.0×10^{-4}	5.53	3.02
	30	1.0	N	2.8000	2.33	2.15	1.0×10^{-4}	7.72	2.89

Table 3.25

Optimised Partial Factors for Stiffened Flanges

β_t	Load COV	Load Bias	Dist Type	$\gamma_m \gamma_f$	γ_f ($\gamma_m = 1.2$)	γ_f ($\gamma_m = 1.3$)	$\bar{p}_{fi}$	β_{min} - β_{max}
2.326	5	1.075	N	1.8733	1.56	1.44	1.0×10^{-2}	1.58 - 12.2
	10	1.15	N	2.0828	1.74	1.60	1.0×10^{-2}	1.63 - 9.72
	25	1.0	LN	2.2198	1.85	1.71	1.0×10^{-2}	1.88 - 4.55
	30	1.0	N	2.2618	1.88	1.74	1.0×10^{-2}	1.82 - 6.20
2.807	5	1.075	N	2.3831	1.73	1.59	2.5×10^{-3}	2.04 - 13.6
	10	1.15	N	2.6444	1.92	1.78	2.5×10^{-3}	2.10 - 11.0
	25	1.0	LN	2.5752	2.15	1.98	2.5×10^{-3}	2.35 - 5.14
	30	1.0	N	2.8762	2.14	1.98	2.5×10^{-3}	2.27 - 7.27
3.719	5	1.075	N	2.5157	2.10	1.94	1.0×10^{-4}	2.99 - 16.4
	10	1.15	N	2.8349	2.36	2.18	1.0×10^{-4}	3.02 - 13.5
	25	1.0	LN	3.4442	2.87	2.65	1.0×10^{-4}	3.24 - 6.26
	30	1.0	N	3.2813	2.73	2.52	1.0×10^{-4}	3.14 - 9.45

Table 3.26

Web Optimised Partial Factors

β_t	Load COV	Load Bias	Dist Type	$\gamma_m\gamma_f$	γ_f / γ_m = 1.2	γ_f / γ_m = 1.3	$\bar{p}_{fi}$	β_{min} - β_{max}
2.326	5	1.075	N	1.7801	1.483	1.369	.0100	1.45 - 8.68
	10	1.15	N	1.8306	1.526	1.408	.0100	1.46 - 7.18
	25	1.0	LN	-	-	-	-	- - -
	30	1.0	N	2.1966	1.831	1.690	.0100	1.48 - 4.72
2.807	5	1.075	N	1.9157	1.596	1.474	.00250	2.09 - 9.58
	10	1.15	N	1.9990	1.666	1.538	.00250	2.09 - 8.06
	25	1.0	LN	-	-	-	-	- - -
	30	1.0	N	2.5345	2.112	1.950	.00250	2.10 - 5.65
3.719	5	1.075	N	2.1800	1.817	1.677	.00010	3.18 - 10.3
	10	1.15	N	2.3400	1.950	1.800	.00010	3.18 - 9.15
	25	1.0	LN	-	-	-	-	- - -
	30	1.0	N	3.3091	2.758	2.545	.00010	3.19 - 7.71

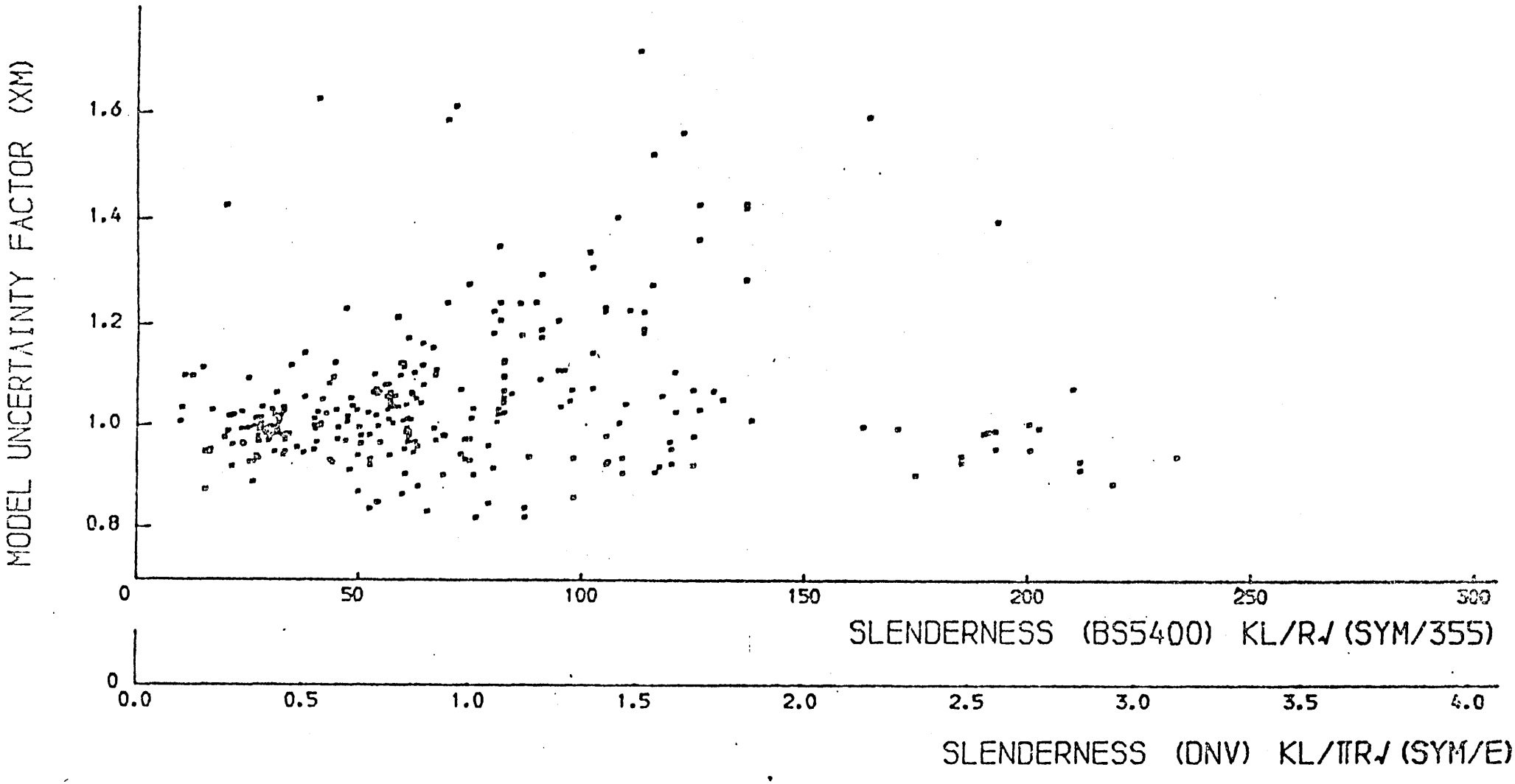

Fig. 3.1 MODEL UNCERTAINTY FACTOR VS SLENDERNESS PARAMETER (BS5400)

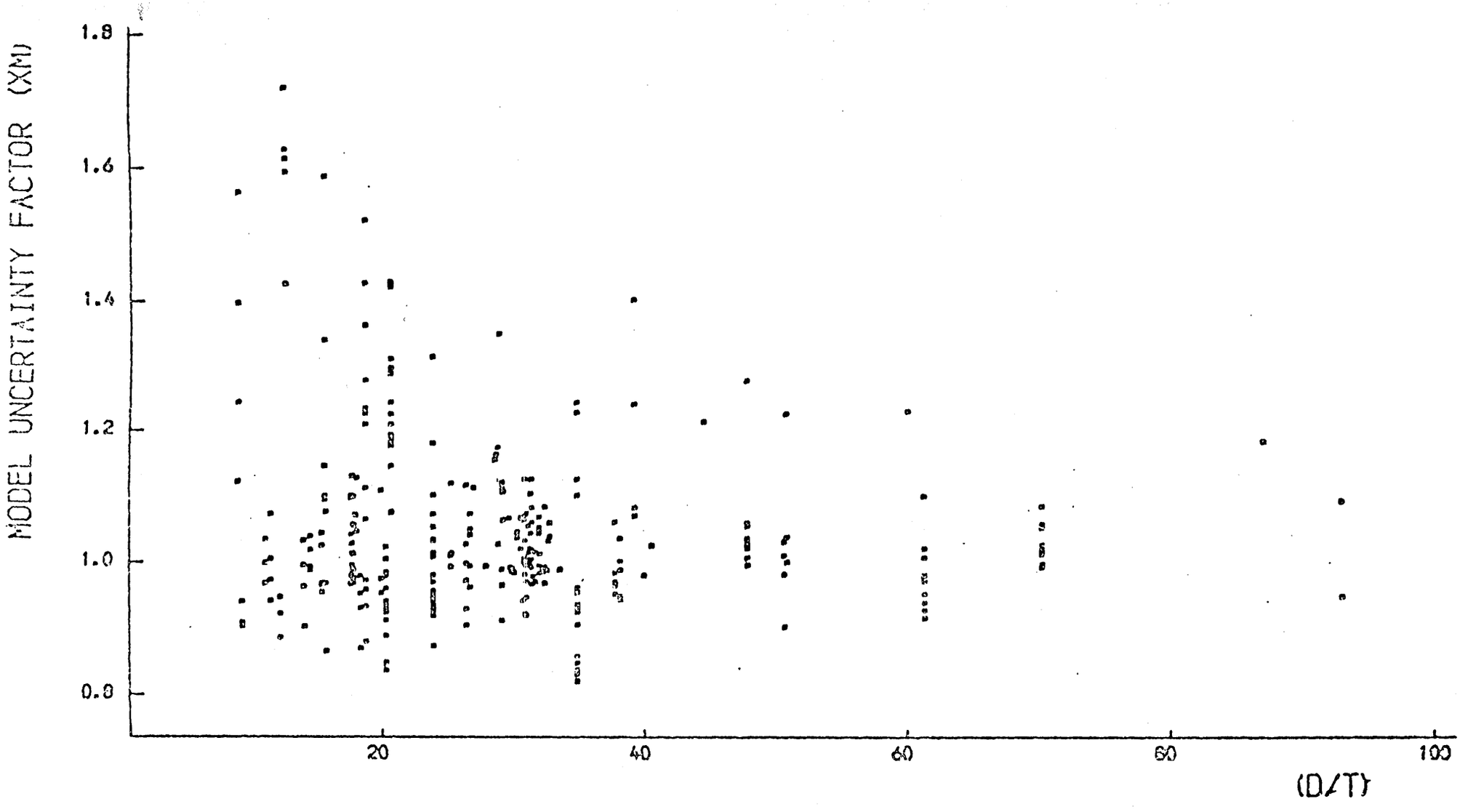

Fig. 3.2 MODEL UNCERTAINTY FACTOR VS D/T RATIO (BS5400)

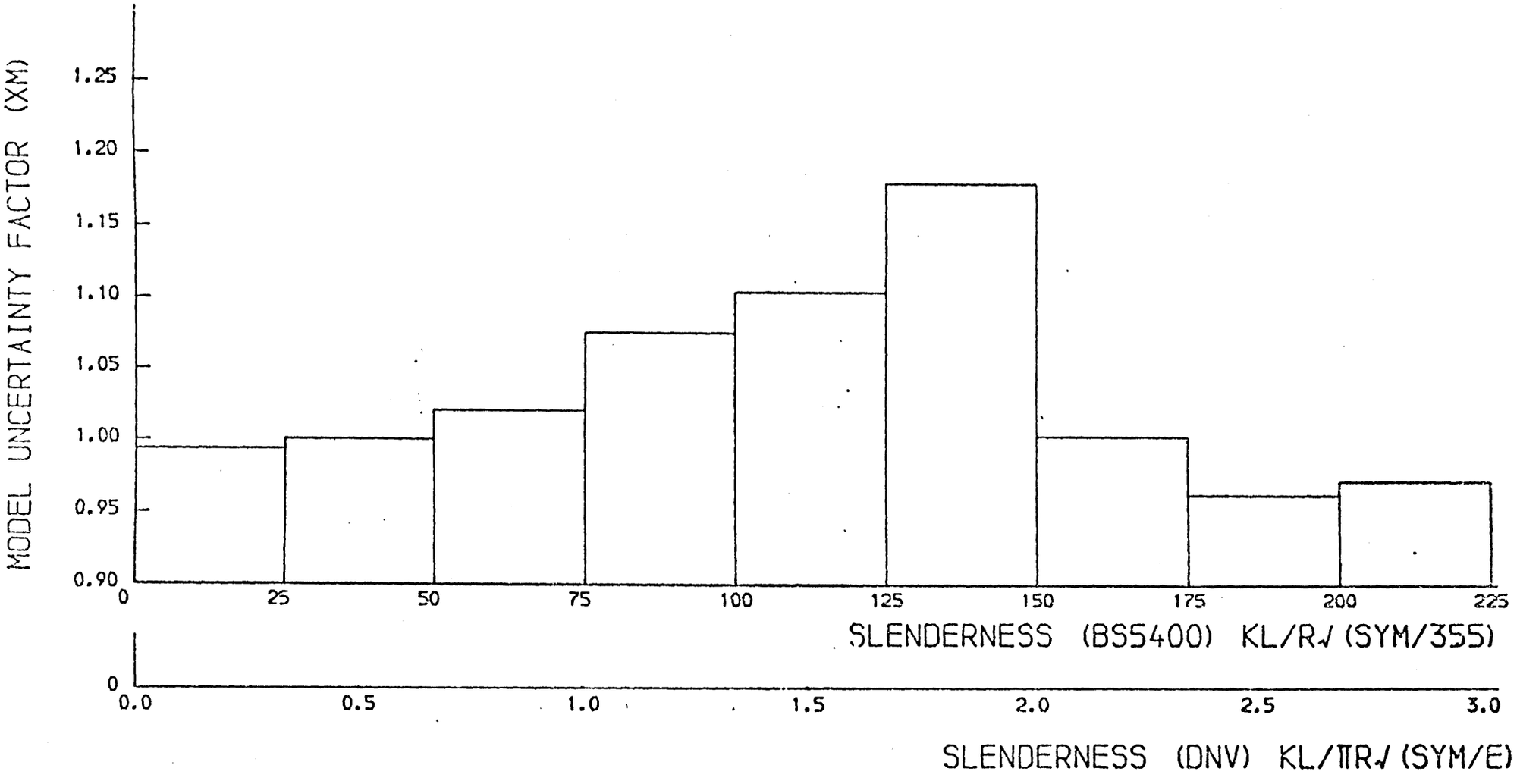

Fig. 3.3 MEAN MODEL UNCERTAINTY FACTOR VS SLENDERNESS PARAMETER (BS5400)

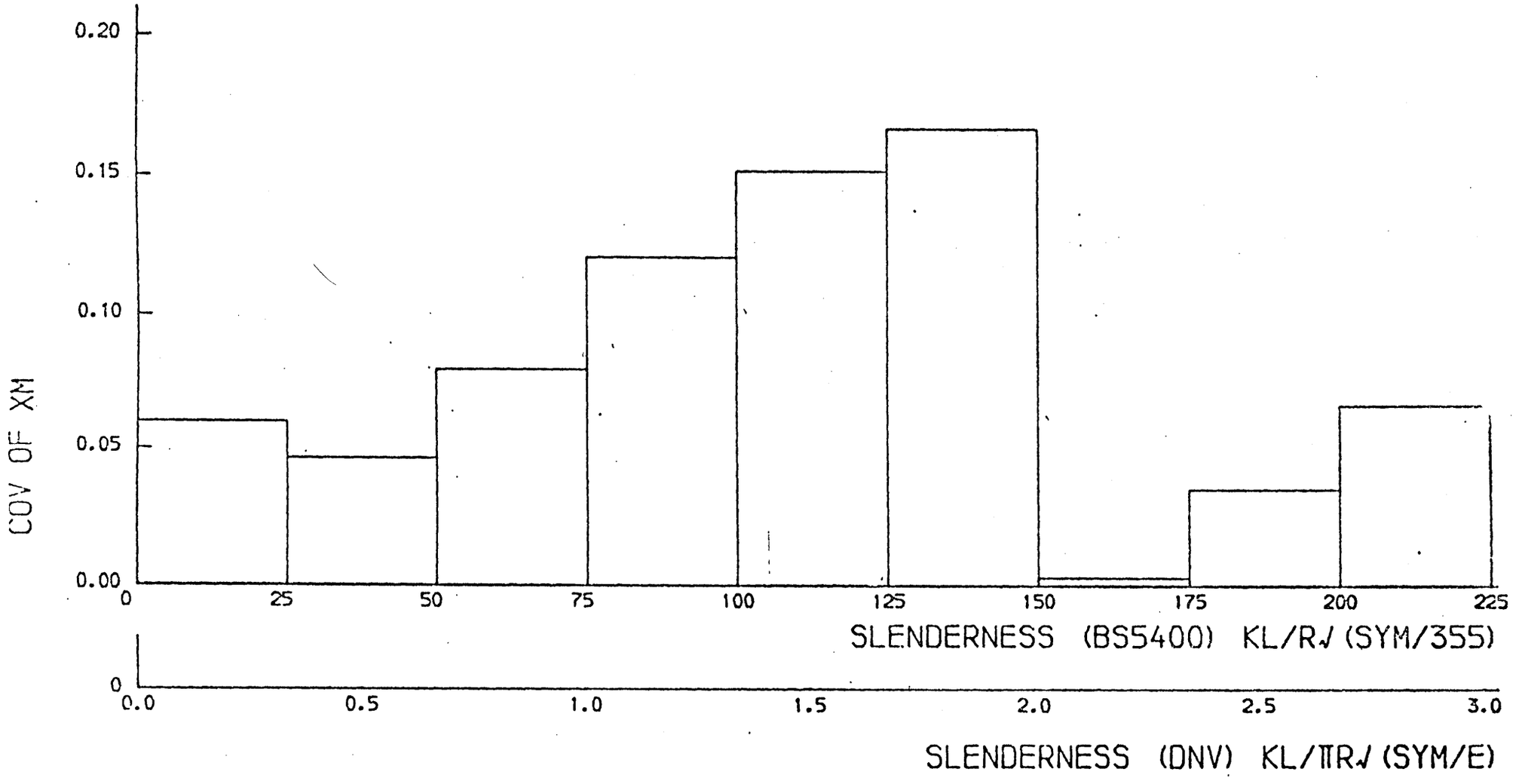

Fig. 3.4 COV OF MODEL UNCERTAINTY FACTOR VS SLENDERNESS PARAMETER (BS5400)

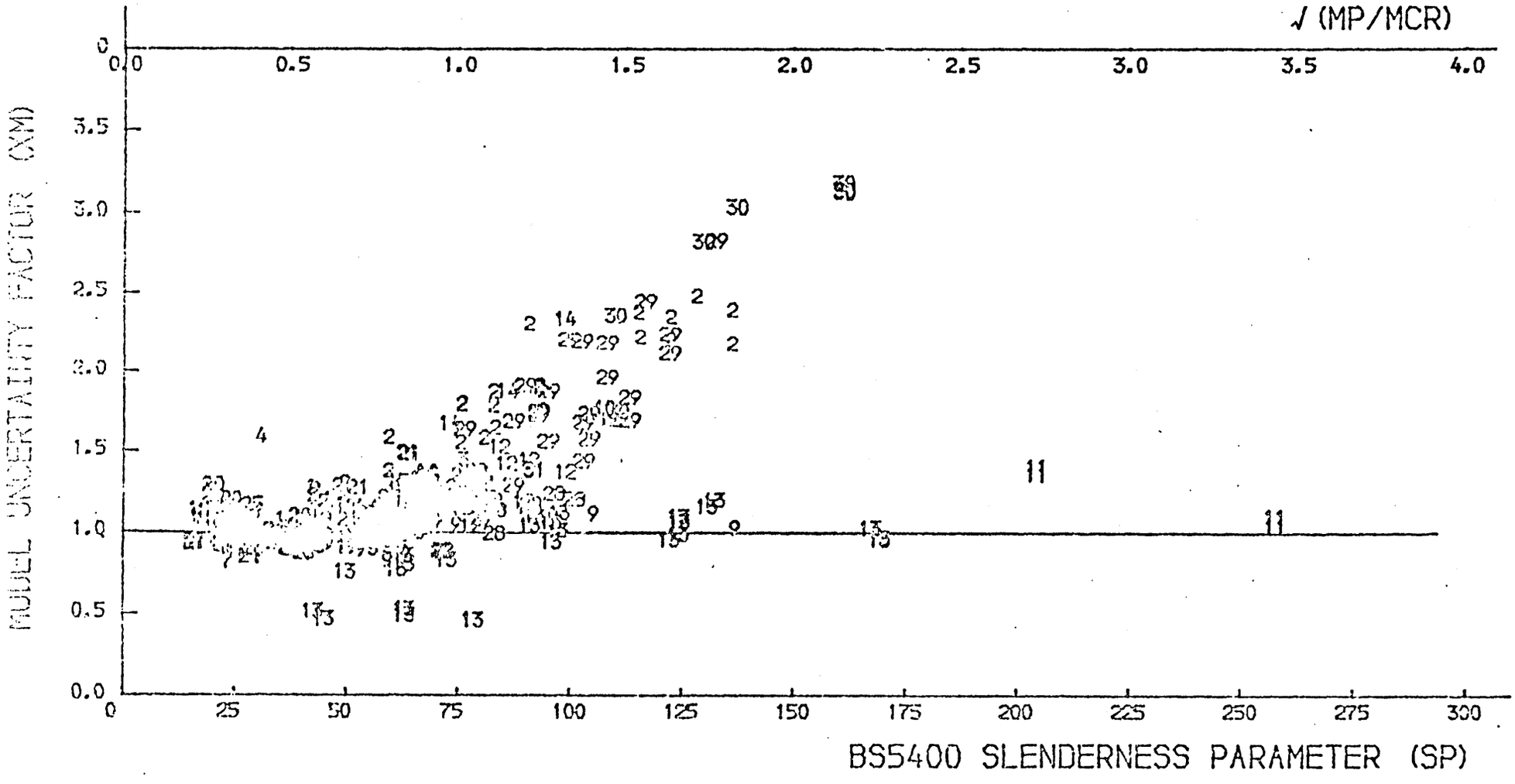

Fig. 3.5 MODEL UNCERTAINTY FACTOR (XM) VS SLENDERNESS PARAMETERS

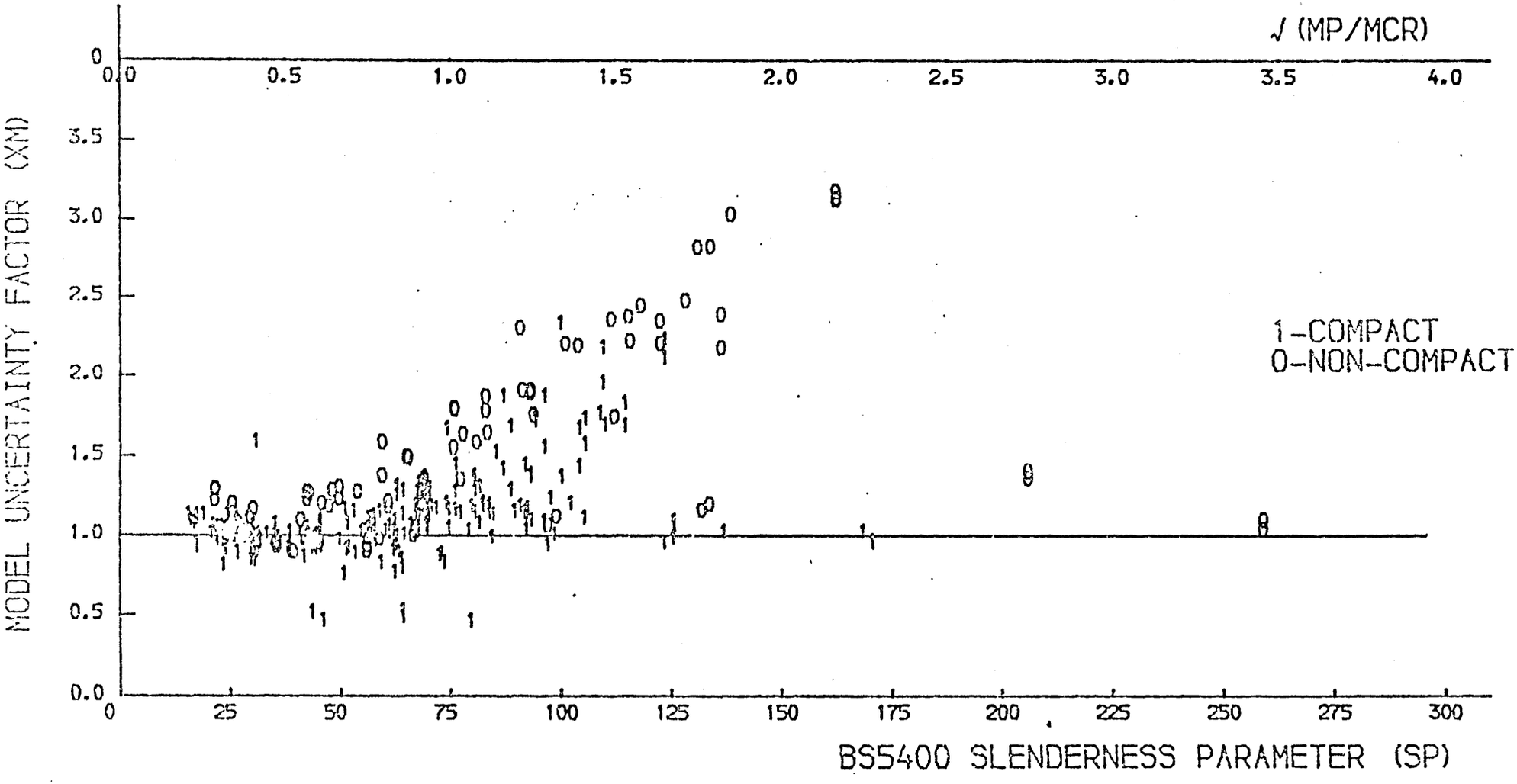

Fig. 3.6 MODEL UNCERTAINTY FACTOR (XM) VS SLENDERNESS PARAMETERS

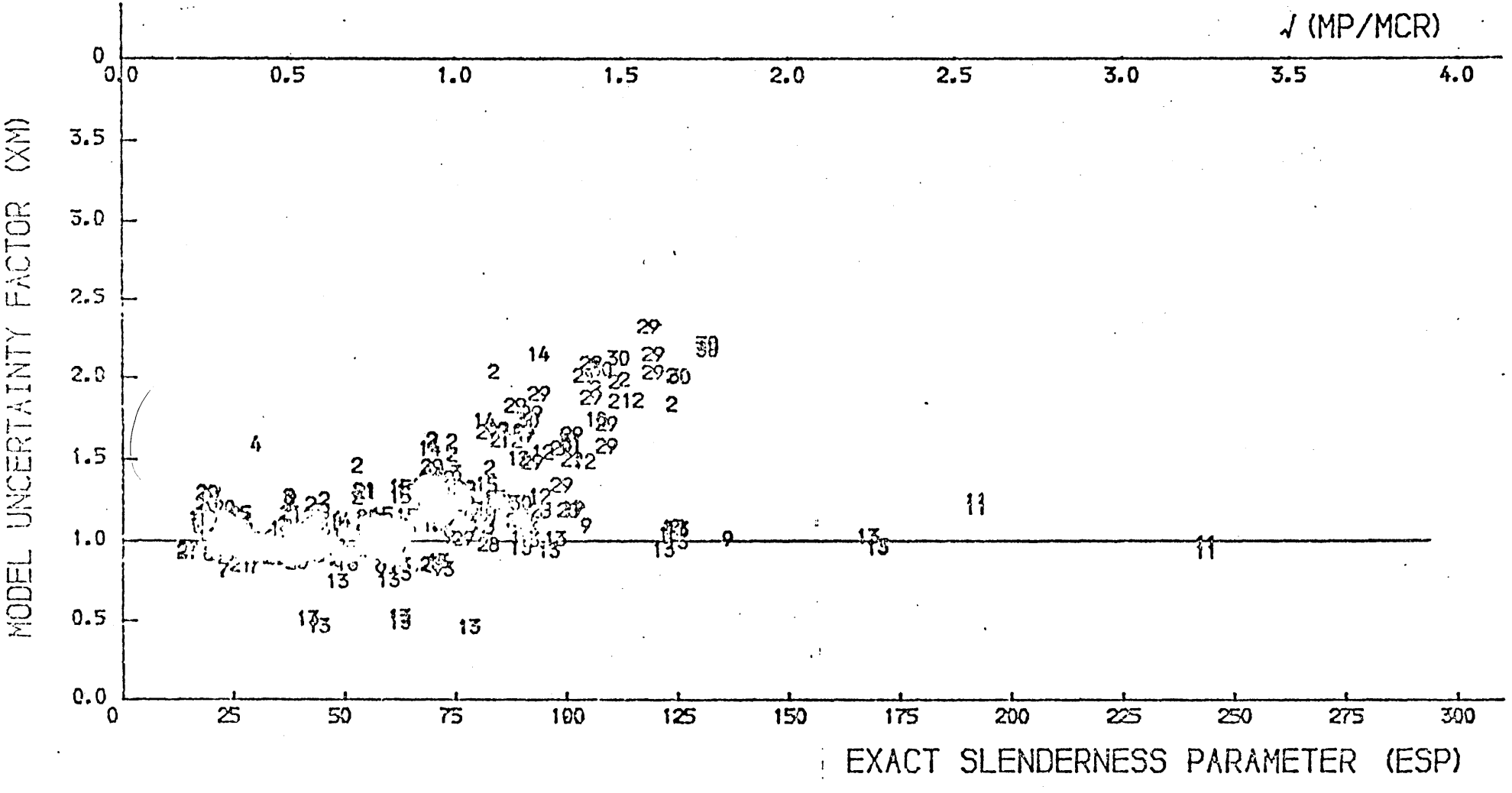

Fig. 3.7 MODEL UNCERTAINTY FACTOR (XM) VS SLENDERNESS PARAMETERS

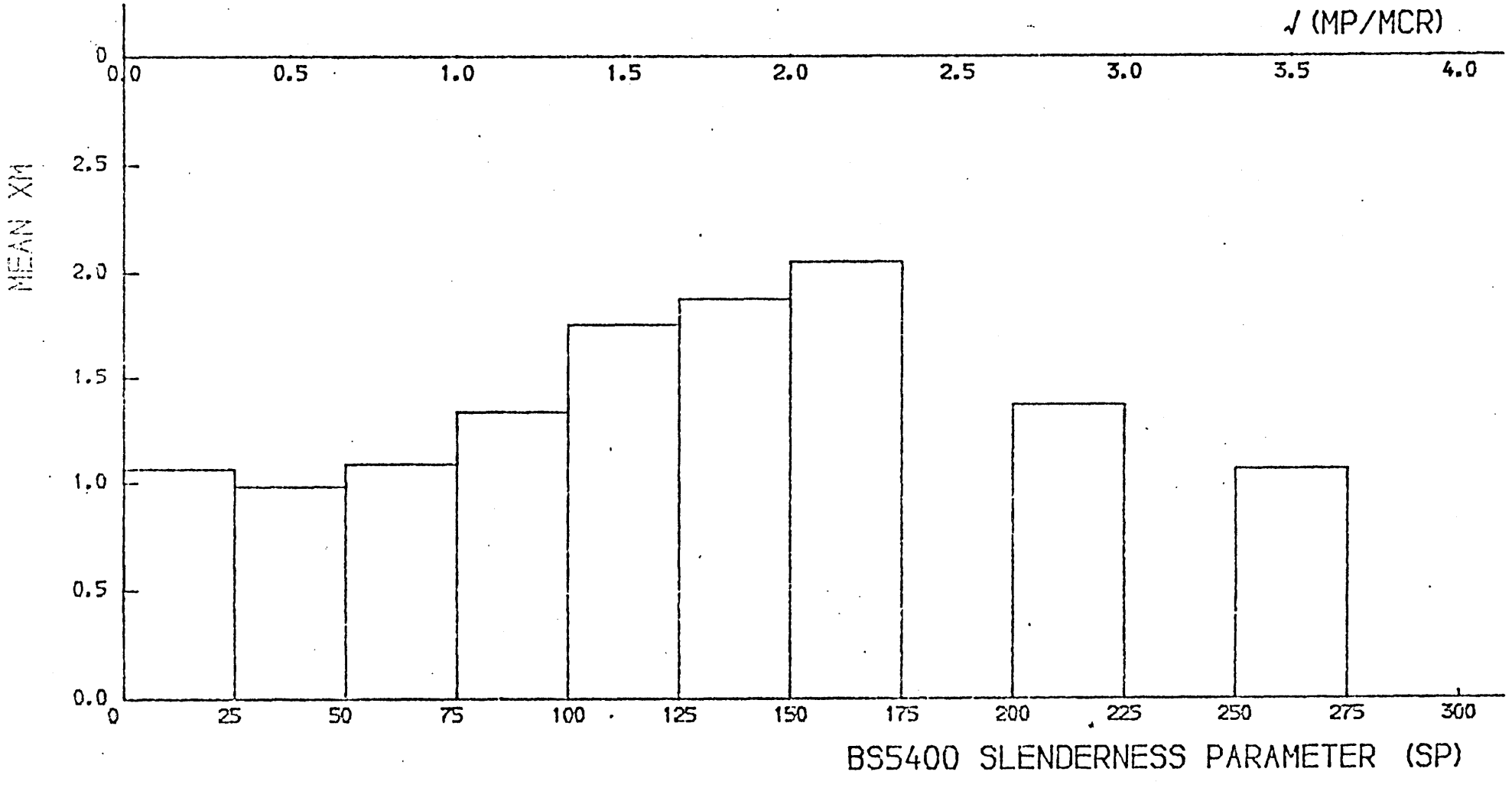

Fig. 3.8 MEAN XM VS SLENDERNESS PARAMETERS

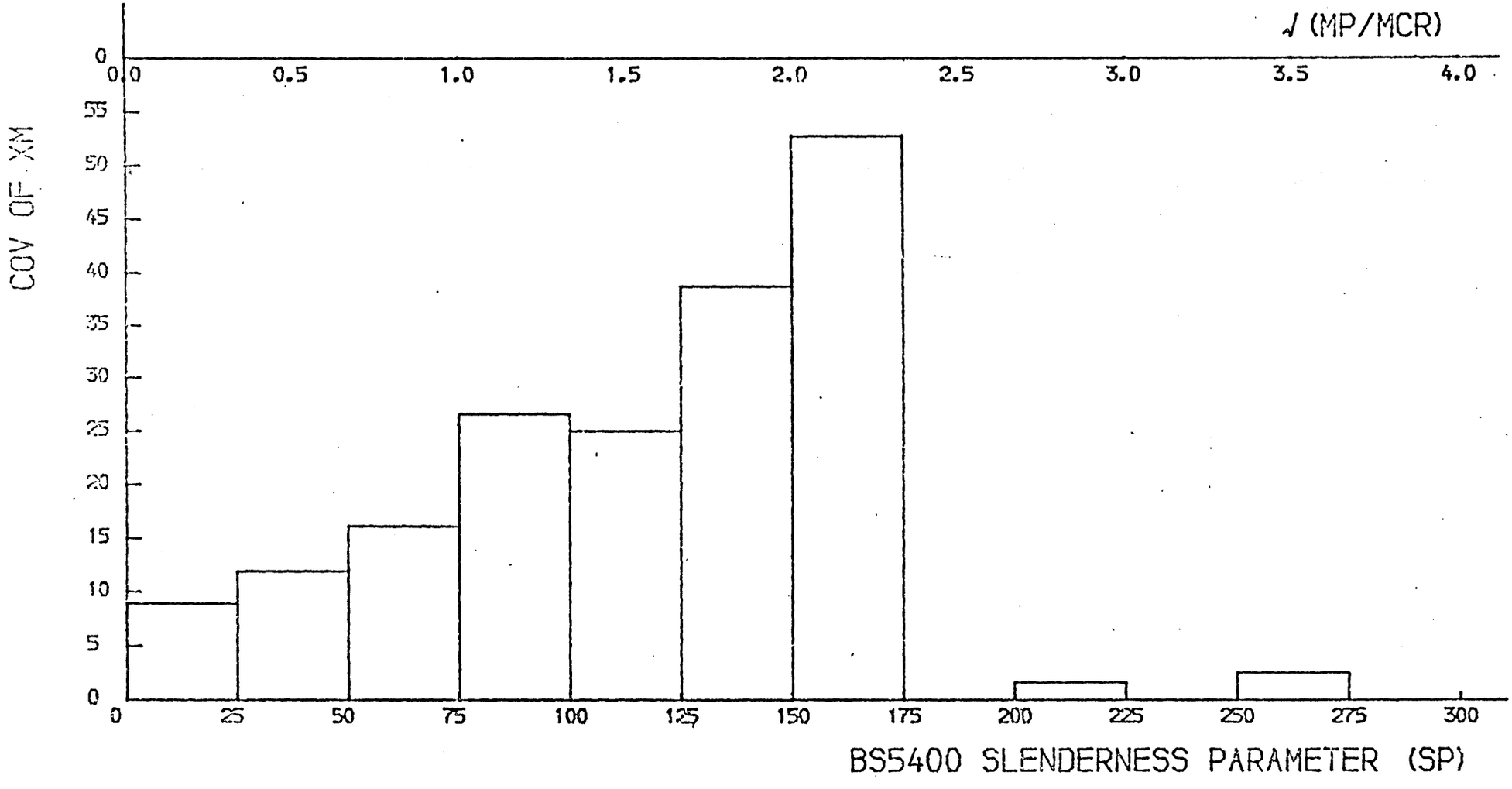

Fig. 3.9 COV OF XM VS SLENDERNESS PARAMETERS

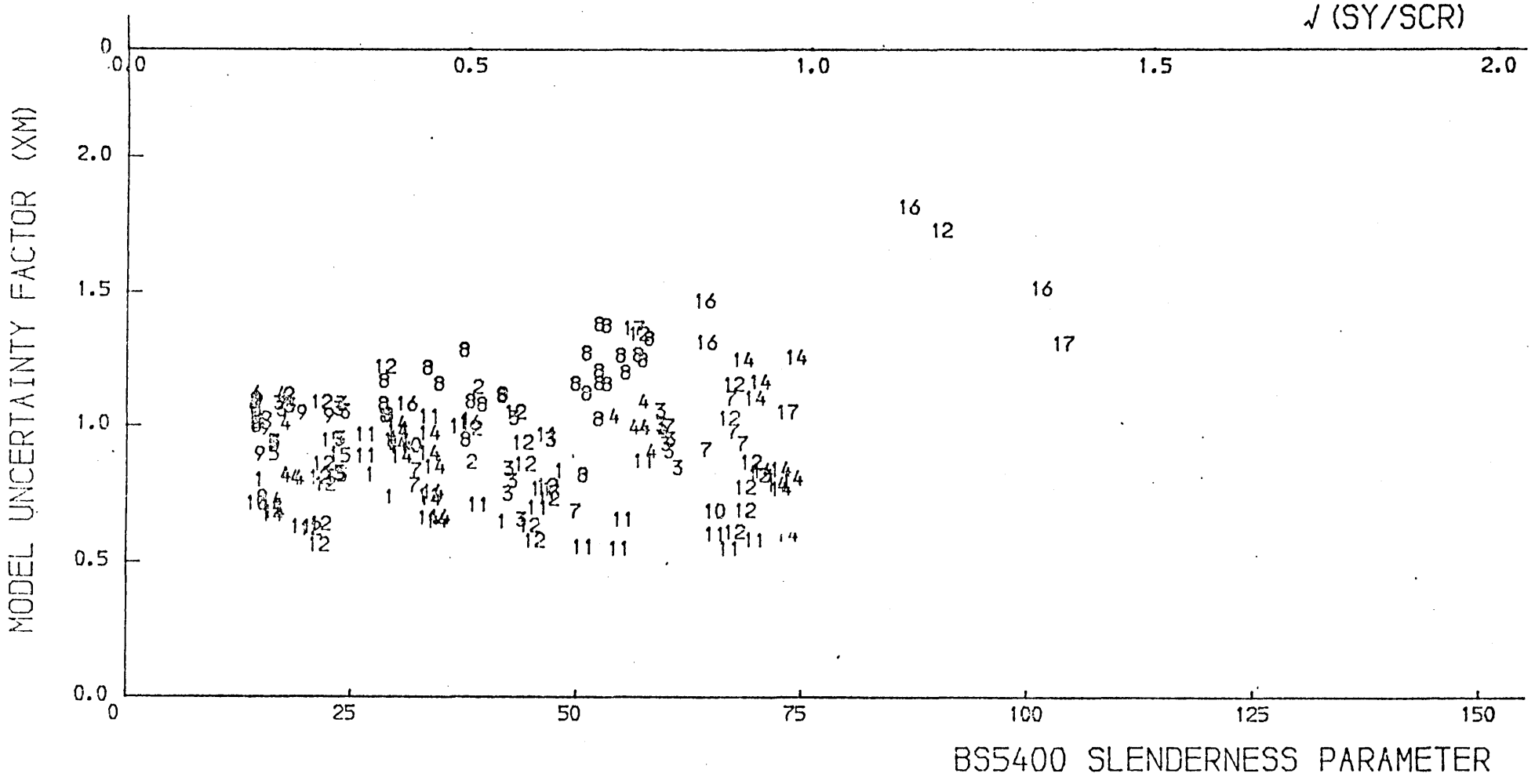

Fig. 3.10 MODEL UNCERTAINTY FACTOR (XM) VS SLENDERNESS PARAMETERS

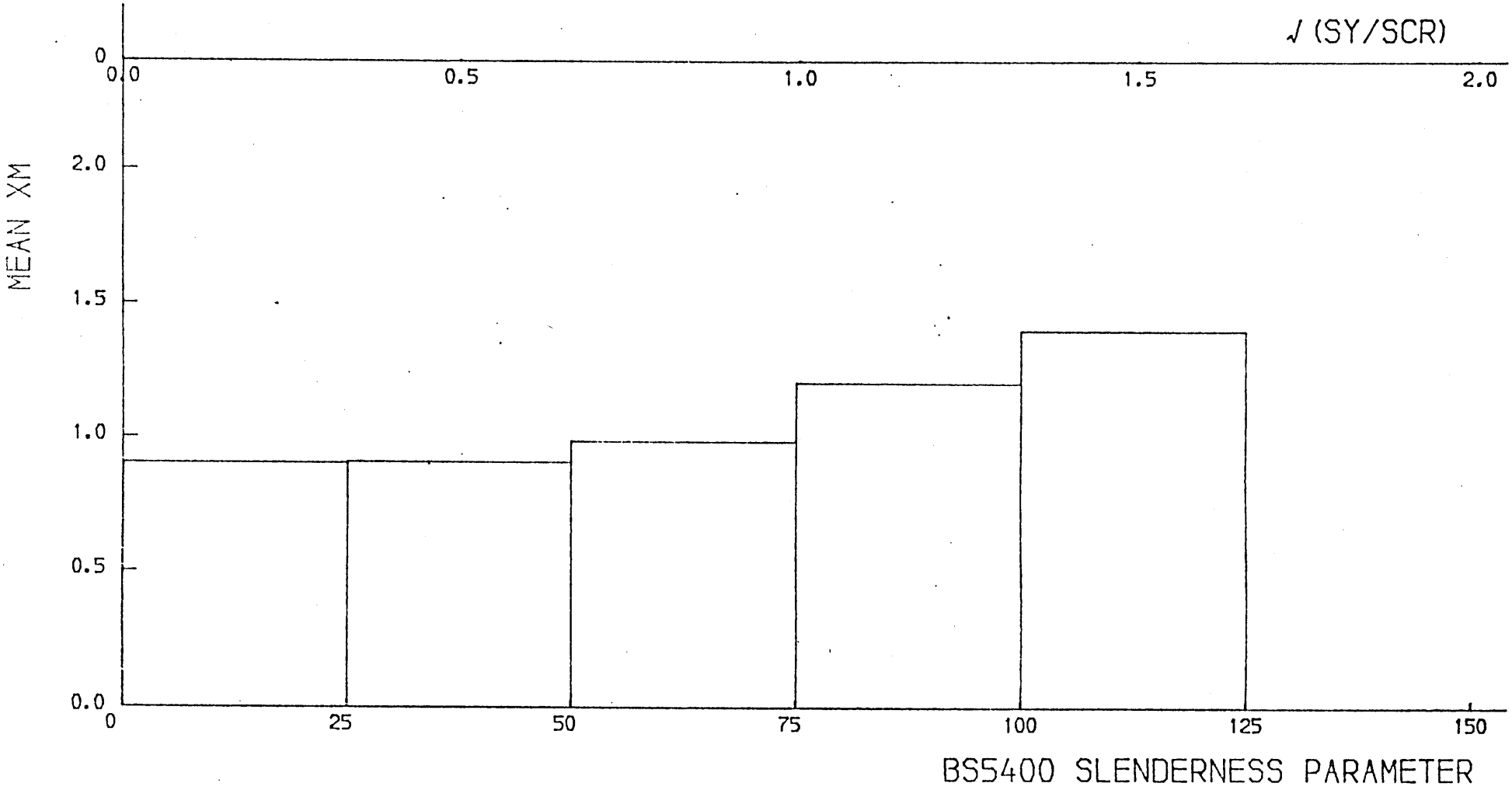

Fig. 3.11 MEAN XM VS SLENDERNESS PARAMETERS

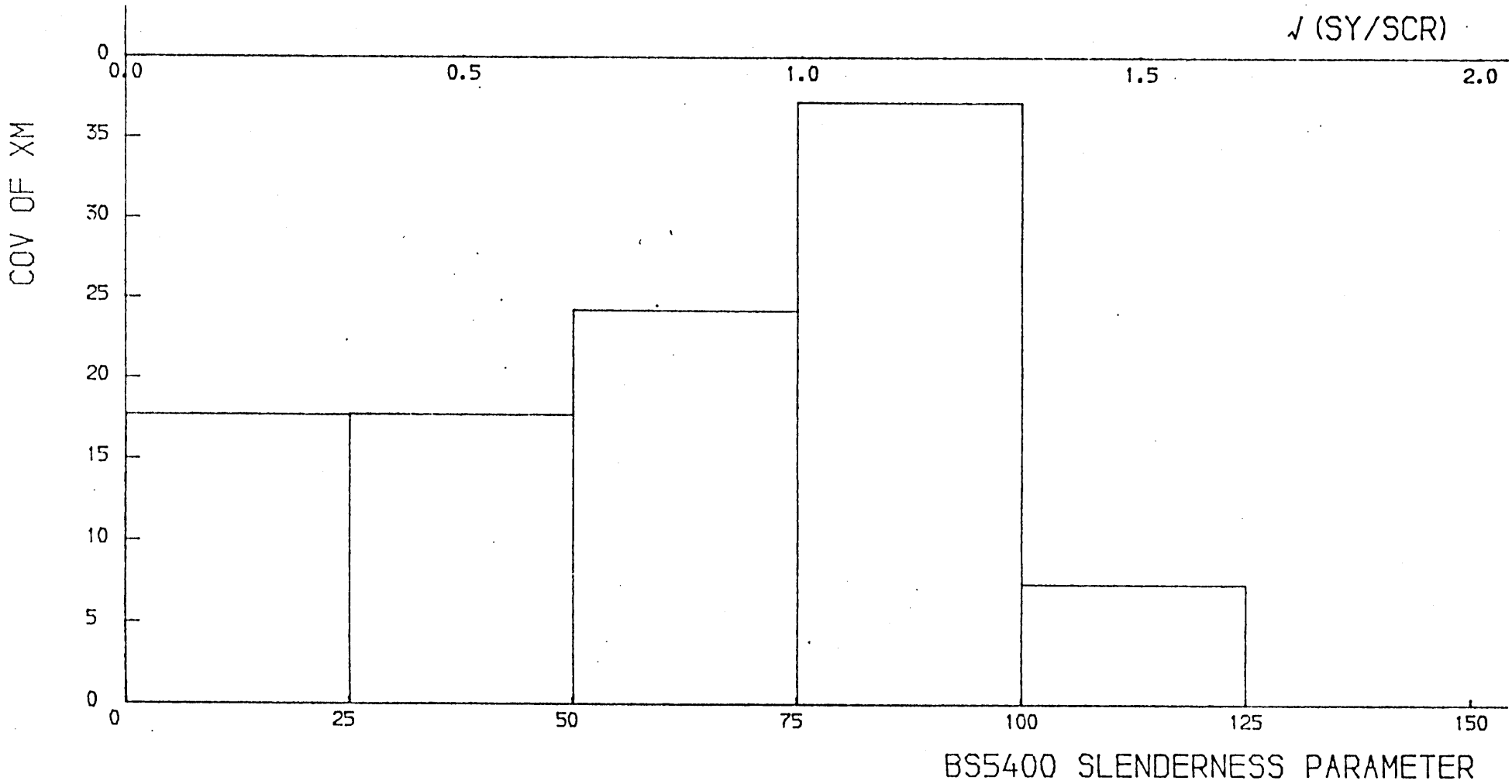

Fig. 3.12 COV OF XM VS SLENDERNESS PARAMETERS

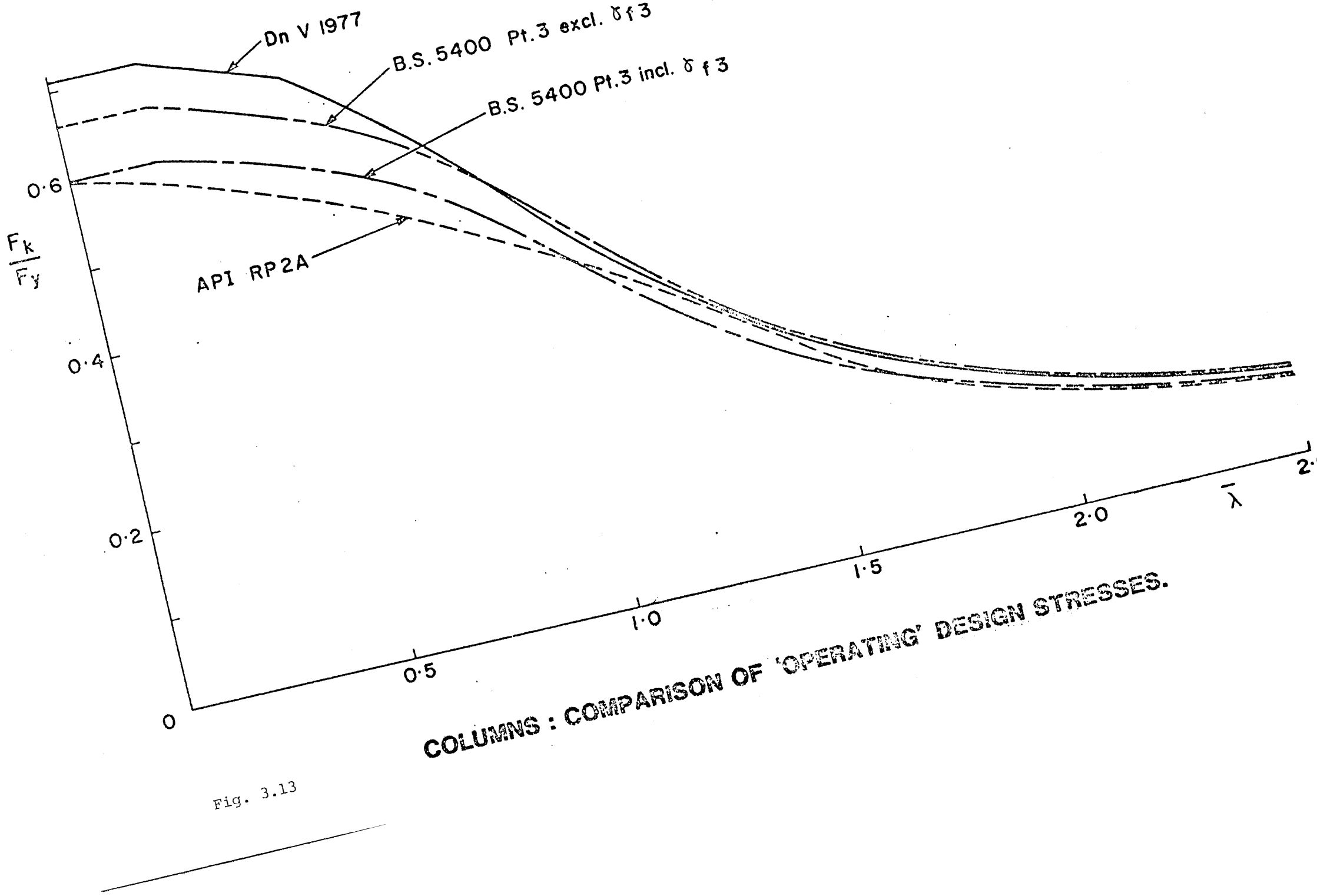
Dn V 1977
B.S. 5400 Pt.3 excl. γf3
B.S. 5400 Pt.3 incl. γf3
API RP2A
Fk/Fy
0·6
0·4
0·2
0
0·5
1·0
1·5
2·0
λ̄
COLUMNS : COMPARISON OF 'OPERATING' DESIGN STRESSES.

Fig. 3.13

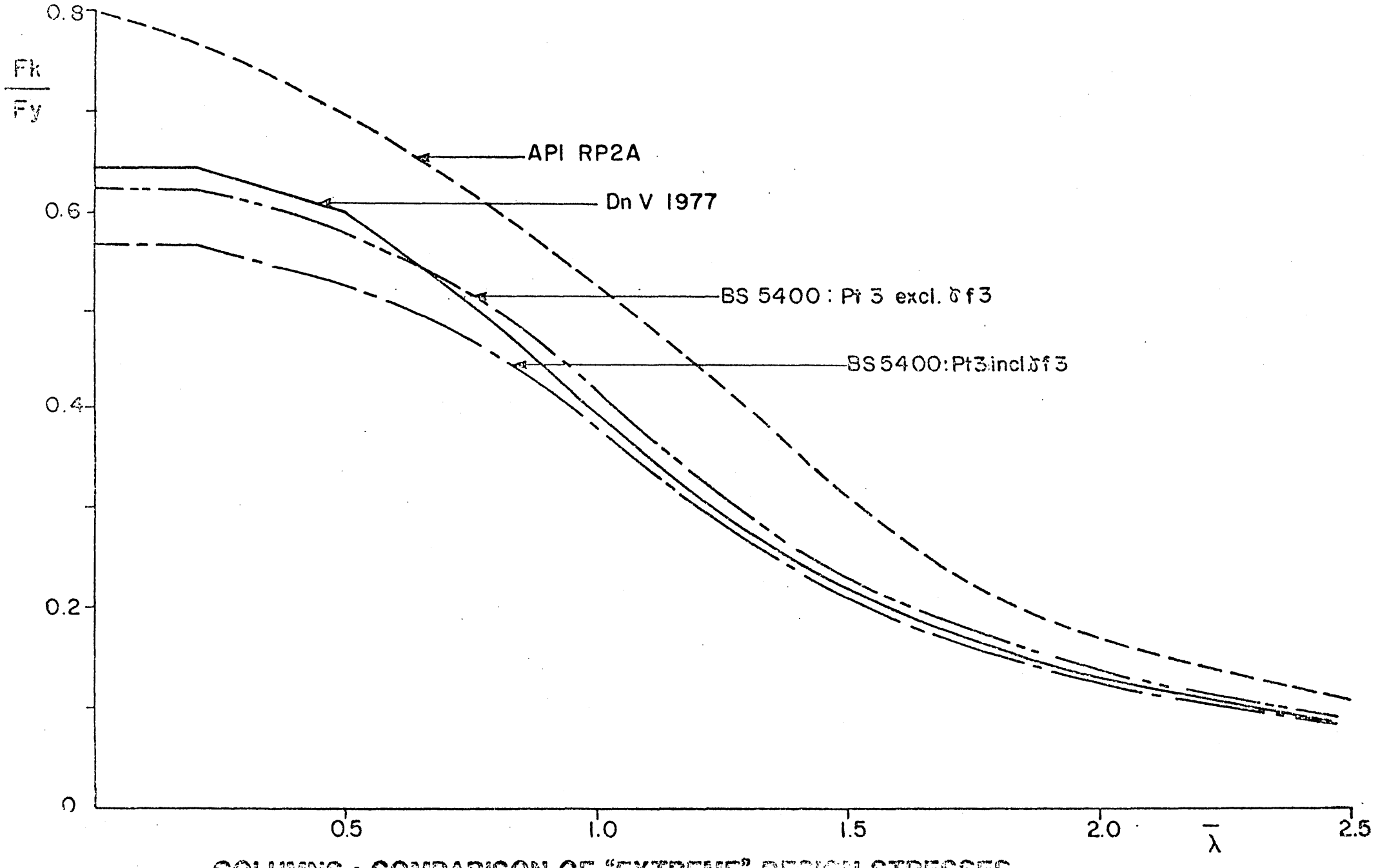

Fig. 3.14 **COLUMNS : COMPARISON OF "EXTREME" DESIGN STRESSES.**

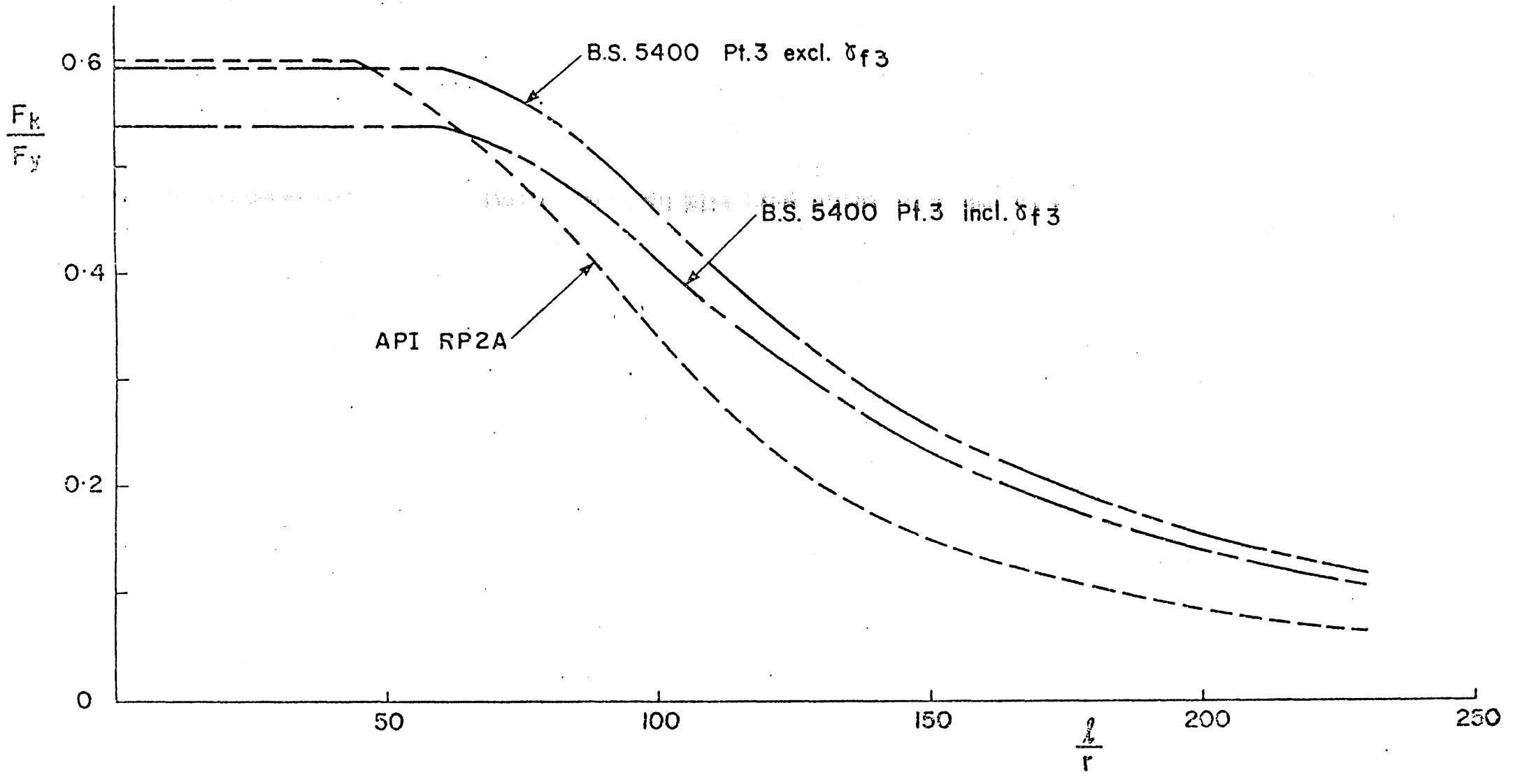

Fig. 3.15 **BEAMS : COMPARISON OF 'OPERATING' DESIGN STRESSES.**

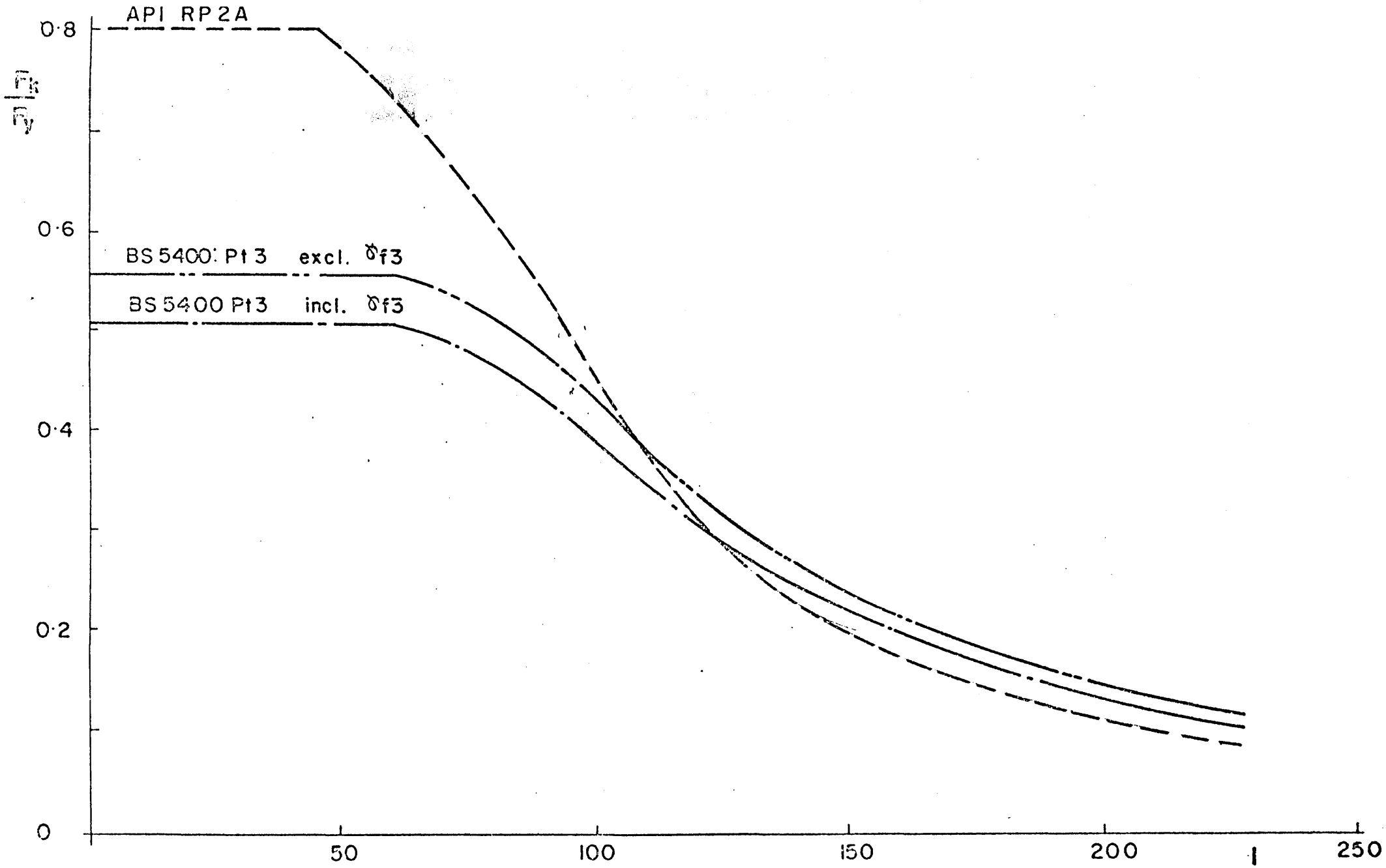

Fig. 3.16 BEAMS : COMPARISON OF 'EXTREME' DESIGN STRESSES

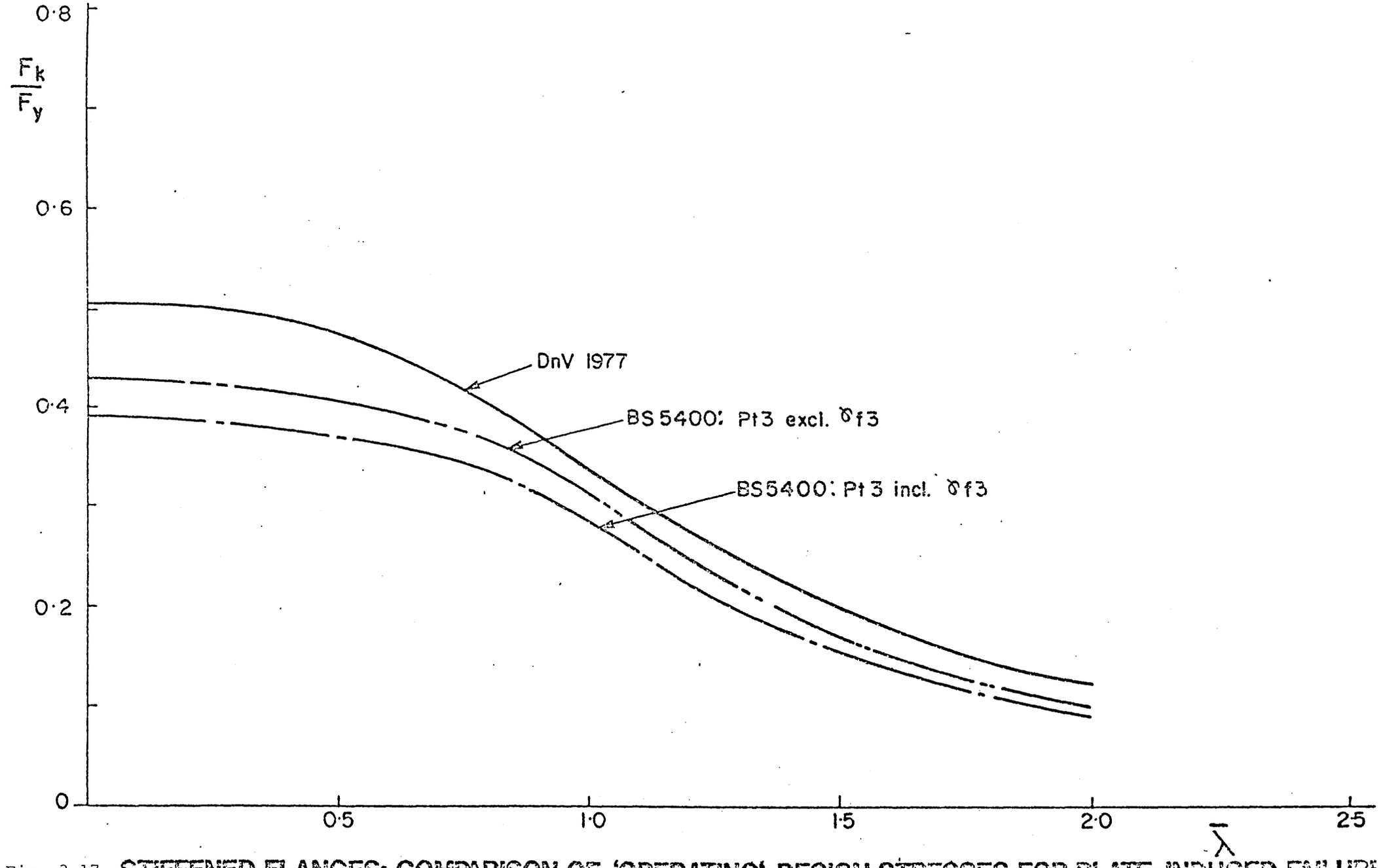

Fig. 3.17 STIFFENED FLANGES: COMPARISON OF 'OPERATING' DESIGN STRESSES FOR PLATE-INDUCED FAILURE

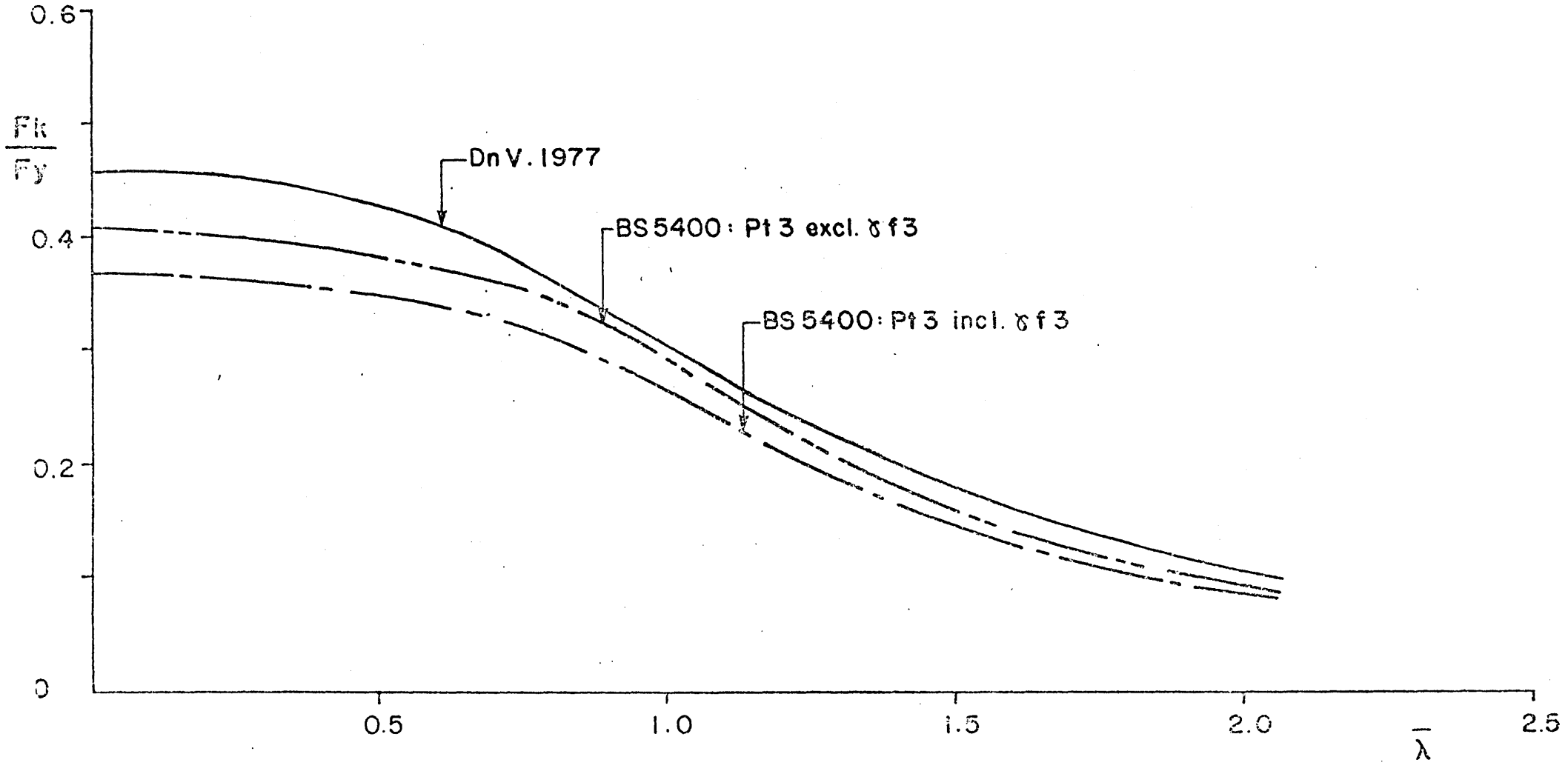

Fig. 3.18 **STIFFENED FLANGES : COMPARISON OF 'EXTREME' DESIGN STRESSES FOR PLATE - INDUCED FAILURE**

SECTION 4

CONNECTIONS: A RE-EVALUATION OF BS5400 PARTIAL FACTORS FOR OFFSHORE USE

4.1 Introduction

Fillet welds under shear and the friction capacity of high strength friction grip bolts are examined in this Section. Data on 789 lap joints with transverse and longitudinal fillet welds and on cruciform test pieces were studied and modelling factors evaluated separately for end fillets, side fillets and combined fillets. Weld area, load and modelling uncertainty were treated as random variables. Experimental data on the friction capacity of 211 HSFG butt splice joints in mild and higher grade plate material were examined. The data covered bolts to BS4395 Parts 1 and 2 and the equivalent US grades. The methods of tightening covered were the 'turn of nut' and a more accurate means of achieving a shank tension to the proof load. Blast cleaned and mill scale faying surfaces were considered as were the effects of surface treatments, weathering and relaxation of shank tension due to creep. Coefficient of friction, shear load and shank tension were treated as random variables.

Three statistical loading definitions corresponding to 'dead', 'live' and 'environmental' loads as identified in the previous Section were used. Combinations of uncertainty are treated using advanced FOSM reliability analysis. Optimisation of partial factors is then presented using the partial factors on load already derived. The effect of different statistical models for weld area on partial factor is demonstrated.

Finally the BS5400 rules for side fillets show signficantly greater conservatism than for end fillets. The consequences for the partial factor and the spread of reliabilities when the two formulations are made more consistent is demonstrated.

Section 4.2 considers suitable target failure probabilities based upon failure consequences and the experience of past design practices. Section 4.3 summarises the statistical definitions of load effects. Sections 4.4 and 4.5 deal with partial factor optimisation of HSFG bolted connections and fillet welded connections respectively. Section 4.6 summarises the material factors and in Section 4.7 the global factors of safety are compared with both BS5400: Part 3 values for bridges and the American codes. Section 4.8 discusses the comparisons.

Conclusions are summarised in Section 4.10.

4.2 Target Reliability

In choosing target reliabilities for connections on offshore structures it was borne in mind that nominally at least connections should be more reliable than the connected components. Two considerations lead to this conclusion:

(1) the consequences of failure are greater (though not catastrophic as in the case of determinate structures)

(2) the warning time of impending failure is likely to be very short.

For the evaluation of reliabilities to BS153 designs[1] it was found that when considering static strength alone fillet welded connections have a higher notional reliability than components. This would not be the case were fracture and fatigue to be modelled in the failure function.

They were excluded from the evaluation of target reliability. Friction grip bolts on the other hand had a significantly lower notional reliability and were likewise excluded. It should be borne in mind that friction grip bolts are designed to a serviceability requirement i.e. no slip and as such do not have severe consequence of failure. The reliability of bolted components against bearing or shear failure are not considered in the present work.

The original calibration[1] proceeded by selecting separate target reliabilities for bolted and welded connections.

The same course was taken in the present study. It was also decided to maintain the same ratio of component reliability to connection reliability as that estimated for BS153.

The lifetime failure probability for all components to BS153 was notionally 3.2×10^{-5} and for fillet welds 4.0×10^{-10}[1]: a reduction of five orders of magnitude. The target lifetime failure probability for components used in the previous section was 2.5×10^{-3}. Reducing this by five orders of magnitude leaves 2.5×10^{-8}. This was the value adopted for fillet welds in this study. For HSFG boted connections to BS153 rules the lifetime failure probability was 2.5×10^{-4}[1]: an order of magnitude greater than the components. Increasing the component target failure probability used in the last section by one order of magnitude results in 2.5×10^{-2}. Because of the not insignificant notional chances of failure this now represented it was felt this value should be reduced to 1.25×10^{-2}. The lifetime failure probabilities are summarised below with

appropriate values of $1/p_f$ and safety index, β.

	p_f	$1/p_f$	β
BS153			
all components(1)	3.2×10^{-5}	31250	4.0
(except connections)			
BS153 fillet welds(1)	4.0×10^{-10}	2500×10^{6}	6.2
BS153 HSFG bolts(1)	2.5×10^{-4}	4000	3.5
current components	2.5×10^{-3}	400	2.8
Proposed -	2.5×10^{-8}	40×10^{6}	5.5
fillet welds			
Proposed -	1.25×10^{-2}	80	2.2
HSFG bolt			

4.3 Statistical Definition of Load Effects

The definitions used in this study are those assumed for the work on components and are summarised at the end of this section.

The following summarises the remarks made in Section 3.

The five load categories in the DEn guidance notes(2) were reduced to three by amalgamating dead with hydrostatic load and dynamic with environmental. The amalgamation was done with load types with a similar degree of variability. The categories are as follows:

(1) 'Dead' - weight of structure and fixed equipment and machinery, hydrostatic loads.

(2) 'Live' - operation loads, stores, portable equipment, crew, berthing and landing loads, motion loads for mobile platforms, thermal stresses, construction forces and buoyancy.

(3) 'Environmental' - wind, wave, slamming, vortex shedding, marine growth effects, snow and ice, currents. Dynamic loads which are those arising from a structure's momentum in response to imposed loads.

Apart from the advantage of handling a reduced number of types this categorisation is consistent with the API RP2A[3] definitions except in RP2A buoyancy is included under dead loads.

The assumed bias, COV and distribution for each load category are summarised below:

Design Variable	Bias	COV%	Distribution
Dead load effect	1.075	5	normal
Live load effect	1.15	10	normal
Environmental load effect	1.0	30	normal

4.4 HSFG Bolted Connections in Friction: Partial Factor Optimisation

4.4.1 Strength Formulation

The friction capacity of HSFG bolts in BS5400 Part 3[4] is

$$P_{dgn} = N_S N_B K_5 K_H \mu P_v / \gamma_m \gamma_{fL} \qquad (4.1)$$

where N_B is the number of bolts

N_S is the number of shear planes

K_H is an allowance for overside or slotted holes.

The K_5 parameter is given by:

$$K_5 = 1 - (L-15d)/200d \quad (K_5 \leq 0.75) \qquad (4.2)$$

where L, the length between centres of end bolts (measured in direction of the load), must exceed 15 bolt diameters d. The allowance becomes necessary due to the large differential strains which exist at either end of a line of bolts and which can give rise to an unbuttoning effect.

The slip factor μ depends on the type of faying surface and a list of values is given in clause 14.5.4.4 of Part 3. The slip factor should be reduced by 10% when the higher grade bolts of BS4395: Part 2[5] are used. This follows the experimental work of Black and Moss[6] who reported a 2% loss in slip factor for every 10kN increase in bolt preload. The two possible reasons for this quoted in Reference 7 are:

(1) 'for treated faying surfaces, increase in bolt load is carried by the thin surface treatment, and part by the steel substance which does not take part in the shear process of the slipping surfaces' and

(2) 'the measured bolt loads are not a true measure of the loads being carried by the surfaces in contact at the time of slip'.

The prestress load, P_v, in the absence of externally applied tension, is defined as the proof load P_{pro}. This should be reduced to 0.85 P_{pro} for the higher grade bolts of BS4395: Part 2. Some justification for this was found in Reference 7 in which the ratio of preload to proof load for bolts tightened by the standard procedure was greater for lower grade bolts than for the higher grade ones.

Appendix A presents typical hand calculations for HSFG bolted connections designed to BS5400:Pt. 3.

4.4.2 Data

The available data on HSFG bolted symmetric butt splices tested in tension are summarised in Table 4.1. The full set of 211 results is tabulated in Appendix B where the original source reference and identifying name can be obtained. The following discusses the data in relation to slip factors and bolt preloads.

References 8 to 12 contain tests on joints with clean mill scale faying surfaces (surface code, IS=1, see Appendix B for a full list of codes). For this type of surface the loose mill scale is usually removed by hand wire brushing and any oil is cleaned using a solvent. This surface type is not categorised in Clause 14.5.4.4 so advantage was taken of that part of the Clause which permits the designer to determine, from published information, a suitable slip factor. Accordingly the average value of

$$\mu = P_{SLIP}/N_S N_B P_{CL} \qquad (4.3)$$

where P_{SLIP} is the load at first slip, and P_{CL} is the average clamping load as measured in tests, was determined from the 85 results in References 8, 10, 11 and 12. Unfortunately Reference 9 did not contain details of clamping loads. The average, 0.349, was used in the analysis. For comparison Reference 7 quotes a mean of 0.336 determined in an identical manner as above from 312 results. The relevant table from Reference 7 has been reproduced herein as Table 4.2. The second row in the table included the results from the first row. The value used in Reference 1 was 0.332.

Surface code 2 refers to blast cleaned faying surfaces for which Clause 14.5.4.4 of Part 3 quotes a slip factor of 0.5. Thirty-one results from References 10, 13, 14 and 15 have been listed in Appendix B. Of these 22 (References 13 and 14) were on a high grade constructional alloy, A514 (yield stress = 620N/mm^2). Due to the surface hardness, blast cleaning has little effect and leaves the average slip factor achieved in tests at around the clean mill scale value. This steel is not appropriate to the evaluation since it contravenes the requirement (Clause 6.3 of Part 3) that the ratio of ultimate to yield strength be not less than 1.2. The remaining 9 results had a mean slip factor of 0.483. Reference 7 quotes an analysis of 171 results for which the mean slip factor was 0.493. Reference 1 used a value of 0.478.

Surface codes 3 to 9 are for faying surfaces treated with various rust inhibitors. Reference 6 was the sole source for the 63 results (see Table 4.1 and Appendix B). Table 4.3 has been reproduced from Reference 6 and is included to enable comparisons to be made between the slip factors in Clause 14.5.4.4 of Part 3 and test results. A considerable amount of scatter is evident and the comparable Part 3 values are seen to underestimate the test values.

Slip factors in general, and these slip factors in particular, were considered to be a major source of modelling error.

Reference 15 gives results on 9 tests with faying surfaces treated with vinyl wash and 3 surfaces treated with linseed oil. These constitute surface code 10. These surfaces are not categorised in Clause 14.5.4.4 and so the mean slip factor from these results 0.27, calculated as above, was used. As can be seen from Table 4.4, which has been reproduced from Reference 15, the small difference in slip factors between vinyl washed and linseed oiled slip surfaces does not warrant separate treatment.

Table 4.5 reproduced from Reference 16, charts the variation of slip factor with exposure time. Except for a small reduction after 6 months for grit blasted surfaces and a reduction during the final 6 months for aluminium sprayed surfaces the factors increase over the two year period. Reference 7 quotes an increase in slip factor from 0.49 to 0.53 for grit blasted surfaces exposed for a short duration (see Table 4.2). In contrast Reference 15 shows a decrease in slip factor from 0.43 after 2 months to 0.39 after 12 months although it increases to 0.47 after 6 months (see Table 4.2). However these particular joints were assembled without first removing the loose rust and involved only one specimen in each time period.

The time factor in joint assembly is not allowed for in the BS5400 strength formulation.

The value of IB in Appendix B is 1 or 2 depending on the type of bolt used. Type 1 corresponds to BS4395 Part 1 bolts while Type 2 corresponds to BS4395 Part 2 bolts so the reductions of 15% of bolt proof load and 10% of slip factor required by Clauses 14.5.4.3 and 14.5.4.4 must be applied.

The tables of ultimate strength, yield strength and proof loads from the relevant UK (BS4395 Parts 1 and 2[5]) and US (ASTM Designations A325 and A490[17]) codes have been reproduced in Appendix C. Table 4.6 summarises the requirements. To facilitate comparison between the bolts specified in these codes the stress levels of the US bolts have been converted in Table 4.6 to N/mm^2. Ignoring the minor difference in the definitions of stress area the A325 bolt is seen to correspond almost exactly to the BS4395 Part 1 (type 1) bolt. The A490 bolt however has slightly higher properties than the BS4395 Part 2 (type 2) bolt.

Accordingly A490 bolts qualify for the reductions in slip factor and proof load as required in Clauses 14.5.4.3 and 14.5.4.4 for BS4395 Part 2 bolts.

The proof loads of the SAE 4140 bolts of Reference 10 were reported in that reference: the values have been reproduced here in Appendix B. None of these exceed the proof loads of type 1 bolts and as such do not qualify for the reductions in proof load and slip factor. In Reference 6 tests on $\frac{7}{8}$ inch bolts to BS3139: Pt 1 (1959)[18] are reported as well as $\frac{7}{8}$ inch 'Y grade' cadminium plated bolts. The former were tightened to 160 kN and the latter to 210 or 260kN. The proof load for $\frac{7}{8}$ inch BS4395 Part 1 bolts is 177 kN and for Part 2 bolts of the same diameter 235.5 kN. The BS3139: Pt. 1 bolts were thus treated as type 1 bolts and the 'Y grade' bolts as type 2.

Table 4.1 gives the method of tightening as either 'to proof load' or by 'turn of nut'. The latter involves tightening the nut until a 'snug' fit is achieved and then rotating an extra $\frac{1}{2}$ or $2/3$ turn depending on grip length. A shank tension in excess of the proof load generally results but interpretation by operatives of what constitutes 'snug' results in some scatter. Another method of tightening, not represented in the data, is by using a calibrated wrench. With this the applied torque can be controlled. Figure 4.1 has been reproduced from Reference 7, and shows distributions of preload/proof load for A490 and A325 bolts tightened by both turn of nut and calibrated wrench methods. A full discussion of distribution parameters follows this section.

The shank tension was obtained experimentally, for all results except those in Reference 6, by measuring with dial gauges, the elongation during tightening. This was then compared with a previously calibrated chart. In

Reference 6 however use was made of a customised device which relied on measuring the difference in elongation between an unstressed rod inserted into a hollowed-out bolt shank and a bolt head. A small difference between the two methods is to be expected but cannot be quantified.

4.4.3 Distribution Parameters

The distribution parameters for slip factor and clamping load to proof load ratio have been calculated from the data. These are presented in this Section with comparable data from References 1 and 7. Lognormal distributions were chosen to represent the data and this is consistent with Reference 1.

Values of the mean of

$$\mu = P_{SLIP}/N_S N_B P_{CL} \qquad (4.4)$$

were calculated for each of the ten types of faying surface indicated in Appendix B. The results are presented in Table 4.7 with comparable values from Reference 1 and 7. The Part 3 values (μ_{CODE}) are also given, those values in parenthesis corresponding to the factors calculated in accordance with Clause 14.5.4.4 of the Code for surfaces not explicitly catered for. A total of 169 results were analysed in this way.

By dividing each of the mean slip factors by the Code value and grouping all surfaces with protective coatings together (IS = 3 to 10 inclusive) the following results were obtained:

IS	Bias	COV	no.
1	1.000	15.1	85
2	0.966	15.4	9
3-10	1.200	13.8	75

These biases and COV's were used as input to the reliability analysis.

The ratio of clamping load to proof load was calculated for all bolts tightened by the turn of nut method and for which clamping loads were given. Seventy-four such results were obtained and their means and COV's are presented below together with comparable results from References 1 and 7.

		Current			Ref. 7			Ref. 1		
Bolt	Type	mean	COV	no.	mean	COV	no.	mean	COV	no
A325	1	1.18	13.60	54	1.35	8	81	-	-	-
A490	2	1.17	6.78	20	1.26	10	-	-	-	-
A325+ A490	1+2	1.18	11.70	74	-	-	-	1.19	14	71

The values used in the analysis were those for the combined bolt types - viz. mean, 1.18 and COV, 11.7.

4.4.4 Reliability Analysis

Using the Advanced Level 2 procedure reliability analyses were performed using the following failure equation:

$$g = \{P_{pro}\}\{\mu_{CODE}\}q[(1/N_p)\Sigma(P_{CL}/P_{pro})]$$
$$[(1/N_\mu)\Sigma(P_{SLIP}/N_S N_B P_{CL}\mu_{CODE})]$$
$$- \{\text{Load Bias} \times P_{pro}\mu_{CODE}\, q/\gamma_m\gamma_{fL}\} \qquad (4.5)$$

where $q = N_S\ N_B\ K_S\ K_H$.

μ_{CODE} is the slip factor from Clause 14.5.4.4 of Part 3 or 0.9 times this value depending on bolt type.

P_{pro} is the proof load or 0.85 times this value depending on bolt type.

N_p is the number of data for which P_{CL}/P_{pro} could be calculated and

N_μ is the number of data for which $P_{SLIP}/(N_S\ N_B\ P_{CL}\ \mu_{CODE})$ could be calculated.

The two terms in square brackets in Equation 4.5 are the biases on proof load and slip factor which have been calculated in Section 3.4.3. The three terms in parenthesis are the basic design variables. Their means and COV's, together with the biases from the previous section, are summarised below:

Basic Variable	Mean		COV%	Bias	
P_{pro}	as specified		11.7	1.18	LN
	(x .85 for type 2)				
		IS=1	15.1	1.00	LN
μ_{CODE}	from CODE	IS=2	15.4	0.966	LN
	(x .9 for type 2)	IS=3,10	13.8	1.20	LN
		Dead	5.0	1.075	N
P_{dgn}	$\frac{P_{pro}\mu_{CODE}q}{\gamma_m\gamma_{fL}}$	Live	10.0	1.15	N
		Env.	30.0	1.00	N

Assuming the same bias and COV adopted herein to represent design dead loading (bias = 1.075, COV = 5%), reliability analysis was carried out on all test results. The load level was determined using $\gamma_m = \gamma_{fL} = 1.3$. The values of P_{pro}, μ_{CODE} (ETA), P_{dgn} and safety index (BETA) are presented in Appendix B. Three results, one from each of the three surface types (IS=1, IS=2 and IS=3 to 10), were selected for presentation of typical sensitivity factors. These results are presented in Tables 4.8 to 4.10.

At the top of each table, general information is given. The identifying group and name enables each test joint in question to be matched with the source reference in Appendix B. The first two columns give the input means and COV's. The third column, the design point, corresponds to the point of maximum probability of failure density and is in general greater than the mean for loading variables and less for resistance variables.

The absolute value of the sensitivity factors indicates the relative sensitivity each variable has to failure. Closer control of the more sensitive variables would more readily result in greater safety. A negative sensitivity factor indicates that the design point is greater than the mean.

Design load is here seen to be least influential. However, for loads representing environmental forces, COV=30%, this will not necessarily be true. Slip factors are the most influential and preload only slightly less so. The order of sensitivities is the same for each example and follows the order of magnitude of COV.

Examination of the safety indices (BETA) in Appendix B reveals a direct correlation between surface type and safety index. Coated surfaces (IS=3 to 10) result in the highest safety index, blast cleaned surfaces (IS=2) the lowest and clean mill scale surfaces (IS=1) occupy an intermediate value.

4.4.5 Partial Factor Determination

Values of the global safety factor $\gamma_G = \gamma_m \gamma_{fL}$ were found for which the weighted mean failure probability equalled the target probability of failure.

$$p_{ft} = \sum_{i=1}^{M} \omega_i \, p_{fi} \qquad (4.6)$$

where p_{fi} is the probability of failure of member i of the data set of M members. Three loading categories were considered (Section 4.3). The weighting applied was on the basis that clean mill scale surfaces, blast cleaned surfaces and coated faying surfaces would occur in equal proportion.

The results are presented in Table 4.11 and Figure 4.2. Columns 1 to 4 in Table 4.11 give the input target probability of failure and design load distribution parameters. The required optimum global factor is given in column 5 and the achieved weighted average probability of failure appears in column 6. The final two columns give the corresponding range of safety indices. The range diminishes as load COV increases which is consistent with the work on components. The variation of global factor with $\log_{10}(p_{ft})$ is shown for each loading category in Figure 4.2. As one would expect global factor increases with load COV.

Determination of γ_m for bolted connections is achieved by dividing the global factors by the load factors determined in Section 2. The process of calculation is presented below:

	Global	Load Factor	γ_m
Dead	1.428	1.20	1.19
Live	1.581	1.35	1.17
Env.	1.689	1.50	1.13
		Average	1.16

The three γ_m's show consistency despite the fact that the load factors were not involved in the optimisation. The above result is summarised together with results from the analysis for welded joints in Section 4.6.

4.5 Welded Connections : Partial Factor Optimisation

4.5.1 Strength Formulation

The International Institute of Welding expression[19] for the combination of stresses acting on the plane of the weld throat as used in Part 3 Clause 14.6.3.11.2 is:

$$(\sqrt{\sigma^2 + 3(\tau_1^2 + \tau_2^2)})^{\frac{1}{2}}$$

σ is the stress normal to the plane.

τ_1 is the shear stress on the plane perpendicular to the length of the weld and

τ_2 is the shear stress on the plane along the length of the weld.

For end fillets τ_2 is zero and for side fillets σ and τ_1 are zero.

The limiting value for this is a function of the average yield stress of parent and weld metal:

$$\frac{k(\sigma_y + 455)}{2\gamma_m\gamma_{f3}}$$

where σ_y is the nominal yield stress (in N/mm^2) of the weaker parent metal and k is 1.4 for side fillets and 0.9 for side fillets. For fillets inclined to the direction of loading k should be taken as 1.0.

Many tests on welded joints had combinations of end and side fillets so it is necessary to express the Clause in load rather than stress terms. This is in keeping with Clause 14.3.3.1 (Elastic Analysis) which requires that all welds share the design axial load in proportion to their respective strengths. Accordingly the design load on any joint was taken as

$$P_{dgn} = \left[\frac{1.4A_1}{\sqrt{2}} + \frac{0.9A_2}{\sqrt{3}} + \frac{1.0A_3}{\sqrt{2}\mathrm{Sin}\theta+3\mathrm{Cos}\theta}\right]\frac{\sigma_y + 455}{2\gamma_m\gamma_{f3}} \qquad (4.7)$$

where A_1 is the throat area of an end fillet

A_2 that of the side fillet and

A_3 that of a fillet inclined at an angle θ to the direction of loading.

Appendix A presents typical hand calculations for fillet welded connections to BS5400:Pt. 3.

4.5.2 Data

Table 4.12 summarises the data used in the evaluation as well as the rejected data. The results from References 20 to 22 were rejected because measured yield stresses were not given. In Reference 23 (Group 11) 152 results were recorded with measured yield stresses. These together with 135 results from Reference 24 (Group 10) constitute the data set of 287 tests from which X_m (see Section 4.5.4) and γ_m (see Section 4.5.5) were calculated.

All the test results in Group 10 were on cruciform test pieces. These were made by welding one one-metre narrow plate either side of a transverse plate and then cutting into 50mm cruciform sections. A tensile load was then

applied to the narrow plates across the thickness of the transverse plate and increased until rupture occurred. The area (A1) given in Appendix B is the sum of the throat thicknesses of the fractured welds times the length of cruciform section. In Appendix B IFIL = 1 is the code used for end fillets.

All of the test pieces in Group 11 had a different configuration consisting of two lap plates welded either side of a wider central plate. The tensile load was applied parallel to the plane of the plates. The various locations of the welds were as follows:

(1) transverse to the direction of loading across the 2 ends of the lap plates (IFIL = 1),
(2) parallel to the direction of loading and along the 2 sides of each lap plate (IFIL = 2), and
(3) both of these i.e. on 3 sides of each lap plate (IFIL = 3).

In Appendix B, therefore, A1 is the sum of two throat areas and A2 sum of four. Twenty-eight test results from Group 11 had end fillets only, 50 had side fillets only and the remaining 74 were of the combined type.

4.5.3 Statistical Definition of Resistance Variables

The definition of yield stress of plate material was discussed at length in the previous section. The conclusion was to select a bias of 1.125 and a COV of 8% with a lognormal distribution. This definition is used herein.

The second and most important basic variable is weld area which will now be discussed.

Reference 1 reports results on 4 groups of measurements of throat thickness. Whether allowance has been made for convexity in the measurements of the fillets is not mentioned. The results are summarised below:

	No.	$\frac{\text{actual}}{\text{nominal}}$	COV%	Distribution
6, 8 and 10mm continuous and intermittent fillets on box girder bridges	198	1.27	16.5	Gamma
6mm tee joints on a plate girder bridge	64	1.20	12.5	Lognormal
6mm fillets on Bridge A	5292	0.95	21.0	Normal
Bridge B	480	1.06	15.1	Lognormal

Evidently, as results from Bridge A suggest, no guarantee can be given that weld area will be greater than nominal. The authors of Reference 1 used the bias and COV of the first group with a lognormal distribution. The reasons for this choice are not clear.

A first attempt at optimisation using the results of the largest group i.e. bias 0.95, COV 21% Normal, failed. For the target reliability selected values of global factor were tried. At a certain level, approximately $\gamma_G = 3.4$, the method began predicting negative design points making convergence impossible. Using the same bias and COV but with a lognormal distribution produced a result albeit rather high. Eventually it was decided to use this definition together with the 'bias 1.27, COV 16.5 Lognormal' definition as bounds on the variability of throat thickness.

4.5.4 Reliability Analysis

4.5.4.1 Model Uncertainty Factor, X_m

The value of the model uncertainty factor,

$$X_m = P_{rupt}/[1.4A_1/2 + 0.9A_2/\sqrt{3})(\sigma_y + 455)/2] \quad (4.8)$$

being the ratio of actual failure load from the test results to the failure load predicted by Equation 4.7, was determined for the entire data set. The third term in Equation 4.7 has been omitted since none of the data had inclined fillets. The results are presented in Appendix B. The most likely sources of modelling error were considered to be k, (the weld orientation parameter) and the assumption of elastic re-distribution. Accordingly, for the purposes of evaluating the mean and COV of X_m the data were categorised as follows:

1) End fillets
2) Side fillets
3) Combined end and side fillets

Side fillets were found to be the most conservatively modelled, X_m=2.07, end fillets the least, X_m=1.44 and combined fillets had an X_m between these two extremes viz. 1.78. The variability in X_m was never greater than 13%. A lognormal distribution was chosen to complete the definition. This is consistent with previous work. Table 4.13 summarises the means and COV's of the modelling factors and of the other basic variables.

4.5.4.2 Results of Typical Analyses

Using the Advanced Level II procedure (Section 1) reliability analyses were performed on all models. Three were selected for the purposes of

illustrating the salient points of the analysis. The load effect selected represented 'design' dead loading in that it had the same bias and degree of uncertainty as adopted herein for this type of action. The load level was determined using $\gamma_m=\gamma_{fL}=1.3$ so that the design effect for which the component was analysed from the limit state equation

$$Z = g(x_1 \ldots\ldots x_6) \qquad (4.9)$$

The basic variables x_1 to x_6 are design load P_{dgn}, throat area of end fillet A_1, throat area of side fillet A_2, throat area of inclined fillet A_3, yield stress σ_y and modelling factor X_m.

The function g has the form:

$$g = X_m P_{ult} - \xi_L P_{dgn} \qquad (4.10)$$

where

$$P_{ult} = \left[\frac{1.4A_1}{\sqrt{2}} + \frac{0.9A_2}{\sqrt{3}} + \frac{1.0A_3}{\sqrt{2}\sin\theta+3\cos\theta}\right] \frac{\sigma_y + 455}{2} \qquad (4.11)$$

P_{dgn} is given by Eqn. 4.1.

ξ_L is the load bias.

The results of the three analyses, one chosen at random from each fillet type are shown in Table 4.14-4.16. In these Tables the source reference can be determined from the group number using Appendix B. An identifying character string is also given enabling each model to be mated with the original. Columns 1 and 2 give the input mean and COV.

The design point corresponds to the point of maximum probability of failure density and is generally greater than the mean for loading variables and less than the mean for resistance variables.

The sensitivity factor gives the slope of the normal to the failure surface with respect to the axis representing the basic variable concerned. Its absolute value indicates the relative sensitivity each basic variable has to failure. A high value indicates a safer design will more readily result from closer inspection of this variable than any other. The partial factor gives the ratio of mean to design point.

Examination of the sensitivities in Tables 3.14-3.16 reveals the same declining order or magnitude of weld area (most influential), modelling factor, design load and yield stress.

4.5.5 Partial Factor Determination

The results of the partial factor optimisation are presented in Tables 4.17 and 4.18 and Figure 4.3. Tables 4.17 and 4.18 show the results using the upper and lower values of weld throat COV respectively. The weighting considered was assuming that each of the three fillet types (IFL = 1, 2 and 3) would occur in equal proportion. The Tables show, in the first four columns, the input values of target safety index, load bias, load COV and distribution type (N= Normal). The fifth and sixth columns show the global optimum safety factors and the achieved weighted average probability of failure respectively. The global optima increase with load COV as would be expected. When the lower value of throat COV is used (Table 4.18) the global optimum safety factors reduce by approximately 24%.

Figure 4.3 shows, for the dead load category (Bias = 1.075, COV = 5%), the variation of $\log_{10}$ of the weighted average probability of failure with

global safety factor. The figure may be used to investigate how a different choice of target probability of failure would influence the global factor and hence the choice of γ_m.

In order to see what final γ_m's the results in Tables 4.17 and 4.18 represent it is necessary to divide out the yield stress bias (1.125) and the load factors. The load factors which were derived in the components study were dead load - 1.20, live load - 1.35, and environmental load - 1.50. The process of calculations is displayed below:

Throat Definition	Load Category	Global Optimum	+1.125	+ Load Factor
LN, 21.5%	Dead	2.898	2.576	2.147
	Live	3.300	2.933	2.173
	Env.	3.964	3.523	2.349
			Average	2.223 = γ_m
LN, 16.5%	Dead	2.332	2.073	1.727
	Live	2.680	2.382	1.765
	Env.	3.300	2.933	1.955
			Average	1.816 = γ_m

The load factors were not included in the optimisation and thus a slight lack of consistency in the γ_m's results. Taking average values to the nearest 0.05 gives γ_m of 2.20 and 1.80 for the 21.5% and 16.5% weld throat defintions respectively.

The outcome of the analysis using two separate defintions of throat thickness lends itself to the suggestion that the final choice of γ_m be left to the designer with an upper bound of 2.20 and a lower bound of 1.80, depending on the confidence held in the welding quality.

4.5.5.1 Modified Strength Formulation

Recalling Section 4.5.4.1, X_m for end fillets was 1.44 and 2.07 for side fillets. This evident lack of consistency seemed to warrant further investigation. If the formulation is modified such that k = 1.0, instead of 1.4, for end fillets the appropriate X_m value becomes 2.01. This is clearly more consistent with the value for side fillets. The consequences for reliability and optimised partial factors are now demonstrated.

Firstly the spread of reliabilities is substantially reduced. Comparison of Figure 4.4, which shows the range of safety indices for any global factor when k is taken as 1.0 for end fillets, with Figure 4.5 which shows the same set of results when k = 1.4 clearly demonstrates this. Figures 4.4 and 4.5 have been plotted for the dead load case and the throat thickness COV = 21.5%. A similar reduction in the spread of reliabilities can be expected for other load categories and throat thickness definitions.

Secondly a substantial reduction in the optimum global factors result - approximately 2.20 (21.5% case) and 1.70 (16.5% case). Carrying out the divisions of yield stress bias (1.125) and dead load factor (1.20) yields 1.63 and 1.26 which compare favourably with the 2.20 and 1.80 obtained above.

Whether added conservatism in the formulation has cancelled out the reduction in partial factor can readily be determined from Equation 4.7. Taking the 16.5% weld throat COV case the various expressions for design load are

	$k = 1.4$ $\gamma_m = 1.73$	$k = 1.0$ $\gamma_m = 1.26$	% Change
End fillet	$\frac{1.4A_1(\sigma_y+455)}{\sqrt{2}x2x1.80x\gamma_{f3}\gamma_{fL}}$	$\frac{1.0A_1(\sigma_y+455)}{\sqrt{2}x2x1x1.26\gamma_{f3}\gamma_{fL}}$	2% less conservative
Side fillet	$\frac{0.9A_2(\sigma_y+455)}{\sqrt{3}x2x1.80x\gamma_{f3}\gamma_{fL}}$	$\frac{0.9A_2(\sigma_y+455)}{\sqrt{3}x2x1.26\gamma_{f3}\gamma_{fL}}$	43% less conservative

A change of the k-factor for end fillets from 1.4 to 1.0 has led to a reduction in material partial factor. Since the same partial factor applies to side fillets a greater capacity can be realised for these at the cost of a reduction in end fillet capacity. The weighted average probability of failure of all fillets remains at the target level and the spread of reliabilities has been substantially reduced.

4.6 SUMMARY OF MATERIAL PARTIAL FACTORS

Values of the partial factors for HSFG bolted connections and fillet welded connections are presented below. The values from the analyses have been rounded to the nearest 0.5.

BS5400 stength formulations:

HSFG bolts		1.15	three loading categories considered
Fillet Welds	Upper	2.20	
	Lower	1.80	

Modified strength formulation with k=1.0 for end fillets:

	Upper	1.60	dead load category considered
	Lower	1.25	

The two values for fillet welds derive from consideration of two separate statistical definitions of weld throat thickness. It is suggested that the two values be regarded as upper and lower bounds and the final choice be made according to the anticipated quality of welding.

4.7 Design Comparisons

4.7.1 HSFG Bolts

The design slip capacity of the HSFG bolts is given by Equation 4.1. In this the slip factor, μ, and prestress load, P_v, both refer to mean values. The global factor of safety against slip is thus the product of partial factors γ_m γ_{fL} times the analysis factor γ_{f3}. For the purpose of comparisons with the American Institute of Steel Construction (AISC) and the original BS5400: Pt. 3 for bridges operating loading conditions are assumed to be represented, for land based structures, by dead load and live load in equal proportion and, for offshore structures, by dead, live and environmental loads in equal proportions.

The AISC allowable shear stress for friction A325 bolts is 103N/mm^2. The API RP2A[3] rules for offshore structures allow an increase of one third on these stresses when they are caused by environmental loads. For the operating condition the allowable stress can thus be increased to (1/3 + 1/3 + 1.33/3)103 = 114N/mm^2. For A490 bolts the allowable shear stress is likewise increased from 138 to 153 N/mm^2. Assuming a coefficient of friction of 0.5 the slip capacity for bolts up to 1 inch diameter is 0.5 x 586 for A325 bolts and 0.5 x 825 for A490 bolts. The factor of safety against slip provided by the AISC allowable stresses are thus 0.5 x 586/114 = 2.54 for A325 bolts and 0.5 x 825/153 = 2.70 for A490 bolts. For a coefficient of friction of 0.35 the factors are respectively 1.80 and 1.89.

The load factors for highway bridges in BS5400: Part 3 are 1.05 for dead load, 1.75 for superimposed load and 1.5 for HA live loading. Assuming for the operating condition the dead and HA line loading occur in equal proportion, and superimposed load to be negligible, the net load factor for highway bridges is

$$0.5 \times 1.05 + 0.5 \times 1.5 = 1.27$$

The BS5400: Part 3 material factor for HSFG bolts is 1.3 and the analysis factor is 1.1 thus the global factor against slip, irrespective of faying surface and bolt type, is 1.3 x 1.1 x 1.27 = 1.82.

For the present study the material factor is 1.15, analysis factor 1.1 and the net loading factor can be obtained for the operating load conditions as

$$1.2/3 + 1.35/3 + 1.5/3 = 1.35$$

The global factor is thus 1.15 x 1.1 x 1.35 = 1.71.

Table 4.19 summarises all comparisons.

For joints designed to resist slip the factors of safety against bearing failure are difficult to establish because the stress distribution on the connected parts in the bearing area is unknown. If, however, bearing failure is assumed to occur when the stress on the rectangular area of plate projected by the bolt reaches the plate yield stress then the factor of safety against bearing is small. However this assumption is very conservative and tests have shown[25] that strength of the net section of a tension member is not effected provided the bearing stress is not larger than 2.25 times the net-section stress.

4.7.2 Fillet Welds

The resulting partial safety factors are expressed as a global factor of safety on electrode yield strength for the purposes of comparisons with the American Institute of Steel Construction (AISC) specification. For this purpose 'operating' conditions of loading are assumed. Comparisons are also made with the original BS5400: Part 3 specification for steel bridges.

The API RP2A[3] rules refer to the AISC specifications for structural steel buildings for details on allowable stresses for welds but allow a 33% increase on these allowable stresses when they are caused by environmental loads. The AISC rules specify the allowable stress on the throat of an end or side fillet of 0.3 times the electrode yield strength[25]. For the purpose of making comparisons with BS5400 rules an 'operating' loading condition can be

identified by assuming the stress on a weld to be composed of one third each of dead, live and environmental loads. For the AISC rules, therefore, the global factor on electrode yield strength under operating conditions is

$$1/(3 \times 0.3) + 1/(3 \times 0.3) + 1/(3 \times 0.4) = 3.06$$

This would be the global factor when the stress on a fillet is assessed as simply the load acting on the throat plane divided by the throat plane area irrespective of the line of action of the load. This is a commonly made assumption. When the IIW expression is used however the stress on an end fillet will be more conservatively assessed by a factor of $\sqrt{2}$ or 1.414. In this case the global factor on electrode yield strength is 1.4141 x 3.06 = 4.33.

The BS5400: Part 3 weld metal strength parameter is $(\sigma_y + 455)/2$. For mild steel with σ_y = 248N/mm^2 this becomes 351 N/mm^2. E60 designated electrodes have a yield strength of 414 N/mm^2 thus for mild steel the BS5400 weld strength parameter is more conservative than the AISC parameter by a factor of 1.18. The load factors, γ_{fL}, for highway bridges in BS5400: Part 3 are 1.05 for dead load, 1.75 for superimposed load and 1.5 for HA loading. Assuming, for the operating condition the dead and HA live loading are equal and assuming superimposed loads to be negligible the net load factor for highway bridges is:

$$0.5 \times 1.05 + 0.5 \times 1.5 = 1.27$$

The material factor in BS5400: Part 3 welds is 1.1 and the analysis factor is also 1.1. Using the simple assessment (Clause 14.6.3.11.1) the BS5400: Part 3

weld strength parameter is reduced by a factor of √3; using the IIW expression (Clause 14.6.3.11.2) the factor is √2 for end fillets since

$$\sqrt{\{(P/\sqrt{2}A_1)^2 + 3[(P/\sqrt{2}A_1)^2 + O^2]\}} = \sqrt{2}\ P/A_1 \qquad (4.12)$$

and √3 for side fillets since:

$$\sqrt{\{O^2 + 3[O^2 + (P/A_2)^2]\}} = \sqrt{3}\ P/A_2 \qquad (4.13)$$

In Equations 4.12 and 4.13 the load P is assumed to be supported by end fillets of total throat area, A_1 or by side fillets of total throat area, A_2.

An additional factor on the BS5400: Part 3 weld metal strength parameter is 1/1.4 for end fillets and 1/0.9 for side fillets. The factors originate from Reference 1 based on data from Reference 26. Average experimental values were obtained for

$$k_1 = 2\ P_{rupt}/(A_1(\sigma_p + \sigma_w)) \qquad (4.14)$$

and

$$k_2 = 2\ P_{rupt}/(A_2(\sigma_p + \sigma_w)) \qquad (4.15)$$

where

σ_p and σ_w are plate and weld metal yield stresses respectively and P_{rupt} is the experimental rupture load.

The average values were $k_1 = 1.4$ and $k_2 = 0.9$. On the basis of these results end fillets were concluded to be 'stronger' than side fillets. However the mode

of analysis strength in Equations 4.14 and 4.15 ignores the direct stress component. Had the more realistic IIW expression been used the differences in strength would not have been so great.

Considering all the above contributory factors the global factor on electrode yield strength in BS5400: Part 3 end fillets in mild steel using the IIW expression under operating conditions is thus

$$1.1 \times 1.1 \times 1.27 \times \sqrt{2} \times 1/1.4 \times 1.18 = 1.83$$

other combinations are tabulated in Table 4.20.

For comparisons with the present study a material factor of 1.8 has been assumed and the same operating load condition has been assumed as for the AISC case i.e. one third dead load, one third live load and one third environmental load. Thus the net load factor is

$$1.2/3 + 1.35/3 + 1.5/3 = 1.35$$

Comparisons have been made for the two cases:

$\gamma_m = 1.8$ with $k_1 = 1.4$

and

$\gamma_m = 1.26$ with $k_1 = 1.0$

For example the global factor on electrode yield strength for end fillets in mild steel under operating conditions using the IIW expression is

$$1.8 \times 1.1 \times 1.35 \times \sqrt{2} \times 1/1.4 \times 1.18 = 3.19$$

when γ_m = 1.8 with k_1 = 1.4 and

$$1.26 \times 1.1 \times 1.35 \times \sqrt{2} \times 1.0 \times 1.18 = 3.12$$

when γ_m = 1.26 with k_1 = 1.10.

All combinations are tabulated in Table 4.20.

4.8 Discussion

The comparisons of global factor of safety with BS5400: Part 3 designs shows the design of HSFG bolted connections are less conservative under the revised partial factors whereas fillet welds are more conservative. Two major factors influence the optimum partial factors: the target reliability and loading model. It will be recalled from Section 4.2 that the difference in target safety indices between bridge and offshore connections was 3.5 - 2.2 = 1.3. For welds the difference was 6.2 - 5.5 = 0.7. Considering target reliabilities alone, the global factors for offshore connections could be expected to be lower than bridge connections but with the difference in bolted connection global factors being greater than the difference in fillet weld global factors.

Considering alone the second major influence on optimum partial factors, i.e. load model, greater global factors should result for offshore connections because of the greater variability in environmental loading offshore. For comparison, HA live loading was modelled[1] as an extreme value distribution with COV = 7%, the environmental load effects offshore, on the other hand, were modelled with a Normal distribution, COV = 30%. Since the same loading model applies to bolted and welded connections a uniform increase in global factor would be expected. Superimposition of the two effects, target reliability and load model, has resulted, for the present case, in bolted connection global factors being smaller and fillet weld global factors being greater than their counterparts in BS5400: Part 3.

Comparisons with the AISC rules indicate similar global factors for clean mill scale joints (i.e. when μ = 0.35). For blast cleaned jonts (μ=0.5) the AISC rules are considerably more conservative. AISC fillet welds on the other hand are generally less conservative than the present recommendations.

The presentation adopted in Figures 4.2 to 4.5 illustrates the relationship between global safety factor and failure probability. As such the figures can be used to re-establish partial factors if and when it is deemed desirable to do so. For example it may be found, upon considering economic criteria and consequences of failure, necessary to adjust the target reliabilities.

4.9 Conclusions

1. The probability that the slip capacity of HSFG bolted connection designed to the BS5400: Part 3 rules with

   γ_m = 1.15

   γ_{fLD} = 1.20

   γ_{fLL} = 1.35

   γ_{fLE} = 1.50

   will be exceeded is on average 1.25×10^{-2}. The range of safety indices was from 2.00 to 3.20.

2. The probability that the rupture load of an end or side weld fillet designed to BS5400: Part 3 rules with

   γ_m = 1.80 for good weld quality

   = 1.20 for poor weld quality

   γ_{fLD} = 1.20

   γ_{fLL} = 1.35

   γ_{fLE} = 1.50

   will be exceeded is on average 2.5×10^{-8}. The range of safety indices was from 5.24 to 8.15.

3. The probability that the rupture load of an end or side fillet designed according to BS5400: Part 3 but with k_1, the weld orientation factor for end fillets, having a value of 1.0 and with

   γ_m = 1.25 for good weld quality

   = 1.60 for poor weld quality

   γ_{fLD} = 1.20

   γ_{fLL} = 1.35

   γ_{fLE} = 1.50

   will be exceeded is on average 2.5×10^{-8}. The range of safety indices in this case is reduced, being between 5.5 and 6.7.

4.10 References

1. Flint, A.R. et al, 'The Derivation of Safety Factors for Design of Highway Bridges'. In the Design of Steel Bridges, ed. Rockey and Evans, Granada, London, 1981, pp11-36.
2. 'Offshore Installations Guidance on Design and Construction', Dept. of Energy, HMSO, July 1977.
3. API RP2A 'API Recommended Practice for Planning, Designing and Construction of Fixed Offshore Platforms', American Petroleum Inst., Dallas, 1981.
4. BS5400: Steel, Concrete and Composite Bridges. British Standards Institution, London, 1982.
5. BS4395: Higher Grade Bolts (waisted shank), Nuts and General Grade Washers. British Standards Institution, London, 1973.
6. Black, W.B. and Moss, D.S., 'High Strength Friction Grip Bolts - Slip Factors of Protected Faying Surfaces', Road Research Lab Report, LR153, 1968.

7. Fisher, J.W. and Struick, J.H., 'Guide to Design Criteria for Bolted and Riveted Joints', John Wiley & Sons, 1974.

8. Sterling, G.H. and Fisher, J.E.W., 'A440 Steel Connected by A490 Joints', Proc. ASCE, J.Struct. Div., ST3, June 1966, pp101-118.

9. Bendigo, R.A., Hansen, R.M. and Rumpf, J.L., 'Long Bolted Joints', Proc. ASCE, J.Struct. Div., Dec. 1963, ST6, pp187- 211.

10. Hechtman, R.A., Young, D.R., Chin, A.G. and Savikho, E.R., 'Slip of Joints under Static Loads', Trans. ASCE, Vol. 1120, 1955, pp1335-1351.

11. Fisher, J.W., Ramseler, P.O. and Beedle, L.S., 'Strength of A440 Steel Joints Fastened with A325 Bolts', IABSE, Vol. 23, 1963, pp135-157.

12. Foreman, R.T. and Rumpf, J.L., 'Static Tension Tests of Compact Bolted Joints', Proc. ASCE, J.Struct. Div., June 1960, ST6, pp73-99.

13. Kulak, G.L. and Fisher, J.W., 'A514 Steel Joints Fastened by A490 Bolts', Proc. ASCE, J.Struct. Div., October 1968, ST10, pp2303-2323.

14. Fisher, J.W. and Kulak, A.M., 'Tests of Bolted Butt Splices', Proc. ASCE, J.Struct. Div., November 1968, ST11, pp2609-2619.

15. Lee, J.H., O'Connor, C. and Fisher, J.W., 'Effect of Surface Coatings and Exposure on Slip', Proc. ASCE, J.Struct. Div., November 1969, ST11, pp2371-2381.

16. Moss, D.S., 'Effect of Two Yars Weathering on High Strength Friction Grip Bolted Joints', Transport and Road Research Laboratory Supplementary Report, 191 UC, 1976.

17. American Society for Testing Materials: Part 1, Steel Piping, Tubing and Fittings, ASTM Designation A325, Specification for High-Strength Steel Bolts, 1970.

18. BS3139: Specification for High Strength Friction Grip Bolts for Structural Engineering. British Standards Institution, London, 1959.

19. Hicks, J.G., 'Welded Joint Design', Crosby Lockwood Staples, London, 1979.

20. Clarke, A.H., 'The Strength of Fillet Welded Connections', Imperial College, November 1970.

21. Harrison, J.D. and Clarke, P.J., 'Static Shear Tests on Fillet Welded Connections', The Welding Institute paper 3364/1/72, October, 1972.

22. Butler, L.J. and Kulak, G.L., 'Strength of Fillet Welds as a Function of Direction of Load', Welding Research Supplement, Vol. 50, No. 5, May 1971, pp231-234.

23. Ligtenberg, F.K., 'International Test Series', Final Report International Institute of Welding Document XV-242-68, 1968.

24. Swedish Institute for Production Engineering Research, 'Vertically Welded Fillet Welds', International Institute of Welding Document XV-272-69, 1969.

25. Gaylord, E.H. and Gaylord, C.N., 'Design of Steel Structures', McGraw Hill, New York, 1972.

26. Strating, J., 'The Strength of Fillet Welds made by Automatic and Semi-automatic Welding Processes'. International Institute of Welding Document XV-316-71, March 1971.

Group (Ref)	Bolt	Dia. in.	P_{CL} given	P_{SLIP} given	Tightening Method	Plate	Surface Code	No. of tests
1 (8)	A490	7/8	8	8	tn	A440	1	8
2 (13)	A490	1 1/8, 1, 7/8	12	11	tn	A514	2	12
3 (9)	A325	7/8	4	0	tn	A7	1	20
4 (14)	A325	1 1/8	10	10	tn	A514	2	10
5 (15)	A325	1	18	18	tn	A36	10(12),2(6)	18
6 (10)	SAE 414(42) A325 (16)	1	58	58	proof	A7	1(55), 2(3)	58
7 (11)	A325	7/8	14	14	tn	A440	1	14
8 (6)	BS 3139(21) 'Y grade'(42)	7/8	63	63	proof	HYBS968 (1962) σy=340	3, 4, 5 6, 7, 8 9 (9 each)	63
9 (12)	A325	7/8, 1, 1 1/8	8	8	tn	A7	1	8

Tightening methods : tn - turn of nut
proof - to proof Load

Table 4.1 Summary of Data on HSFG Bolted Joint Tests

Summary of Slip Coefficients[a]

Type Steel	Treatment	Average	Standard Deviation	Number of Tests
A7, A36, A440	Clean mill scale	0.322	.062	180
A7, A36, A440 Fe37, Fe52	Clean mill scale	0.336	.070	312
	Red lead paint	0.065	—	6
A7, A36, Fe37	Grit blasted	0.493	.074	168
A7, A36, Fe37	Grit blasted, exposed (short period)	0.527	.056	51
A514	Grit blasted	0.331	.043	19
A7, A36	Semi polished	0.279	.043	12
A7, A36, Fe37	Hot dip galvanized	0.184	.041	27
	Vinyl treated	0.275	.023	15
	Cold zinc painted	0.30	—	3
	Metallized	0.48	—	2
	Rust preventing paint	0.60	—	3
	Galvanized and sand blasted	0.34	—	1
	Sand blasted and treated with linseed oil (exposed)	0.26	—	3
	Sand blasted	0.47	—	3

[a] Determined from tension type specimens.

Table 4.2 - Reproduced from Reference 7 Table 5.1

p: 78

Comparison of slip factors, measured during present tests with other British measurements

1	2	3	4	5	6	7	8
	Bolt load 160 kN (16.1 tonf)					Bolt load 295 kN (29.5 tonf)	
	Slip Factors						
Preparation of Faying Surfaces	RRL Nominal bolt load	RRL Actual bolt load (Corrected)	BIE Actual bolt load	MET Actual bolt load	BR Actual bolt load	RRL Nominal bolt load (Extra-polated	BR Actual bolt load
Grit blasted, etch primer	0.33	0.34	0.32			0.32	
Shot Blasted, etch primer	0.30	0.31	0.30			0.29	
Grit Blasted, zinc silicate primer	0.43	0.50	0.56			0.27	
Shot Blasted, zinc silicate primer	0.51	0.59	0.63		0.38	0.36	0.32
Grit Blasted, zinc metal spray	0.59	0.71	0.78	0.75		0.52	
Grit Blasted, zinc metal spray (Wire)	0.62	0.75				0.43	0.37
Grit Blasted, aluminium spray (Powder)	0.71	0.72	0.76			0.56	
Grit Blasted, aluminium spray (Wire)				0.77			

Column 2. Present results. Slip factor = Slip Load ÷ Nominal Bolt Load
3. Present results. Slip factor = Slip Load ÷ Load in bolts immediately prior to testing.

Slip factor corrected to value at 16.1 tons bolt load, assuming that slip factor decreases by 2 per cent per ton of bolt load.

Column 4. B.I.E. tests; bolts retightened to nominal value before test.
Column 5. Results from Metalisation Ltd. testing immediately after bolting up, ∴ actual bolt load.
Columns 6 & 8 British Rail results. Testing immediately after bolting.

TABLE 4.3 Reproduced from Reference 6

Specimen number[1]	Load at first slip, in kips	Maximum load before 0.02 in. movement, in kips	Initial clamping force, in kips	K_1	K_2	Remarks
(1)	(2)	(3)	(4)	(5)	(6)	(7)
SB1–1	290	303	463	0.31	0.33	Blast cleaned; treated
SB1–2	200	210	360	0.28	0.29	with vinyl wash
SB1–3	270	280	489	0.28	0.29	MIL-C15328A.
Average	—	—	—	0.29	0.30	
SB2–1	294	294	379	0.39[2]	—	Blast cleaned; exposed
SB2–2	310	310	360	0.43[2]	—	12, 2 and 6 months.
SB2–3	340	340	360	0.47[2]	—	
Average	—	—	—	0.43	—	
SB3–1	210	210	408	0.26	—	Blast cleaned; treated
SB3–2	212	212	394	0.27	—	with linseed oil and
SB3–3	220	220	421	0.26	—	exposed 2 months.
Average	—	—	—	0.26	—	
SB4–1	205	205	459	0.22	—	Blast cleaned; treated
SB4–2	215	215	387	0.28	—	with vinyl wash
SB4–3	275	275	443	0.31	—	MIL-C15328A and exposed 2 months
Average	—	—	—	0.27	—	
SB5–1	260	260	514	0.25	—	Blast cleaned; treated
SB5–2	250	260	480	0.27	—	with vinyl wash
SB5–3	240	240	487	0.25	—	MIL-P15328B and exposed 2 months.
Average	—	—	—	0.26	—	
SH1–1	345	345	360	0.48	—	Blast cleaned; longi-
SH1–2	360	360	360	0.50	—	tudinal slotted holes.
SH1–3	359	359	360	0.50	—	
Average	—	—	—	0.49	—	

[1] SOH2–1 exposed 12 months; SOH2–2 exposed 2 months; SOH2–3 exposed 6 months.

TABLE 4.4 Test results reproduced from Reference 15

Variation in slip factor with exposure time

Exposure Time	Grit Blasted		Grit Blasted + Zinc Spray		Grit Blasted + Aluminium Spray	
	Slip Factor	Spec.	Slip Factor	Spec. No.	Slip Factor	Spec. No.
24 hours after assembly (unexposed)	0.683	8	0.711	33	0.596	73
	0.693	9	0.678	44	0.555	75
	0.670	15	0.728	45	0.590	81
	0.675	21	0.648	57	0.691	87
	0.665	32	0.645	68	0.515	93
	Mean 0.677		Mean 0.682		Mean 0.589	
6 months	0.652	1	0.738	38	0.673	74
	0.707	14	0.783	50	0.575	76
	0.633	16	0.745	58	0.687	86
	0.648	22	0.766	67	0.679	91
	0.700	27	0.810	59	0.645	95
	Mean 0.668		Mean 0.768		Mean 0.652	
1 year	0.700	2	0.825	37	0.695	72
	0.745	13	0.763	49	0.640	83
	0.672	17	0.721	66	0.674	84
	0.683	23	0.810	59	0.678	97
	0.733	31	0.842	40	0.669	90
	Mean 0.707		Mean 0.792		Mean 0.671	
2 years	0.766	5	0.800	34	0.707	69
	0.783	12	0.825	39	0.630	71
	0.731	18	0.804	43	0.605	78
	0.721	24	0.815	46	0.594	79
	0.790	30	0.806	60	0.634	82
	Mean 0.758		Mean 0.810		Mean 0.634	

TABLE 4.5 Reproduced from Reference 16

	UTS N/mm²	Yield N/mm²	Proof N/mm²	Proof / UTS x 100%
BS 4395				
Part 1	827 M12–M24	635	589	71
	725 M27–M36	558	512	71
Part 2	981 all	882	776	79
[Stress area = $\pi/16$ (eff. diameter + minor diameter)^2]				
BS 3139 (1959)				
Part 1	827 $^1/_2$ – $^3/_4$ in.	–	586	–
	792 $^7/_8$ –1 in.	–	538	–
	724 $1^1/_8$–$1^1/_2$in.	–	510	–
[Stress area = 0.7854 (nom. diameter – .9743/no. of threads per inch)^2]				
ASTM				
A325 (1982)	827 $^1/_2$ –1 in.	634	586	70
	724 $1^1/_8$–$1^1/_2$in.	558	510	70
A490 (1981)	1035 all	895	825	80
[Stress area = 0.7854 (nom. diameter – .9743/no. of threads per inch)^2]				

TABLE 4.6 Summary of UK and US Code Requirements

Surface Code (IS)	μ Code	Current Mean	Current COV	Current No.	Ref.7 Mean	Ref.7 COV	Ref.7 No.	Ref.1 Mean	Ref.1 COV	Ref.1 No.
1	(0.349)	0.349	15.10	85	0.336	21.0	312	0.332	21.0	312
2	0.50	0.483	15.40	9	0.493	15.0	171	0.478	15.0	153
3	0.25	0.320	5.18	9	0.275	8.4	15	–	–	–
4	0.25	0.290	4.06	9	–	–	–	–	–	–
5	0.35	0.385	18.2	9	0.300	–	3	–	–	–
6	0.35	0.459	12.4	9	–	–	–	–	–	–
7	0.40	0.516	8.13	9	–	–	–	–	–	–
8	0.40	0.532	12.0	9	–	–	–	–	–	–
9	0.50	0.615	7.97	9	–	–	–	–	–	–
10	(0.27)	0.270	9.29	12	0.272	–	18	–	–	–

TABLE 4.7 Comparison of distribution parameters for slip factors

TABLE 4.8

RELIABILITY ANALYSIS RESULTS
BOLTED CONNECTIONS

GROUP 1 K42A
FAYING SURFACE CODE= 1
NUMBER OF BOLTS= 8
NO. OF SHEAR PLANES= 2
BOLT TYPE= 2
K5= 1.000
KH= 1.000

PARAMETER	MEAN	COV	DESIGN POINT	SENSITIVITY FACTOR	PARTIAL FACTOR	1/PARTIAL FACTOR
PDGN (KN)	670.456	5.000	695.623	-0.246	1.038	0.964
PRO (KN)	209.730	11.700	168.550	0.595	0.804	1.244
ETA	0.314	15.100	0.219	0.766	0.696	1.437

BETA= 3.055
PF= 0.11245E-02

TABLE 4.9

RELIABILITY ANALYSIS RESULTS
BOLTED CONNECTIONS

GROUP 2 J42A
FAYING SURFACE CODE= 2
NUMBER OF BOLTS= 8
NO. OF SHEAR PLANES= 2
BOLT TYPE= 2
K5= 1.000
KH= 1.000

PARAMETER	MEAN	COV	DESIGN POINT	SENSITIVITY FACTOR	PARTIAL FACTOR	1/PARTIAL FACTOR
PDGN (KN)	1259.353	5.000	1302.972	-0.244	1.035	0.967
PRO (KN)	274.975	11.700	224.751	0.588	0.817	1.223
ETA	0.450	15.400	0.318	0.772	0.706	1.416

BETA= 2.844
PF= 0.22258E-02

TABLE 4.10

RELIABILITY ANALYSIS RESULTS
BOLTED CONNECTIONS

GROUP 5 SOH11
FAYING SURFACE CODE= 10
NUMBER OF BOLTS= 8
NO. OF SHEAR PLANES= 2
BOLT TYPE= 1
K5= 0.996
KH= 1.000

PARAMETER	MEAN	COV	DESIGN POINT	SENSITIVITY FACTOR	PARTIAL FACTOR	1/PARTIAL FACTOR
PDGN (KN)	627.220	5.000	660.778	-0.255	1.054	0.949
PRO (KN)	229.111	11.700	167.481	0.626	0.731	1.368
ETA	0.270	13.800	0.175	0.737	0.647	1.545

BETA= 4.201
PF= 0.13294E-04

B_t (P_{ft})	Load Bias	Load COV	Distribution	$\gamma_m\gamma_{fL} = \gamma_G$	$\Sigma\omega_i P_{fi}$	β_{min}	β_{max}
	1.075	5	Normal	1.428	0.012500	2.00	3.30
2.24	1.15	10	Normal	1.581	0.012500	2.00	3.20
(0.0125)	1.0	30	Normal	1.689	0.012500	2.04	2.93

TABLE 4.11 Optimised Partial Factors : HSFG Bolts Acting in Friction

Equal weighting for clean mill scale, blast cleaned and coated faying surfaces.

GROUP	Ref.	Throat dimen.	measured yield stress	Prupt	No. of tests	Remarks
–	20	given	not given	given	18	
–	21	given	not given	given	5	
–	22	nominal	not given	–	23	average results given
10	24	given	given	given	135	Cruciform test pieces
–	23	given	not given	given	456	The International
11	23	given	given	given	152	Test Series

TABLE 4.12 Summary of Data for Welded Joints

Variable	Sample Size	Mean	COV %	Distribution
Weld Area/Nominal	5292*	.95	21.5	Lognormal
	198	1.27	16.5	Lognormal
Yield Stress/Nominal	-	1.125	8	Lognormal
X_m end fillets	163	1.437	12.85	Lognormal
X_m side fillets	50	2.071	12.85	Lognormal
X_m combined	74	1.780	9.96	Lognormal
Dead Load		1.075	5	Normal
Live		1.15	10	Normal
Environmental		1.0	30	Normal

* first choice

TABLE 4.13 Summary of Proposed Statistical Definitions for Welded Joints.

TABLE 4.14

RELIABILITY ANALYSIS RESULTS
WELDED CONNECTIONS

GROUP 10 NO 1

END FILLET

ARAMETER	MEAN	COV	DESIGN POINT	SENSITIVITY FACTOR	PARTIAL FACTOR	1/PARTIAL FACTOR
DGN (KN)	115.458	5.000	116.998	-0.108	1.013	0.987
1 (MM2)	486.850	21.500	239.928	0.956	0.493	2.029
2 (MM2)	0.000	0.000	0.000	0.000	0.000	0.000
5 (MM2)	0.000	0.000	0.000	0.000	0.000	0.000
Y (N/MM2)	298.224	8.000	293.282	0.069	0.983	1.017
M	1.434	12.067	1.317	0.264	0.918	1.089

BETA= 2.467
PF= 0.68078E-02

TABLE 4.15

RELIABILITY ANALYSIS RESULTS
WELDED CONNECTIONS

GROUP 11 IB3 NL

SIDE FILLET

PARAMETER	MEAN	COV	DESIGN POINT	SENSITIVITY FACTOR	PARTIAL FACTOR	1/PARTIAL FACTOR
PDGN (KN)	210.606	5.000	213.139	-0.077	1.012	0.988
A1 (MM2)	0.000	0.000	0.000	0.000	0.000	0.000
A2 (MM2)	1545.000	21.500	528.402	0.976	0.342	2.924
A5 (MM2)	0.000	0.000	0.000	0.000	0.000	0.000
SY (N/MM2)	369.837	8.000	363.608	0.055	0.983	1.017
XM	2.071	12.855	1.897	0.199	0.916	1.092

BETA= 3.137
PF= 0.85270E-03

TABLE 4.16

RELIABILITY ANALYSIS RESULTS
WELDED CONNECTIONS

GROUP 11 IIIB NL

COMBINED FILLETS

PARAMETER	MEAN	COV	DESIGN POINT	SENSITIVITY FACTOR	PARTIAL FACTOR	1/PARTIAL FACTOR
PDGN (KN)	467.284	5.000	478.162	-0.120	1.023	0.977
A1 (MM2)	1181.000	21.500	346.642	0.849	0.294	3.407
A2 (MM2)	1178.000	21.500	742.273	0.444	0.630	1.587
A5 (MM2)	0.000	0.000	0.000	0.000	0.000	0.000
SY (N/MM2)	369.837	8.000	358.910	0.087	0.970	1.030
XM	1.780	9.965	1.612	0.245	0.906	1.104

BETA= 3.871
PF= 0.54220E-04

TABLE 4.17

OPTIMISATION RESULTS : FILLET WELDS

WELD AREA COV: 21.5%
DISTRIBUTION: Lognormal

β_t (φ_{ft})	Load Bias	Load COV	Distribution	$\gamma_m\gamma_{fL}$	$\Sigma\omega_i P_{fi}$	β_{min}	β_{max}
5.5	1.015	5	N	2.898	2.500×10^{-8}	5.24	8.12
(2.5×10^{-8})	1.15	10	N	3.299	2.501×10^{-8}	5.24	7.89
	1.0	30	N	3.964	2.501×10^{-8}	5.24	7.36

Size of data set : 287

TABLE 4.18

OPTIMISATION RESULTS : FILLET WELDS

WELD AREA COV: 16.5%
DISTRIBUTION: Lognormal

β_t (ρ_{ft})	Load Bias	Load COV	Distribution	$\gamma_m\gamma_{fL}$	$\Sigma\omega_i P_{fi}$	β_{min}	β_{max}
5.5	1.015	5	N	2.332	2.501×10^{-8}	5.24	8.15
(2.5×10^{-8})	1.15	10	N	2.679	2.501×10^{-8}	5.24	7.87
	1.0	30	N	3.300	2.501×10^{-8}	5.24	7.28

The size of the data set was 287.

Code	Bolt Type	μ = O.5	μ = O.35
AISC	1 (A325*)	2.54	1.8O
	2 (A49O)	2.7O	1.89
BS54OO:Pt. 3	1	1.82	1.82
	2	1.82	1.82
Present	1	1.71	1.71
	2	1.71	1.71

* bolt diameters up to 1 inch

Table 4.19 Comparison of global factors of safety against slip under operating conditions

Code	Stress Expression	End	Side
AISC*	IIW	4.33	3.06
	Simple	3.06	3.06
BS5400:Pt. 3	IIW	1.83	3.49
	Simple	2.24	3.49
Present k_1=1.4 and γ_m=2.0	IIW	3.19	6.07
	Simple	3.91	6.07
Present k_1=1.0 and γ_m=1.26	IIW	3.12	4.25
	Simple	3.82	4.25

* allowing 33% on environmental loads

Table 4.20 Global factors on electrode yield strength for fillet welds in mild steel under operating conditions of loading.

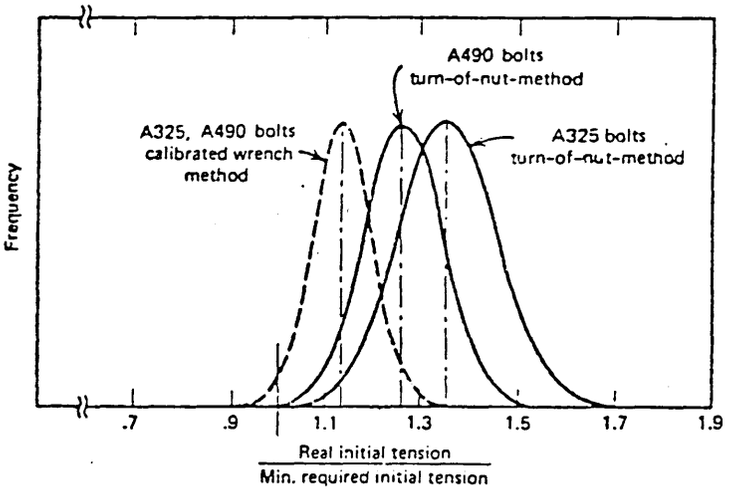

Distribution curves $T_i/T_{i\,spec}$ for different installation procedures.

FIGURE 4.1 Bolt tension distributions. Reproduced from Reference 7

Figure 5.8 p.82

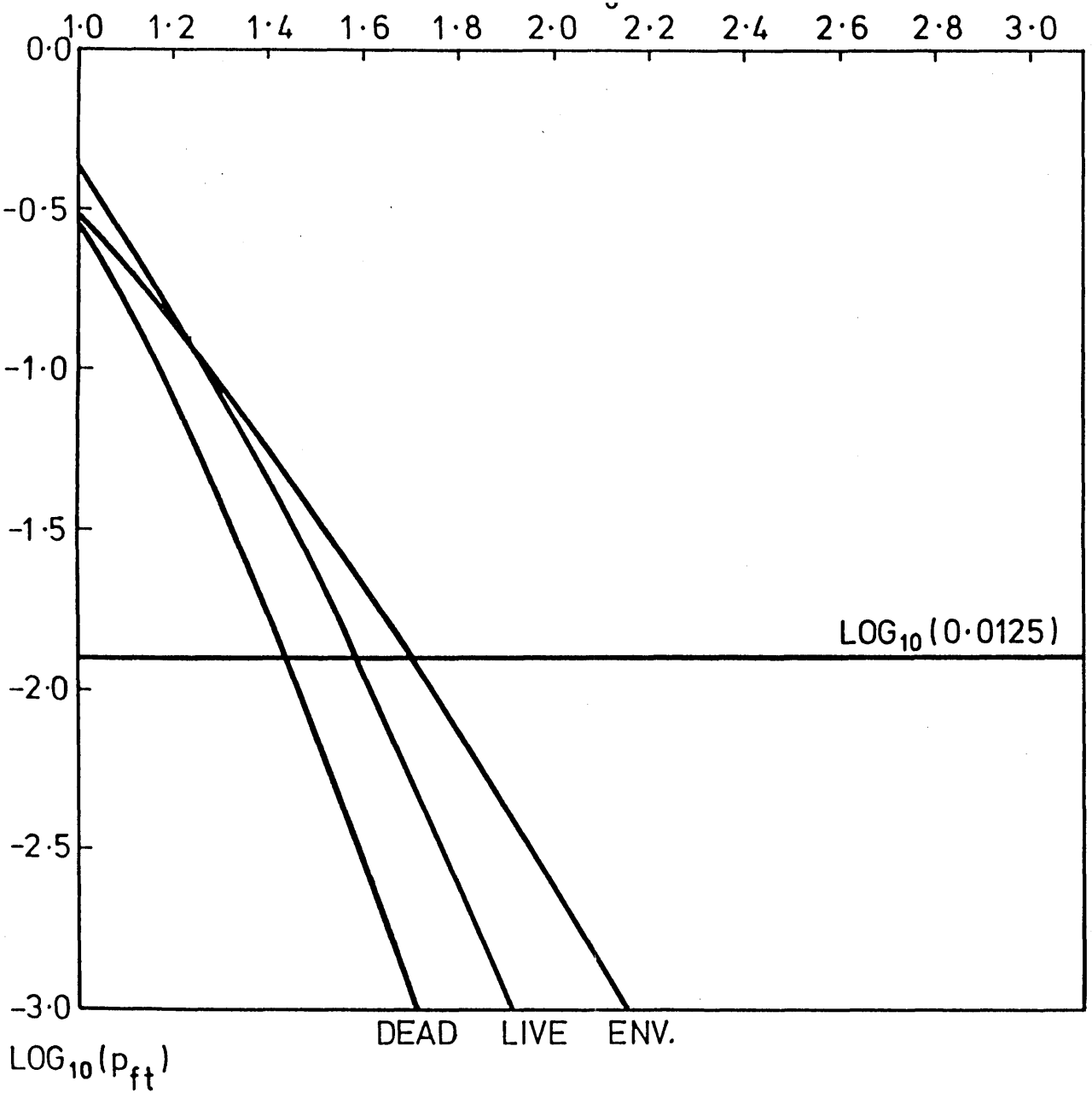

Fig. 4.2

BOLTED CONNECTIONS - γ_G vs. $LOG_{10}(p_{ft})$

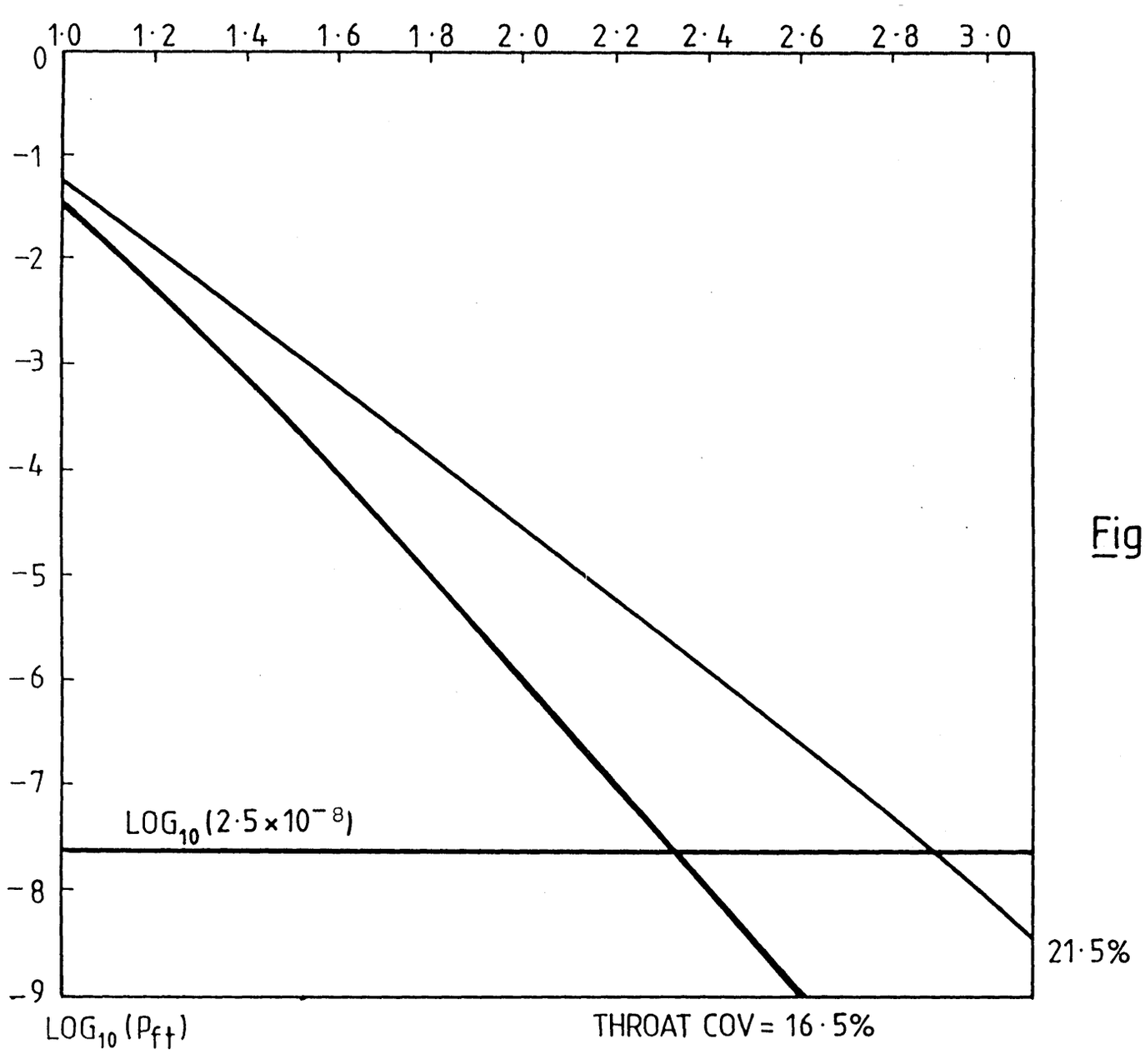

Fig. 4.3 WELDED CONNECTIONS

γ_g VS. $LOG_{10}(P_{ft})$

DEAD LOAD CASE

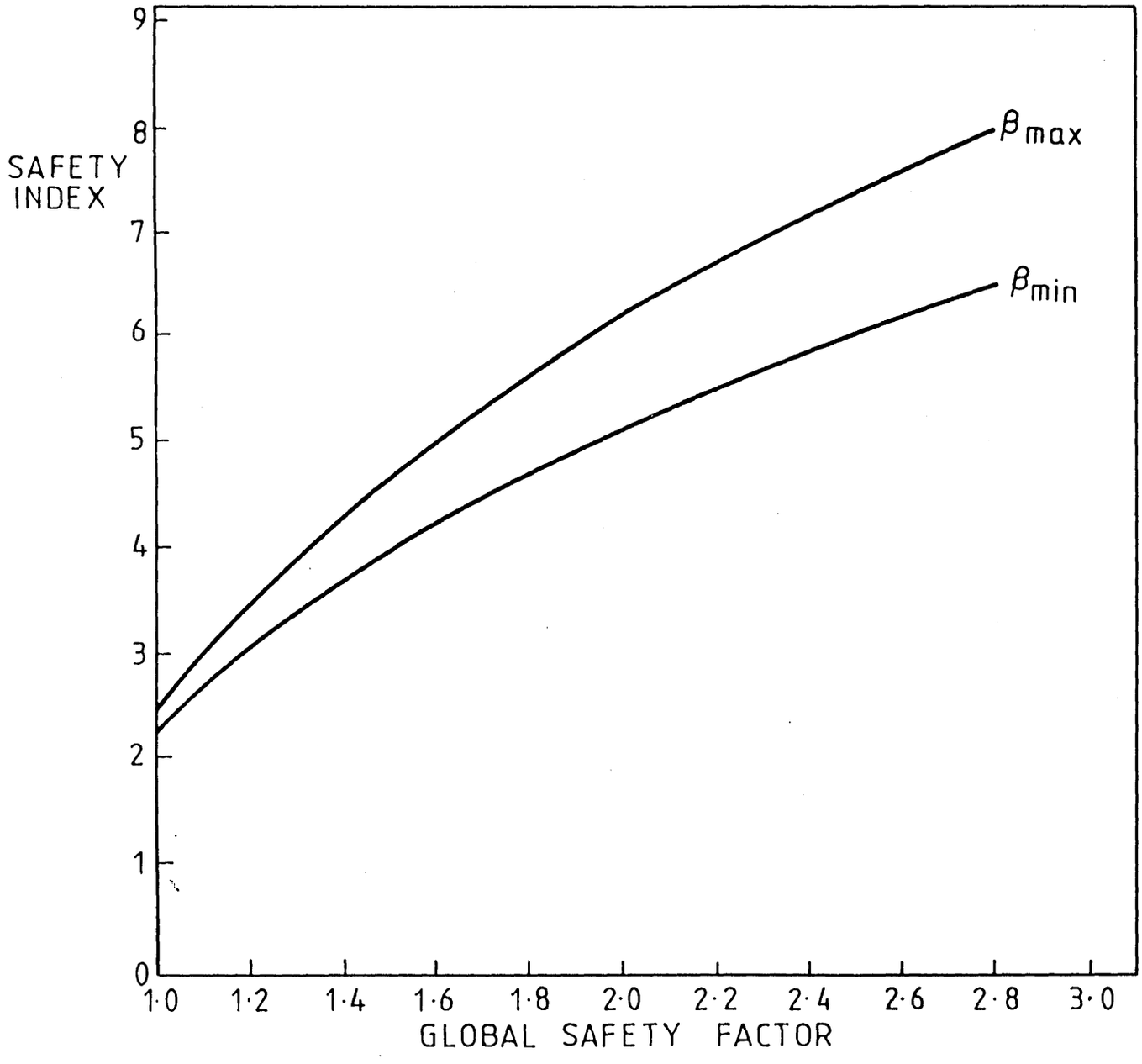

Fig. 4.4 SAFETY INDEX vs. GLOBAL SAFETY FACTOR

k FOR END FILLETS: 1·0
WELD AREA DEFINITION: 21·5%
LOG NORMAL, DEAD LOAD CASE.

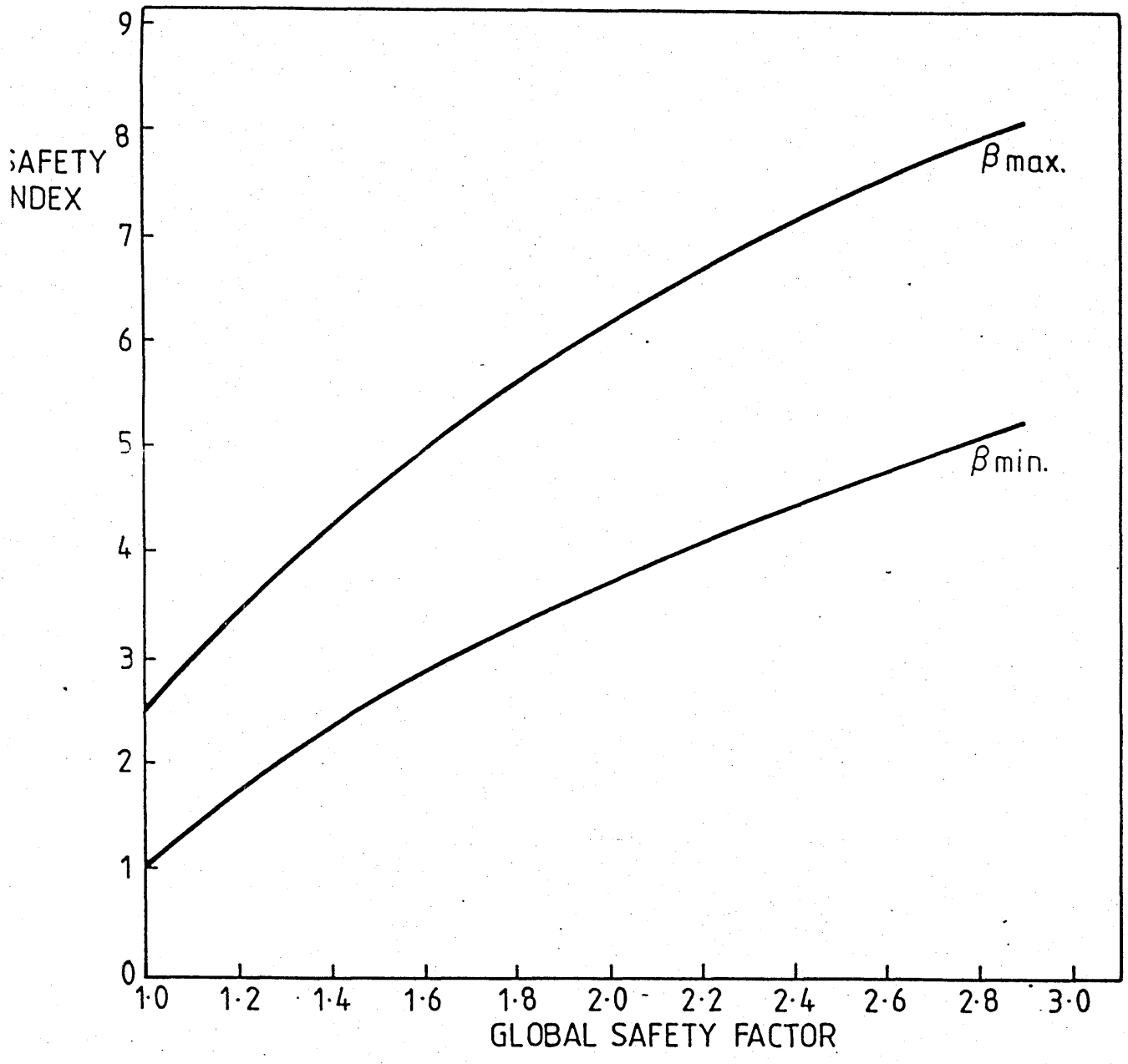

Fig. 4.5 SAFETY INDEX v.s. GLOBAL SAFETY FACTOR.

k FOR END FILLETS 1·4
WELD AREA DEFINITION: 21·5% LOG NORMAL, DEAD LOAD CASE.

APPENDIX A

SAMPLE CALCULATIONS

Calculations for the design capacity of HSFG bolted joint acting in friction and of welded joints are presented in the following pages. In each case the capacity is found from multiplying the characteristic resistance by the assumed bias on dead load, 1.075 and dividing by the trial values of material and load partial factors.

The notation used is consistent with Appendix B.

1. BOLTED JOINT : GROUP 1 K131 (Ref. 8)

IS	=	1
NS	=	2
NB	=	13
IB	=	2
BD	=	22.225 mm ($^{7}/_{8}$ inch)
ETA	=	0.349 but IB=2 $\therefore$ 0.9 ETA = 0.314
PRO	=	246.7 kN but IB=2 $\therefore$ 0.85 PRO = 209.73 kN
LENGTH	=	802.64 > 15BD
$\therefore$ K5	=	1 - (LENGTH - 15 BD)/200 BD
	=	1 - (802.64 - 15 X 22.225)/200 X 22.225
	=	0.894
PDGN	=	NB NSx.85 PROx.9 ETAxK5xKHx1.075/$Y_m Y_{fL}$
	=	13x2x209.73x0.314x0.894x1.0x1.075/1.3x1.3
PDGN	=	974.5 kN

2. END FILLET : GROUP 10 1 (REF. 24)

$A1 = 486.85\ mm^2$

$SY = 298.224\ N/mm^2$

$PDGN = 115.46\ KN$

$$PDGN = \frac{1.075 \times A1 \times 1.4(SY + 455)}{\gamma_m \gamma_{fL} \quad 2\sqrt{2}}$$

$$= \frac{1.075 \times 436.85 \times 1.4 \times (298.224) + 455)}{1.3 \times 1.3 \times 1000 \times 2 \times \sqrt{2}}$$

PDGN = 115.46 KN

3. SIDE FILLET : GROUP 11 IB3 NL (REF. 23)

$A2 = 1545.0\ mm^2$

$SY = 369.837\ N/mm^2$

$PDGN = 210.6\ KN$

$$PDGN = \frac{1.075 \times 0.9 \times A2\ (SY+455)}{2\sqrt{3} \quad \gamma_m \gamma_{fL}}$$

$$= \frac{1.075 \times 0.9 \times 1545(369.84 + 455)}{2\sqrt{3} \times 1.3 \times 1.3 \times 1000}$$

PDGN = 210.6 KN

4. COMBINED END AND SIDE FILLETS : GROUP 11 IIIB NL (REF. 23)

$A1 = 1181.0\ mm^2$

$A2 = 1178.0\ mm^2$

$SY = 369.84\ N/mm^2$

$PDGN = 467.28\ KN$

$$PDGN = \frac{1.075 \times 1.4 \times A1(SY + 455)}{2\sqrt{2} \times \gamma_m \times \gamma_{fL}} + \frac{1.075 \times 0.9 \times A2(SY+455)}{2\sqrt{3}\ \gamma_m \quad \gamma_{fL}}$$

$$= \frac{1.075\ (369.84 + 455)}{2 \times 1.3 \times 1.3 \times 1000} \left(\frac{1.4 \times 1181.0}{\sqrt{2}} + \frac{0.9 \times 1178}{\sqrt{3}} \right)$$

PDGN = 467.28 KN

APPENDIX B

DATA

The data used for the evaluation of material factors for HSFG bolted joints acting in friction and fillet welds are presented in the following pages. The notation and source references are indicated below:

GR — Group Number

IS — faying surface type as follows:

1 Clean mill scale

2 Blast cleaned

3 Grit blasted, etch primer

4 Shot blasted, etch primer

5 Grit blasted, zinc silicate paint

6 Shot blasted, zinc spray (powder process)

8 Grit blasted, zinc spray (wire process)

9 Grit blasted, aluminium spray (powder process)

10 Vinyl wash or linseed oil

1B — Bolt Type

NS — Number of shear planes

NB — Number of bolts

ETA — Coefficient of friction for faying surface type (x 0.9 if IB = 2)

PRO — Proof Load (x 0.85 if IB = 2)

PCL — Bolt clamping force or preload

BS — Bolt diameter

LENGTH — Length of joint between centres of end bolts. In the case of Reference 12 the maximum length is given.

K5	Reduction factor for long joints
PDGN	Design friction capacity for $\gamma_m = \gamma_{fL} = 1.3$ and Load bias = 1.075
P_{SLIP}	Experimental slip load
BETA	Reliability index for dead load case with $\gamma_m = \gamma_{fL} = 1.3$
IFIL	1 end fillets
	2 side fillets
	3 combined end and side fillets
A1	Throat area of end fillet
A2	Throat area of side fillet
A5	Throat area of combined fillets
SY	Yield stress of parent metal
PRUPT	Rupture load of joint
XM	Modelling factor = PRUPT x 1.075/PDGN x 1.3 x 1.3

GROUP	REFERENCE
1	8
2	13
3	9
4	14
5	15
6	10
7	11
8	6
9	12
10	24
11	23

NO	GR	NAME	IS	NS	NB	IB	ETA	PRO	PCL	BD	LENGTH	KS	PDGN	PSLIP	BETA
								KN	KN	MM	MM		KN	KN	
1	1	K42A	1	2	8	2	0.314	209.730	266.988	22.225	266.700	1.000	670.456	1557.430	3.055
2	1	K42B	1	2	8	2	0.314	209.730	264.763	22.225	266.700	1.000	670.456	1397.237	3.055
3	1	K42C	1	2	8	2	0.314	209.730	255.864	22.225	266.700	1.000	670.456	1441.735	3.055
4	1	K42D	1	2	8	2	0.314	209.730	265.208	22.225	266.700	1.000	670.456	1704.273	3.055
5	1	K131	1	2	13	2	0.314	209.730	290.127	22.225	802.640	0.894	974.471	2411.791	3.055
6	1	K132	1	2	13	2	0.314	209.730	290.127	22.225	1600.199	0.750	817.118	2580.884	3.055
7	1	K133	1	2	13	2	0.314	209.730	289.682	22.225	1600.199	0.750	817.118	2438.490	3.055
8	1	K191	1	2	19	2	0.314	209.730	291.462	22.225	1600.199	0.750	1194.250	3764.530	3.055
9	2	J42A	2	2	8	2	0.450	274.975	382.683	25.400	266.700	1.000	1259.353	2135.904	2.844
10	2	J42B	2	2	8	2	0.450	274.975	355.984	25.400	266.700	1.000	1259.353	2251.598	2.844
11	2	J42C	2	2	8	2	0.450	274.975	355.984	25.400	266.700	1.000	1259.353	2304.996	2.844
12	2	J42D	2	2	8	2	0.450	274.975	355.984	25.400	266.700	1.000	1259.353	1993.510	2.844
13	2	J071	2	2	7	2	0.450	209.730	317.271	22.225	533.400	0.955	802.649	1201.446	2.844
14	2	J072	2	2	7	2	0.450	209.730	310.151	22.225	533.400	0.955	802.649	1619.727	2.844
15	2	J131	2	2	13	2	0.450	209.730	313.711	22.225	1065.800	0.835	1303.329	2758.875	2.844
16	2	J132	2	2	13	2	0.450	346.272	491.703	28.575	1066.800	0.888	2289.290	4334.112	2.844
17	2	J171	2	2	17	2	0.450	209.730	296.356	22.225	1422.400	0.755	1541.062	3248.354	2.844
18	2	J172	2	2	17	2	0.450	209.730	297.691	22.225	1422.400	0.755	1541.062	3114.860	2.844
19	2	J251	2	2	25	2	0.450	209.730	320.831	22.225	2133.599	0.750	2251.265	0.000	2.844
20	2	J252	2	2	25	2	0.450	209.730	320.386	22.225	2133.599	0.750	2251.265	4173.910	2.844
21	3	D31	1	2	6	1	0.349	174.641	0.000	22.225	177.800	1.000	465.238	769.815	3.055
22	3	D41	1	2	8	1	0.349	174.641	0.000	22.225	266.700	1.000	620.317	1027.458	3.055
23	3	D51	1	2	10	1	0.349	174.641	0.000	22.225	355.600	0.995	771.519	1535.181	3.055
24	3	D61	1	2	12	1	0.349	174.641	0.000	22.225	444.500	0.975	907.213	1469.323	3.055
25	3	D71	1	2	14	1	0.349	174.641	0.000	22.225	533.400	0.955	1036.704	1587.688	3.055
26	3	D81	1	2	16	1	0.349	174.641	0.000	22.225	622.300	0.935	1159.992	2464.299	3.055
27	3	D91	1	2	18	1	0.349	174.641	0.000	22.225	711.200	0.915	1277.077	1771.910	3.055
28	3	D101	1	2	20	1	0.349	174.641	0.000	22.225	800.100	0.895	1387.958	2481.653	3.055
29	3	D701	1	2	14	1	0.349	174.641	0.000	22.225	533.400	0.955	1036.704	3167.812	3.055
30	3	D801	1	2	16	1	0.349	174.641	0.000	22.225	622.300	0.935	1159.992	2652.080	3.055
31	3	D901	1	2	18	1	0.349	174.641	0.000	22.225	711.200	0.915	1277.077	3792.119	3.055
32	3	D1001	1	2	20	1	0.349	174.641	0.000	22.225	800.100	0.895	1387.958	4439.563	3.055
33	3	D10	1	2	20	1	0.349	174.641	0.000	22.225	800.100	0.895	1387.958	3956.317	3.055
34	3	D13A	1	2	26	1	0.349	174.641	0.000	22.225	800.100	0.895	1804.347	4185.480	3.055
35	3	D13	1	2	26	1	0.349	174.641	0.000	22.225	1066.800	0.835	1683.385	4185.480	3.055
36	3	D16	1	2	32	1	0.349	174.641	0.000	22.225	1333.500	0.775	1922.982	1637.526	3.055

NO	GR	NAME	IS	NS	NR	IP	ETA	PRO	PCL	BD	LENGTH	KS	PDGN	PSLIP	BETA
								KN	KN	MM	MM		KN	KN	
37	3	L2	1	1	4	1	0.349	174.641	216.260	22.225	88.900	1.000	155.079	275.888	3.055
38	3	L5	1	1	10	1	0.349	174.641	215.370	22.225	355.600	0.995	385.760	476.128	3.055
39	3	L7	1	1	14	1	0.349	174.641	216.705	22.225	533.400	0.955	518.353	867.711	3.055
40	3	L10	1	1	20	1	0.349	174.641	216.260	22.225	800.100	0.895	693.980	1557.430	3.055
41	4	F42A	2	2	8	1	0.500	251.334	307.036	28.575	266.700	1.000	1278.974	1762.121	2.844
42	4	F42B	2	2	8	1	0.500	251.334	311.486	28.575	266.700	1.000	1278.974	1477.333	2.844
43	4	F42C	2	2	8	1	0.500	251.334	304.811	28.575	266.700	1.000	1278.974	1450.635	2.844
44	4	F42D	2	2	8	1	0.500	251.334	313.711	28.575	266.700	1.000	1278.974	1521.831	2.844
45	4	F42E	2	2	8	1	0.500	251.334	307.036	28.575	266.700	1.000	1278.974	1539.631	2.844
46	4	F42G	2	2	8	1	0.500	251.334	311.486	28.575	266.700	1.000	1278.974	1771.020	2.844
47	4	F191	2	2	19	1	0.500	251.334	347.084	28.575	1600.199	0.795	2414.862	3648.835	2.844
48	4	F192	2	2	19	1	0.500	251.334	335.515	28.575	1600.199	0.795	2414.862	3942.522	2.844
49	4	F131	2	2	13	1	0.500	251.334	383.573	28.575	1065.800	0.888	1846.253	3292.852	2.844
50	4	F111	2	2	11	1	0.500	251.334	371.558	28.575	889.000	0.919	1616.925	2669.880	2.844
51	5	SOH11	10	2	8	1	0.270	229.111	257.643	25.400	400.050	0.996	627.220	1290.442	4.201
52	5	SOH12	10	2	8	1	0.270	229.111	200.241	25.400	400.050	0.996	627.220	889.960	4.201
53	5	SOH13	10	2	8	1	0.270	229.111	271.883	25.400	400.050	0.996	627.220	1201.446	4.201
54	5	SOH21	2	2	8	1	0.500	229.111	210.253	25.400	400.050	0.996	1161.518	1308.241	2.844
55	5	SOH22	2	2	8	1	0.500	229.111	200.241	25.400	400.050	0.996	1161.518	1379.438	2.844
56	5	SOH23	2	2	8	1	0.500	229.111	200.241	25.400	400.050	0.996	1161.518	1512.932	2.844
57	5	SOH31	10	2	8	1	0.270	229.111	226.940	25.400	400.050	0.996	627.220	934.458	4.201
58	5	SOH32	10	2	8	1	0.270	229.111	219.153	25.400	400.050	0.996	627.220	943.357	4.201
59	5	SOH33	10	2	8	1	0.270	229.111	234.060	25.400	400.050	0.996	627.220	978.956	4.201
60	5	SOH41	10	2	8	1	0.270	229.111	255.307	25.400	400.050	0.996	627.220	912.209	4.201
61	5	SOH42	10	2	8	1	0.270	229.111	215.259	25.400	400.050	0.996	627.220	956.707	4.201
62	5	SOH43	10	2	8	1	0.270	229.111	246.408	25.400	400.050	0.996	627.220	1223.695	4.201
63	5	SOH51	10	2	8	1	0.270	229.111	285.899	25.400	400.050	0.996	627.220	1156.948	4.201
64	5	SOH52	10	2	8	1	0.270	229.111	266.988	25.400	400.050	0.996	627.220	1156.948	4.201
65	5	SOH53	10	2	8	1	0.270	229.111	270.881	25.400	400.050	0.996	627.220	1067.952	4.201
66	5	SSH11	2	2	8	1	0.500	229.111	200.241	25.400	400.050	0.996	813.063	1535.191	2.844
67	5	SSH12	2	2	8	1	0.500	229.111	200.241	25.400	400.050	0.996	813.063	1601.928	2.844
68	5	SSH13	2	2	8	1	0.500	229.111	200.241	25.400	400.050	0.996	813.063	1597.478	2.844
69	6	10	1	2	4	1	0.349	200.241	200.686	25.400	152.400	1.000	355.623	550.792	3.055
70	6	11	1	2	4	1	0.349	200.241	199.351	25.400	152.400	1.000	355.623	542.404	3.055
71	6	12A	1	2	4	1	0.349	200.241	200.686	25.400	152.400	1.000	355.623	536.812	3.055
72	6	12B	1	2	4	1	0.349	200.241	200.686	25.400	152.400	1.000	355.623	612.301	3.055
73	6	13	1	2	4	1	0.349	200.241	200.686	25.400	152.400	1.000	355.623	480.894	3.055
74	6	14	1	2	4	1	0.349	200.241	201.576	25.400	152.400	1.000	355.623	690.596	3.055
75	6	15A	1	2	4	1	0.349	200.241	200.686	25.400	152.400	1.000	355.623	603.914	3.055
76	6	15B	1	2	4	1	0.349	200.241	199.351	25.400	152.400	1.000	355.623	615.097	3.055
77	6	16	1	2	4	1	0.349	200.241	198.906	25.400	152.400	1.000	355.623	651.444	3.055
78	6	17	1	2	4	1	0.349	200.241	198.461	25.400	152.400	1.000	355.623	525.629	3.055
79	6	18	1	2	4	1	0.349	200.241	197.571	25.400	152.400	1.000	355.623	738.117	3.055
80	6	19	1	2	4	1	0.349	200.241	199.796	25.400	152.400	1.000	355.623	603.914	3.055
81	6	20	1	2	4	1	0.349	200.241	198.461	25.400	152.400	1.000	355.623	704.566	3.055
82	6	21	1	2	4	1	0.349	200.241	199.796	25.400	152.400	1.000	355.623	679.403	3.055
83	6	31	1	2	4	1	0.349	106.795	107.685	25.400	152.400	1.000	189.666	349.487	3.055
84	6	32	1	2	4	1	0.349	106.795	107.685	25.400	152.400	1.000	189.666	324.324	3.055

NO	GR	NAME	IS	NS	NB	IB	ETA	PRO	PCL	BD	LENGTH	KS	PDGN	PSLIP	BETA
								KN	KN	MM	MM		KN	KN	
85	6	33	1	2	4	1	0.349	106.795	105.905	25.400	152.400	1.000	189.666	293.569	3.055
86	6	37	1	2	4	1	0.349	160.193	158.858	25.400	152.400	1.000	284.498	444.548	3.055
87	6	38	1	2	4	1	0.349	160.193	162.418	25.400	152.400	1.000	284.498	564.771	3.055
88	6	39	1	2	4	1	0.349	160.193	157.523	25.400	152.400	1.000	284.498	452.935	3.055
89	6	54	2	2	4	1	0.500	200.241	159.303	25.400	152.400	1.000	509.489	732.525	2.844
90	6	55	2	2	4	1	0.500	200.241	198.906	25.400	152.400	1.000	509.489	629.077	2.844
91	6	56	2	2	4	1	0.500	200.241	198.906	25.400	152.400	1.000	509.489	967.380	2.844
92	6	57	1	2	4	1	0.349	160.193	159.303	25.400	152.400	1.000	284.498	472.506	3.055
93	6	58	1	2	4	1	0.349	160.193	165.978	25.400	152.400	1.000	284.498	520.037	3.055
94	6	59	1	2	4	1	0.349	160.193	163.753	25.400	152.400	1.000	284.498	506.058	3.055
95	6	63	1	2	6	1	0.349	189.117	188.672	25.400	152.400	1.000	503.799	826.187	3.055
96	6	64	1	2	6	1	0.349	189.117	190.006	25.400	152.400	1.000	503.799	792.636	3.055
97	6	65	1	2	6	1	0.349	189.117	189.117	25.400	152.400	1.000	503.799	910.064	3.055
98	6	66	1	2	8	1	0.349	189.117	188.672	25.400	152.400	1.000	671.733	1017.706	3.055
99	6	67	1	2	8	1	0.349	189.117	188.672	25.400	152.400	1.000	671.733	961.788	3.055
100	6	68	1	2	8	1	0.349	189.117	189.562	25.400	152.400	1.000	671.733	967.380	3.055
101	6	77	1	2	4	1	0.349	189.117	188.672	25.400	152.400	1.000	335.866	466.915	3.055
102	6	78	1	2	4	1	0.349	189.117	189.562	25.400	152.400	1.000	335.866	475.303	3.055
103	6	79A	1	2	4	1	0.349	189.117	189.562	25.400	152.400	1.000	335.866	592.730	3.055
104	6	79B	1	2	4	1	0.349	189.117	187.782	25.400	152.400	1.000	335.866	500.465	3.055
105	6	80	1	2	4	1	0.349	189.117	188.227	25.400	152.400	1.000	335.866	559.179	3.055
106	6	81	1	2	4	1	0.349	189.117	188.672	25.400	152.400	1.000	335.866	427.772	3.055
107	6	82	1	2	4	1	0.349	189.117	189.562	25.400	152.400	1.000	335.866	520.037	3.055
108	6	101	1	2	4	1	0.349	189.117	187.782	25.400	152.400	1.000	335.866	525.629	3.055
109	6	102	1	2	4	1	0.349	189.117	187.782	25.400	152.400	1.000	335.866	461.323	3.055
110	6	103	1	2	4	1	0.349	189.117	186.892	25.400	152.400	1.000	335.866	422.180	3.055
111	6	104	1	2	4	1	0.349	189.117	188.672	25.400	152.400	1.000	335.866	559.179	3.055
112	6	105	1	2	4	1	0.349	189.117	187.782	25.400	152.400	1.000	335.866	570.362	3.055
113	6	106	1	2	4	1	0.349	189.117	189.562	25.400	152.400	1.000	335.866	570.362	3.055
114	6	107	1	2	4	1	0.349	231.390	231.390	25.400	152.400	1.000	410.942	556.383	3.055
115	6	108	1	2	4	1	0.349	231.390	234.504	25.400	152.400	1.000	410.942	517.241	3.055
116	6	109	1	2	4	1	0.349	231.390	231.390	25.400	152.400	1.000	410.942	455.731	3.055
117	6	128A	1	2	4	1	0.349	189.117	184.222	25.400	152.400	1.000	335.866	464.119	3.055
118	6	128B	1	2	4	1	0.349	189.117	189.562	25.400	152.400	1.000	335.866	394.221	3.055
119	6	129	1	2	4	1	0.349	189.117	187.782	25.400	152.400	1.000	335.866	374.650	3.055
120	6	130	1	2	4	1	0.349	189.117	188.227	25.400	152.400	1.000	335.866	478.098	3.055
121	6	131	1	2	4	1	0.349	189.117	189.562	25.400	152.400	1.000	335.866	478.098	3.055
122	6	132	1	2	4	1	0.349	189.117	188.227	25.400	152.400	1.000	335.866	383.038	3.055
123	6	133	1	2	4	1	0.349	189.117	191.341	25.400	152.400	1.000	335.866	413.793	3.055
124	6	137	1	2	4	1	0.349	231.390	231.835	25.400	152.400	1.000	410.942	609.506	3.055
125	6	138	1	2	4	1	0.349	231.390	233.170	25.400	152.400	1.000	410.942	623.485	3.055
126	6	139	1	2	4	1	0.349	231.390	233.615	25.400	152.400	1.000	410.942	595.526	3.055
127	7	E41A	1	2	8	1	0.349	174.655	227.385	22.225	266.700	1.000	620.365	1165.847	3.055
128	7	E41B	1	2	8	1	0.349	174.655	227.830	22.225	266.700	1.000	620.365	881.060	3.055
129	7	E41C	1	2	8	1	0.349	174.655	223.825	22.225	266.700	1.000	620.365	1156.948	3.055
130	7	E41E	1	2	8	1	0.349	174.655	229.610	22.225	266.700	1.000	620.365	1254.843	3.055
131	7	E41F	1	2	8	1	0.349	174.655	214.925	22.225	266.700	1.000	620.365	1201.446	3.055
132	7	E41G	1	2	8	1	0.349	174.655	227.830	22.225	266.700	1.000	620.365	1254.843	3.055

NO	GR	NAME	IS	NS	NR	IR	ETA	PRO	PCL	BD	LENGTH	KS	PDGN	PSLIP	RETA
								KN	KN	MM	MM		KN	KN	
133	7	E41	1	2	8	1	0.349	174.655	216.260	22.225	265.700	1.000	620.365	1112.450	3.055
134	7	E71	1	2	14	1	0.349	174.655	214.925	22.225	533.400	0.995	1336.783	1779.920	3.055
135	7	E101	1	2	20	1	0.349	174.655	217.595	22.225	800.100	0.995	1388.065	2732.177	3.055
136	7	E131	1	2	26	1	0.349	174.655	214.035	22.225	1066.800	0.995	1483.515	3666.675	3.055
137	7	E161	1	2	32	1	0.349	174.655	214.480	22.225	1333.500	0.995	1923.129	4574.391	3.055
138	7	E46	1	2	24	1	0.349	174.655	217.595	22.225	265.700	1.000	1841.094	3550.940	3.055
139	7	E74	1	2	28	1	0.349	174.655	216.260	22.225	533.400	0.995	2073.568	4058.217	3.055
140	7	E741	1	2	28	1	0.349	174.655	214.925	22.225	533.400	0.995	2073.568	3025.864	3.055
141	8	L19	3	2	2	1	0.250	160.000	160.600	22.000	228.600	1.000	101.775	200.300	4.200
142	8	L22	3	2	2	1	0.250	160.000	159.600	22.000	228.600	1.000	101.775	209.200	4.200
143	8	L25	3	2	2	1	0.250	160.000	159.800	22.000	228.600	1.000	101.775	196.300	4.200
144	8	L21	3	2	2	2	0.225	178.500	207.900	22.000	228.600	1.000	102.189	284.000	4.200
145	8	L23	3	2	2	2	0.225	178.500	209.400	22.000	228.600	1.000	102.189	284.000	4.200
146	8	L26	3	2	2	2	0.225	178.500	209.100	22.000	228.600	1.000	102.189	267.000	4.200
147	8	L20	3	2	2	2	0.225	221.000	258.200	22.000	228.600	1.000	126.519	337.800	4.200
148	8	L24	3	2	2	2	0.225	221.000	258.200	22.000	228.600	1.000	126.519	297.900	4.200
149	8	L27	3	2	2	2	0.225	221.000	258.000	22.000	228.600	1.000	126.519	324.800	4.200
150	8	L28	4	2	2	1	0.250	160.000	160.800	22.000	228.600	1.000	101.775	191.300	4.200
151	8	L31	4	2	2	1	0.250	160.000	160.800	22.000	228.600	1.000	101.775	187.300	4.200
152	8	L34	4	2	2	1	0.250	160.000	160.800	22.000	228.600	1.000	101.775	182.300	4.200
153	8	L29	4	2	2	2	0.225	178.500	209.200	22.000	228.600	1.000	102.189	236.100	4.200
154	8	L32	4	2	2	2	0.225	178.500	209.200	22.000	228.600	1.000	102.189	222.200	4.200
155	8	L33	4	2	2	2	0.225	178.500	209.200	22.000	228.600	1.000	102.189	258.100	4.200
156	8	L30	4	2	2	2	0.225	221.000	259.100	22.000	228.600	1.000	126.519	302.900	4.200
157	8	L33	4	2	2	2	0.225	221.000	259.100	22.000	228.600	1.000	126.519	297.900	4.200
158	8	L36	4	2	2	2	0.225	221.000	259.100	22.000	228.600	1.000	126.519	301.900	4.200
159	8	L37	5	2	2	1	0.350	160.000	160.000	22.000	228.600	1.000	142.485	249.100	4.200
160	8	L40	5	2	2	1	0.350	160.000	160.400	22.000	228.600	1.000	142.485	306.900	4.200
161	8	L43	5	2	2	1	0.350	160.000	159.900	22.000	228.600	1.000	142.485	274.000	4.200
162	8	L38	5	2	2	2	0.315	178.500	206.700	22.000	228.600	1.000	143.064	328.800	4.200
163	8	L41	5	2	2	2	0.315	178.500	209.200	22.000	228.600	1.000	143.064	410.500	4.200
164	8	L44	5	2	2	2	0.315	178.500	209.200	22.000	228.600	1.000	143.064	269.000	4.200
165	8	L39	5	2	2	2	0.315	221.000	259.100	22.000	228.600	1.000	177.127	328.800	4.200
166	8	L42	5	2	2	2	0.315	221.000	259.100	22.000	228.600	1.000	177.127	314.900	4.200
167	8	L45	5	2	2	2	0.315	221.000	259.100	22.000	228.600	1.000	177.127	351.700	4.200
168	8	L46	6	2	2	1	0.350	160.000	160.800	22.000	228.600	1.000	142.485	306.900	4.200
169	8	L49	6	2	2	1	0.350	160.000	160.400	22.000	228.600	1.000	142.485	319.800	4.200
170	8	L52	6	2	2	1	0.350	160.000	160.400	22.000	228.600	1.000	142.485	357.700	4.200
171	8	L47	6	2	2	2	0.315	178.500	209.200	22.000	228.600	1.000	143.064	377.600	4.200
172	8	L50	6	2	2	2	0.315	178.500	209.200	22.000	228.600	1.000	143.064	391.600	4.200
173	8	L53	6	2	2	2	0.315	178.500	209.200	22.000	228.600	1.000	143.064	387.600	4.200
174	8	L48	6	2	2	2	0.315	221.000	259.100	22.000	228.600	1.000	177.127	431.400	4.200
175	8	L51	6	2	2	2	0.315	221.000	259.100	22.000	228.600	1.000	177.127	448.400	4.200
176	8	L54	6	2	2	2	0.315	221.000	259.100	22.000	228.600	1.000	177.127	364.700	4.200
177	8	L1	7	2	2	1	0.400	160.000	160.400	22.000	228.600	1.000	162.840	297.900	4.200
178	8	L6	7	2	2	1	0.400	160.000	160.400	22.000	228.600	1.000	162.840	324.800	4.200
179	8	L7	7	2	2	1	0.400	160.000	160.400	22.000	228.600	1.000	162.840	306.900	4.200
180	8	L2	7	2	2	2	0.360	178.500	209.200	22.000	228.600	1.000	163.502	400.600	4.200

NO	GR	NAME	IS	LS	NB	IB	ETA	PRO	PCL	BD	LENGTH	KS	PDGN	PSLIP	BETA
								KN	KN	MM	MM		KN	KN	
181	[illegible]	L5	7	[illegible]	[illegible]	2	0.360	178.500	209.200	22.000	228.600	1.000	163.502	429.400	4.200
182	[illegible]	L8	7	[illegible]	[illegible]	2	0.360	178.500	209.200	22.000	228.600	1.000	163.502	462.300	4.200
183	[illegible]	L3	7	[illegible]	[illegible]	2	0.360	221.000	259.100	22.000	228.600	1.000	202.431	613.800	4.200
184	[illegible]	L4	7	[illegible]	[illegible]	2	0.360	221.000	259.100	22.000	228.600	1.000	202.431	533.100	4.200
185	[illegible]	L9	7	[illegible]	[illegible]	2	0.360	221.000	259.100	22.000	228.600	1.000	202.431	573.900	4.200
186	[illegible]	L10	8	[illegible]	[illegible]	1	0.400	160.000	160.800	22.000	228.600	1.000	162.840	369.700	4.200
187	[illegible]	L13	8	[illegible]	[illegible]	1	0.400	160.000	161.200	22.000	228.600	1.000	162.840	404.500	4.200
188	[illegible]	L16	8	[illegible]	[illegible]	1	0.400	160.000	160.800	22.000	228.600	1.000	162.840	387.600	4.200
189	[illegible]	L11	8	[illegible]	[illegible]	2	0.360	178.500	209.200	22.000	228.600	1.000	163.502	431.400	4.200
190	[illegible]	L14	8	[illegible]	[illegible]	2	0.360	178.500	209.200	22.000	228.600	1.000	163.502	435.400	4.200
191	[illegible]	L17	8	[illegible]	[illegible]	2	0.360	178.500	209.200	22.000	228.600	1.000	163.502	480.300	4.200
192	[illegible]	L12	8	[illegible]	[illegible]	2	0.360	221.000	260.100	22.000	228.600	1.000	202.431	502.200	4.200
193	[illegible]	L15	8	[illegible]	[illegible]	2	0.360	221.000	259.100	22.000	228.600	1.000	202.431	467.300	4.200
194	[illegible]	L18	8	[illegible]	[illegible]	2	0.360	221.000	259.100	22.000	228.600	1.000	202.431	471.300	4.200
195	[illegible]	L55	9	[illegible]	[illegible]	1	0.500	160.000	160.400	22.000	228.600	1.000	203.550	467.300	4.200
196	[illegible]	L58	9	[illegible]	[illegible]	1	0.500	160.000	160.400	22.000	228.600	1.000	203.550	399.600	4.200
197	[illegible]	L61	9	[illegible]	[illegible]	1	0.500	160.000	160.400	22.000	228.600	1.000	203.550	399.600	4.200
198	[illegible]	L56	9	[illegible]	[illegible]	2	0.450	178.500	209.200	22.000	228.600	1.000	204.377	494.200	4.200
199	[illegible]	L59	9	[illegible]	[illegible]	2	0.450	178.500	209.200	22.000	228.600	1.000	204.377	507.200	4.200
200	[illegible]	L62	9	[illegible]	[illegible]	2	0.450	178.500	209.200	22.000	228.600	1.000	204.377	516.100	4.200
201	[illegible]	L57	9	[illegible]	[illegible]	2	0.450	221.000	259.100	22.000	228.600	1.000	253.038	568.900	4.200
202	[illegible]	L60	9	[illegible]	[illegible]	2	0.450	221.000	259.100	22.000	228.600	1.000	253.038	601.800	4.200
203	[illegible]	L63	9	[illegible]	[illegible]	2	0.450	221.000	259.100	22.000	228.600	1.000	253.038	639.700	4.200
204	9	B1	1	[illegible]	30	1	0.349	174.655	215.237	22.225	533.400	0.955	2221.681	5508.852	3.055
205	9	B2	1	[illegible]	25	1	0.349	174.655	215.548	22.225	355.600	0.995	1928.946	4658.938	3.055
206	9	B3	1	[illegible]	21	1	0.349	174.655	215.815	22.225	266.700	1.000	1550.911	4053.767	3.055
207	9	B4	1	[illegible]	23	1	0.349	174.655	210.654	22.225	355.600	0.995	1774.630	3782.330	3.055
208	9	B5	1	[illegible]	20	1	0.349	174.655	211.143	22.225	355.600	0.995	1543.156	2709.928	3.055
209	9	B6	1	[illegible]	18	1	0.349	174.655	210.609	22.225	177.800	1.000	1395.820	2994.715	3.055
210	9	A3	1	[illegible]	16	1	0.349	229.165	269.213	25.400	304.800	1.000	1627.963	3751.181	3.055
211	9	G1	1	[illegible]	12	1	0.349	251.191	347.084	28.575	203.200	1.000	1338.327	4093.815	3.055

NO	GR	NAME	IFIL	A1	A2	SY	PRUPT	PDGN	XM	BETA
				MM2	MM2	N/MM2	KN	KN		
1	10	1	1	486.850	0.000	298.224	261.927	115.458	1.443	2.467
2	10	2	1	532.350	0.000	298.224	279.192	126.248	1.407	2.467
3	10	3	1	511.875	0.000	298.224	377.979	121.393	1.981	2.467
4	10	4	1	530.740	0.000	380.628	318.727	139.637	1.452	2.465
5	10	5	1	533.120	0.000	380.628	314.803	140.263	1.428	2.465
6	10	6	1	583.100	0.000	380.628	342.271	153.412	1.419	2.465
7	10	7	1	562.875	0.000	431.640	343.350	157.132	1.390	2.464
8	10	8	1	555.750	0.000	431.640	348.942	155.143	1.431	2.464
9	10	9	1	577.125	0.000	431.640	357.771	161.110	1.413	2.464
10	10	10	1	566.475	0.000	298.224	286.550	134.341	1.357	2.467
11	10	11	1	555.100	0.000	298.224	307.544	131.644	1.486	2.467
12	10	12	1	534.625	0.000	298.224	296.262	126.788	1.486	2.467
13	10	13	1	559.120	0.000	380.628	310.585	147.103	1.343	2.465
14	10	14	1	603.200	0.000	380.628	307.838	158.701	1.234	2.465
15	10	15	1	598.560	0.000	380.628	321.277	157.480	1.298	2.465
16	10	16	1	586.845	0.000	431.640	338.151	163.823	1.313	2.464
17	10	17	1	601.335	0.000	431.640	344.429	167.868	1.305	2.464
18	10	18	1	627.900	0.000	431.640	366.109	175.284	1.329	2.464
19	10	19	1	549.780	0.000	298.224	279.291	130.382	1.363	2.467
20	10	20	1	602.140	0.000	298.224	279.291	142.799	1.244	2.467
21	10	21	1	637.840	0.000	298.224	297.733	151.266	1.252	2.467
22	10	22	1	457.040	0.000	298.224	224.747	108.388	1.319	2.467
23	10	23	1	470.960	0.000	298.224	231.516	111.690	1.319	2.467
24	10	24	1	477.920	0.000	298.224	205.814	113.340	1.155	2.467
25	10	25	1	565.245	0.000	298.224	319.708	134.050	1.517	2.467
26	10	26	1	605.790	0.000	298.224	326.477	143.665	1.446	2.467
27	10	27	1	608.175	0.000	298.224	337.856	144.231	1.490	2.467
28	10	28	1	558.035	0.000	380.628	324.417	146.818	1.406	2.465
29	10	29	1	584.380	0.000	380.628	341.780	153.749	1.414	2.465
30	10	30	1	603.540	0.000	380.628	343.546	158.790	1.376	2.465
31	10	31	1	604.910	0.000	431.640	354.435	168.866	1.335	2.464
32	10	32	1	613.120	0.000	431.640	342.859	171.158	1.274	2.464
33	10	33	1	658.625	0.000	431.640	346.980	183.861	1.200	2.464
34	10	34	1	496.080	0.000	298.224	281.841	117.647	1.524	2.467
35	10	35	1	503.235	0.000	298.224	277.132	119.344	1.477	2.467

NO	GR	NAME	IFIL	A1	A2	SY	PRUPT	PDGN	XM	BETA
				MM2	MM2	N/MM2	KN	KN		
36	10	36	1	503.235	0.000	298.224	277.231	119.344	1.478	2.467
37	10	37	1	528.190	0.000	380.628	316.372	138.966	1.448	2.465
38	10	38	1	518.630	0.000	380.628	297.930	136.450	1.389	2.465
39	10	39	1	509.070	0.000	380.628	281.449	133.935	1.337	2.465
40	10	40	1	516.460	0.000	431.640	301.952	144.175	1.332	2.464
41	10	41	1	348.800	0.000	431.640	209.836	97.371	1.371	2.464
42	10	42	1	635.460	0.000	431.640	289.787	177.394	1.039	2.464
43	10	43	1	631.040	0.000	298.224	265.066	149.653	1.127	2.467
44	10	44	1	603.200	0.000	298.224	276.053	143.051	1.228	2.467
45	10	45	1	621.760	0.000	298.224	302.344	147.452	1.304	2.467
46	10	46	1	559.120	0.000	380.628	277.427	147.103	1.200	2.465
47	10	47	1	619.440	0.000	380.628	306.759	162.973	1.197	2.465
48	10	48	1	654.240	0.000	380.628	314.705	172.129	1.163	2.465
49	10	48	1	654.240	0.000	380.628	314.705	172.129	1.163	2.465
50	10	49	1	580.000	0.000	431.640	361.498	161.912	1.420	2.464
51	10	50	1	584.640	0.000	431.640	315.195	163.208	1.228	2.464
52	10	51	1	591.600	0.000	431.640	329.322	165.151	1.268	2.464
53	10	52	1	589.280	0.000	298.224	306.464	139.750	1.395	2.467
54	10	53	1	547.520	0.000	298.224	308.524	129.846	1.511	2.467
55	10	54	1	547.520	0.000	298.224	310.585	129.846	1.522	2.467
56	10	55	1	556.800	0.000	380.628	306.268	146.493	1.330	2.465
57	10	56	1	549.840	0.000	380.628	303.521	144.662	1.335	2.465
58	10	57	1	552.160	0.000	380.628	320.198	145.272	1.402	2.465
59	10	58	1	596.240	0.000	431.640	362.970	166.446	1.387	2.464
60	10	59	1	575.360	0.000	431.640	356.299	160.617	1.411	2.464
61	10	60	1	570.720	0.000	431.640	353.356	159.322	1.411	2.464
62	10	61	1	475.475	0.000	298.224	250.449	112.760	1.413	2.467
63	10	62	1	520.975	0.000	298.224	264.772	123.551	1.363	2.467
64	10	63	1	520.975	0.000	298.224	278.996	123.551	1.436	2.467
65	10	64	1	549.780	0.000	380.628	327.850	144.646	1.442	2.465
66	10	65	1	566.440	0.000	380.628	319.708	149.029	1.365	2.465
67	10	66	1	561.680	0.000	380.628	325.398	147.777	1.401	2.465
68	10	67	1	574.785	0.000	431.640	348.549	160.456	1.382	2.464
69	10	68	1	561.680	0.000	431.640	351.198	156.798	1.425	2.464
70	10	69	1	574.785	0.000	431.640	349.530	160.456	1.386	2.464

NO	GR	NAME	IFIL	A1	A2	SY	PRUPT	PDGN	XM	BETA
				MM2	MM2	N/MM2	KN	KN		
71	10	70	1	516.425	0.000	298.224	274.974	122.472	1.428	2.467
72	10	71	1	511.875	0.000	298.224	296.360	121.393	1.553	2.467
73	10	72	1	509.600	0.000	298.224	280.075	120.853	1.474	2.467
74	10	73	1	533.600	0.000	380.628	300.186	140.389	1.360	2.465
75	10	74	1	547.520	0.000	380.628	303.227	144.051	1.339	2.465
76	10	75	1	542.880	0.000	380.628	301.461	142.831	1.343	2.465
77	10	76	1	572.355	0.000	431.640	334.717	159.778	1.333	2.464
78	10	77	1	596.505	0.000	431.640	329.714	166.520	1.259	2.464
79	10	78	1	591.675	0.000	431.640	355.024	165.171	1.367	2.464
80	10	79	1	584.675	0.000	298.224	302.442	138.657	1.387	2.467
81	10	80	1	616.525	0.000	298.224	287.237	146.211	1.250	2.467
82	10	82	1	521.220	0.000	380.628	302.148	137.132	1.402	2.465
83	10	83	1	502.180	0.000	380.628	311.762	132.123	1.501	2.465
84	10	84	1	514.080	0.000	380.628	310.683	135.253	1.461	2.465
85	10	85	1	544.920	0.000	431.640	313.626	152.119	1.311	2.464
86	10	86	1	554.480	0.000	431.640	295.968	154.788	1.216	2.464
87	10	87	1	509.070	0.000	431.640	321.376	142.112	1.438	2.464
88	10	88	1	539.175	0.000	298.224	254.471	127.867	1.266	2.467
89	10	89	1	536.900	0.000	298.224	280.370	127.327	1.401	2.467
90	10	90	1	532.350	0.000	298.224	275.072	126.248	1.386	2.467
91	10	91	1	524.055	0.000	380.628	289.787	137.878	1.337	2.465
92	10	92	1	504.560	0.000	380.628	286.452	132.749	1.373	2.465
93	10	93	1	504.560	0.000	380.628	278.996	132.749	1.337	2.465
94	10	94	1	535.360	0.000	431.640	334.521	149.451	1.424	2.464
95	10	95	1	506.680	0.000	431.640	320.493	141.444	1.441	2.464
96	10	96	1	547.310	0.000	431.640	325.005	152.787	1.353	2.464
97	10	97	1	590.240	0.000	298.224	338.739	139.977	1.539	2.467
98	10	98	1	595.000	0.000	298.224	317.550	141.106	1.431	2.467
99	10	99	1	606.900	0.000	298.224	334.325	143.928	1.478	2.467
100	10	100	1	562.695	0.000	380.628	351.198	148.044	1.509	2.465
101	10	101	1	579.600	0.000	380.628	362.577	152.492	1.512	2.465
102	10	102	1	615.825	0.000	380.628	361.793	162.022	1.420	2.465
103	10	103	1	573.580	0.000	431.640	405.938	160.120	1.613	2.464
104	10	104	1	606.900	0.000	431.640	394.264	169.422	1.480	2.464
105	10	105	1	595.000	0.000	431.640	390.732	166.100	1.496	2.464

NO	GR	NAME	IFIL	A1	A2	SY	PRUPT	PDGN	XM	BETA
				MM2	MM2	N/MM2	KN	KN		
106	10 106		1	523.600	0.000	298.224	280.468	124.173	1.437	2.467
107	10 107		1	530.740	0.000	298.224	293.319	125.867	1.482	2.467
108	10 108		1	554.540	0.000	298.224	284.686	131.511	1.377	2.467
109	10 109		1	555.450	0.000	380.628	338.837	146.138	1.475	2.465
110	10 110		1	550.620	0.000	380.628	334.815	144.867	1.470	2.465
111	10 111		1	543.375	0.000	380.628	330.106	142.961	1.469	2.465
112	10 112		1	593.960	0.000	431.640	360.027	165.809	1.381	2.464
113	10 113		1	567.615	0.000	431.640	347.568	158.455	1.395	2.464
114	10 114		1	550.850	0.000	431.640	357.672	153.775	1.480	2.464
115	10 115		1	521.020	0.000	298.224	318.236	123.561	1.638	2.467
116	10 116		1	535.360	0.000	298.224	330.891	126.962	1.658	2.467
117	10 117		1	535.360	0.000	298.224	324.711	126.962	1.627	2.467
118	10 118		1	500.850	0.000	380.628	320.395	131.773	1.547	2.465
119	10 119		1	486.540	0.000	380.628	331.970	128.008	1.650	2.465
120	10 120		1	498.465	0.000	380.628	326.673	131.145	1.584	2.465
121	10 121		1	486.820	0.000	431.640	351.885	135.900	1.647	2.464
122	10 122		1	498.870	0.000	431.640	390.438	139.264	1.783	2.464
123	10 123		1	503.690	0.000	431.640	382.884	140.610	1.732	2.464
124	10 124		1	544.920	0.000	298.224	274.386	129.229	1.351	2.467
125	10 125		1	523.410	0.000	298.224	282.332	124.128	1.447	2.467
126	10 126		1	554.480	0.000	298.224	267.420	131.497	1.294	2.467
127	10 127		1	546.060	0.000	380.628	273.306	143.667	1.210	2.465
128	10 128		1	538.875	0.000	380.628	292.338	141.777	1.312	2.465
129	10 129		1	548.455	0.000	380.628	285.667	144.297	1.259	2.465
130	10 130		1	518.840	0.000	431.640	300.676	144.839	1.320	2.464
131	10 131		1	528.360	0.000	431.640	288.414	147.496	1.244	2.464
132	10 132		1	512.775	0.000	431.640	319.021	143.146	1.418	2.464
133	10 133		1	555.450	0.000	298.224	346.391	131.727	1.673	2.467
134	10 134		1	557.865	0.000	298.224	349.923	132.299	1.682	2.467
135	10 135		1	603.750	0.000	298.224	342.859	143.181	1.523	2.467
136	11 IB	NL	3	445.000	1123.000	369.837	894.672	268.648	2.118	4.004
137	11 IB1	NL	1	392.000	0.000	369.837	235.440	101.803	1.471	2.465
138	11 IB2	NL	2	0.000	1243.000	369.837	622.935	169.439	2.339	3.137
139	11 IB3	NL	2	0.000	1545.000	369.837	681.795	210.606	2.059	3.137
140	11 IIA	NL	3	398.000	1378.000	369.837	804.420	291.202	1.757	3.893

NO	GR	NAME	IFIL	A1	A2	SY	PRUPT	PDGN	XM	BETA
				MM2	MM2	N/MM2	KN	KN		
141	11	IIA1 NL	1	442.000	0.000	369.837	303.129	114.788	1.680	2.465
142	11	IIA2 NL	2	0.000	1392.000	369.837	564.075	189.750	1.891	3.137
143	11	IIA3 NL	2	0.000	1738.000	369.837	660.213	236.915	1.773	3.137
144	11	IIB NL	3	719.000	1235.000	369.837	814.230	355.073	1.459	4.035
145	11	IIB1 NL	1	734.000	0.000	369.837	348.255	190.620	1.162	2.465
146	11	IIB2 NL	2	0.000	1293.000	369.837	531.702	176.255	1.919	3.137
147	11	IIB3 NL	2	0.000	1725.999	369.837	673.947	235.278	1.822	3.137
148	11	IIC NL	3	804.000	996.000	369.837	917.235	344.568	1.693	3.959
149	11	IIC1 NL	1	882.000	0.000	369.837	522.873	229.056	1.452	2.465
150	11	IIC2 NL	2	0.000	961.000	369.837	470.880	130.998	2.286	3.137
151	11	IIC3 NL	2	0.000	1566.000	369.837	657.270	213.468	1.959	3.137
152	11	IIIB NL	3	1181.000	1178.000	369.837	1137.960	467.284	1.549	3.871
153	11	IIIB1 NL	1	1162.000	0.000	369.837	719.073	301.772	1.516	2.465
154	11	IIIB2 NL	2	0.000	1228.000	369.837	529.740	167.394	2.013	3.137
155	11	IIIB3 NL	2	0.000	1272.000	369.837	578.790	173.392	2.123	3.137
156	11	II1B NL	3	525.000	986.000	369.837	740.655	270.749	1.740	4.039
157	11	II2B NL	3	609.000	1098.000	369.837	797.553	307.831	1.648	4.038
158	11	II3B NL	3	533.000	1167.000	369.837	830.907	297.499	1.777	4.031
159	11	II4B NL	3	532.000	1136.000	369.837	735.750	293.014	1.597	4.033
160	11	II5B NL	3	562.000	1092.000	369.837	830.907	294.807	1.793	4.039
161	11	II6B NL	3	588.000	1058.000	369.837	769.104	296.924	1.648	4.038
162	11	II7B NL	3	585.000	1012.000	369.837	779.895	289.875	1.711	4.035
163	11	II8B NL	3	634.000	1146.000	369.837	809.325	320.866	1.604	4.038
164	11	IIB NL	3	612.000	1215.000	369.837	882.900	324.559	1.730	4.039
165	11	IIB NL	3	566.000	1245.000	369.837	851.508	316.702	1.710	4.037
166	11	IIB NL	3	567.000	1126.000	369.837	910.368	300.740	1.926	4.039
167	11	IIB NL	3	532.000	1090.000	369.837	860.337	286.743	1.909	4.037
168	11	IIB NL	3	591.000	1091.000	369.837	889.767	302.202	1.873	4.039
169	11	IB D	3	277.000	1070.000	435.564	780.876	235.148	2.112	3.840
170	11	IB1 D	1	350.000	0.000	435.564	291.357	98.138	1.888	2.464
171	11	IB2 D	2	0.000	982.000	435.564	549.360	144.527	2.418	3.136
172	11	IB3 D	2	0.000	1330.000	435.564	593.505	195.745	1.929	3.136
173	11	IIA D	3	348.000	1285.000	435.564	839.736	286.699	1.863	3.861
174	11	IIA1 D	1	381.000	0.000	435.564	331.578	106.830	1.974	2.464
175	11	IIA2 D	2	0.000	1278.000	435.564	622.935	188.092	2.107	3.136

NO	GR	NAME	IFIL	A1	A2	SY	PRUPT	PDGN	XM	BETA
				MM2	MM2	N/MM2	KN	KN		
176	11	IIA3	D 2	0.000	1645.000	435.564	688.662	242.105	1.809	3.136
177	11	IIB	D 3	532.000	1140.000	435.564	953.532	316.951	1.914	4.035
178	11	IIB1	D 1	538.000	0.000	435.564	409.077	150.852	1.725	2.464
179	11	IIB2	D 2	0.000	1036.000	435.564	505.215	152.475	2.108	3.136
180	11	IIB3	D 2	0.000	1664.999	435.564	672.966	245.049	1.747	3.136
181	11	IIC	D 3	935.000	880.000	435.564	1077.138	391.684	1.749	3.841
182	11	IIC1	D 1	885.000	0.000	435.564	572.904	248.149	1.469	2.464
183	11	IIC2	D 2	0.000	866.000	435.564	432.621	127.455	2.159	3.136
184	11	IIC3	D 2	0.000	1700.000	435.564	684.738	250.200	1.741	3.136
185	11	IIIB	D 3	955.000	990.000	435.564	1147.770	413.481	1.766	3.885
186	11	IIIB1	D 1	970.000	0.000	435.564	806.382	271.983	1.886	2.464
187	11	IIIB2	D 2	0.000	935.000	435.564	425.754	137.610	1.968	3.136
188	11	IIIB3	D 2	0.000	1530.000	435.564	603.315	225.180	1.704	3.136
189	11	IIB	D 3	582.000	1070.000	435.564	902.520	320.669	1.790	4.035
190	11	IIB	D 3	590.000	1190.000	435.564	907.425	340.573	1.695	4.034
191	11	IIB	D 3	550.000	1110.000	435.564	869.166	317.583	1.741	4.034
192	11	IIB	D 3	549.000	1155.000	435.564	926.064	323.926	1.819	4.031
193	11	IIB	D 3	534.000	1045.000	435.564	918.216	303.530	1.924	4.035
194	11	IIB	D 3	582.000	1120.000	435.564	902.520	328.027	1.750	4.035
195	11	IIB	D 3	560.000	1140.000	435.564	921.159	324.802	1.804	4.034
196	11	IIB	D 3	527.000	1140.000	435.564	901.539	315.549	1.817	4.028
197	11	IB	I 3	386.000	1059.000	399.757	833.850	253.474	2.093	3.979
198	11	IB1	I 1	460.000	0.000	399.757	277.132	123.796	1.424	2.464
199	11	IB2	I 2	0.000	1158.000	399.757	562.113	163.578	2.186	3.137
200	11	IB3	I 2	0.000	1460.000	399.757	686.700	206.238	2.118	3.137
201	11	IIA	I 3	382.000	1490.000	399.757	843.660	313.280	1.713	3.837
202	11	IIA1	I 1	563.000	0.000	399.757	358.065	151.515	1.503	2.464
203	11	IIA2	I 2	0.000	1460.000	399.757	663.156	206.238	2.045	3.137
204	11	IIA3	I 2	0.000	1554.000	399.757	698.472	219.517	2.024	3.137
205	11	IIB	I 3	499.000	1145.000	399.757	826.983	296.033	1.777	4.022
206	11	IIB1	I 1	572.000	0.000	399.757	339.426	153.937	1.403	2.464
207	11	IIB2	I 2	0.000	1197.000	399.757	534.645	169.087	2.011	3.137
208	11	IIB3	I 2	0.000	1702.000	399.757	739.674	240.423	1.957	3.137
209	11	IIC	I 3	884.000	1018.000	399.757	1064.385	381.705	1.774	3.931
210	11	IIC1	I 1	932.000	0.000	399.757	570.942	250.821	1.448	2.464

NO	GR	NAME	IFIL	A1	A2	SY	PRUPT	PDGN	XM	BETA
				MM2	MM2	N/MM2	KN	KN		
211	11	IIC2	I	2	0.000	990.000	399.757	495.405	139.847	2.253	3.137
212	11	IIC3	I	2	0.000	1774.000	399.757	756.351	250.594	1.920	3.137
213	11	IIIB	I	3	1076.000	1149.000	399.757	1151.694	451.881	1.621	3.900
214	11	IIIB1	I	1	1038.000	0.000	399.757	559.170	279.347	1.273	2.464
215	11	IIIB2	I	2	0.000	966.000	399.757	461.070	136.456	2.149	3.137
216	11	IIIB3	I	2	0.000	1546.000	399.757	639.612	218.387	1.863	3.137
217	11	IIB	I	3	489.000	1168.000	399.757	776.265	296.591	1.665	4.015
218	11	IIB	I	3	555.000	1175.000	399.757	820.116	315.342	1.654	4.033
219	11	IIB	I	3	537.000	1146.000	399.757	810.698	306.401	1.683	4.032
220	11	IIB	I	3	564.000	1279.000	399.757	877.995	332.454	1.680	4.024
221	11	IIB	I	3	559.000	1281.000	399.757	881.919	331.391	1.693	4.022
222	11	IIB	I	3	553.000	1224.000	399.757	845.033	321.725	1.671	4.028
223	11	IIB	I	3	557.000	1284.000	399.757	876.033	331.277	1.682	4.021
224	11	IIB	I	3	574.000	1105.000	399.757	842.679	310.567	1.726	4.038
225	11	IB	S	3	312.000	974.000	361.989	656.289	211.762	1.971	3.936
226	11	IB1	S	1	281.000	0.000	361.989	227.592	72.281	2.003	2.466
227	11	IB2	S	2	0.000	777.000	361.989	480.690	104.908	2.915	3.137
228	11	IB3	S	2	0.000	1560.000	361.989	663.156	210.627	2.003	3.137
229	11	IIA	S	3	402.000	1243.000	361.989	761.256	271.233	1.785	3.940
230	11	IIA1	S	1	389.000	0.000	361.989	280.566	100.062	1.784	2.466
231	11	IIA2	S	2	0.000	1156.000	361.989	561.132	156.080	2.287	3.137
232	11	IIA3	S	2	0.000	1451.000	361.989	702.396	195.910	2.281	3.137
233	11	IIB	S	3	524.000	987.000	361.989	864.261	268.050	2.051	4.041
234	11	IIB	S	3	582.000	1056.000	361.989	852.489	292.286	1.855	4.039
235	11	IIB	S	3	578.000	1041.000	361.989	792.648	289.231	1.743	4.039
236	11	IIB1	S	1	540.000	0.000	361.989	392.400	138.904	1.797	2.465
237	11	IIB1	S	1	545.000	0.000	361.989	398.286	140.190	1.807	2.465
238	11	IIB1	S	1	583.000	0.000	361.989	399.267	149.965	1.694	2.465
239	11	IIB2	S	2	0.000	1000.000	361.989	466.956	135.017	2.200	3.137
240	11	IIB2	S	2	0.000	1077.000	361.989	482.652	145.414	2.111	3.137
241	11	IIB2	S	2	0.000	964.000	361.989	534.645	130.157	2.613	3.137
242	11	IIB3	S	2	0.000	1550.000	361.989	709.263	209.277	2.156	3.137
243	11	IIB3	S	2	0.000	1472.000	361.989	680.814	198.746	2.179	3.137
244	11	IIB3	S	2	0.000	1476.000	361.989	702.396	199.286	2.242	3.137
245	11	IIC	S	3	860.000	843.000	361.989	1012.392	335.037	1.922	3.863

NO	GR	NAME	IFIL	A1	A2	SY	PRUPT	PDGN	XM	PETA
				MM2	MM2	N/MM2	KN	KN		
246	11	IIC1	S	1	858.000	0.000	361.989	618.070	220.703	1.781	2.466
247	11	IIC2	S	2	0.000	741.000	361.989	465.975	100.048	2.963	3.137
248	11	IIC3	S	2	0.000	1496.000	361.989	705.339	201.986	2.221	3.137
249	11	IIB	S	3	795.000	968.000	361.989	1047.708	335.194	1.988	3.954
250	11	IIIB1	S	1	866.000	0.000	361.989	710.244	222.761	2.028	2.466
251	11	IIIB2	S	2	0.000	1009.000	361.989	463.032	136.233	2.162	3.137
252	11	IIIB3	S	2	0.000	1658.000	361.989	657.270	223.859	1.868	3.137
253	11	IIB	S	3	600.000	1056.000	361.989	931.950	296.916	1.997	4.037
254	11	IIB	S	3	550.000	1016.000	361.989	990.810	278.654	2.262	4.039
255	11	IIB	S	3	451.000	1108.000	361.989	961.380	265.610	2.302	4.011
256	11	IIB	S	3	532.000	1077.000	361.989	1010.430	282.260	2.277	4.038
257	11	IIB	S	3	578.000	985.000	361.989	969.228	281.670	2.189	4.034
258	11	IA	D	3	313.000	1897.000	373.761	853.470	341.492	1.590	3.615
259	11	IA	D	3	331.000	1810.000	373.761	843.660	334.273	1.605	3.668
260	11	IA	D	3	296.000	1631.000	373.761	784.800	300.623	1.661	3.664
261	11	IA1	D	1	327.000	0.000	373.761	176.580	85.326	1.316	2.465
262	11	1A2	D	2	0.000	1732.001	373.761	667.080	237.220	1.789	3.137
263	11	IB	D	3	476.000	1449.000	373.761	784.800	322.665	1.547	3.945
264	11	IB	D	3	372.000	1287.000	373.761	755.370	273.339	1.758	3.893
265	11	IB	D	3	446.000	1502.000	373.761	804.420	322.096	1.589	3.905
266	11	IB1	D	1	395.000	0.000	373.761	225.630	103.070	1.392	2.465
267	11	IB2	D	2	0.000	1262.000	373.761	549.360	172.847	2.022	3.137
268	11	IIA	D	3	345.000	1497.000	373.761	794.610	295.056	1.713	3.786
269	11	IIA	D	3	380.000	1547.000	373.761	824.040	311.037	1.685	3.817
270	11	IIA	D	3	425.000	1468.000	373.761	784.800	311.959	1.600	3.894
271	11	IIA1	D	1	414.000	0.000	373.761	215.820	108.027	1.271	2.465
272	11	IIA2	D	2	0.000	1334.000	373.761	480.690	182.709	1.674	3.137
273	11	IIB	D	3	582.000	1294.000	373.761	863.280	329.095	1.669	4.028
274	11	IIB	D	3	576.000	1210.000	373.761	843.660	316.024	1.698	4.035
275	11	IIB	D	3	563.000	1234.000	373.761	863.280	315.919	1.738	4.030
276	11	IIB1	D	1	599.000	0.000	373.761	333.540	156.301	1.357	2.465
277	11	IIB2	D	2	0.000	1237.000	373.761	500.310	169.423	1.878	3.137
278	11	IIIA	D	3	582.000	1458.000	373.761	1039.860	351.556	1.881	4.006
279	11	IIIA	D	3	750.000	1557.000	373.761	1010.430	408.953	1.572	4.036
280	11	IIIA	D	3	717.000	1465.000	373.761	981.000	387.742	1.609	4.037

NO	GR	NAME	IFIL	A1	A2	SY	PRUPT	PDGN	XM	BETA
				MM2	MM2	N/MM2	KN	KN.		
281	11	IIIA1	D 1	654.000	0.000	373.761	421.830	170.652	1.572	2.465
282	11	IIIA2	D 2	0.000	1348.000	373.761	490.500	184.626	1.690	3.137
283	11	IIB	D 3	880.000	949.000	373.761	961.380	359.601	1.701	3.905
284	11	IIB	D 3	936.000	936.000	373.761	931.950	372.433	1.592	3.872
285	11	IIIB	D 3	911.000	975.000	373.761	1020.240	371.251	1.748	3.902
286	11	IIIB1	D 1	891.000	0.000	373.761	627.840	232.494	1.718	2.465
287	11	IIIB2	D 2	0.000	930.000	373.761	382.590	127.375	1.911	3.137

APPENDIX C

BS4395 and ASTM specifications for HSFG bolts.

TABLE III.—TENSILE REQUIREMENTS FOR FULL-SIZE BOLTS.

Bolt Size, Threads per Inch and Series Designation	Stress Area,[a] sq in.	Tensile Strength,[b] min, lb	Proof Load,[b] Length Measurement Method, lb	Alternate Proof Load, Yield Strength Method, min, lb[b]
Column 1	Column 2	Column 3	Column 4	Column 5
½ - 13 UNC	0.142	17 050	12 050	13 050
⅝ - 11 UNC	0.226	27 100	19 200	20 800
¾ - 10 UNC	0.334	40 100	28 400	30 700
⅞ - 9 UNC	0.462	55 450	39 250	42 500
1 - 8 UNC	0.606	72 700	51 500	55 750
1⅛ - 7 UNC	0.763	80 100	56 450	61 600
1⅛ - 8 UN	0.790	82 950	58 450	64 000
1¼ - 7 UNC	0.969	101 700	71 700	78 500
1¼ - 8 UN	1.000	105 000	74 000	81 000
1⅜ - 6 UNC	1.155	121 300	85 450	93 550
1⅜ - 8 UN	1.233	129 500	91 250	99 870
1½ - 6 UNC	1.405	147 500	104 000	113 800
1½ - 8 UN	1.492	156 700	110 400	120 850

[a] The stress area is calculated as follows:

$$A_s = 0.7854\left(D - \frac{0.9743}{n}\right)^2$$

where:

A_s = stress area,
D = nominal bolt size, and
n = threads per inch.

[b] Loads tabulated are based on the following:

Bolt Size	Column 3	Column 4	Column 5
½, to 1 incl.	120 000 psi	85 000 psi	92 000 psi
1⅛ to 1½, incl.	105 000 psi	74 000 psi	81 000 psi

ASTM A 490

TABLE 5 Tensile Requirements for Full-Size Bolts

Bolt Size, Threads per Inch, and Series Designation	Stress Area,[A] in.² (cm²)	Tensile Load,[B] lbf(kN)		Proof Load,[B] lbf(kN)	Alternative Proof Load,[B] min, lbf(kN)
		min	max	Length Measurement Method	Yield Strength Method
Column 1	Column 2	Column 3	Column 4	Column 5	Column 6
½-13 UNC	0.142 (0.92)	21 300 (95)	24 150 (107)	17 050 (76)	18 500 (82)
⅝-11 UNC	0.226 (1.46)	33 900 (151)	38 400 (171)	27 100 (121)	29 400 (131)
¾-10 UNC	0.334 (2.15)	50 100 (223)	56 800 (253)	40 100 (178)	43 400 (193)
⅞-9 UNC	0.462 (2.98)	69 300 (308)	78 550 (349)	55 450 (247)	60 100 (267)
1-8 UNC	0.606 (3.91)	90 900 (404)	103 000 (458)	72 700 (323)	78 800 (351)
1⅛-7 UNC	0.763 (4.92)	114 450 (509)	129 700 (577)	91 550 (407)	99 200 (441)
1⅛-8 UN	0.790 (5.10)	118 500 (527)	134 300 (597)	94 800 (422)	102 700 (457)
1¼-7 UNC	0.969 (6.25)	145 350 (647)	164 750 (733)	116 300 (517)	126 000 (560)
1¼-8 UN	1.000 (6.45)	150 000 (667)	170 000 (756)	120 000 (534)	130 000 (578)
1⅜-6 UNC	1.155 (7.45)	173 250 (771)	196 350 (873)	138 600 (617)	150 200 (668)
1⅜-8 UN	1.233 (7.95)	185 000 (823)	209 600 (932)	148 000 (658)	160 300 (713)
1½-6 UNC	1.405 (9.06)	210 750 (937)	238 850 (1062)	168 600 (750)	182 600 (812)
1½-8 UN	1.492 (9.63)	223 800 (996)	253 650 (1128)	175 050 (779)	194 000 (863)

[A] The stress area is calculated as follows:

$$A_s = 0.7854\,[D - (0.9743/n)]^2$$

where:
A_s = stress area, in.²,
D = nominal bolt size, and
n = threads per inch.

[B] Loads tabulated and loads to be used for tests of full size bolts larger than 1½ in. in diameter are based on the following:

Bolt Size	Column 3	Column 4	Column 5	Column 6
½ to 1½ in., incl	150 000 psi (1035 MPa)	170 000 psi (1170 MPa)	120 000 psi (825 MPa)	130 000 psi (895 MPa)

TABLE 4. MECHANICAL PROPERTIES OF BOLTS

1	2	3	4	5	6	7	8	9	10	11	12	13	14	15	16
Nominal size and thread diameter	Pitch of thread (coarse pitch series)	Tensile stress area (see Note 1)	Ultimate load (see Note 2) min.		Yield load or load at permanent set limit $R_{0.2\ min}$ (see Note 3) min.		Proof load (see Note 4) min.		Elongation after fracture	Hardness (see Note 5)					
										Brinell HB		Rockwell HRC		Vickers HV 30	
d mm	p mm	A_s mm²	tonne-force (1000 kgf)	kilo-newtons	tonne-force (1000 kgf)	kilo-newtons	tonne-force (1000 kgf)	kilo-newtons	per cent min.	Max.	Min.	Max.	Min.	Max.	Min.
M 12*	1·75	84·3	7·1	69·6	5·45	53·5	5·04	49·4	12	321	255	34	25	330	260
M 16	2·0	157	13·25	130	10·16	99·7	9·39	92·1	12	321	255	34	25	330	260
M 20	2·5	245	20·71	203	15·85	155	14·64	144	12	321	255	34	25	330	260
M 22	2·5	303	25·57	250	19·60	192	18·1	177	12	321	255	34	25	330	260
M 24	3·0	353	29·79	292	22·94	225	21·10	207	12	321	255	34	25	330	260
M 27	3·0	459	33·89	333	26·04	259	23·88	234	12	295	223	30	19	292	225
M 30	3·5	561	41·42	406	31·82	313	29·19	286	12	295	223	30	19	292	225
M 36	4·0	817	60·32	591	46·35	445	42·51	418	12	295	223	30	19	292	225

* Non-preferred. Only to be used for the lighter type of construction where practical conditions, such as material thickness, do not warrant the usage of a larger size bolt than M 12.

NOTE 1. The tensile stress area is calculated from the following formula:

$$A_s = \frac{\pi}{4}\left(\text{mean of effective and minor diameters}\right)^2 = \frac{\pi}{16}\left(\text{effective diameter} + \text{minor diameter}\right)^2$$

NOTE 2. Based on 84·38 kgf/mm² (827 N/mm²) for sizes M 12 to M 24 inclusive and 73·83 kgf/mm² (725 N/mm²) for sizes M 27 to M 36 inclusive.

NOTE 3. Based on 64·7 kgf/mm² (635 N/mm²) for sizes M 12 to M 24 inclusive and 56·73 kgf/mm² (558 N/mm²) for sizes M 27 to M 36 inclusive. Equivalent to stress at permanent set limit $R_{0.2\ min}$.

NOTE 4. Based on 59·77 kgf/mm² (587 N/mm²) for sizes M 12 to M 24 inclusive and 52·04 kgf/mm² (512 N/mm²) for sizes M 27 to M 36 inclusive.

NOTE 5. Hardness values are given for guidance only.

NOTE 6. See Appendix B for method of carrying out: (1) ultimate load test;
(2) yield load (or load at permanent set limit $R_{0.2\ min}$), proof load and elongation tests;
(3) hardness tests.

BS 4395 : Part 2 : 1969

TABLE 4. MECHANICAL PROPERTIES OF BOLTS

1	2	3	4	5	6	7	8	9	10	11	12	13	14	15	16
Nominal size and thread diameter	Pitch of thread ISO metric coarse series	Tensile stress area (see Note 1)	Ultimate load (see Note 2) min.		Load at permanent set limit $R_{0.2\ min}$ (see Note 3) min.		Proof load (see Note 4) min.		Elongation after fracture	Hardness (see Note 5)					
										Brinell HB		Rockwell HRC		Vickers HV 30	
d mm	p mm	A_s mm²	tonne force (1000 kgf)	kilo-newtons	tonne force (1000 kgf)	kilo-newtons	tonne force (1000 kgf)	kilo-newtons	% min.	max.	min.	max.	min.	max.	min.
M 16	2·0	157	15·7	154·1	14·13	138·7	12·45	122·2	9	365	280	38	27	380	280
M 20	2·5	245	24·5	240·0	22·05	216	19·41	190·4	9	365	280	38	27	380	280
M 22	2·5	303	30·3	296·5	27·2	266	24·0	235·5	9	365	280	38	27	380	280
M 24	3·0	353	35·3	346	31·8	312	28·0	274·6	9	365	280	38	27	380	280
M 27	3·0	459	45·9	450	41·4	406	36·3	356	9	365	280	38	27	380	280
M 30	3·5	561	56·1	550	50·5	495	44·4	435	9	365	280	38	27	380	280
M 33	3·5	694	69·4	680	62·4	612	55·0	540	9	365	280	38	27	380	280

NOTE 1. The tensile stress area is calculated from the following formula:

$$A_s = \pi/4\ (\text{mean of pitch (effective) and minor diameters})^2 = \pi/16\ (\text{pitch (effective) diameter} + \text{minor diameter})^2$$

NOTE 2. Based on 100 kgf/mm² (981 N/mm²) for all sizes.

NOTE 3. Based on 90 kgf/mm² (882 N/mm²) for all sizes.

NOTE 4. Based on 79·2 kgf/mm² (776 N/mm²) for all sizes.

NOTE 5. Hardness values are given for guidance only.

NOTE 6. See Appendix B for method of carrying out:
(1) ultimate load test,
(2) load at permanent set limit ($R_{0.2\ min.}$) proof load and elongation tests,
(3) hardness tests.

SECTION 5

FRACTURE MECHANICS CONCEPTS AND BACKGROUND TO THE CTOD DESIGN CURVE

5.1 Introduction

The major part of this Section follows the development of fracture mechanics from Griffith in the 1920's to the PD6493 Design Curve, published in 1980. The developments since 1980 will also be introduced. The ability of the fracture models to predict applied crack opening displacement (COD) will be reviewed and the uncertainties associated with the models and assessment variables will be described. In the light of this discussion the suitability of a model for use in a failure function for reliability analysis of defect assessment will be considered.

Most of the earlier development was concerned with linear elastic fracture mechanics (LEFM). This approach is suitable for sub-critical crack growth due to fatigue loading and for the failure of purely brittle materials: its application to lower strength ductile materials where extensive plasticity preceeds and accompanies fracture is however less appropriate. The more recent development has been concerned with elastic-plastic fracture mechanics (EPFM) where failure initiation and subsequent crack advance occurs under elastic-plastic conditions. EPFM has developed to a stage where there are recommended procedures such as crack-tip opening displacement (CTOD) for failure assessments of defects in fusion welded joints.

5.2 Elastic Strain Energy Release Rate

The earliest engineering approach to describe the fracture phenomenum was by Griffith[1] in 1920. He proposed that if the rate of change of elastic strain energy was greater than or equal to the rate of change in the energy required to create new crack surfaces then unstable fracture would occur by increasing the crack length. The requirement was expressed as

$$\frac{dU_e}{da} \geqslant \frac{dW}{da} \qquad (5.1)$$

where U_e is the elastic strain energy of the system

$$= -\tfrac{1}{2} \frac{\sigma^2 \pi a^2}{E'}$$

a is half the crack length

σ is the nominal applied stress

$E' = E$ for plane stress

$E' = E/(1-\nu^2)$ for plane strain

E is Young's modulus

ν is Poisson's ratio

W is the work required to create new surfaces

$= 2aT_e$

T_e is the specific surface tension

The strain energy release rate dU_e/da was regarded as characterising the potential for fracture and was symbolised by G:

$$G = \frac{dU_e}{da} = \frac{\sigma^2 \pi a}{E'} \qquad (5.2)$$

The level at which fracture takes place was designated G_c, the critical strain energy release rate, and was found to be a constant material property for any particular strain rate and temperature.

The critical stress level, the stress below which brittle fracture in a material containing a critical crack of length $2a_c$, would not initiate, would therefore have been

$$\sigma_c = (2E'T_e/\pi a_c)^{\frac{1}{2}} \qquad (5.3)$$

Furthermore for any given stress level the limiting crack size could have been calculated.

The Griffith model, validated by his experiments using glass, has become the basis for modern fracture mechanics. The limitations of his model were:

1) the material is entirely brittle.
2) the material considered was a large plate of unit thickness containing a very small through crack in the form of a flat ellipse so that no boundary or size effects are imposed other than the crack size.
3) the condition analysed is the onset of instability disregarding events prior to and after it.
4) material properties E and T_e are assumed constant.

Most metals exhibit plastic deformation before and during fracture. In 1947 Irwin[2] modified the Griffith approach to attempt to account for surface plastic energy absorption T_p

$$G = \frac{\sigma^2 \pi a}{E} = 2(T_e + T_p) \qquad (5.4)$$

In 1952 Irwin and Kies[3] postulated that fracture would occur if the elastic strain energy equalled the work done by a remotely applied load P to cause an incremental displacement δ at the crack tip

$$U_e = P\delta/2 = P^2C/2 \qquad (5.5)$$

where C is the linear elastic compliance of the specimen. The strain energy release rate is found by differentiating the elastic strain energy

$$\frac{dU_e}{da} = G = \frac{P^2}{2}\frac{dC}{da} \qquad (5.6)$$

It was anticipated that by measuring the linear elastic compliance of similar specimens which contained different crack lengths it would be possible to evaluate dC/da as a function of crack length. By substituting the appropriate value of load and dC/da at initiation the material parameter G_c could then be determined.

5.3 The Stress Intensity Factor (SIF)

In 1939 Westergaard[4] developed the mathematical functions for the stress field in the vicinity of an elliptical internal void. Sneddon[5] used these to calculate the rate of elastic strain energy and presented a series of solutions for the linear elastic stress at the tip of a sharp crack. In 1957 Irwin[6] expressed the stress distribution near to the crack tip in a form inversely proportional to the square root of the radial distance, r, from the crack tip (Fig. 4.1).

$$\sigma_{ij} = \frac{K}{\sqrt{rk}} F_{ij}(\theta) \qquad (5.7)$$

where σ_{ij} is the direct stress magnitude in the x, y and z coordinate direction at any point.

k is a constant.

$F_{ij}(\theta)$ is a function of the angle of inclination θ to the crack plane and is dependent on the overall geometry.

K here is a function of the applied stress, crack length and geometry. K can be considered as a measure of the amplitude of the stress field singularity and is called the stress intensity factor (SIF).

The stress intensity factor at the tip of a crack in a loaded body is unique for the particular mode of loading. The three principal types of loading are shown in Figure 5.2. They are

MODE I Normal displacement of the crack surfaces relative to one another (opening mode).

MODE II In plane displacement of the crack surfaces perpendicular to the crack front (shearing mode).

MODE III In plane displacement of the crack surfaces parallel to the crack front (sliding mode).

The opening mode is the most common and the stress intensity factor in the opening mode is given the appropriate suffix K_I. For this mode the stresses and displacements ahead of a crack are as follows:

$$\begin{bmatrix} \sigma_{xx} \\ \sigma_{yy} \\ \tau_{xy} \end{bmatrix} = \frac{K_I}{\sqrt{2\pi r}} \begin{bmatrix} \cos\frac{\theta}{2}\left(1-\sin\frac{\theta}{2}\sin\frac{3\theta}{2}\right) \\ \cos\frac{\theta}{2}\left(1+\sin\frac{\theta}{2}\sin\frac{3\theta}{2}\right) \\ \cos\frac{\theta}{2}\quad \sin\frac{\theta}{2}\cos\frac{3\theta}{2} \end{bmatrix} \qquad (5.8)$$

$$u = 2(1+\nu)\frac{K_I}{E}\sqrt{\frac{r}{2\pi}}\,\mathrm{Cos}\frac{\theta}{2}\left(2-2\nu-\mathrm{Cos}^2\frac{\theta}{2}\right) \qquad (5.9)$$

$$v = 2(1+\nu)\frac{K_I}{E}\sqrt{\frac{r}{2\pi}}\,\mathrm{Sin}\frac{\theta}{2}\left(2-2\nu-\mathrm{Cos}^2\frac{\theta}{2}\right) \qquad (5.10)$$

$$w = 0 \text{ for plane strain} \qquad (5.11)$$

The limiting value of K_I is a property of the material, the fracture toughness, K_c. When conditions of plain strain prevail (i.e. small plastic zone) $K_c = K_{Ic}$.

For a central crack of length 2a infinite body under a remote stress σ

$$K_I = \sigma\sqrt{\pi a} \qquad (5.12)$$

For a material with fracture toughness K_{Ic} the stress at the onset of instability is

$$\sigma_c = K_{Ic}/\sqrt{\pi a_c} \qquad (5.13)$$

This approach is more reliable than the critical strain energy release rate, G_c, since it is based on conditions at the crack tip. They are, however, related since

$$G = \sigma^2\pi a/E' = K^2/E' \qquad (5.14)$$

The general expression for K is

$$K = F(g)\,\sigma\sqrt{\pi a} \qquad (5.15)$$

where F(g) is a function dependent on specimen geometry, crack shape and boundary conditions. There has been a considerable amount of research effort into the determination of stress intensity factors. Tada et al[7] is one of the many handbooks available which catalogue comprehensive values of stress intensity factors.

5.4 Small Scale Yielding

According to Equation 5.8 at the crack tip (r = 0) the stress would be infinite. Naturally in practise yielding takes place and a volume of plasticity surrounds the tip. If the plastic zone is small the energy content would likewise be small and the overall stress distribution would be unaffected. As the plastic zone increases so does the energy content and the effect on the overall stress distribution becomes significant. In such circumstances K_I and G will not fully represent the problem.

Irwin in 1970 proposed an adaptation of the model to incorporate plasticity. The allowance for a small amount of plasticity was made by assuming the crack length was $a+r_y$ where r_y is the radius of the plastic zone. r_y was estimated by assuming the normal stress ahead of the crack tip equal to the yield stress. Using his earlier solution for the stress distribution around the crack tip he obtained the radius of the plastic zone:

$$r_y = \frac{1}{2\pi} (K/\sigma_y)^2 \qquad (5.16)$$

for plane stress. The stress intensity factor was now modified as

$$K = F(g, r_y)\sigma\sqrt{\pi(a+r_y)} \qquad (5.17)$$

Such a correction to the linear elastic SIF is only valid if r_y is small compared to the crack length and the specimen width. Fracture mechanics condition, where the region of plasticity is small compared with crack length, has become known as small scale yielding (SSY).

5.5 Toughness Testing

Validity of LEFM depends on the experimental determination of a unique material fracture toughness value. Most materials exhibit a thickness effect where thicker materials have lower apparent toughness than thin materials (see Fig. 5.3). The reason for this is the greater amount of plastic constraint within thick sections. The thicker the section the greater the region of plane strain leading to the minimum plane strain fracture toughness K_{Ic} (see Fig. 5.4). For thinner sections the plane stress region is dominant and evaluation of K_c would lead to very conservative results. Valid fracture toughness testing therefore requires a minimum proportion of plane strain. The US and UK standards for fracture toughness testing both impose validity checks on the toughness test results so that a minimum proportion of plane strain exists

$$a,\ (W-a),\ B \geqslant 2.5\left[\frac{K_{Ic}}{\sigma_y}\right]^2 \qquad (5.18)$$

where a, W, and B are crack length, specimen width and specimen thickness respectively and $(K_{Ic}/\sigma_y)^2$ is a measure of the plastic zone size.

5.6 Summary of LEFM

Since the early work of Griffith the use of stress intensity factors to characterise cracks has been the most significant development. The precondition

of the approach, that plasticity must be restricted to a small volume around the crack tip, is very limiting since in many practical situations the volume of plasticity is much larger. Furthermore for tough materials the size of test specimen necessary to determine valid K_{Ic} is very large. The subsequent development of elastic-plastic fracture mechanics (EPFM) overcame many of the restrictions.

5.7 Elastic-Plastic Fracture Mechanics

Brittle fracture accompanied by small scale plasticity described above is one extreme mode of failure: the opposite extreme being plastic collapse on the uncracked ligament. In between these two fracture takes place with large scale plasticity which is sufficient to invalidate LEFM concepts but insufficient to initiate plastic collapse. This is the regime of elastic-plastic fracture mechanics.

The fracture characterising parameter described here is the crack-tip opening displacement COD or CTOD. Other parameters not included are the J-integral which relates the strain energy of a cracked body to a given increment in crack length and the two-criteria approach used by the Central Electricity Generating Board in the UK.

5.8 Crack Opening Displacement

Wells[8] in 1961 proposed that the separation of the crack faces, which is a measure of the extent of normal deformation, could be considered as a characterisation parameter of the strain and thus the stress field at the crack tip. Crack extension will occur at some critical value of this separation called the critical CTOD.

Using the Irwin analysis (Equations 5.10) with $r = r_y$, the plasticity correction factor, and $\theta=\pi$

$$v = \frac{4K}{E}\sqrt{\frac{r_y}{2\pi}} \qquad (5.19)$$

The total crack opening δ is twice the normal displacement so substituting for r_y from Equation 5.16 gives

$$\delta = 2v = \frac{4K^2}{\pi E \sigma_y} \qquad (5.20)$$

If K is expressed in terms of G using Equation 5.14

$$\delta = 4G/\pi\sigma_y \qquad (5.21)$$

Wells in 1963[9] proposed that the energy balance required to produce an increment in crack length is equal to the work done at the crack tip prior to extension. Since σ_y is the only stress acting across the plastic zone then

$$G = \delta\sigma_y \qquad (5.22)$$

and

$$\delta = G/\sigma_y \qquad (5.23)$$

Comparison of the two above expressions for δ shows a factor of $4/\pi$ difference. Wells[9] argued that this factor could be replaced by unity without disturbing the energy balance at the crack tip. The above expression was considered a lower bound value for CTOD:

$$\delta \geq G/\sigma_y \qquad (5.24)$$

Expressing this in terms of K gives rise to

$$\delta \geqslant K^2/E\sigma_y \qquad (5.25)$$

The approach to EPFM adopted by Dugdale[10] was different. He suggested that by equating the work done in closing the crack with the change in internal energy due to shortening the crack, the displacement at the crack tip could be estimated. Burdekin and Stone[11] used Westergaard stress functions to evaluate the COD

$$\delta = (8\sigma_y a/\pi E) \ln \sec(\pi\sigma/2\sigma_y) \qquad (5.26)$$

where σ is the remotely applied tensile stress. For $\sigma = \sigma_y$ in this expression the COD becomes infinite. This is because as yet strain hardening was not accounted for.

Expanding Equation 5.26 yields

$$\delta = \frac{8\sigma_y a}{\pi E}\left[\tfrac{1}{2}\left[\frac{\pi\sigma}{2\sigma_y}\right]^2 + \tfrac{1}{2}\left[\frac{\pi\sigma}{2\sigma_y}\right]^4 + \ldots\right] \qquad (5.27)$$

Taking the first term of this expression and substituting the MODE I expression for K

$$\delta = \frac{\pi\sigma^2 a}{E\sigma_y} = \frac{K^2}{E\sigma_y} \qquad (5.28)$$

which agrees with the lower bound value of δ in Equation 5.25.

5.9 Critical CTOD

EPFM using crack opening displacement is based on the assumption that failure occurs when the CTOD reaches a critical value, δ_{crit}. The critical CTOD may be a material constant independent of the degree of plastic deformation. Three critical CTOD values can be identified depending on the physical nature of the fracture event:

i) CTOD at the onset of instability δ_c if stable crack extension is followed by unstable fast fracture.

ii) CTOD at maximum load, δ_m, if failure occurs by plastic collapse of the remaining ligament.

iii) CTOD at the initiation of crack extension δ_i.

Many authors agree that δ_c is affected by section thickness and crack acuity of the test piece while δ_m is dependent on specimen dimensions. Under sufficient plane strain conditions however δ_i, the COD at the initiation of crack extension, is independent of specimen dimensions. Thus δ_i is potentially the best measure of the material property. Even so work by Hancock and Cowling[12] has shown that for high strength steel δ_i is dependent on the state of stress at the crack tip. An order of magnitude difference was reported between δ_i for high and low constraint geometries. Despite this observation it is regarded as a well established toughness parameter in the elastic plastic regime.

5.10 Experimental Determination of δ_i

Due to practical difficulty in detecting the exact incident of crack initiation δ_i is usually determined from a crack growth resistance curve. This is a plot of COD versus physical crack extension Δa. On the same plot is drawn the 'blunting line' which models the transition of a sharp crack-tip to a semicircular or other shaped crack-tip under the tensile load. From simple geometric considerations the blunting line has the equation

$$\delta = 2\Delta a \qquad (5.29)$$

The R-curve is represented in Figure 5.5.

Physical measurement of crack extension is done visually or by electrical potential drop methods. The COD is usually measured by a clip gauge rigidly attached across the mouth of the crack (geometric reckoning is then used to convert the crack mouth opening to crack tip opening). Other methods include replication techniques using hardening silicon rubber, and visual measurements.

5.11 The CTOD Design Curve

The application of the COD concept has been shown to be relevant for conditions of small scale yielding. As the extent of plasticity increases so the relationship between COD and SIF (Equation 5.25) loses its validity. The COD design curve is a compound curve for which the lower portion (for low stresses) derives directly from analytical considerations and the upper portion (for higher stresses and more widespread plasticity) is a lower bound to

experimental results. The curve is given by

$$\bar{a}_m = \frac{\delta_c / e_y}{2\pi \left[\frac{\sigma}{\sigma_y}\right]^2} \qquad \frac{\sigma}{\sigma_y} \leqslant 0.5 \qquad (5.30)$$

$$\bar{a}_m = \frac{\delta_c / e_y}{2\pi \left[\frac{e}{e_y} - 0.25\right]^2} \qquad \frac{\sigma}{\sigma_y} > 0.5 \qquad (5.31)$$

and it is continuous at $\sigma/\sigma_y = 0.5$. $\bar{a}_m$ is the tolerable defect parameter which for through thickness cracks in wide plates would be the crack half length. The BSI document PD6493[13] in which the design curve was published in 1980 provides graphs for converting $\bar{a}_m$ into tolerable dimensions for other defect geometries. The conversion is based on equating the stress intensity factor of any particular geometry to that of a through crack in a wide plate.

The expression for $\bar{a}_m$ in the lower portion of the curve is exactly one half of the quantity obtained from expanding and rearranging Equation 5.26. Restated this is

$$\delta = (8\sigma_y a/\pi E) \ln \sec(\pi\sigma/2\sigma_y) \qquad (5.32)$$

Expanding, replacing σ_y/E with e_y and simplifying

$$\delta = e_y a \pi \left[\frac{\sigma}{\sigma_y}\right]^2 \qquad (5.33)$$

Rearranging

$$a = \frac{\delta / e_y}{\pi \left[\frac{\sigma}{\sigma_y}\right]^2} \qquad (5.34)$$

Thus the lower portion of the curve incorporates a safety factor of 2.0.

The method of obtaining tolerable defect sizes based on COD presented in PD6493 is straightforward to use. Because the overall strain of the body is used as input secondary effects such as residual and thermal stresses can be taken into account.

The major omission in the method is that no consideration is given to the amount of plastic constraint. The bend specimens used to determine critical CTOD have a highly constrained geometry and therefore would lead to over-conservative estimates of tolerable flaw sizes in real cracks in less constrained geometries.

5.12 Summary of EPFM

The successful application of fracture mechanics concepts to assessing defects in structures depends largely on the characterisation of the fracture toughness of materials. Many of the 'tougher' materials used in various structures are medium to low strength steels which develop large plastic zones at the tip of a crack under load. Therefore assessment based on K_{Ic} toughness and LEFM is inappropriate in these cases. CTOD toughness on the other hand has been shown to be a valid characteristing parameter in the EPFM regime.

The use of the CTOD at the initiation of crack extension can lead to over-conservative judgements since many materials in elastic-plastic conditions undergo a period of stable crack growth prior to instability. However there is a lack of clear understanding about instability conditions so such conservatism may be justified.

5.13 Developments since 1980

The major shortcoming of the Design Curve is that modelling beyond 50% of yield is not based on knowledge of the physical phenomena occurring at these stresses. To base it on a lower bound to experimental data is one way of making up for the lack of knowledge but unless the parameters which control the physics are recognised and accounted, for such an approach cannot give wholly satisfactory predictions. It was these considerations which lead in recent years to the development of the so called collapse modified strip yield model[14].

This approach attempts to model the fracture and plastic collapse phenomena with an interaction equation of the form

$$\checkmark\delta_r = \frac{S_r}{\checkmark\left[\frac{8}{\pi^2} \ln\sec\left(\pi/2\ S_r\right)\right]} \qquad (5.35)$$

The equation describes a curve in the plane of S_r, the stress as a proportion of the plastic collapse stress, and $\checkmark\delta_r$, the ratio of applied to critical COD. By plotting the values of these parameters for any particular defect 'failure' is predicted if the point lies outside of the interaction curve. The type of failure predicted would be by brittle fracture at low S_r values, by plastic collapse at S_r values $\approx$ 1.0 and by tearing with large plastic deformation at intermediate values of S_r.

In order to validate the model Anderson, Legatt, Garwood[15] used it to compare actual COD measurements with COD predicted using Equation 5.35.

Their results have been reproduced in Figure 5.6 which shows the modified strip yield model to follow the trend of the experimental points. The design curve on the other hand can be seen to be wholly unrepresentative of the experimental points in the upper stress range. The other result in Figure 5.6 is for the so-called 'reference stress equation'[15] which uses the stress/strain characteristics of the material to predict CODs at stresses beyond yield. Both the strip yield and reference stress methods are likely to supplement the design curve in a coming revision to PD6493.

5.14 Discussion: Uncertainties in Defect Assessment

The safety factor of 2.0 which is implicit in the COD design curve at stresses below $0.5\sigma_y$ is often described[15,16,17] as 'variable'. The sources of this variability are usually put down to random and systematic uncertainties in the material toughness and to the fact that differing degrees of safety result depending on the stress level. Figure 5.7 reproduced from Reference 15 shows the variation of safety factor, being the ratio of predicted to actual COD, to stress level.

The first accredited source of uncertainty is in principle, as far as treatment under reliability analysis is concerned, no different from the uncertainty in material yield stress seen in problems of static strength. The random uncertainty in toughness comes about because of the difficulty in obtaining similar values in separate, nominally identical tests. The systematic error comes about because of the lower bound toughness value employed to offset this random uncertainty. (In the past the minimum of three values from nominally identical tests has been used).

The second accredited source of uncertainty is a modelling uncertainty, X_m. The model predicting applied COD has an accuracy which depends on the level of stress. The parallel in static strength prediction is the variation of mean and random modelling uncertainty parameters with slenderness observed in strut, flange and beam strength prediction. Figure 5.7 can also be interpreted, even though it is for only one specimen, as the variation of $1/X_m$ since, generally, modelling uncertainty is treated as the ratio of actual to predicted values. For the strip yield model $1/X_m$ varies between 1.15 and 1.5 for stresses below net section yield, this corresponds to X_m values between 0.67 and 0.87. To fully quantify modelling uncertainty for the strip yield model a large sample of such data would be required from which values of X_m could be obtained for different ranges of stress. Without such data modelling uncertainty would have to be treated using nominal values.

As well as the uncertainties generally believed to be the cause of the 'variable safety factor' there are additional uncertainties associated with assessment of defects as well as other modelling uncertainties. Firstly there are random and systematic uncertainties in assessing stress comparable to those described in Section 3 for offshore structures. Recapping, these were divided into three main groupings:

- dead and hydrostatic,
- live, operation and berthing loads,
- environmental (wave, wind and current) and dynamic.

The calculation of load effects from these primary sources also adds uncertainty since there is a need to choose a wave theory, suitable

hydrodynamic constants and type of structural analysis. Additionally local stresses used in defect assessment depend on stress concentration effects (caused by joint geometry) and residual welding stresses. This last category is generally considered to dominate the total uncertainty in stress assessment in conditions where residual stress is known to approach yield magnitude.

Secondly, assessment of defect size is subject to large systematic and random uncertainty[18]. The degree of which depends largely on the type of NDE equipment used, the skill of the operator and the ardour of the conditions in which assessment is being made.

Finally a source of modelling uncertainty, in addition to the uncertainty in predicting applied COD, is in the choice of plastic collapse stress used to evaluate the plastic collapse ratio, S_r, in the collapse modified strip yield model. For tubular joint geometries where plastic failure is accompanied by distortions of the circular cross sections the plastic collapse stress based on a cracked wide plate in tension is adequate.

Clearly the need and scope for probabilistic assessment of defects is great. The strip yield model is a suitable tool from which to evaluate an unbiased critical defect size. The difference between this and the actual current defect size would then constitute the safety margin. The strip yield model is essentially an interaction equation expressing interaction between failure by brittle fracture, parametised by $\delta_r > 1$, and failure by plastic collapse, parametised by $S_r > 1$. The use of a probabilistic failure model involving an interaction equation is not unprecedented in reliability analysis. In Section 3 failure of stiffened webs was modelled as the interaction between shear capacity and flexural capacity.

Once the failure function has been set up in terms of the basic uncertainties of material fracture toughness, stress and actual defect size answers to the more pertinent questions of operators of offshore structures can be tackled. Questions such as:

1. in what order should an operator repair a series of known defects?
2. would it be economic to use a more or less expensive NDE detection and sizing equipment?
3. would it be more economic to perform finite element analysis on a joint to gain a more accurate estimate of stress.
4. considering the uncertainties in stress and defect size, is three COD tests sufficient to ensure a reasonable lower bound toughness?
5. what safety factors should be applied to stress, defect size and toughness to obtain a specified reliability against failure.

Section 6 deals with the setting up of the failure function as the difference between actual and critical defect size. Thus given estimates of means and COVs of each of the uncertain variables the probability that actual defect size exceeds critical defect size can be estimated. The first question can then be answered as 'in order of decreasing probability'. Section 7 should provide answers to questions 2, 3 and 4 since they relate to the relative sensitivities of the different variables for different combinations of the means and COVs of the three basic variables. Thus only if the sensitivity factor of a particular variable were high would it be worth considering obtaining a better estimate, and conversely, for variables having little influence on 'failure probability' consideration might be given to using cheaper alternative assessment methods. The answer to question 5 should be found in Section 8 where partial safety factors on stress, toughness and defect size are calculated for three different required probabilities.

5.15 Conclusions

1. The CTOD design curve although capable of safely predicting defect sizes at low stresses does not model correctly the behaviour of applied crack opening displacements in the elastic-plastic region. As such it is not suitable for the formulation of a failure function for reliability analysis.
2. The collapse modified strip yield model does predict the essential characteristics of the applied stress/applied COD curve and would be suitable for use in a failure function for reliability assessment of defects. The resulting values of failure probability would however be strictly notional since there is an absence of data from which modelling uncertainties could be determined.

5.16 References

1. Griffith, A.A., 'The Phenomena of Rupture and Flow in Solids', Phil. Trans. Roy. Soc., London, Series, A., Vol. 221, 1921, pp163-198.
2. Irwin, G.R., 'Fracture Dynamics', ASM Seminar on the fracturing of metals, 29th Nat. Metal Cong., Chicago, 1947.
3. Irwin, G.R. and Kies, J.A., 'Fracturing and Fracture Dynamics', Supplement to the Welding Journal, Vol. 31, No. 2, 1952, pp95-s - 100-s.
4. Westergaard, H.M., 'Bearing Pressures and Cracks', J. Appl. Mechs., Trans. ASME, Vol. 6, 1939, ppA-49 - A-53.
5. Sneddon, I.N., 'The Distribution of Stress in the Neighbourhood of a Crack in an Elastic Solid', Proc. Roy. Soc., London, Vol. A187, 1946, pp229-260.
6. Irwin, G.R., 'Analysis of Stresses and Strains near the End of a Crack Traversing a Plate', J. Appl. Mechs., Trans. ASME, Vol. 24, 1957, pp361-364.

7. Tada, H., Paris, P.C. and Irwin, G.R., 'The Stress Analysis of Cracks Handbook', DEL Research Corp., Pennsylvania, 1973.

8. Wells, A.A., 'Unstable Crack Propagation in Metals-cleavage and Fast Fracture', Symp. on Crack Propagation, College of Aeronautics, Paper B4, Cranfield, 1961.

9. Wells, A.A., 'Application of Fracture Mechanics at and Beyond General Yielding', Brit. Weld. J., Vol. 10, 1963, pp563-570.

10. Dugdale, D.S., 'Yielding of Steel Sheets Containing Slits', J. Mech. Phys. Solids, Vol. 8, 1960, pp100-104.

11. Burdekin, F.M. and Stone, D.E.W., 'The Crack Opening Displacement Approach to Fracture Mechnics in Yielding Materials', J. Strain Analysis, Vol. 1, 1966, pp145-153.

12. Hancock, J.W. and Cowling, M.J., 'Role of State of Stress in Crack Tip Failure Processes', J. Metal Science, 1980, pp239-304.

13. British Standards Institution: PD6493, 'Guidance on Some Methods for the Derivation of Acceptance Levels for Defects in Fusion Welded Joints', BSI, 1980.

14. Garwood, S.J., 'A Crack Tip Opening Displacement (CTOD) Method for the Analysis of Ductile Materials', Welding Institute research report No. 277/1985, June 1985.

15. Anderson, T.L., Leggatt, R.H. and Garwood, S.J., 'The Use of CTOD Methods in Fitness for Purpose Analysis', Welding Institute Staff Papers, Prsented at Workshop on CTOD Methodology, GKSS Research Centre, Geesthacht, 23-25 April, 1985.

16. Kamath, M.S., 'The COD Design Curve: an Assessment of Validity Using Wide Plate Tests', International Journal of Pressure Vessels and Piping, Vol. 9, 1981, pp79-105.

17. Burdekin, F.M. and Townsend, P.H., 'Reliability Aspects of Fracture on Stress Concentration Regions in Offshore Structures', Integrity of Offshore Structures Second International Symposium. Eds. D. Faulkner, M.J. Cowling and P.A. Frieze, Applied Science Publishers, 1981.

18. Tam, J.C.P. and Dover, W.D., 'Structural Integrity of Welded Tubular Joints in Random Load Fatigue Combined with Size Effects', Department of Mechanical Engineering, University College, London.

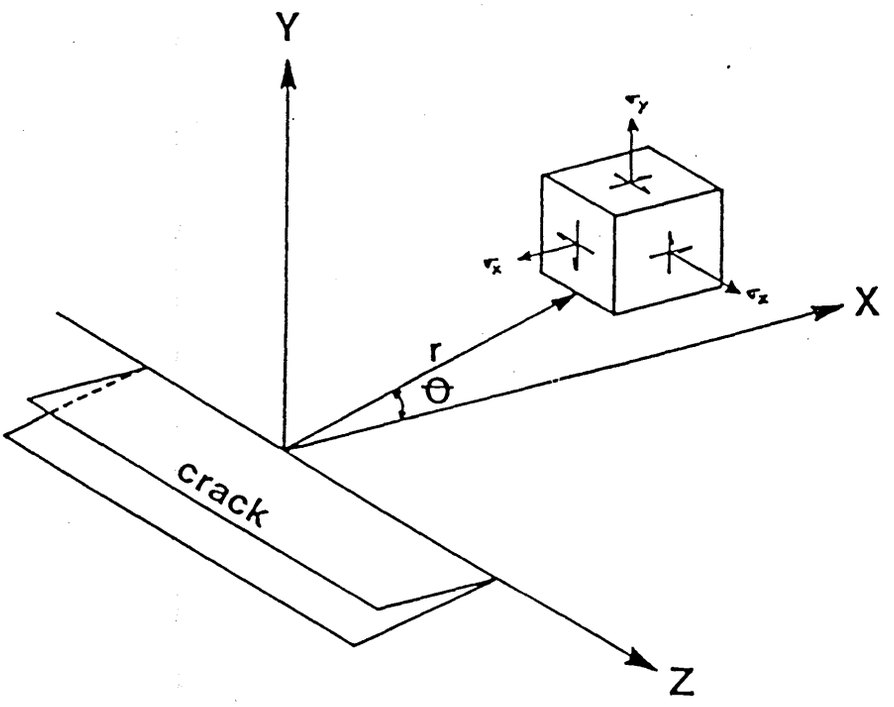

Fig. 5.1 Stress components ahead of a crack tip

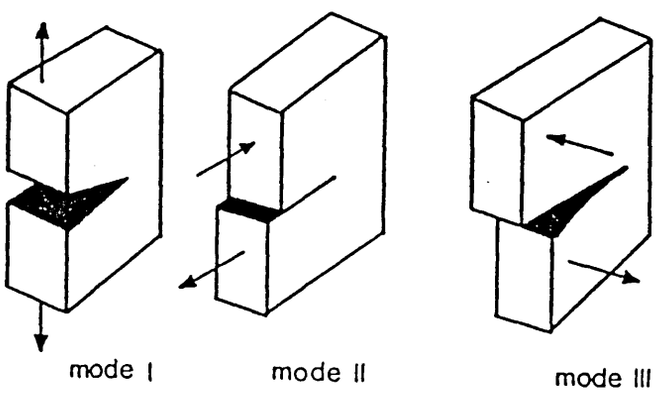

Fig 5.2 Fracture modes

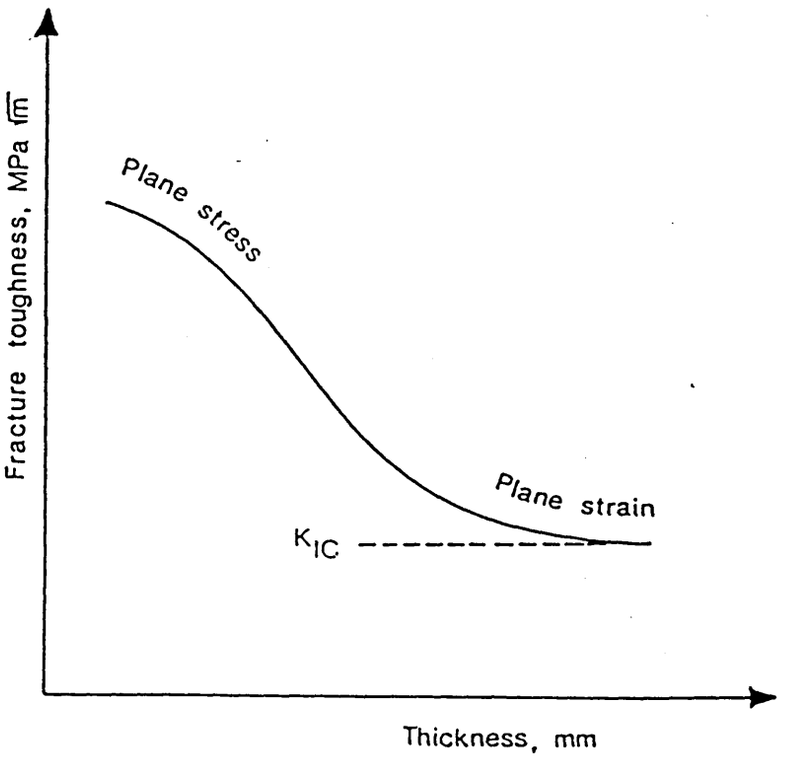

Fig. 5.3 Variation of fracture toughness with specimen thickness.

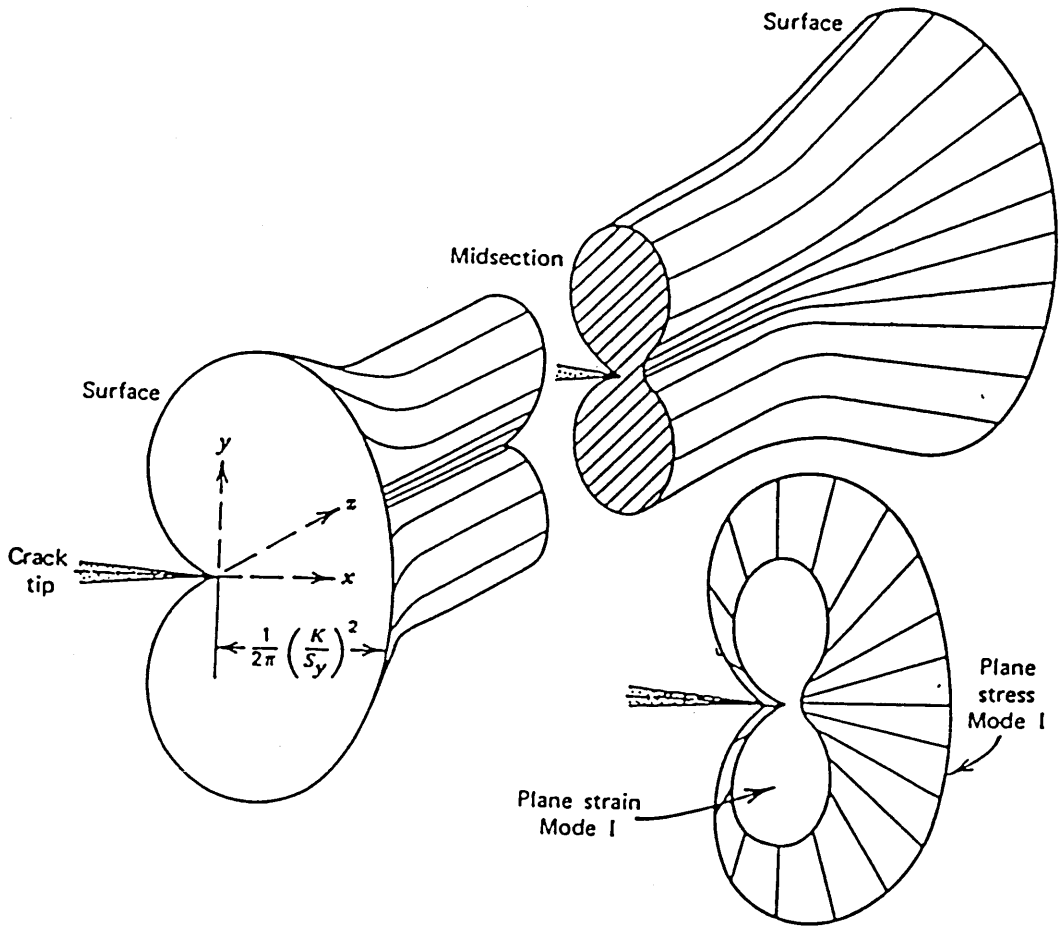

Fig. 5.4 Plastic zone ahead of a crack tip

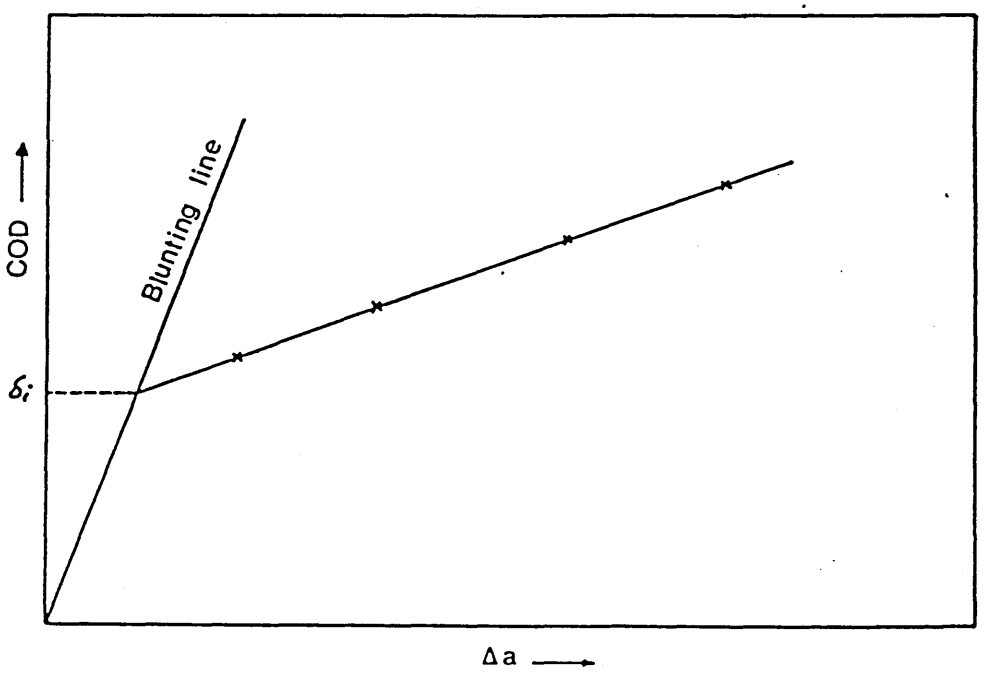

Fig. 5.5 Schematic COD-R-curve

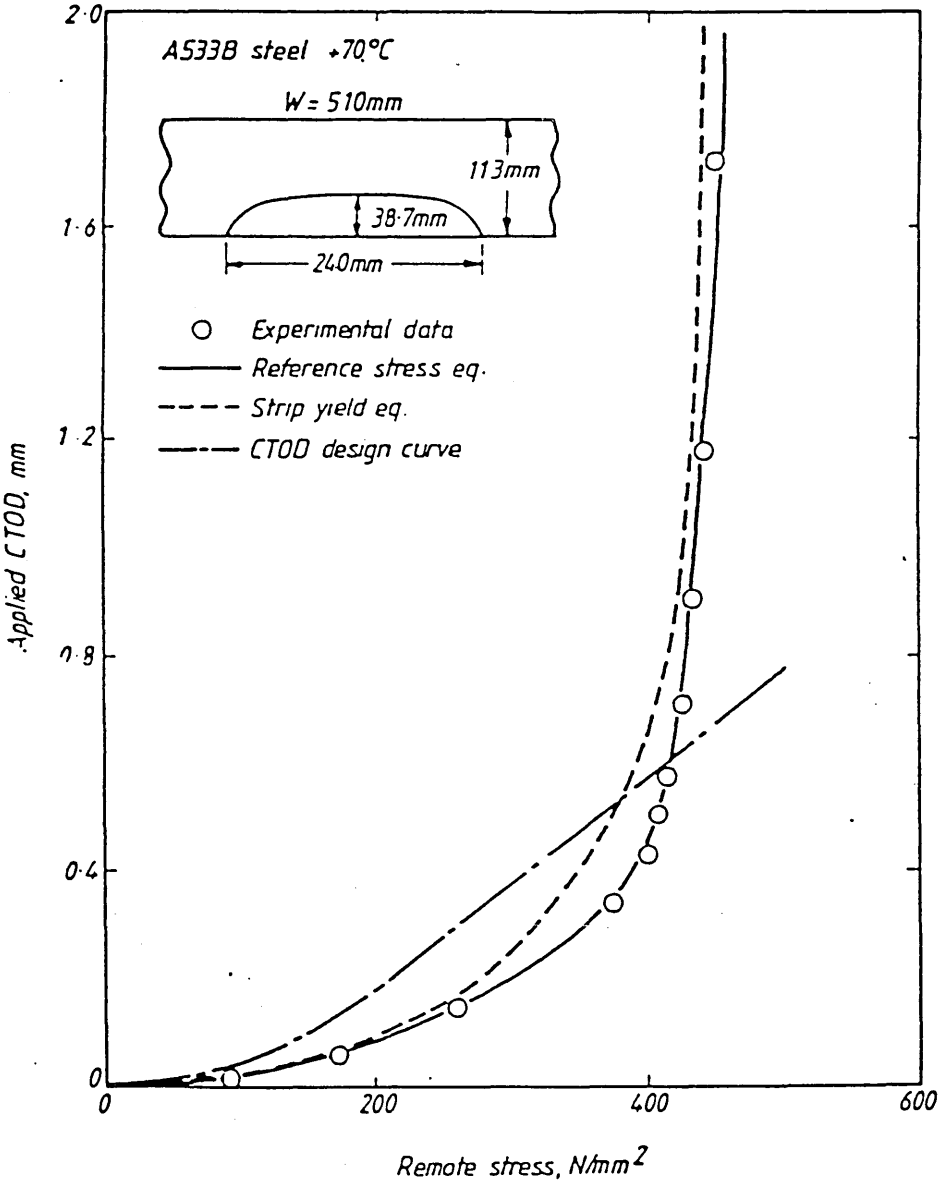

Fig. 5.6 Comparison of predicted and experimental CTOD in A533B steel wide plate

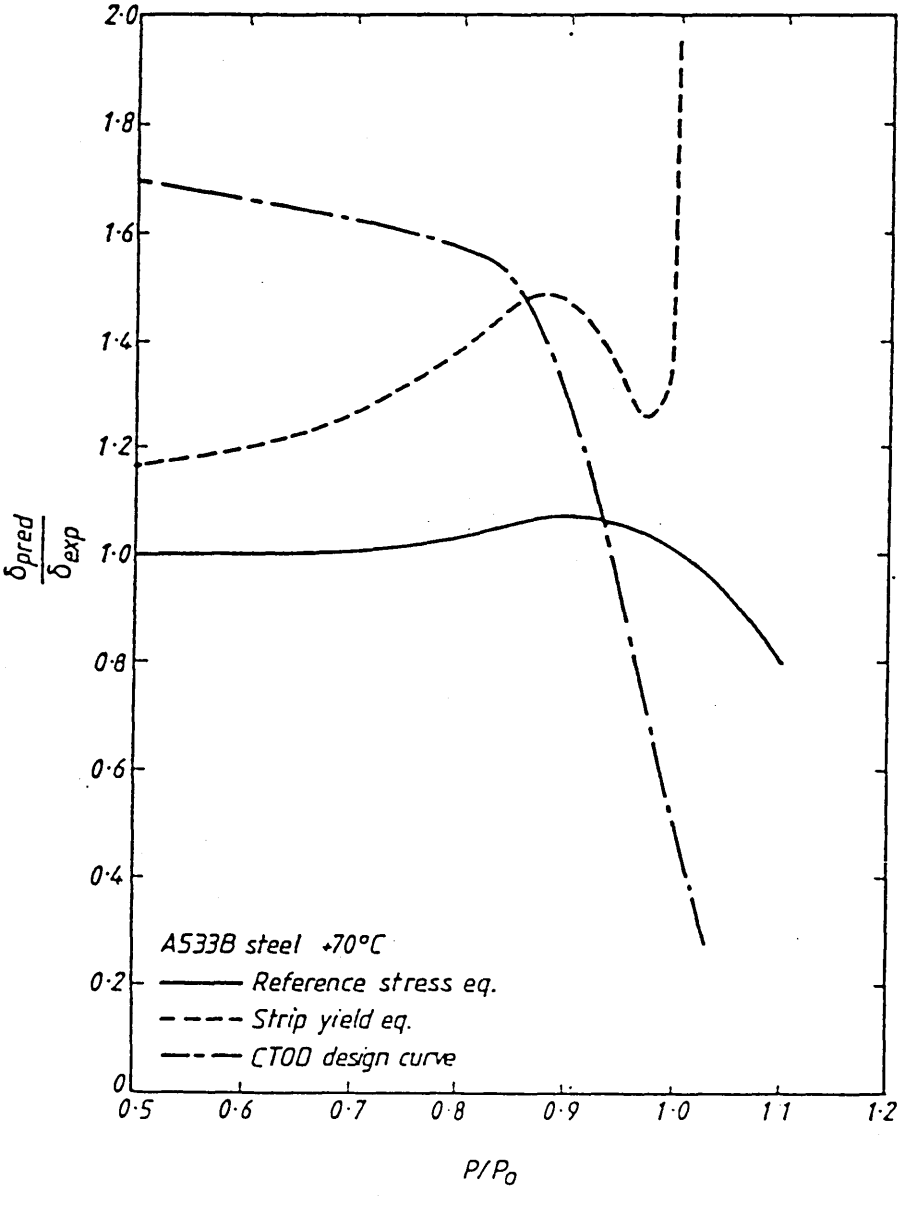

Fig. 5.7 Safety factor on applied CTOD

SECTION 6

RELIABILITY STUDY OF EXISTING AND PROPOSED DEFECT ASSESSMENT PROCEDURES

Foreword

The work in Sections 6, 7 and 8 was carried out at the instigation of the Methodology Working Group (MWG) which comprises dedicated representatives from a dozen UK industries and researchers with an interest in steel offshore structures. Funding derives from subscriptions of the industrial members of the Group as well as from the U.K. Government through the Marine Technology Directorate Ltd. and the Department of Energy. The program of research in reliability and several other steel offshore structures - linked topics was carried out in a number of U.K. universities during the period 1985-87. It was titled 'Defect Assessment in Offshore Structures'. The MWG activity encompassed the collaborative university/industry research of Glasgow University, University College, London and the University of Manchester Institute of Science and Technology. The objective of the MWG was to provide substantial recommendations for, and specific methodology for the assessment of defects in steel offshore structures.

The BSI recommendations for the treatment of in-service defects are set out in published document PD6493 (not a British Standard). The document has provided a readily useable decision tool for operators faced with the problem of whether or not to repair a known defect but has several widely recognised shortcomings. Firstly the lack of a plastic collapse check has meant that modelling of crack behaviour at stresses in excess of 0.8 of yield is

non-conservative. Secondly the stress field is conservatively taken as being constant through the thickness at the level of the total stress at the surface. Thirdly the modelling at stresses below 0.5 yield incorporates an unspecified factor of safety of 2.0 that is out of keeping with current design code philosophy which calls for limit state design/assessment equations with explicitly stated partial safety factors reflecting the various degrees of uncertainty.

In proposed revisions to the document the limit state equations are based on the collapse modified strip yield model (see Section 6.4). This and the following two Sections are directed at establishing partial safety factors to be used with the new assessment equations in the revision.

The major distinction between this and earlier Sections of the thesis is the range of application of the code in question. Unlike the bridge code (Section 2) and offshore structures codes (Sections 3 and 4) the defect assessment code is not structure-specific. The ramifications of this will become evident in Section 7 where an attempt is made to present the results of reliability calculations for the multitude of combinations of different levels of uncertainty in the basic variables. Fortunately the complexity of offshore jacket structures means that by concentrating on this specific application almost every other case will be catered for. Users of the revised assessment document in other fields will have to make subjective assessment of the uncertainty in the basic variables before selecting the appropriate safety factors.

The diversity of application exacerbates the task of identifying target reliabilities, the final choice being highly dependent on an arbitrary set of "typical" assessments. Although such a target has been identified in this study

for offshore jackets (and partial factors evaluated) the final recommendation to operators of defect-prone structures in any field is to develop their own (or acquire the necessary) software and use it with the failure functions to be described herein in order to get a feeling for the level of failure probabilities for defects which they have hitherto considered as safe. Having established such a target the problems of dealing with different toughness distributions, different levels of stress uncertainty as well as different levels of NDT accuracy will be readily overcome. Although the explicit objective in the following Sections is to derive partial safety factors to be used with the revised code it is intended that the approach adopted will serve as a model for operators wishing to obtain "hands-on" experience with defect assessment reliability.

In this Section stress level, defect size and fracture toughness are identified as being the pertinent sources of uncertainty in defect assessment. They are treated as time-independent random variables and combined using the First Order-Second Moment reliability analysis method to generate the notional failure probability of a known defect. The use of the method to make one-off assessments is illustrated. Notional failure probabilities are found for defects which the PD6493 Design Curve and the revision based on the modified strip yield model classify as safe and a means of ensuring consistent safety at an adequate level is proposed.

6.1 Introduction

As part of the revisions to the UK recommendations for the assessment of in-service defects, the CTOD design curve in BSI PD6493[1] is to be

supplemented by a routine based on a modification of the Dugdale[2] strip yield model. This new proposal, referred to as the Level 2 assessment route, incorporates both fracture and plastic collapse considerations and is less conservative in its treatment of defects in through-thickness stress gradients. This Section describes a pilot study into how the reliability of the Level 2 route might be calibrated probabilistically using the safety record of the CTOD design curve.

The problem has been approached from consideration of the uncertainties in stress, defect size and fracture toughness and the combination of these to estimate the probability that a known defect is greater than the critical size for the same stress field and material toughness. This probability has been referred to herein as the failure probability. Estimation of the notional failure probabilities of those defects which the assessment rules class as safe provides a fundamental means of quantifying the margin of safety inherrent in any assessment route. Where the safety record of the existing assessment route is acknowledged as being adequate a datum failure probability, or target reliability, can be set. By means of a safety factor on defect size or by using lower bound values (characteristic values) of the input variables or both the reliability of the proposed route can be made to match this datum: this is what is meant by calibration of an assessment route. The major advantage of this appraoch to reliability is that the influence on safety of each of the three uncertain variables is made apparent; each is assigned a sensitivity factor as part of the calculation of reliability.

The scope of this section is limited to finding reliability indices using the modified strip yield model and the existing CTOD design curve to evaluate

"critical" and "tolerable" defect sizes. The presentation of sensitivity factors and discussion of their considerable use is the subject of Section 7. They have also been reported in a separate paper[3].

The advanced First Order-Second Moment (FOSM) reliability analysis method is used to determine safety indices. The limitations of the method are discussed in relation to probabilistic fracture mechanics. The existing and newly proposed assessment routes are described and a failure criterion for use with the FOSM method is proposed. Attention is drawn to the problem of identifying a model uncertainty factor.

Results of reliability calculations on two types of defect are presented for an assumed set of statistical parameters for stress, toughness and detection accuracy.

Notation

a	defect size - half width of through crack, height of surface crack or half height of embedded crack.
COV	coefficient of variation
e	plate thickness
e_y	yield strain
E	Young's Modulus
E(.)	expected value
K	stress intensity factor
N	number of CTOD tests
P(x)	probability of x
w	plate width
β	safety index
γ	safety factor
δ	crack tip opening displacement (CTOD)
m	mean value
s	standard deviation
σ_T	ultimate tensile stress
σ_y	yield stress
Φ(.)	normal distribution function

Other notation is defined in the text.

6.2 Reliability Analysis Method

The advanced First Order-Second Moment method is well documented in the literature, in particular References 4 and 5. A full description was presented in Section 1. Essentially a safety index, β, is found which corresponds to the minimum distance in the space of normalized independent design variables from the origin to the failure surface. If x is a design variable then the transformation

$$z = \frac{x - m_X}{s_X} \qquad (6.1)$$

ensures that any distance measured in the transformed design space is non-dimensional and gives β its unique meaning. (It also ensures that the origin, corresponding to the mean values of the design variables, is in the safe domain).

If all the design variables are normally distributed and the failure surface is linear then the probability of failure is exactly given by

$$p_f = \Phi(-\beta) \qquad (6.2)$$

In defect assessment reliability both the failure surface is non-linear and the toughness distribution is widely recognised to be highly skewed. To improve upon the approximation of Equation 6.2 m_X and s_X in Equation 6.1 are replaced by m_X^N and s_X^N being the mean and standard variation of the normal distribution having the same cdf and pdf as the non-normal variable at the design point. The transformations are due to Rackwitz and Fiesler (Reference 5, Section 1) and their derivations are presented in Appendix A of this Section.

It should be emphasised that the Rackwitz-Fiesler transformations are not estimates of the first and second moments of the given non-normal distribution. These are unique values which may be evaluated in terms of the parameters of the particular distribution (for an example with the Weibull distribution see Appendix B). The R-F transformations are not unique since they are dependent upon the point of evaluation as Equations A4 and A5 in Appendix A clearly show.

Comparisons by Chang[6] between the R-F algorithm and an 'exact' solution obtained from Monte-Carlo simulation showed the former to predict a safety index within 0.1 of the value predicted by the latter in all but 2 of the 13 examples analysed. These two related to a failure surface functions of many Chi-square variables all having COVs of 140%. The question of whether the advanced FOSM method gives sufficiently accurate results with highly skewed variables such as those attributed to material toughness is investigated in Section 7 by making comparisons with the Monte Carlo method.

6.3 Toughness Distribution

It is generally recognised that toughness distributions differ according to steel type, thickness, position of crack tip within the same plate (anisotropic) state of stress at the crack tip and testing temperature. This makes development of assessment codes with Level I reliability philosophy complex. To recall Section 1, in Level I codes the partial safety factors are made functions of the distribution characteristics of the basic design variables and thus eliminate the need of code users to apply reliability methods. The choices available to developers of Level I assessment codes are:

either to produce partial factors for combinations of different toughness distributions with the distributions of the other variables.

or to assume a 'cover-all' value for toughness variability and distribution type and rely on a small number of toughness tests to locate the mean of the distribution.

The first option would require the user to perform enough toughness tests (at least 20) to be confident of the distribution and would significantly complicate the presentation of assessment rules. The second option has been taken herein since, primarily, there is little experimental evidence to suggest that there are great differences in toughness reliability (although significant differences occur in mean toughness). What evidence there is suggests that variability in the mid-transition zone is greater than at either upper or lower shelf temperatures. Consequently the cover-all value assumed related to data at mid-transition temperatures.

Approximately 100 CTOD test results from 14 European laboratories were analysed in Reference 7. The tests were all at transition temperatures on BS4360-50D steel using 52mm thick plates. No significant inter-laboratory bias was present and the data gave a reasonable fit to a Weibull distribution with shape factor 2.0. The Weibull has the property that the distribution of minima of random samples of size N is also Weibull with the same shape factor as the original (parent) distribution. A simple relationship exists between the scale factors of the parent and derived distributions - see Appendix B.

Since the toughness input in assessment calculations is generally obtained from the minimum of three or more CTOD tests the Weibull property gives it a distinct operational advantage over the lognormal. Accordingly it was used in this study.

6.4 Defect Assessment Procedures

6.4.1 Introduction

The most widely used assessment procedure in the offshore industry is that embodied in BS PD6493[1]. This procedure is based on the CTOD design curve:

$$a_m = C\delta / e_y \qquad (6.3)$$

where $C = \frac{1}{2}\pi(\sigma/\sigma_y)^2 \qquad \sigma/\sigma_y < 0.5$

$= \frac{1}{2}\pi(\sigma/\sigma_y - 0.25) \qquad \sigma/\sigma_y \geq 0.5$

For some considerable time this has been believed to produce an excessive degree of conservatism as a result of the inherent limitations of the procedure and the aim of widespread applicability.

In particular the following specific limitations are inherent in PD6493:

(i) Through thickness stress gradients are not allowed for.

(ii) For applied stresses greater than 50% of the yield stress the CTOD design curve is an empirial fit to available data.

(iii) Plastic collapse is not an integrated failure mechanism.

(iv) The inherent safety factor varies and is often ill defined.

In addition specific restrictions on the use of PD6493 are applicable, but

not explicitly stated. These are:

(a) Primary stresses should be less than yield.

(b) Crack size must not exceed 10% of the component width.

(c) Separate plastic collapse calculations are required for defected sections.

Recent work[8] has proposed correction factors to the CTOD design curve in PD6493 to extend the crack size restriction to 50% of component width.

Proposed revisions of PD6493 [9,10] include a revised CTOD design curve approach as a basic assessment routine with increasingly more complex procedures available in Levels 2 and 3. Level 2 is summarised briefly below.

6.4.2 Level 2 Assessment [9]

The proposed Level 2 assessment procedure is based on the original Dugdale[2] strip yield model for the plastic zone ahead of a loaded notch. This original model has been widely used to derive fractures characterising parameters. Modification[11] of the original model to incorporate plastic collapse led to a formulation in terms of the ratio of applied CTOD to critical CTOD, δ_r,

$$\delta_r = (\pi^2/8) S_r^2 \ (\ln \sec \pi/2 \ S_r)^{-1} \qquad (6.4)$$

where $S_r = \sigma_n/\sigma_{pc}$, the stress ratio

$\sigma n = \sigma/(1-2a/w)$ for through thickness cracks

$= \sigma/(1-a/e)$ for long surface cracks, the net stress

$\sigma_{pc} = (\sigma_y + \sigma_T)/2$, the flow stress.

$\delta_r = \delta_I/\delta_{mat}$

δ_{mat} = the material toughness

$\delta_I = K^2/\sigma_y E$, the applied CTOD

$K = \sigma\surd\pi a$ for through cracks in tension

$= \sigma\surd a$ times appropriate stress intensity correction factors for other defect geometries and loading types.

A flaw is assessed by plotting values of $\surd\delta_r$ and S_r on a Universal Assessment Diagram. A plotted point outside the curve indicates an unacceptable defect. The value of defect size a which satisfies Equation 6.4 may also be found using a simple computer routine which increments a in appropriately small steps (1mm is an obvious first choice), calculates the ratios S_r and δ_r and terminates when the equation is satisfied. The solution, a_{crit}, is unique and the graphical and computer methods are equivalent.

The Level 2 assessment procedure has been shown[11] to be significantly more accurate than the CTOD design curve approach and may be applied for net section stress levels up to yield. Options exist regarding the degree of sophistication utilised in the estimation of primary and secondary stresses.

6.5 Failure Function for One-Off Assessments

For cracks found in service failure may be assumed to occur when

$$M = a_{crit} - a_{actual} \qquad (6.5)$$

becomes negative. a_{crit} is the crack size (either half length of a through crack, height of a surface crack or half-height of an embedded crack) which satisfies Equation 6.4. It may be called the calculated critical crack size. The uncertainties in material toughness, stress level and crack modelling all contribute to uncertainty in the calculated critical crack size. Actual crack size has uncertainties stemming from the NDT method.

The failure probability is the probability that actual crack size exceeds the critical crack size, i.e. $P(M < 0)$. Given estimates of the toughness distribution, stress (treated either deterministically or as a random variable with subjective assessment of the COV) and actual defect size (treated likewise) the Level II method may be used to obtain β and a notional failure probability. For this purpose the measured or estimated values of stress and actual defect size would be taken as mean values of the respective random variables and both distributions assumed to be normal unless there was evidence to suggest otherwise. Results for a selection of distribution parameters are presented in Table 6.1.

Also shown in Table 6.1 are values of the tolerable through thickness defect sizes in a wide plate (470 x 112.5mm) made from mild steel (σ_y = 400N/mm^2) using both the design curve and strip yield approaches. A mean

COD toughness of 0.125mm has been assumed. The estimate of the minimum of three toughness obviously varies with the COV of the parent Weibull distribution (see Appendix B) and this has been taken in account in the Table. An indication is made whether on the basis of each approach a repair is necessary. The most sensitive variable based on the sensitivity factors, α, from Equation 1.7 is shown in the final column. For the Table a standard deviation of 2mm has been assumed for defect size.

The solution algorithm for the advanced FOSM method is iterative and involves repeated calls to a routine returning the value of the failure function (i.e. M in Equation 6.5). Evaluation of M involves calculating a_{crit} which is the result of a separate iterative solution to Equation 6.4. For one-off assessments the time to compute the β-value is not excessive despite the two separate sets of iterations. When a large number of β-evaluations is required however, such as in code calibrating work, a short cut may be used to "merge" the separate iterative calculations into a single one and thus considerably speed up the calculation. This is described in Section 6.7.

6.6 Model Uncertainty

Modelling of physical behaviour inevitably necessitates assumptions being made to simplify the model as well as providing a means of understanding the processes involved. The variations of test results about predicted behaviour for example in column buckling are attributed to deviations from the assumptions or indeed to other physical behaviour omitted in the model. Model uncertainty is usually evaluated as

$$X_m = \frac{\text{actual behaviour}}{\text{predicted behaviour}} \qquad (6.6)$$

In the column buckling model in Section 3 uncertainty was treated as a random variable, X_m, and used in the failure function as follows:

$$M = X_m \times \text{critical buckling capacity} - \text{load}$$

The modelling uncertainty factor provides a convenient way of dealing with random and systematic "errors" arising out of modelling. In a purely deterministic sense X_m serves to "correct" the model for any conservatism (or non-conservatism). Note that for resisting variables $X_m > 1$ implies underprediction of performance (i.e. safe) and $X_m < 1$ implies overprediction (unsafe).

Following the spirit of the buckling modelling uncertainty X_m for fracture/tearing could be expressed as:

$$\frac{\text{actual fracture load}}{\text{predicted fracture load}}$$

or, since it is crtical crack size which is being modelled:

$$\frac{\text{actual crticial crack size}}{\text{predicted critical crack size}}$$

The denominators of both of these expressions imply knowledge of the material toughness δ_{mat} and because of this neither, as the following shows, are viable.

Unlike buckling, where the material properties can be known accurately before a test is performed, with fracture repeated nominally identical 3-point

bend tests result in a wide scatter of values of the toughness, δ_{mat}. The physical reasons for the scatter are not of immediate concern. It is relevant however that the modelling of the fracture process does not account completely for the observed physical phenomena. The 3-point bend test produces a random sample of the value of a material property called toughness. By obtaining increased numbers of samples a better picture is obtained of the toughness distribution. However this does not increase the accuracy with which a_{crit} can be predicted since the value of the crack-tip opening displacement at fracture in any large scale test is not any particular characteristic of the toughness distribution. Fracture in the large scale test also occurs at a random value of COD. In repeated large scale tests however the distribution of critical COD's would be expected to resemble the distribution of δ_{mat} obtained in repeated 3-point bend tests. This is the assumption on which the ability to predict critical and tolerable defect sizes rests.

The consequence of the random nature of toughness is that scatter in either of the above expressions for model uncertainty may derive either from the variation in "toughness" or from other modelling assumptions not realised in the test. Since toughness scatter is already taken into account by assuming a distribution for toughness in a_{crit} in Equation 6.5 any account of the variability in X_m would duplicate this.

The following describes an alternative approach to model uncertainty in fracture. Unlike buckling the model used in fracture/tearing/collapse failures can be used to predict displacement (i.e. the COD) at varying stress levels up the fracture event. Failure is predicted when this exceeds the critical COD,

δ_{mat}. Modelling accuracy can thus properly be expressed as

$$X_{m_\delta} = \frac{\text{actual COD}}{\text{predicted COD}} \qquad (6.7)$$

and ideally would be known at discrete stress levels. This modelling variable is independent of δ_{mat} and thus free of the duplicity described above.

The only available data on this value is contained in Reference 10 and is limited to a single test. This test indicates $X_{m_\delta} \approx 1.15$ at stresses below 0.5 of yield rising to 1.5 at 0.9 of yield. In view of the lack of representative data it was considered appropriate for this study to treat X_{m_δ} as deterministic with a value of 1.0 throughout the stress range. It has consequently been omitted from Equation 6.5 and from following references to the failure function.

6.7 Failure Function for Defect Assessment Codes

It is required to determine the reliability inherrent in code procedures. In other words what is the failure probability of the largest defect deemed by the code to be tolerable? If the largest defect determined using the PD6493 design curve is a_{DC} then $P(M < 0)$ where

$$M = a_{crit} - a_{DC} \qquad (6.8)$$

is the required failure probability. In this case a_{DC} is equal to a_m given in Equation 6.3. Similarly if the defect deemed tolerable using a revised procedure based on the strip yield model is a_{SY} the appropriate failure function would be

$$M = a_{crit} - a_{SY}/\gamma_a \qquad (6.9)$$

and P(M < 0) would be the required failure probability.

a_{SY} here is the solution to Equation 6.4 when the input values of toughness and stress are modified by partial factors γ_τ and γ_σ respectively. Additionally a lower bound toughness $\delta_{min\,3}$ being the minimum of three COD tests is used. γ_a is a partial factor on defect size. These factors are fully described in the discussion on a Model Code in Section 8.

By writing the (iterative) solution to Equation 6.4 as

$$a = f_2(\sigma \ , \ \delta) \tag{6.10}$$

then

$$a_{SY} = f_2(m_\sigma \gamma_\sigma \ , \ \delta_{min\,3}/\gamma_\tau) \tag{6.11}$$

and

$$a_{crit} = f_2(m_\sigma \ , \ m_\delta) \tag{6.12}$$

Equation 6.9 becomes

$$M = f_2(m_\sigma \ , \ m_\delta) - \frac{f_2(m_\sigma \gamma_\sigma \ , \ \delta_{min\,3}/\gamma_\tau)}{\gamma_a} \tag{6.13}$$

Identifying the mean and standard deviation of the random variables as $[m_X , s_X]$ gives

$$M = f_2([m_\sigma , s_\sigma] , [m_\delta , s_\delta]) - \frac{[f_2(m_\sigma \gamma_\sigma , \delta_{min3}/\gamma_\tau) , s_a]}{\gamma_a} \qquad (6.14)$$

where s_a is the standard deviation assumed for the random variable modelling detection accuracy.

The Level II safety index, β, is found by finding a stress, σ^*, toughness, δ^* and defect size, a^* such that

$$x^* = m_X + \alpha_X \beta s_X \qquad x=\sigma , \delta , a \qquad (6.15)$$

and

$$M(x^*) = 0$$

$$\text{i.e.} \quad M(x^*) = f_2(\sigma^* , \delta^*) - a^* = 0 \qquad (6.16)$$

$$\text{or} \quad a^* = f_2(\sigma^* , \delta^*) \qquad (6.17)$$

By comparing Equation 6.17 to 6.10 it is clear that the failure function is in precisely the same form as the solution to Equation 6.4. Evaluation of M in Equation 6.9 does not therefore require separate iterative solutions for a_{crit} and a_{SY} as Equations 6.11 and 6.12 would suggest. Rather, a single iterative solution to Equation 6.16 is necessary for each new design point created in the advanced FOSM solution algorithm. Only one prior additional iterative solution is required to determine m_a which is given by a_{SY}/γ_a where a_{SY} is given in Equation 6.11.

Figure 6.1 presents plots of safety index, β, versus total stress nondimensionalised by yield stress. The dashed curve derives from Equation 6.8 (i.e. $\beta = \Phi^{-1}(1 - p_f)$, $p_f = P(M < 0)$, M from Equation 6.8) when a_{DC} is calculated using the estimate of the minimum of three 3-point bend tests for toughness (see Appendix B). The solid curves derive from Equation 6.9 but with

$$a_{SY} = \frac{f_2(m_\sigma , m_\delta)}{\gamma_a}$$

and γ_a = 1.75, 2.5 and 4.0, i.e. partial factors on stress and toughness are assumed to be 1.0 and the mean toughness used. In Figure 6.1 the stress is assumed to be pure tension and in Figure 6.2, pure bending.

6.8 Discussion

The reasons of the seemingly low reliabilities in Table 6.1 and Figures 6.1 and 6.2 raise the need for verification. For this Equation 1.8, the mean value FOSM method can be invoked:

$$\beta = \frac{m_R - m_L}{\sqrt{(s_R^2 + s_L^2)}} \qquad (6.18)$$

whence, provided $m_L \neq 0$

$$\beta = \frac{\theta - 1}{\sqrt{V_R^2\ \theta^2 + V_L^2}} \qquad (6.19)$$

where V = s/m, the COV, and

$\theta = m_R/m_L$ can be called a global safety factor.

For $\theta = 1$ obviously $\beta = 0$. As θ becomes large the numerator in Equation 6.19 is dominated by θ and the denominator by $V_R \theta$. Hence

$$\lim_{\theta \to \infty} \beta = \frac{1}{V_R} \qquad (6.20)$$

The R in the context of defect assessment represents calculated critical defect size, a_{crit}, which is a function of material toughness and stress level. Since the COV of a_{crit} is at least as large as the COV of toughness for which a value of 50% has been indicated then it must be expected that $\beta < 2.0$. This is true for any arbitrary large safety factor and thus for any actual defect size greater than zero. Performing a similar calculation for static collapse of columns, say, where the largest COV on the resistance side was for modelling uncertainty and approximately 15% then for any column, regardless of safety factor, $\beta < 6.7$. The Mean Value FOSM method underestimates the exact safety indices by approximately 0.5. Nonetheless the point is clear that there is a limiting upper bound to reliability which for fracture is much smaller than for static collapse.

Table 6.1 shows the deterministic margin between actual defect size and allowable defect size in two assessments may be the same but the probabilities of actual defect size being greater than the critical defect size (as parametised by β) can vary substantially. The latter, of course, depends upon the degree of variability in the input information whilst the former does not.

Figures 6.1 and 6.2 show the extent to which safety index depends on stress ratio. For one-off assessments it would be expected that the reliability for similar defect sizes reduces as the stress level increases. For making defect

assessments, however, such a dependency is not at all desirable: ideally the curve would be flat indicating a similar degree of confidence in assessing defects at higher stresses as at lower stresses. In other words the assessment procedure should compensate for the effect. The analytical reason is that a singularity exists in Equation 6.4 at $S_r = 1$ where S_r is the plastic collapse ratio of net to flow stress. When flow stress is taken as the average of yield and ultimate tensile stress (as it is here) the singularity corresponds to $\sigma/\sigma_y \approx 1.15$ (BS4360 Grade 500). Thus, although mean values of both a_{crit} and a_{SY} in Equation 6.9 reduce as stress is increased, near the singularity they both approach zero and the difference between them becomes smaller. The deterministic safety margin and consequently β is thus reduced.

The dependence would be offset if the modelling factor, with a mean value rising with increasing stress level, had been employed. The degree to which the curve would be restored would of course depend on the rate of increase of modelling uncertainty to stress ratio. It is unlikely that the value of 1.5 suggested in Section 6.5 for modelling uncertainty at stresses close to yield would have significant impact. The apparent decline in safety with increasing stress must therefore be viewed as a real phenomenum, i.e. making assessments at stresses approaching yield contains more risk than for lower stresses.

A second striking characteristic of Figures 6.1 and 6.2 is the dissimilarity between the Design Curve (dashed curve) and the curve for the strip yield method (designated Level 2). Although the same general function has been used to plot all the curves the way a_{DC} varies with stress is different from the variation of a_{SY}. Had they been plotted on a toughness base the distinction would have been less obvious.

Lastly the steeply rising values of β at low stresses are apparent for the strip yield method in both figures. The tolerable defects in these cases were very large compared to the plate width and unlikely to be tolerated in any structure. In a later refinement to the strip yield approach a penalty applied to stress intensity factor is imposed when the defect size is greater than 10% of the load bearing area. This will be seen to completely alter the shape of the β versus stress curve at low stresses and cause it to plunge rather than climb. This emphasises a point brought out in earlier Sections that the calculated reliability is only as good as the model which it uses to calculate critical values. Little heed should be paid to reliability values for stresses below $0.4\sigma_y$ shown in the figures. For higher stresses there is relative consistency between the two approaches and the β-values are more relevant.

The results pose a problem for calibration since assessments are usually carried out where the total stress could be any value up to and beyond yield magnitude. Given this variation how does one choose a discrete target reliability to represent all stress levels?

Two alternative solutions to this problem are examined in Sections 7 and 8.

6.9 Conclusions

1. Model uncertainty is most usefully described by values of

$$\frac{\text{actual applied COD}}{\text{predicted applied COD}}$$

Data should be sought on this expression at different stress levels and used to refine the model.

2. When the coefficient of variation for the toughness distribution is V_T the maximum value of safety index cannot be greater than $1/V_T$ whatever the size of defect or magnitude of safety factor. This limits the safety index for fracture to approximately 2.0.

3. Level II reliability analysis using the failure function derived provides a reasonable way of assessing a known defect. The advantages over any deterministic approach are that it can cope with individual estimates of the uncertainties involved in the input parameters. Users of this method would gain additional information on the relative sensitivity of the input variables.

4. In assessments using either existing or proposed rules there is significantly more risk in assessing a defect in a region of high stress than for one in a low stressed region.

6.10 References

1. PD6493 : 1980, Guidance on some methods for the derivation of acceptable levels for defects in fusion welded joints. British Standards Institution, London, 1980.
2. Dugdale, D.S. 'Yielding in Steel Sheets Containing Slits', J. Mech. Phys. Solids, Vol. 8, 1960, pp100-104.
3. Plane, C.A. and Cowling, M.J., 'Further Studies on Reliability Aspects of Defect Assessment'. Final Report, Vol. 3, Defect Assessment in Offshore Structures 1985/87.
4. "Rationalisation of Safety and Serviceability Factors in Structural Codes' - Construction Industry Research and Information Association, London, CIRIA Report 63, 1977.

5. Leporati, E., 'The Assessment of Structural Safety', Series in Cement and Concrete Research, Vol. 1, Edited by A. Short, Research Studies Press, Oregon 1979.

6. Chang, J.T.L., 'Investigation of the Wu Algorithm for Computing Structural Reliability'. Engineering Experiment Station, College of Engineering, The University of Arizona, October 1985.

7. Towers, O.L., Williams, S. and Harrison, J.D., 'ECSC Collaborative Elastic-Plastic Fracture Toughness Testing and Assessment Methods', Final Contract Report for the Commission of the European Communities, Report No. 3571/10M/84 The Welding Institute, June 1984, Cambridge.

8. Dawes, M.G., 'The CTOD Design Curve Approach: Limitations and Finite Size'. Welding Institute Report 278/1985, June 1985.

9. Proposed revisions to PD6493 Section 2 revision 4: Private communication.

10. Anderson, T.L., Leggatt, R.H., Garwood, S.J., 'The Use of CTOD Methods in Fitness for Purpose Analysis', Welding Institute Staff Paper, April, 1985.

11. Garwood, S.J., 'A Crack Tip opening Displacement (CTOD) Method for the Analysis of Ductile Materials', Welding Institute research report no. 277/1985, June 1985.

12. Hancock, J.W. and Cowling, M.J., 'Role of State of Stress in Crack-Tip Failure Processes', Metal Science, August-September, 1980, pp293-304.

13. Flint, et al. 'The Derivation of Safety Factors for Design of Highway Bridges', in the Design of Steel Bridges, ed. Rockey and Evans, Granada, London, 1981, pp11-36.

14. Anderson, T.L., 'Elastic-Plastic Fracture Mechanics Assessments Based on CTOD'. Welding Institute Research Report No.276/1985.

15. Benjamin, J.R. and Cornel, C.A., 'Probability, Statistics and Decision for Civil Engineers', McGraw-Hill Book Co., 1970.

σ/σ_Y (tension)	stress cov% (Normal)	toughness cov% (Weibull)	defect size (mm)	β	a_{DC}* (mm)	repair? (Y/N)	a_{SY}** (mm)	repair? (Y/N)	most sensitive
0.3	5	20	60	2.73	98.0	N	78.7	N	tough.
0.3	5	20	80	1.20	98.0	N	78.7	Y	tough.
0.3	5	50	60	1.27	68.2	N	67.6	N	tough.
0.3	5	50	80	0.44	68.2	Y	67.6	Y	tough.
0.3	30	20	60	1.64	98.0	N	73.0	N	stress
0.3	30	20	80	0.51	98.0	N	73.0	Y	stress
0.3	30	50	60	1.04	68.2	N	61.5	N	tough.
0.3	30	50	80	0.31	68.2	Y	61.5	Y	stress
0.9	5	20	8	1.93	13.6	N	9.80	N	tough.
0.9	5	20	10	1.45	13.6	N	9.80	Y	tough.
0.9	5	50	8	0.97	9.40	N	7.00	Y	tough.
0.9	5	50	10	0.68	9.40	Y	7.00	Y	tough.
0.9	30	20	8	0.58	13.6	N	6.10	Y	stress
0.9	30	20	10	0.43	13.6	N	6.10	Y	stress
0.9	30	50	8	0.52	9.40	N	4.40	Y	stress
0.9	30	50	10	0.36	9.40	Y	4.40	Y	stress

Table 6.1 Comparison of safety indices, β, for different input parameters

* a_{DC} = tolerable defect size using design curve with estimate of minimum-of-three toughness
** a_{SY} = tolerable defect size using strip yield approach with estimate of minimum-of-three toughness and stress partial factors of 1.1 and 1.2 for stress cov = 5% and 30% respectively.

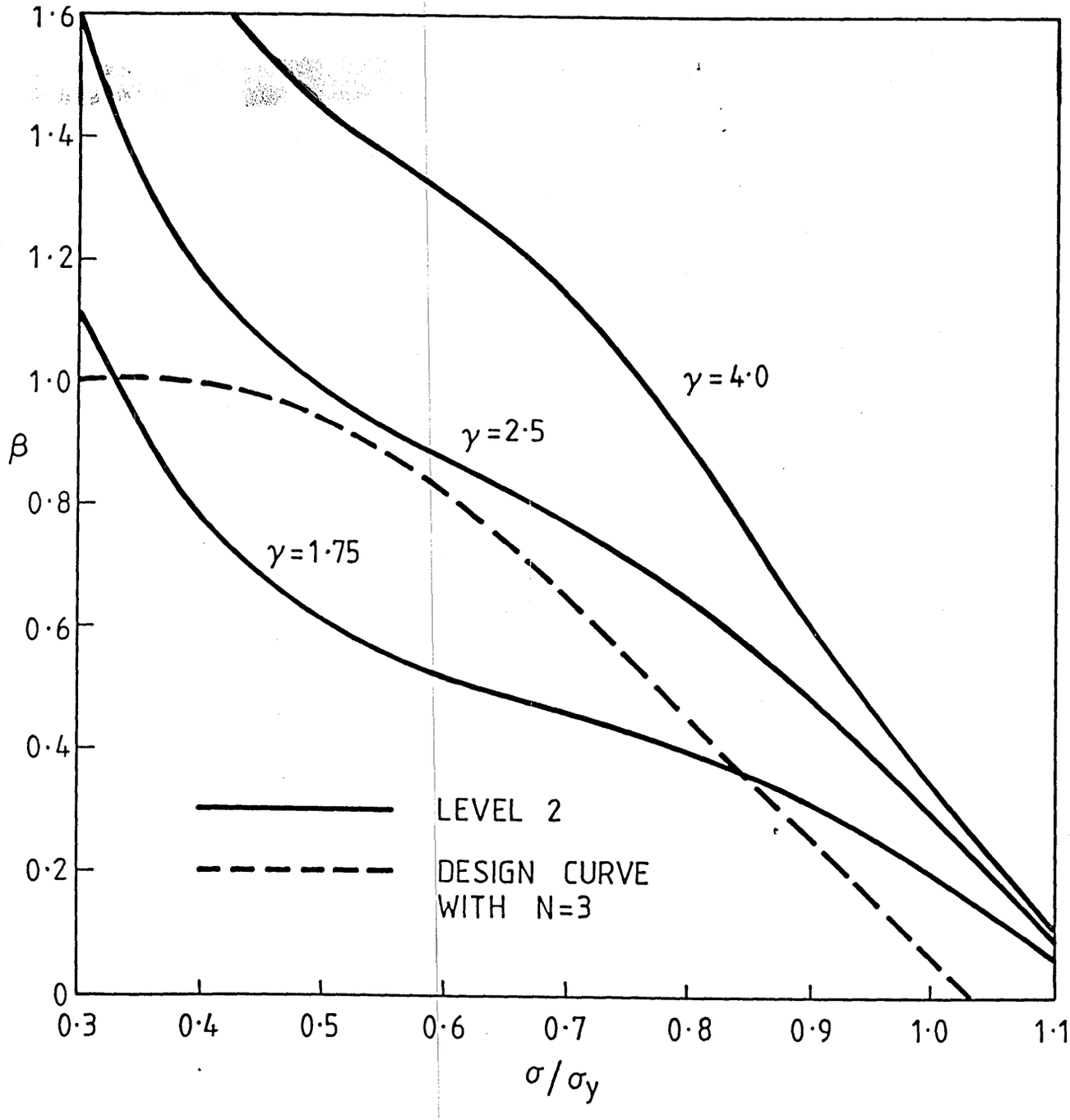

Fig. 6.1
SAFETY INDEX vs. STRESS RATIO FOR A THROUGH CRACK IN PURE TENSION

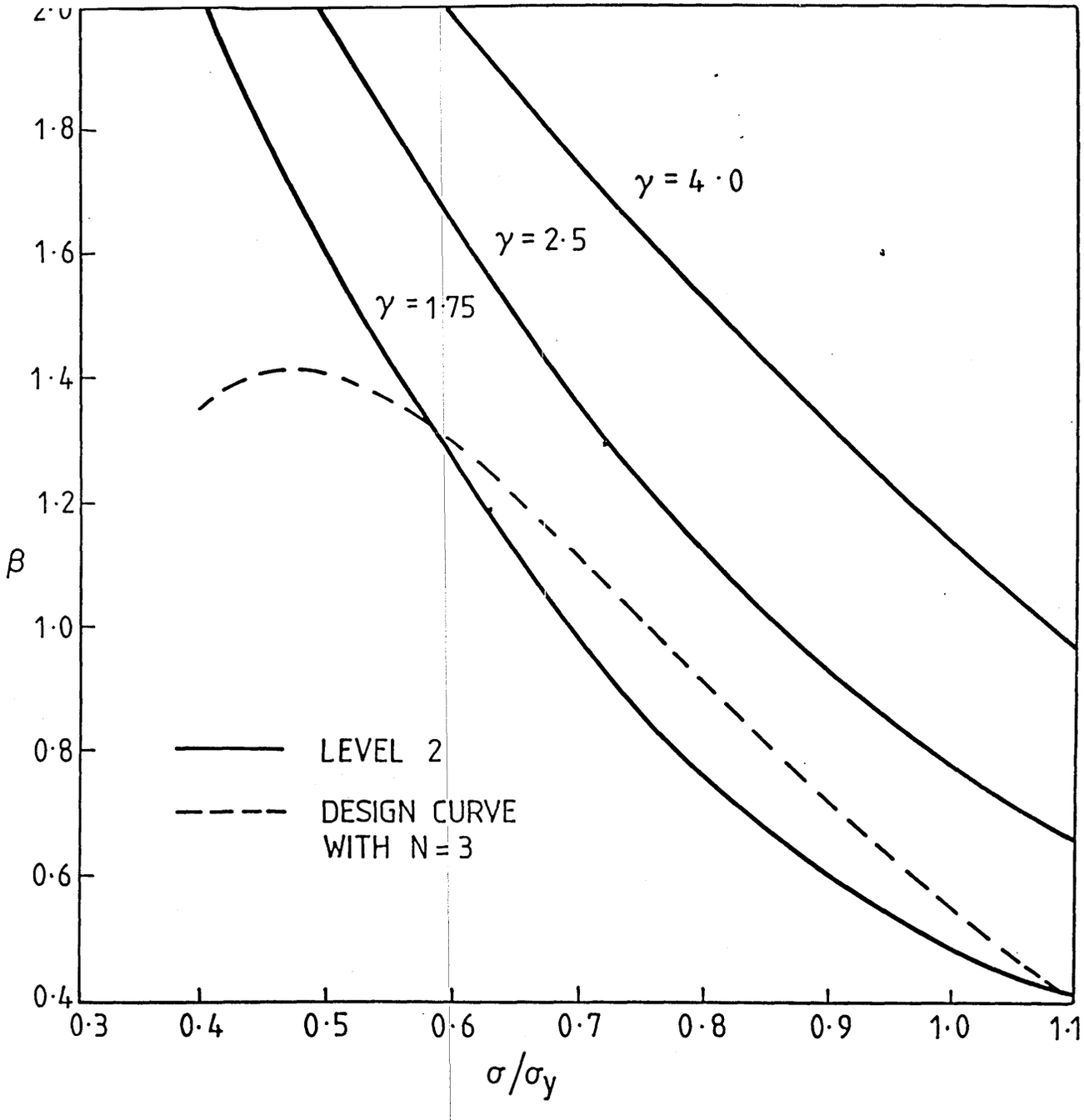

Fig. 6.2
SAFETY INDEX vs. STRESS RATIO FOR A SEMI-ELLIPTICAL SURFACE DEFECT IN PURE BENDING

Where f and φ are the probability density functins (pdf) corresponding to the cummulative distribution functions (cdf) F and Φ respectively.

Rearranging:

$$u_i \approx \frac{x_i - x_i^* - \left[\frac{\Phi^{-1}[F(x_i^*)]\varphi\{\Phi^{-1}[F(x_i^*)]\}}{f(x_i^*)}\right]}{\frac{\varphi\{\Phi^{-1}[F(x_i^*)]\}}{f(x_i^*)}} \qquad \text{A3}$$

Comparison of Equation A3 and A2 gives

$$s_x^N = \frac{\varphi\{\Phi^{-1}[F(x_i^*)]\}}{f(x_i^*)} \qquad \text{A4}$$

and

$$m_x^N = x_i^* - \Phi^{-1}[F(x_i^*)]\, s_x^N \qquad \text{A5}$$

If Equation A1 is corrected as shown only at the design point the transformation gives good approximation in the proximity of this point i.e. in the region of major interest for checking safety. The transformation is equivalent to fitting any given distribution by a normal distribution both having the same cdf and pdf at the design point.

Finally if x_i is lognormally distributed and for convenience dropping the i subscript and * superscript,

$$F(x) = \Phi\left[\frac{\ln(x/\tilde{m}_x)}{\sigma_{\ln x}}\right] \qquad \text{A6}$$

APPENDIX A

Derivation of Rackwitz-Fiesler transformations m^N and s^N for non-normal variables.

In theory it is possible to replace a random variable x_i, having a given cummulative distribution function $F(x_i)$ by a normal standardised variable u_i. The two variables are related by

$$F(x_i) = \Phi(u_i)$$

i.e. $$u_i = \Phi^{-1}[F(x_i)] \qquad A1$$

Let y_i be a normal variable such that

$$u_i = (y_i - m_i^N)/s_i^N$$

where m_i^N and s_i^N are the mean and standard deviation of y_i respectively. The problem is to find m_i^N and s_i^N for $y_i = x_i$.

By a Taylor power series expansion of Equation A1 at x_i^* and considering linear terms only.

$$u_i \approx \Phi^{-1}[F(x_i^*)] + \left[\frac{\partial \Phi^{-1}[F(x_i)]}{\partial x_i}\right]_{x_i^*} (x_i - x_i^*)$$

Where the notation indicates derivatives are calculated at the design point. Differentiating the inverse function gives

$$u_i \approx \Phi^{-1}[F(x_i^*)] + \frac{f(x_i^*)(x_i - x_i^*)}{\varphi\{\Phi^{-1}[F(x_i)]\}}$$

and

$$f(x) = \frac{1}{x\sigma_{\ln x}} \varphi \frac{\ln(x/\tilde{m}_x)}{\sigma_{\ln x}} \qquad \text{A7}$$

where $\sigma_{\ln x} = \sqrt{\ln(V_x^2 + 1)}$,

$\tilde{m}_x = m_x \exp(-\frac{1}{2}\sigma_{\ln x}^2)$,

V_x = the standard deviation $\div$ m_x

Substituting A6 and A7 into A4 and A5 and reintroducing the i subscript and * superscripts gives:

$$s_x^N = x_i^* \sigma_{\ln x} \qquad \text{A8}$$

$$m_x^N = x_i^* - \ln(x_i^*/\tilde{m}_x) x_i^* \qquad \text{A9}$$

When iterating to find the minimum distance, β, for lognormally distributed variables the s_i and m_i in Equations 1.23 and 1.25 must be replaced by s_x^N and m_x^N using Equations A8 and A9 respectively.

APPENDIX B

The relationship between the Weibull scale factors of a parent distribution of toughness and the distribution derived from selecting the minima of samples of size N is shown by example. The same relationship is shown to exist between the expected values of the two distributions.

Example

If δ follows a Weibull distribution with shape and scale parameters α and β respectively

a) find $E(\delta)$

b) show that the derived distribution of the minima, δ_N, of a number of random samples of size N from the parent Weibull population is also Weibull.

c) find the parameters α^1 and β^1 of the derived distribution.

d) show that the ratio of the expected values of the two distributions is $N^{1/\alpha}$.

Solution:

a) any statistical text-book, for example Reference 15, carries this solution:

$$E(\delta) = \beta\Gamma(1 + \frac{1}{\alpha})$$

where $\Gamma(-)$ is the gamma function.

b) Let $F_\delta(\delta)$ be the parent distribution of toughness and let $F_{\delta_N}(\delta_N)$ be the distribution derived from selecting the minima of random samples of size N.

For any toughness T

$$Pr(\delta > T) = 1 - Pr(\delta < T)$$

$$= 1 - F_\delta(T)$$

If N tests to determine toughness are carried out the probability that all N values are greater than T is $[1 - F_\delta(T)]^N$ and the probability that at least one value is less than T is $1 - [1-F_\delta(T)]^N$.

This probability is identical to the probability that the minimum of N δ values is less than T, i.e.

$$Pr(\delta_N < T) = 1 - [1 - F_\delta(T)]^N$$

If many tests are carried out in groups of N and the minimum, δ_N, is selected from each group the distribution of δ_N's is defined by

$$F_{\delta_N}(T) = Pr(\delta_N < T)$$

Thus

$$F_{\delta_N}(T) = 1 - [1 - F_\delta(T)]^N$$

If F_δ is Weibull it has the form

$$F_\delta(T) = 1 - \exp[-(\frac{T}{\beta})^\alpha]$$

Therefore

$$F_{\delta_N}(T) = 1 - [\exp[-(\frac{T}{\beta})^\alpha]]^N$$

$$= 1 - \exp[-(\frac{T}{\beta/N^{1/\alpha}})^\alpha]$$

i.e. F_{δ_N} is Weibull

c) From b)

$$\alpha^1 = \alpha$$

$$\beta^1 = \beta / N^{1/\alpha}$$

d)
$$E(\delta_N) = \beta^1 \Gamma(1 + \frac{1}{\alpha^1})$$
$$= \frac{\beta}{N^{1/\alpha}} \Gamma(1 + \frac{1}{\alpha})$$

Therefore, using a)

$$\frac{E(\delta)}{E(\delta_N)} = N^{1/\alpha}$$

SECTION 7

FURTHER STUDIES ON RELIABILITY ASPECTS OF DEFECT ASSESSMENT

7.1 Introduction

In order to verify the results of the FOSM method for defect assessment reliability both Monte-Carlo simulation and FOSM methods are used to solve the same reliability problem. The latter is found to have a good degree of accuracy despite the highly skewed toughness distribution.

The FOSM method is then used to tabulate safety indices and relative sensitivity codes for different combinations of distribution characteristics of the basic variables: stress, toughness and defect size. Tabulation is carried out for the case when actual defect is assumed to be the largest allowable defect according to the strip yield model and when actual defect size is assumed to be the largest allowable defect according to the current PD6493[1] design curve.

The problem of calibrating defect assessment codes when there is a strong dependence of assessment reliability on stress was raised in Section 6. If it can be assumed that assessments carried out according to the design curve at a specific stress level have adequate, but not excessive, reliability then this can be used to identify a target reliability. Using this target and the tables presented in this section a safety factor on Level I[2] assessments can then be obtained. The process of this defect by defect calibration is demonstrated by example.

Notation

a	half width of through defect, height of surface defect or half height of embedded defect
COD	crack tip opening displacement
E	Young's Modulus
K	stress intensity factor
w	width of section
α	sensitivity factor
β_T	target safety index
γ	safety factor
δ_{mat}	critical COD
σ_f	flow stress (= mean of yield and tensile stress)
σ_m	membrane stress
σ_n	net stress
σ_y	yield stress

Other notation is defined in the text.

7.2 Comparisons with Monte-Carlo Simulation

The validity of advanced Level II reliability analysis when highly skewed (non-normal) variables make up the design space is examined in this sub-section. Comparison will be made with a single reliability calculation using Monte-Carlo Simulation.

7.2.1 Random Number Generators

The Multiplicative Congruence method produces a series of pseudo-random numbers using the following algorithm:

$$r_{n+1} = a\ r_n \text{(modulo } m\text{)}$$

where a and m are prime integer constants. Using an integer "seed" i_0 the first pseudo-random number r_1 in the interval [0,1] is obtained from

$$\frac{a i_0}{m} = j_1 + \frac{a i_0 - j_1 m}{m} + \frac{i_1}{m} = j_1 + r_1 \qquad (7.1)$$

i.e. r_1 is the fractional part of the quotient ai_0/m and j_1 is the integer part. The description "pseudo" is used because the series eventually repeats itself. Provided a and m are correctly chosen the cycle is sufficiently large for most purposes (in excess of 10^{12} cycles).

This method generates numbers such that any number in the interval [0,1] has an equal chance of occuring. In order to produce random deviates with a specific probability distribution it is sufficient to calculate the inverse function:

$$x = F_X^{-1}(r) \qquad (7.2)$$

where r is the random number and F_X is the cummulative distribution of x. (For cummulative distribution functions which cannot be inverted in closed form numerical integration must be used). For the Weibull distribution the CDF is

$$F_X(x) = 1 - \exp[-(\frac{x}{\beta})^{\alpha}] \qquad (7.3)$$

whence

$$x = \beta[\ln(\frac{1}{1 - F_X(x)})]^{1/\alpha} \qquad (7.4)$$

Hence of series of independent random deviates x_i may be obtained from:

$$x_i = \beta[\ln(\frac{1}{1 - r_i})]^{1/\alpha} \qquad (7.5)$$

where the r_i have a rectangular distribution in the interval [0,1]. The Normal and Lognormal distributions are generally treated as special cases. Use is made of the Central Limit Theorum and random numbers are derived from the sum of n, (n>12) rectangularly distributed random numbers. Random numbers on the Glasgow University Computing Services ICL3988 computer are called from a source program specifying the parameters of the distribution. This greatly facilitates the application of Monte-Carlo Simulation.

7.2.2 Monte-Carlo Simulation for Defect Assessment

In a single trial random values of stress, defect size and toughness are generated by calling the relevant library sub-routine with the appropriate distribution paramters. Failure is assumed to have occured for the trial if M<0 where

$$M = a_{crit}(\text{stress}, \text{toughness}) - \text{defect size} \qquad (7.6)$$

i.e. a_{crit} is evaluated as the solution to Equation 6.4 using the random values of stress and toughness. The failure probability is the ratio of the number of failures to the number of trials, N, when N is large. Table 7.1 presents the first 20 random values of stress, defect size and toughness and the corresponding values of M. Table 7.2 presents the values of failure probability, the numbers of failures, and safety index, β for various values of N up to 300,000. Table 7.3 presents the input and output information when the advanced Level II method is used to solve the same problem. The OCP (central processor) times from which cost is calculated are given for each calculation.

7.3 Sensitivity Factors

The method of determining safety indices used in the previous Section is an Advanced Level II procedure and is fully documented in References 3 and 4 as well as elsewhere in this thesis. Variables are not all equally influential on safety. A one standard deviation shift in one variable will, in general, have a different influence on the safety margin than the same shift in another. Knowledge of sensitivities is thus essential to the design code drafter when deciding which variables should be represented in the assessment equations by their characteristic (lower bound) value. This same knowledge is also useful to designers who, conscious of the need to allocate resources prudently, may need to decide on which assessment variable to concentrate the most resources.

The relative sensitivity of any variable is governed by the form of the failure function, (see Section 6.7) as well as its degree of uncertainty relative to other variables; it is generally not obvious from cursary examination of the failure function and is only revealed by the type of analysis referred to here. The prime interest in sensitivities is their order rather than in their absolute value.

7.4 Failure Function

The failure function adopted to determine the failure probability of a defect assessed as being safe is

$$M = a_{crit}(x_1, x_3) - a_{tol}(x_2) \qquad (7.7)$$

where x_1 = stress

x_2 = defect size

x_3 = COD toughness.

a_{crit} = critical defect size

a_{tol} = tolerable defect size

Failure is assumed to occur when M becomes negative.

The collapse modifed strip yield model[5] was used to define the critical defect. This requires the solution of

$$\frac{S_r}{\frac{8}{\pi^2} \ln \sec\left(\frac{\pi}{2} S_r\right)} - \surd\delta_r = 0 \qquad (7.8)$$

where S_r is the ratio of net to flow stress and δ_r is the ratio of applied to critical COD. Both are functions of defect size and an iterative solution is required.

For a through crack in pure tension

$$S_r = \frac{\sigma_n}{\sigma_f} = \frac{\sigma_m}{(1 - \frac{2a}{W})\sigma_f} \qquad (7.9)$$

$$\delta_r = \delta_I / \delta_{mat} \qquad (7.10)$$

$$\delta_I = K^2 / \sigma_y E \qquad (7.11)$$

$$= \sigma_m{}^2 \pi a / \sigma_y E$$

For other defect geometries and loading types appropriate net stresses, σ_n, and correction factors to the stress intensity factors, K, were used.

Tolerable defects sizes were calculated

a) using the strip yield model (Equation 7.8) with mean toughness and with defect size factored by three choices of safety factor,

b) for the target reliability study from the PD6493 design curve[1] assuming a toughness equivalent to the minimum of three COD tests and no factor on defect size.

The tolerable defect parameter in PD6493 was converted using Figures 12 and 13 of that document[1] to obtain defect heights for surface and embedded cracks.

7.5 Results

The distribution characteristics considered for the basic variables are presented in Table 7.4. Table 7.5 defines the defect geometry and loading types.

The pattern of changing sensitivities and safety indices with different means and COVs of the basic variables is complex and does not lend itself to two-dimensional graphical representation. A means of presentation which is

concise yet does not sacrifice much detail has therefore been adopted. For any combination of mean and COV of the design variables a code has been used indicating the order of sensitivities. Where any particular variable is predominantly influential this has also been indicated. The sensitivity codes are given in Table 7.6.

Two groups of results are presented. The first, Tables 7.7 to 7.30, give the safety index and sensitivity codes for every combination of the design variable distribution characteristics using the strip yield method to define the tolerable defect size. The second group, Tables 7.31 to 7.36 give safety index only for the same combinations of distribution characteristics but with tolerable defect size defined by the PD6493 design curve (assuming a toughness equivalent to the minimum of three COD tests). This is consistent with past usage of PD6493 and therefore these results provide a datum safety level.

The results can be used to identify an appropriate safety factor for use with the strip yield method or to determine the order of sensitivities, or both. The two uses are now described in more detail.

7.5.1 To Determine Safety Factors for the Strip Yield Method on a Defect by Defect Basis

In the main study, Tables 7.7 to 7.30, three safety indices are presented - one for each value of safety factor. Note that the safety factor is applied to the defect size assessed assuming mean toughness. When the minimum of N COD tests is to be used the safety factors must be made to compensate by dividing each by $N^{\frac{1}{2}}$. The safety factor should be chosen such that the safety index matches the appropriate value in the tables of target reliabilities.

Choice of target reliability

It was shown in Section 6 that for through thickness defects in tension assessed using the COD design curve the reliability drops steeply and steadily from stresses of $0.3\sigma_y$ to yield. The same problem is noticeable but not as pronounced for other defect types. This complicates the choice of target reliability since one must first ascertain an appropriate stress level and then translate this to a target safety index using Tables 7.31 to 7.36. The object of indentifying a target reliability is to determine a reliability acknowledged through past experience as being adequate. The bounds on possible choices may be identified as follows:

Upper bound

Recent work at the Welding Institute[6] suggests that in A533B steel at least the COD design curve used with mean toughness is overconservative at stresses below 90% of yield and unsafe at higher stresses. These conclusions arise from results of seven centre cracked and semi-elliptical surface notched tension panels in 110mm thick material at upper shelf temperatures. No comparable result is available for cracks in pure bending. For cracks in tension the smallest practicable safety margin is considered to be that obtained using the COD design curve with a minimum-of-three toughness input at 80% of yield.

Lower bound

If the stress level used to obtain the target reliability is equal to that at which the defect is being assessed both the COD design curve and the strip

yield method will lead to the same tolerable defect. The lower bound of stress (corresponding to the upper bound of reliability) is thus that to which the defect is subject.

The stress levels indicated in Tables 7.31 to 7.36 (the target reliability tables) are 80%, 60% and 40% of yield. The final choice will vary with the application and be obtained by considering the maximum stress level at which past use of the COD design curve has proved satisfactory.

As the example below illustrates, any choice greater than the stress at which the defect is being assessed will result in an increase in tolerable defect size (of the strip yield method over the COD design curve predictions) yet maintain safety at a level known to be adequate.

To determine the relative sensitivities

The order of sensitivities of the three basic variables; stress, defect size and fracture toughness can be obtained from the code in the appropriate table.

To use the tables knowledge of stress COV, approximate stress level, approximate fracture toughness and defect size standard deviation is required. Choice of stress COV and defect size standard deviation should be confirmed by consulting available literature. Some general guidance on stress COV may be found in Reference 3 whilst Reference 7 gives COV information relevant to offshore structures. Consideration should be given to the type of environment as well as the detection method when choosing the defect standard deviation.

Both uses are illustrated by the following example:

7.5.2 Example

Assume a situation with high uncertainties in stress and detection accuracy i.e. stress COV=40%, defect size standard deviation = 10mm. Also assume a high toughness material ($\delta_{mat} \simeq 0.257$). For a through crack in uniform tension find the safety indices when the tolerable defect is determined using the approach with a single safety factor or defect size of γ = 1.75, 2.5 and 4.0. What is the most sensitive variable? Assuming a target reliability corresponding to that obtained using the COD Design Curve at σ/σ_y = 0.8 find a suitable safety factor on assessments using the strip yield method.

Assume σ/σ_y = a) 0.4, b) 0.6, c) 0.8.

Given the values of the tolerable defect size using the Design Curve, $a_{DC}(TOL)$, and the critical defect using the strip yield method $a_{SY}(CRIT)$ complete the following table:

σ/σ_y	$a_{DC}(TOL)$	$a_{SY}(CRIT)$	Sensitive Variables	γ	$a_{L2}(TOL)$
0.4	70.7	143.1			
0.6	30.3	73.9			
0.8	19.3	37.3			

where $a_{SY}(TOL)$ is the defect size using the strip yield method and factored by γ.

Solution

Defect is Type 1 (see Table 7.5)

a) $\sigma/\sigma_y = 0.4$

From Table 7.7:

γ =	1.75	2.5	4.0
β =	0.8	1.2	1.7

The sensitivity code is 4 for γ=1.75 and 2 for other safety factors (Table 3) indicating that stress and toughness are approximately equally sensitive.

From Table 7.31 at $\sigma/\sigma_y = 0.8$, $\beta_T = 0.5$.

Since γ=1.75 gives a reliability greater than β=0.5 it may be considered that this is adequate. (Extrapolation is not recommended since the β vs. γ relationship is non-linear. Interpolation between the tabulated values however will not lead to significant errors).

b) $\sigma/\sigma_y = 0.6$

From Table 7.7

γ =	1.75	2.5	4.0
β =	0.5	0.9	1.3

The sensitivity code is 4 therefore (Table 7.6) stress is most influential.

The target safety index is achieved with γ=1.75.

c) σ/σ_y = 0.8

From Table 7.7

γ =	1.75	2.5	4.0
β =	0.4	0.7	0.9

The sensitivity code 7 indicates that stress is dominantly influential.

A safety factor between 1.75 and 2.5 is necessary to achieve a target safety index of 0.5. By interpolation γ = 2.0.

σ/σ_y	a_{DC}(TOL)	a_{SY}(CRIT)	Sensitive Variables	γ	a_{SY}(TOL)
0.4	70.7	143.1	σ and δ	1.75	81.8
0.6	30.3	73.9	σ	1.75	42.2
0.8	19.3	37.3	σ (>0.9)	2.00	18.6

N.B. The defect assessed using the strip yield method with a toughness obtained from the minimum of three COD tests would, on average, be the value in column 3 divided by $\sqrt{3}$. The safety factor would then need to be factored by the same amount. The value of tolerable defect size in the final column would thus remain unchanged.

7.6 Discussion

The validity of the FOSM method is clearly verified from examination of the safety indices in Tables 7.2 and 7.3. The Monte-Carlo solution after 300,000 trials agrees with the FOSM solution to one decimal place. Table 7.1 has been included because it provides a visual verification that the modelling of randomness is reasonable. This is especially useful in the case of toughness. Often the results of repeated COD tests appear so scattered as to be unyielding to any probabilistic description. The 20 random values shown range from 0.303 down to 0.032. The degree of scatter is realistic but to be more representative of actual data values as low as 0.001 might also be expected.

The values of safety margin M are not in millimetre units as might be supposed from Equation 7.7, they are, rather, non-dimensional. None of the 20 values is negative: at the failure rate predicted an average of one negative value in the first 156 trials would be expected. Note that the lowest toughness corresponds to the lowest safety margin although in this trial both stress and defect size are well on the unsafe side of the mean. The largest toughness does not correspond to the greatest safety margin. From these results it is clear that there is no direct way of determining the relative sensitivity of each variable to the overall result.

The FOSM method on the other hand gives a direct value, the sensitivity factor as shown in Table 7.3. The factors are such that their squares sum to unity. Toughness is seen to be the most sensitive in this instance. The negative simply distinguishes between loading and resistance variables (see Section 1 for definitions) and does not affect the order of ranking. Defect size is least

sensitive. The method also provides a design point - the point on the failure surface with the highest joint probability density - and can be taken to be the most likely combination of values of the variables at failure. Note that the design point for toughness, 0.019, is well below the expected value of the minimum of three COD tests = $0.125/3^{1/2.101}$ or 0.074 (see Appendix B of Section 6). The central partial safety factor in Table 7.3 is the ratio of design point to mean. These would be the actual code partial factors applied to mean values of the basic variables if the target value of safety index was 2.48 and if the statistical parameters assumed for stress, defect size and toughness were representative of all defect assessments. Since this is clearly not the case optimisation has to be entered into to determine optimal values of partial factors to suit the range of assessment parameters. This is described in Section 8.

Comparison of processing times (directly related to cost) in Tables 7.2 and 7.3 show the Monte-Carlo method to be 70 times more expensive. For one-off assessments and where random number generators are available in a system the method may nevertheless be preferable. The transparent logic of the method does make it attractive but this has to be balanced against the lack of information on sensitivity.

Where there is no access to software Tables 7.7 to 7.36 will serve to give information on safety indices and sensitivities for discrete values of the input variables. The following summarises the general trends in safety indices, β, and sensitivities observed in the Tables.

- β decreases with increasing stress COV and increasing defect size standard deviation.

- β decreases as mean stress increases. The change in β with increasing mean toughness is apparent but insignificant compared to the rate for stress.
- β naturally increases with safety factor.
- the type of defect (geometry and loading) affects β but not such that any one type has consistantly higher β's than any other, e.g. semi-circular defects in tension (Table 7.11) with stress COV = 40%, stress level = $0.9\sigma_y$ and defect standard deviation = 10mm has the lowest β of all types. When stress COV = 0.1%, stress level = $0.4\sigma_y$ and defect standard deviation = 2mm the safety index for this type is relatively large. It is similarly large for stress COV = 30%, stress level = $0.6\sigma_y$ and defect size standard deviation = 5mm.
- the large β values for types 4, 6 and 8 defects have little meaning other than "very safe".
- at lower stresses toughness is usually most sensitive: stress becomes more sensitive as stress level and/or stress COV increase. For stress > $0.8\sigma_y$ stress is usually dominantly sensitive.
- defect size is most sensitive only for the isolated cases of surface and embedded defects in bending where stress level and stress COV are low. Since these are the cases corresponding to large β's it can be concluded that variability in estimates of defect size have little affect on safety. This would not necessarily be true for defect size standard deviations greater than 10mm.

This last trend leaves open to question how to decide on a defect size standard deviation for any particular NDT method. A simple estimate can be made by trying to answer the question: within what range would the NDT

method be accurate, say, 95% of the time? If, for example, there is confidence that the NDT method is accurate to within ±7mm 95% of the time then a reasonable estimate of the defect size standard deviation would be 7.0/1.64 = 4.3mm. (1.64 being the standard normal deviate at a 95% probability level, i.e. $\Phi(1.64) = 0.95$). If manufacturers' claims for NDT accuracy were to be accepted allowance should be made for the deleterious effects on accuracy of marine fouling and operator conditions. Note that a defect size standard deviation of 10mm corresponds to an accuracy of within ±16.4mm 95% of the time - considered to be achieveable by most NDT methods used offshore.

The example given illustrates one method by which an assessment procedure based on the strip yield model could be calibrated to a desired safety level. It is a defect by defect approach and has several drawbacks not least of which is the lack of a clear choice of target reliability. It does have the advantage however that the order of sensitivities are indicated. In the method of calibration by optimisation, to be described in Section 8, sensitivities are not revealed.

7.7 Conclusions

1. The FOSM method of reliability analysis applied to a defect assessment problem with highly skewed toughness distribution gives a value of safety index with an accuracy approaching that of an exact method. Unlike the exact method it also provide valuable information on relative sensitivities.
2. In general toughness is the most sensitive variable when the level of stress is low. It is dominantly sensitive when, in addition, the COV in stress is low.

3. Stress is generally the most sensitive variable when the stress level is high ($>0.8\sigma_y$). It is dominantly sensitive when, in addition, the COV in stress is large.
4. For defect size standard deviations up to 10mm defect size is rarely the most sensitive variable.
5. Provided a clear choice of target reliability, based on passed experience with the PD6493 design curve, can be made, a defect assessment procedure based on the strip yield model can be calibrated on a defect by defect basis using the tabulated results herein.

7.8 References

1. British Standards PD6493:1980, Guidance on some methods for the derivation of acceptable levels for defects in fusion welded joints, London 1980.

2. Burdekin, F.M., Proposed revisions to PD6493 Section 2 revision 4 : Private communication.

3. 'Rationalisation of Safety and Serviceability Factors in Structural Codes' - Construction Industry Research and Information Association, London, CIRIA Report 63, 1977.

4. Leporati, E., 'The Assessment of Structural Safety', Series in Cement and Concrete Research, Vol. 1, Edited by A. Short, Research Studies Press, Oregon, 1979.

5. Garwood, S.J., 'A Crack Tip Opening Displacement (CTOD) Method for the Analysis of Ductile Materials', Welding Institute Research Report No. 277/1985, June 1985.

6. Anderson, T.L., 'Elastic-Plastic Fracture Mechanics Assessment Based on CTOD', Welding Institute Research Report No. 276/1985.

7. Fjeld, S., 'Reliability of Offshore Structures', Jnl. Pel. Tech. 1978, October, pp1486-1496.

	stress	defect size	toughness
mean	200	5	0.125
std. dev.	60	2	.0625
distribution	Normal	Normal	Weibul(α = 2.101, β = 0.141)

stress	defect size	toughness	M
209.1	4.69	0.070	0.654
207.3	4.94	0.239	0.749
283.3	5.92	0.032	0.137
277.0	5.40	0.052	0.359
289.1	4.16	0.072	0.473
164.6	4.68	0.130	0.828
120.7	5.17	0.096	0.861
224.4	5.65	0.054	0.493
195.3	7.30	0.197	0.760
326.1	6.25	0.084	0.302
186.2	1.67	0.120	0.801
324.2	7.61	0.132	0.357
154.7	5.88	0.115	0.815
176.2	5.06	0.157	0.810
104.0	4.95	0.177	0.931
150.7	2.55	0.242	0.867
202.9	1.36	0.159	0.766
321.0	3.64	0.116	0.435
223.2	6.24	0.194	0.702
191.2	3.19	0.303	0.788

Table 7.1 Random Values of Input Variables and Safety Margin

Input data as for Table 7.1

Processing Time 104 secs.

No. of Trials	No. of Failures	Failure Probability	Safety Index
1000	11	0.0110	2.290
2000	18	0.0090	2.366
3000	27	0.0090	2.366
4000	34	0.0085	2.387
5000	36	0.0072	2.447
10000	65	0.0065	2.484
20000	134	0.0067	2.473
50000	341	0.0068	2.467
100000	664	0.0066	2.476
300000	1923	0.0064	2.489

Table 7.2 Monte-Carlo Simulation Result

Input data as for Table 7.1

Processing time 1.56 secs.

	Distn.	COV%	Design Point	Sensitivity Factor	Central Factor
stress	N(200,60)	30	260	0.40	1.30
defect size	N(5,2)	40	6.17	0.24	1.23
toughness	W(2.10, 0.141)	50	0.019	-0.88	1/6.58

safety index = 2.480
failure probability = 0.00657

Table 7.3 Advanced Level II Reliability Result

Variable	Mean	COV%	Distribution
Stress σ/σ_y	0.4,0.6,0.8	0.1,20,30,40	Normal
Defect size (mm)	a_{tol}	2,5,10*	Normal
Toughness (mm)	0.05,0.15,0.257	52.3 (shape=2.0)	Weibull

* standard deviation.

Table 7.4 Distribution Characteristics

Type	Defect	Aspect Ratio(a/2c)	Loading
1	T	-	T
2	T	-	B
3	S	O.1O	T
4	S	O.1O	B
5	E	O.1O	T
6	E	O.1O	B
7	S	O.5	T
8	S	O.5	B

Defects: T - through thickness
S - surface
E - embedded

Loading: T - uniform tension
B - pure bending

Table 7.5 Defect Types

CODE	Most Sensitive		Least Sensitive
1	σ	a	δ
2	δ	σ	a
3	a	δ	σ
4	σ	δ	a
5	δ	a	σ
6	a	σ	δ
7	α_σ>O.9		
8	α_a>O.9		
9	α_δ>O.9		

σ - stress, a - size (detection), δ - toughness

Table 7.6 Sensitivity Codes

Notation and Values Used in Tables 7.7 - 7.36

COVS	Coefficient of variation for stress
D1	Toughness (COD) in mm = 0.257
D2	Toughness (COD) in mm = 0.150
D3	Toughness (COD) in mm = 0.050
G1	Value of safety factor = 1.75
G2	Value of safety factor = 2.50
G3	Value of safety factor = 4.00
SDA1	Standard deviation on defect size = 2mm
SDA2	Standard deviation on defect size = 5mm
SDA3	Standard deviation on defect size = 10mm
S/SY	Ratio of bending or membrane stress to yield stress.

COVS		SDA1			SDA2			SDA3		
S/SY		G1	G2	G3	G1	G2	G3	G1	G2	G3
0.1	D_4	1.2	1.6	2.1	1.2	1.6	2.1	1.2	1.6	2.1
0.1	D_6	9 1.0	9 1.4	9 1.9	9 1.0	9 1.4	9 1.9	9 0.9	9 1.4	9 1.9
0.1	D_8	9 0.9	9 1.4	9 1.9	9 0.9	9 1.4	9 1.9	9 0.9	9 1.3	9 1.8
20.0	D_4	9 1.1	9 1.5	9 2.0	9 1.1	9 1.5	9 2.0	9 1.1	9 1.5	9 2.0
20.0	D_6	2 0.8	9 1.2	9 1.7	2 0.8	9 1.2	9 1.7	2 0.8	9 1.2	9 1.7
20.0	D_8	2 0.7	2 1.1	9 1.6	2 0.7	2 1.1	9 1.6	2 0.7	2 1.1	9 1.6
30.0	D_4	4 0.9	2 1.4	2 1.8	4 0.9	2 1.4	2 1.8	4 0.9	2 1.4	2 1.8
30.0	D_6	2 0.7	2 1.1	2 1.6	2 0.7	2 1.1	2 1.6	2 0.7	2 1.1	2 1.5
30.0	D_8	4 0.5	2 0.9	2 1.2	4 0.5	2 0.9	2 1.2	4 0.5	2 0.8	2 1.2
40.0	D_4	4 0.8	4 1.2	7 1.7	4 0.8	4 1.2	7 1.7	4 0.8	4 1.2	7 1.7
40.0	D_6	4 0.5	2 0.9	2 1.4	4 0.5	2 0.9	2 1.4	4 0.5	2 0.9	2 1.3
40.0	D_8	4 0.4	4 0.7	4 0.9	4 0.4	4 0.7	4 0.9	4 0.4	4 0.7	4 0.9
		7	7	7	7	7	7	7	7	7

BETA VALUES & SENSITIVITY CODES FOR TYPE 1 DEFECTS,
TOUGHNESS (CTOD)=0.257 MM

Table 7.7

COVS		SDA1			SDA2			SDA3		
	S/SY	G1	G2	G3	G1	G2	G3	G1	G2	G3
0.1	0.4	1.1	1.5	2.0	1.1	1.5	2.0	1.1	1.5	2.0
0.1	0.6	9 0.9	9 1.3	9 1.8	9 0.9	9 1.3	9 1.8	9 0.9	9 1.3	9 1.8
0.1	0.8	9 0.8	9 1.3	9 1.8	9 0.8	9 1.3	9 1.8	9 0.8	9 1.3	9 1.8
20.0	0.4	9 1.0	9 1.4	9 1.9	9 1.0	9 1.4	9 1.9	9 1.0	9 1.4	9 1.9
20.0	0.6	2 0.8	9 1.2	9 1.7	2 0.8	9 1.2	9 1.7	2 0.7	9 1.2	9 1.7
20.0	0.8	2 0.7	2 1.1	9 1.6	2 0.7	2 1.1	9 1.6	2 0.7	2 1.1	9 1.6
30.0	0.4	2 0.9	2 1.3	9 1.8	2 0.9	2 1.3	9 1.8	2 0.9	2 1.3	2 1.8
30.0	0.6	2 0.7	2 1.1	2 1.6	2 0.6	2 1.1	2 1.6	2 0.6	2 1.1	2 1.5
30.0	0.8	2 0.6	2 1.0	2 1.5	2 0.6	2 1.0	2 1.5	2 0.6	2 1.0	2 1.5
40.0	0.4	2 0.8	2 1.2	2 1.6	2 0.8	2 1.2	2 1.6	4 0.8	2 1.2	2 1.6
40.0	0.6	4 0.6	2 0.9	2 1.4	4 0.6	2 0.9	2 1.4	4 0.6	2 0.9	2 1.4
40.0	0.8	4 0.5	4 0.9	2 1.3	4 0.5	4 0.9	2 1.3	4 0.5	4 0.9	2 1.3
		4	4	2	4	4	2	4	4	2

BETA VALUES & SENSITIVITY CODES FOR TYPE 2 DEFECTS,
TOUGHNESS (CTOD)=0.257 MM

Table 7.8

COVS		SDA1			SDA2			SDA3		
	S/SY	G1	G2	G3	G1	G2	G3	G1	G2	G3
0.1	0.4	1.6	2.1	2.6	1.6	2.1	2.6	1.6	2.1	2.6
		9	9	9	9	9	9	9	9	9
0.1	0.6	1.3	1.8	2.3	1.3	1.8	2.2	1.2	1.7	2.2
		9	9	9	9	9	9	9	9	9
0.1	0.8	1.2	1.6	2.1	1.1	1.6	2.1	1.0	1.5	2.0
		9	9	9	9	9	9	5	9	9
20.0	0.4	1.5	2.0	2.5	1.5	2.0	2.5	1.4	2.0	2.4
		9	9	9	2	9	9	2	9	9
20.0	0.6	1.1	1.6	2.1	1.1	1.6	2.1	1.1	1.6	2.1
		2	2	9	2	2	9	2	2	9
20.0	0.8	0.8	1.3	1.8	0.8	1.3	1.8	0.7	1.2	1.7
		4	4	7	4	4	4	4	4	4
30.0	0.4	1.3	1.9	2.3	1.3	1.9	2.3	1.3	1.8	2.3
		2	2	9	2	2	9	2	2	9
30.0	0.6	0.9	1.4	1.9	0.9	1.4	1.9	0.9	1.4	1.9
		4	2	2	4	2	2	4	2	2
30.0	0.8	0.6	0.9	1.2	0.6	0.9	1.2	0.6	0.9	1.2
		7	7	7	7	7	7	1	7	7
40.0	0.4	1.2	1.7	2.2	1.2	1.7	2.2	1.1	1.7	2.2
		4	2	2	4	2	2	4	2	2
40.0	0.6	0.8	1.2	1.7	0.8	1.2	1.7	0.7	1.2	1.6
		4	4	4	4	4	4	4	4	4
40.0	0.8	0.5	0.7	0.9	0.5	0.7	0.9	0.5	0.7	0.9
		7	7	7	7	7	7	7	7	7

BETA VALUES & SENSITIVITY CODES FOR TYPE 3 DEFECTS,
TOUGHNESS (CTOD)=0.257 MM

Table 7.9

COVS		SDA1			SDA2			SDA3		
	S/SY	G1	G2	G3	G1	G2	G3	G1	G2	G3
0.1	0.4	21.9	43.7	87.4	8.8	17.5	35.0	4.4	8.8	17.5
		8	8	8	8	8	8	8	8	8
0.1	0.6	1.9	2.2	2.5	1.9	2.2	2.4	1.9	2.1	2.4
		9	9	9	9	9	9	9	9	9
0.1	0.8	1.4	1.8	2.1	1.4	1.8	2.1	1.4	1.7	2.1
		9	9	9	9	9	9	9	9	9
20.0	0.4	2.4	2.6	2.8	2.4	2.6	2.8	2.4	2.6	2.8
		9	9	9	9	9	9	9	9	9
20.0	0.6	1.8	2.0	2.3	1.8	2.0	2.3	1.7	2.0	2.3
		9	9	9	2	9	9	2	9	9
20.0	0.8	1.2	1.6	2.0	1.2	1.6	2.0	1.2	1.5	1.9
		2	2	9	2	2	9	2	2	9
30.0	0.4	2.3	2.5	2.7	2.3	2.5	2.7	2.3	2.5	2.7
		9	9	9	2	9	9	2	9	9
30.0	0.6	1.6	1.9	2.2	1.6	1.9	2.2	1.5	1.9	2.2
		2	2	9	2	2	9	2	2	2
30.0	0.8	1.0	1.4	1.8	1.0	1.4	1.8	1.0	1.4	1.8
		4	2	2	4	2	2	4	2	2
40.0	0.4	2.1	2.4	2.6	2.1	2.4	2.6	2.1	2.4	2.6
		2	2	9	2	2	9	2	2	9
40.0	0.6	1.3	1.7	2.1	1.3	1.7	2.1	1.3	1.7	2.0
		4	2	2	4	2	2	4	2	2
40.0	0.8	0.8	1.2	1.6	0.8	1.2	1.6	0.8	1.1	1.6
		7	4	4	7	4	4	4	4	4

BETA VALUES & SENSITIVITY CODES FOR TYPE 4 DEFECTS,
TOUGHNESS (CTOD)=0.257 MM

Table 7.10

COVS		SDA1			SDA2			SDA3		
	S/SY	G1	G2	G3	G1	G2	G3	G1	G2	G3
0.1	0.4	2.2	2.6	3.0	2.1	2.6	3.0	2.0	2.5	2.9
0.1	0.6	9 1.8	9 2.2	9 2.6	9 1.7	9 2.2	9 2.6	9 1.5	9 2.0	9 2.5
0.1	0.8	9 1.6	9 2.0	9 2.5	9 1.4	9 1.9	9 2.4	5 1.1	9 1.7	9 2.2
20.0	0.4	9 2.0	9 2.5	9 2.9	5 2.0	9 2.4	9 2.9	3 1.8	5 2.4	9 2.8
20.0	0.6	9 1.5	9 2.0	9 2.5	2 1.4	9 2.0	9 2.5	5 1.2	9 1.8	9 2.4
20.0	0.8	2 0.9	9 1.4	9 1.7	2 0.9	2 1.3	9 1.7	6 0.7	2 1.2	2 1.6
30.0	0.4	7 1.8	7 2.3	7 2.8	7 1.8	7 2.3	7 2.8	1 1.7	1 2.2	7 2.7
30.0	0.6	2 1.2	2 1.8	9 2.3	2 1.1	2 1.7	9 2.3	4 1.0	2 1.6	9 2.2
30.0	0.8	7 0.6	4 0.9	7 1.1	4 0.6	4 0.9	7 1.1	1 0.6	1 0.8	2 1.1
40.0	0.4	7 1.6	7 2.2	7 2.6	7 1.6	7 2.1	7 2.6	7 1.4	7 2.1	7 2.6
40.0	0.6	4 0.9	2 1.4	2 1.7	4 0.9	2 1.3	2 1.7	1 0.8	2 1.3	2 1.7
40.0	0.8	7 0.5	7 0.7	7 0.8	7 0.5	7 0.7	7 0.8	1 0.4	7 0.7	7 0.8
		7	7	7	7	7	7	7	7	7

BETA VALUES & SENSITIVITY CODES FOR TYPE 5 DEFECTS,
TOUGHNESS (CTOD)=0.257 MM

Table 7.11

COVS		SDA1			SDA2			SDA3		
	S/SY	G1	G2	G3	G1	G2	G3	G1	G2	G3
0.1	0.4	14.7	29.3	58.6	5.9	11.7	23.5	2.9	5.9	11.7
		8	8	8	8	8	8	8	8	8
0.1	0.6	2.2	2.5	2.8	2.2	2.5	2.8	2.1	2.4	2.8
		9	9	9	9	9	9	8	9	9
0.1	0.8	1.9	2.2	2.6	1.8	2.2	2.6	1.5	2.1	2.5
		9	9	9	9	9	9	8	9	9
20.0	0.4	2.5	2.8	3.1	2.5	2.8	3.1	2.2	2.7	3.1
		9	9	9	9	9	9	9	6	9
20.0	0.6	2.0	2.4	2.7	2.0	2.3	2.7	1.6	2.3	2.7
		9	9	9	2	9	9	6	2	9
20.0	0.8	1.6	2.0	2.5	1.5	2.0	2.4	1.2	1.9	2.3
		2	9	9	2	2	9	6	2	2
30.0	0.4	2.3	2.7	3.0	2.5	2.7	3.0	1.9	2.6	3.0
		2	9	9	1	9	9	1	9	9
30.0	0.6	1.8	2.2	2.6	1.7	2.2	2.6	1.4	2.1	2.5
		2	2	9	1	2	9	1	2	2
30.0	0.8	1.3	1.8	2.3	1.2	1.8	2.3	1.0	1.6	2.2
		7	2	2	1	4	2	1	1	2
40.0	0.4	2.1	2.5	2.9	2.0	2.5	2.9	1.6	2.5	2.9
		2	2	9	1	2	9	1	2	9
40.0	0.6	1.5	2.0	2.5	1.4	2.0	2.5	1.2	1.9	2.4
		7	2	2	7	2	2	1	1	2
40.0	0.8	1.0	1.5	2.0	0.9	1.4	2.0	0.8	1.3	1.8
		7	7	7	7	7	7	1	1	7

BETA VALUES & SENSITIVITY CODES FOR TYPE 6 DEFECTS,
TOUGHNESS (CTOD)=0.257 MM

Table 7.12

COVS		SDA1			SDA2			SDA3		
	S/SY	G1	G2	G3	G1	G2	G3	G1	G2	G3
0.1	0.4	2.3	2.7	3.0	2.3	2.7	3.0	2.3	2.6	3.0
0.1	0.6	9 1.8	9 2.2	9 2.6	9 1.8	9 2.2	9 2.6	9 1.8	9 2.2	9 2.6
0.1	0.8	9 1.6	9 2.0	9 2.4	9 1.6	9 2.0	9 2.4	9 1.5	9 1.9	9 2.4
20.0	0.4	9 2.2	9 2.5	9 2.9	9 2.2	9 2.5	9 2.9	9 2.1	9 2.5	9 2.9
20.0	0.6	9 1.6	9 2.0	9 2.5	9 1.6	9 2.0	9 2.5	9 1.5	9 2.0	9 2.4
20.0	0.8	2 0.9	9 1.3	9 1.7	2 0.9	9 1.3	9 1.7	2 0.9	2 1.3	9 1.6
30.0	0.4	7 2.0	7 2.4	7 2.8	7 2.0	7 2.4	7 2.8	7 2.0	7 2.4	7 2.8
30.0	0.6	2 1.2	9 1.8	9 2.3	2 1.2	9 1.8	9 2.3	2 1.2	2 1.7	9 2.3
30.0	0.8	7 0.6	7 0.9	7 1.1	7 0.6	7 0.9	7 1.1	7 0.6	7 0.9	2 1.1
40.0	0.4	7 1.8	7 2.3	7 2.7	7 1.8	7 2.2	7 2.7	7 1.7	7 2.2	7 2.7
40.0	0.6	4 0.9	2 1.3	2 1.7	4 0.9	2 1.3	2 1.7	4 0.9	2 1.3	2 1.7
40.0	0.8	7 0.5	7 0.7	7 0.8	7 0.5	7 0.7	7 0.8	7 0.5	7 0.7	7 0.8
		7	7	7	7	7	7	7	7	7

BETA VALUES & SENSITIVITY CODES FOR TYPE 7 DEFECTS,
TOUGHNESS (CTOD)=0.257 MM

Table 7.13

COVS		SDA1			SDA2			SDA3		
	S/SY	G1	G2	G3	G1	G2	G3	G1	G2	G3
0.1	0.4	21.9	43.7	87.4	8.8	17.5	35.0	4.4	8.8	17.5
		8	8	8	8	8	8	8	8	8
0.1	0.6	2.3	2.5	2.8	2.2	2.5	2.8	2.2	2.5	2.8
		9	9	9	9	9	9	9	9	9
0.1	0.8	1.9	2.2	2.6	1.9	2.2	2.6	1.8	2.2	2.5
		9	9	9	9	9	9	9	9	9
20.0	0.4	2.6	2.9	3.2	2.6	2.9	3.2	2.4	2.9	3.2
		9	9	9	9	9	9	9	9	9
20.0	0.6	2.1	2.4	2.7	2.1	2.4	2.7	2.0	2.4	2.7
		9	9	9	9	9	9	2	9	9
20.0	0.8	1.6	2.0	2.4	1.6	2.0	2.4	1.5	2.0	2.4
		2	9	9	2	9	9	4	2	9
30.0	0.4	2.5	2.8	3.1	2.5	2.8	3.1	2.5	2.8	3.1
		9	9	9	9	9	9	2	9	9
30.0	0.6	1.9	2.3	2.6	1.9	2.3	2.6	1.8	2.2	2.6
		2	2	9	2	2	9	1	2	9
30.0	0.8	1.3	1.8	2.3	1.3	1.8	2.3	1.2	1.8	2.2
		7	2	2	7	2	2	1	4	2
40.0	0.4	2.4	2.7	3.0	2.3	2.7	3.0	2.3	2.6	3.0
		2	2	9	2	2	9	1	2	9
40.0	0.6	1.6	2.1	2.5	1.6	2.1	2.5	1.4	2.0	2.5
		7	2	2	7	2	2	1	2	2
40.0	0.8	1.0	1.5	2.0	1.0	1.5	2.0	0.9	1.4	2.0
		7	7	7	7	7	7	7	7	7

BETA VALUES & SENSITIVITY CODES FOR TYPE 8 DEFECTS,
TOUGHNESS (CTOD)=0.257 MM

Table 7.14

COVS		SDA1			SDA2			SDA3		
	S/SY	G1	G2	G3	G1	G2	G3	G1	G2	G3
0.1	0.4	0.9	1.4	1.9	0.9	1.4	1.9	0.9	1.4	1.9
0.1	0.6	9 0.9	9 1.3	9 1.8	9 0.9	9 1.3	9 1.8	9 0.8	9 1.3	9 1.8
0.1	0.8	9 0.9	9 1.3	9 1.8	9 0.8	9 1.3	9 1.8	9 0.7	9 1.2	9 1.7
2D_D	0.4	9 0.8	9 1.2	9 1.7	9 0.8	9 1.2	9 1.7	5 0.8	9 1.2	9 1.7
2D_D	0.6	2 0.7	9 1.2	9 1.6	2 0.7	9 1.1	9 1.6	2 0.7	2 1.1	9 1.6
2D_D	0.8	2 0.7	2 1.1	9 1.5	2 0.6	2 1.0	9 1.5	2 0.6	2 1.0	2 1.5
3D_D	0.4	2 0.7	2 1.1	2 1.6	2 0.7	2 1.1	2 1.6	2 0.7	2 1.1	2 1.6
3D_D	0.6	2 0.6	2 1.0	2 1.5	2 0.6	2 1.0	2 1.5	2 0.6	2 1.0	2 1.5
3D_D	0.8	4 0.5	2 0.8	2 1.2	4 0.5	2 0.8	2 1.2	4 0.5	2 0.8	2 1.2
4D_D	0.4	4 0.6	4 1.0	7 1.5	4 0.6	4 1.0	7 1.5	4 0.6	4 1.0	4 1.5
4D_D	0.6	4 0.5	4 0.9	2 1.3	4 0.5	4 0.9	2 1.3	4 0.5	4 0.8	2 1.3
4D_D	0.8	4 0.4	4 0.7	4 0.9	4 0.4	4 0.7	4 0.9	4 0.4	4 0.6	4 0.9
		7	7	7	4	7	7	4	4	7

BETA VALUES & SENSITIVITY CODES FOR TYPE 1 DEFECTS,
TOUGHNESS (CTOD)=0.150 MM

Table 7.15

COVS		SDA1			SDA2			SDA3		
	S/SY	G1	G2	G3	G1	G2	G3	G1	G2	G3
0.1	0.4	0.9	1.3	1.8	0.9	1.3	1.8	0.9	1.3	1.8
0.1	0.6	9 0.8	9 1.3	9 1.8	9 0.8	9 1.3	9 1.8	9 0.8	9 1.2	9 1.7
0.1	0.8	9 0.8	9 1.3	9 1.8	9 0.8	9 1.2	9 1.7	9 0.7	9 1.2	9 1.7
20.0	0.4	9 0.8	9 1.2	9 1.7	9 0.8	9 1.2	9 1.7	9 0.8	9 1.2	9 1.7
20.0	0.6	2 0.7	9 1.1	9 1.6	2 0.7	9 1.1	9 1.6	2 0.7	9 1.1	9 1.6
20.0	0.8	2 0.7	2 1.1	9 1.6	2 0.7	2 1.1	9 1.6	2 0.6	2 1.1	9 1.5
30.0	0.4	2 0.7	2 1.1	9 1.6	2 0.7	2 1.1	9 1.6	2 0.7	2 1.1	2 1.6
30.0	0.6	2 0.6	2 1.0	2 1.5	2 0.6	2 1.0	2 1.5	2 0.6	2 1.0	2 1.5
30.0	0.8	2 0.6	2 1.0	2 1.5	2 0.6	2 1.0	2 1.5	2 0.6	2 0.9	2 1.4
40.0	0.4	2 0.6	2 1.0	2 1.4	2 0.6	2 1.0	2 1.4	4 0.6	2 1.0	2 1.4
40.0	0.6	4 0.5	2 0.9	2 1.4	4 0.5	2 0.9	2 1.4	4 0.5	2 0.9	2 1.4
40.0	0.8	4 0.5	4 0.9	2 1.3	4 0.5	4 0.8	2 1.3	4 0.5	4 0.8	2 1.3
		4	4	2	4	4	2	4	4	2

BETA VALUES & SENSITIVITY CODES FOR TYPE 2 DEFECTS,
TOUGHNESS (CTOD)=0.150 MM

Table 7.16

COVS		SDA1			SDA2			SDA3		
	S/SY	G1	G2	G3	G1	G2	G3	G1	G2	G3
0.1	0.4	1.4	1.9	2.3	1.4	1.8	2.3	1.3	1.8	2.3
		9	9	9	9	9	9	9	9	9
0.1	0.6	1.1	1.6	2.0	1.1	1.6	2.0	1.0	1.5	2.0
		9	9	9	9	9	9	9	9	9
0.1	0.8	1.0	1.4	1.9	0.9	1.4	1.9	0.8	1.2	1.7
		9	9	9	9	9	9	5	5	9
20.0	0.4	1.2	1.7	2.2	1.2	1.7	2.2	1.2	1.7	2.2
		2	9	9	2	9	9	2	9	9
20.0	0.6	0.9	1.4	1.9	0.9	1.4	1.9	0.9	1.3	1.8
		2	2	9	2	2	9	2	2	2
20.0	0.8	0.7	1.2	1.6	0.7	1.1	1.6	0.6	1.0	1.5
		4	2	2	4	2	2	4	2	2
30.0	0.4	1.1	1.6	2.1	1.1	1.6	2.1	1.0	1.6	2.1
		2	2	2	2	2	2	2	2	2
30.0	0.6	0.8	1.2	1.7	0.8	1.2	1.7	0.7	1.2	1.7
		4	2	2	4	2	2	4	2	2
30.0	0.8	0.6	0.9	1.2	0.5	0.9	1.2	0.5	0.8	1.2
		4	7	7	4	4	7	1	4	7
40.0	0.4	1.0	1.4	1.9	0.9	1.4	1.9	0.9	1.4	1.9
		4	2	2	4	2	2	4	2	2
40.0	0.6	0.7	1.0	1.5	0.7	1.0	1.5	0.6	1.0	1.5
		4	4	4	4	4	4	4	4	4
40.0	0.8	0.4	0.7	0.9	0.4	0.7	0.9	0.4	0.7	0.9
		7	7	7	7	7	7	1	7	7

BETA VALUES & SENSITIVITY CODES FOR TYPE 3 DEFECTS,
TOUGHNESS (CTOD)=0.150 MM

Table 7.17

COVS		SDA1			SDA2			SDA3		
	S/SY	G1	G2	G3	G1	G2	G3	G1	G2	G3
0.1	0.4	21.9	43.7	87.4	8.8	17.5	35.0	4.4	8.8	17.5
0.1	0.6	8 1.4	8 1.7	8 2.0	8 1.4	8 1.7	8 2.0	8 1.4	8 1.7	8 2.0
0.1	0.8	9 1.0	9 1.3	9 1.7	9 0.9	9 1.3	9 1.7	9 0.9	9 1.3	9 1.7
20.0	0.4	9 2.0	9 2.2	9 2.5	9 2.0	9 2.2	9 2.5	9 2.0	9 2.2	9 2.4
20.0	0.6	9 1.2	9 1.5	9 1.9	9 1.2	9 1.5	9 1.9	9 1.2	9 1.5	9 1.9
20.0	0.8	2 0.8	9 1.1	9 1.6	2 0.8	9 1.1	9 1.6	2 0.7	2 1.1	9 1.5
30.0	0.4	2 1.9	2 2.1	9 2.3	2 1.9	2 2.1	2 2.3	2 1.8	2 2.1	2 2.3
30.0	0.6	2 1.1	9 1.4	9 1.8	2 1.1	9 1.4	9 1.8	2 1.1	2 1.4	9 1.7
30.0	0.8	2 0.6	2 1.0	2 1.4	2 0.6	2 1.0	2 1.4	2 0.6	2 1.0	2 1.4
40.0	0.4	4 1.7	2 1.9	2 2.2	4 1.7	2 1.9	2 2.2	4 1.7	2 1.9	2 2.2
40.0	0.6	2 0.9	2 1.2	2 1.6	2 0.9	2 1.2	2 1.6	2 0.9	2 1.2	2 1.6
40.0	0.8	4 0.5	4 0.8	2 1.2	4 0.5	4 0.8	2 1.2	4 0.5	4 0.8	2 1.2
		4	4	4	4	4	4	4	4	4

BETA VALUES & SENSITIVITY CODES FOR TYPE 4 DEFECTS,
TOUGHNESS (CTOD)=0.150 MM

Table 7.18

COVS		SDA1			SDA2			SDA3		
	S/SY	G1	G2	G3	G1	G2	G3	G1	G2	G3
0.1	0.4	1.8	2.2	2.7	1.7	2.2	2.6	1.6	2.1	2.6
		9	9	9	9	9	9	5	9	9
0.1	0.6	1.4	1.9	2.3	1.3	1.8	2.3	1.1	1.7	2.2
		9	9	9	9	9	9	5	9	9
0.1	0.8	1.2	1.7	2.2	1.1	1.6	2.1	0.8	1.3	1.9
		9	9	9	5	9	9	3	5	5
20.0	0.4	1.6	2.1	2.5	1.6	2.1	2.5	1.4	2.0	2.5
		9	9	9	2	9	9	5	2	9
20.0	0.6	1.2	1.7	2.2	1.1	1.6	2.1	1.0	1.5	2.0
		2	2	9	2	2	9	5	2	2
20.0	0.8	0.9	1.3	1.7	0.8	1.2	1.7	0.6	1.1	1.6
		4	4	7	4	4	7	6	1	1
30.0	0.4	1.4	2.0	2.4	1.4	1.9	2.4	1.3	1.9	2.4
		2	2	9	2	2	9	2	2	2
30.0	0.6	1.0	1.5	2.0	0.9	1.4	2.0	0.8	1.3	1.9
		4	2	2	4	4	2	1	4	2
30.0	0.8	0.6	0.9	1.2	0.6	0.9	1.2	0.5	0.8	1.1
		7	7	7	1	7	7	1	1	7
40.0	0.4	1.3	1.8	2.3	1.2	1.8	2.3	1.1	1.7	2.2
		4	2	2	4	2	2	4	2	2
40.0	0.6	0.8	1.2	1.7	0.8	1.2	1.7	0.7	1.1	1.6
		4	4	7	4	4	7	1	4	4
40.0	0.8	0.5	0.7	0.9	0.5	0.7	0.9	0.4	0.7	0.9
		7	7	7	7	7	7	1	7	7

BETA VALUES & SENSITIVITY CODES FOR TYPE 5 DEFECTS,
TOUGHNESS (CTOD)=0.150 MM

Table 7.19

COVS		SDA1			SDA2			SDA3		
	S/SY	G1	G2	G3	G1	G2	G3	G1	G2	G3
0.1	0.4	2.2	2.5	2.8	2.2	2.5	2.8	2.1	2.5	2.8
0.1	0.6	9 1.7	9 2.1	9 2.5	9 1.7	9 2.1	9 2.5	9 1.6	9 2.0	9 2.4
0.1	0.8	9 1.4	9 1.8	9 2.2	9 1.3	9 1.8	9 2.2	9 1.1	9 1.6	9 2.1
20.0	0.4	9 2.1	9 2.4	9 2.7	9 2.1	9 2.4	9 2.7	5 2.0	9 2.4	9 2.7
20.0	0.6	9 1.5	9 1.9	9 2.4	9 1.5	9 1.9	9 2.3	2 1.4	9 1.8	9 2.3
20.0	0.8	2 1.2	9 1.6	9 2.1	2 1.1	9 1.6	9 2.1	2 0.9	2 1.4	9 1.9
30.0	0.4	2 1.9	2 2.3	9 2.6	2 1.9	2 2.3	9 2.6	6 1.8	2 2.2	2 2.6
30.0	0.6	2 1.4	9 1.8	9 2.2	2 1.3	9 1.8	9 2.2	2 1.2	2 1.7	9 2.2
30.0	0.8	2 1.0	2 1.4	9 1.9	4 0.9	2 1.4	2 1.9	1 0.8	2 1.3	2 1.8
40.0	0.4	4 1.7	2 2.1	2 2.5	4 1.7	2 2.1	2 2.5	1 1.5	4 2.1	2 2.5
40.0	0.6	2 1.1	2 1.6	2 2.1	4 1.1	2 1.6	2 2.1	1 1.0	2 1.5	2 2.0
40.0	0.8	4 0.8	2 1.2	2 1.7	4 0.8	2 1.2	2 1.7	1 0.7	4 1.1	2 1.6
		7	4	4	4	4	4	1	1	4

BETA VALUES & SENSITIVITY CODES FOR TYPE 6 DEFECTS,
TOUGHNESS (CTOD)=0.150 MM

Table 7.20

COVS		SDA1			SDA2			SDA3		
	S/SY	G1	G2	G3	G1	G2	G3	G1	G2	G3
0.1	0.4	1.9	2.3	2.7	1.9	2.3	2.7	1.9	2.3	2.6
0.1	0.6	9 1.4	9 1.8	9 2.3	9 1.4	9 1.8	9 2.3	9 1.4	9 1.8	9 2.3
0.1	0.8	9 1.2	9 1.7	9 2.1	9 1.2	9 1.6	9 2.1	9 1.1	9 1.6	9 2.0
20.0	0.4	9 1.7	9 2.1	9 2.5	9 1.7	9 2.1	9 2.5	5 1.7	9 2.1	9 2.5
20.0	0.6	9 1.2	9 1.7	9 2.1	9 1.2	9 1.7	9 2.1	2 1.1	9 1.6	9 2.1
20.0	0.8	2 0.8	2 1.3	9 1.7	2 0.8	2 1.3	9 1.7	2 0.8	2 1.2	9 1.7
30.0	0.4	4 1.6	4 2.0	7 2.4	4 1.6	4 2.0	7 2.4	4 1.5	4 2.0	7 2.4
30.0	0.6	2 1.0	2 1.5	9 1.9	2 1.0	2 1.4	9 1.9	2 0.9	2 1.4	9 1.9
30.0	0.8	4 0.6	2 0.9	2 1.1	4 0.6	4 0.9	2 1.1	4 0.6	4 0.9	2 1.1
40.0	0.4	7 1.4	7 1.8	7 2.3	7 1.4	7 1.8	7 2.3	7 1.3	7 1.8	7 2.3
40.0	0.6	4 0.8	2 1.2	2 1.7	4 0.8	2 1.2	2 1.7	4 0.8	2 1.2	2 1.6
40.0	0.8	7 0.5	4 0.7	7 0.9	7 0.5	4 0.7	7 0.9	4 0.4	4 0.7	7 0.9
		7	7	7	7	7	7	7	7	7

BETA VALUES & SENSITIVITY CODES FOR TYPE 7 DEFECTS,
TOUGHNESS (CTOD)=0.150 MM

Table 7.21

COVS		SDA1			SDA2			SDA3		
	S/SY	G1	G2	G3	G1	G2	G3	G1	G2	G3
0.1	0.4	21.9	43.7	87.4	8.8	17.5	35.0	4.4	8.8	17.5
		8	8	8	8	8	8	8	8	8
0.1	0.6	1.8	2.1	2.5	1.8	2.1	2.5	1.7	2.1	2.4
		9	9	9	9	9	9	9	9	9
0.1	0.8	1.4	1.8	2.2	1.4	1.8	2.2	1.3	1.7	2.1
		9	9	9	9	9	9	9	9	9
20.0	0.4	2.2	2.5	2.8	2.2	2.5	2.8	2.2	2.5	2.8
		9	9	9	9	9	9	9	9	9
20.0	0.6	1.6	2.0	2.4	1.6	2.0	2.3	1.6	1.9	2.3
		2	9	9	2	9	9	2	9	9
20.0	0.8	1.2	1.6	2.0	1.2	1.6	2.0	1.1	1.5	2.0
		2	2	9	2	2	9	2	2	9
30.0	0.4	2.1	2.4	2.7	2.1	2.4	2.7	2.1	2.4	2.7
		2	9	9	2	9	9	2	9	9
30.0	0.6	1.4	1.8	2.2	1.4	1.8	2.2	1.4	1.8	2.2
		2	2	9	2	2	9	2	2	2
30.0	0.8	1.0	1.4	1.9	1.0	1.4	1.9	0.9	1.4	1.8
		4	2	2	4	2	2	4	2	2
40.0	0.4	1.9	2.3	2.6	1.9	2.3	2.6	1.9	2.3	2.6
		2	2	9	2	2	9	2	2	2
40.0	0.6	1.2	1.7	2.1	1.2	1.7	2.1	1.2	1.6	2.0
		4	2	2	4	2	2	4	2	2
40.0	0.8	0.8	1.2	1.7	0.8	1.2	1.7	0.8	1.2	1.6
		4	4	4	4	4	4	4	4	4

BETA VALUES & SENSITIVITY CODES FOR TYPE 8 DEFECTS,
TOUGHNESS (CTOD)=0.150 MM

Table 7.22

COVS		SDA1			SDA2			SDA3		
	S/SY	G1	G2	G3	G1	G2	G3	G1	G2	G3
0.1	0.4	0.8	1.3	1.8	0.8	1.3	1.7	0.8	1.2	1.7
		9	9	9	9	9	9	9	9	9
0.1	0.6	0.8	1.3	1.7	0.8	1.2	1.7	0.6	1.1	1.6
		9	9	9	9	9	9	5	5	9
0.1	0.8	0.8	1.2	1.7	0.6	1.1	1.6	0.4	0.8	1.3
		9	9	9	5	5	9	3	3	5
20.0	0.4	0.7	1.1	1.6	0.7	1.1	1.6	0.7	1.1	1.6
		2	2	9	2	2	9	2	2	9
20.0	0.6	0.7	1.1	1.6	0.6	1.1	1.5	0.6	0.9	1.4
		2	2	9	2	2	2	5	5	5
20.0	0.8	0.6	1.0	1.5	0.5	0.9	1.4	0.4	0.7	1.1
		2	2	2	2	2	2	3	3	5
30.0	0.4	0.6	1.0	1.5	0.6	1.0	1.5	0.6	1.0	1.5
		2	2	2	2	2	2	2	2	2
30.0	0.6	0.6	1.0	1.4	0.6	0.9	1.4	0.5	0.8	1.3
		4	2	2	4	2	2	4	2	2
30.0	0.8	0.5	0.8	1.2	0.4	0.8	1.1	0.4	0.6	1.0
		4	4	4	4	4	4	6	1	1
40.0	0.4	0.5	0.9	1.4	0.5	0.9	1.4	0.5	0.9	1.3
		4	4	2	4	4	2	4	4	2
40.0	0.6	0.5	0.8	1.3	0.5	0.8	1.2	0.4	0.7	1.1
		4	4	4	4	4	4	4	4	4
40.0	0.8	0.4	0.7	0.9	0.4	0.6	0.9	0.3	0.5	0.8
		4	7	7	4	4	7	1	1	1

BETA VALUES & SENSITIVITY CODES FOR TYPE 1 DEFECTS,
TOUGHNESS (CTOD)=0.050 MM

Table 7.23

COVS		SDA1			SDA2			SDA3		
	S/SY	G1	G2	G3	G1	G2	G3	G1	G2	G3
0.1	0.4	0.8	1.3	1.7	0.8	1.2	1.7	0.8	1.2	1.7
		9	9	9	9	9	9	9	9	9
0.1	0.6	0.8	1.2	1.7	0.8	1.2	1.7	0.7	1.1	1.6
		9	9	9	9	9	9	5	5	9
0.1	0.8	0.8	1.2	1.7	0.7	1.1	1.6	0.5	0.9	1.4
		9	9	9	5	5	9	3	5	5
20.0	0.4	0.7	1.1	1.6	0.7	1.1	1.6	0.7	1.1	1.6
		2	9	9	2	2	9	2	2	9
20.0	0.6	0.7	1.1	1.6	0.7	1.1	1.6	0.6	1.0	1.5
		2	2	9	2	2	2	5	5	5
20.0	0.8	0.7	1.1	1.6	0.6	1.0	1.5	0.5	0.8	1.3
		2	2	9	5	2	2	3	3	5
30.0	0.4	0.6	1.0	1.5	0.6	1.0	1.5	0.6	1.0	1.5
		2	2	2	2	2	2	2	2	2
30.0	0.6	0.6	1.0	1.5	0.6	1.0	1.4	0.5	0.9	1.3
		2	2	2	2	2	2	2	2	2
30.0	0.8	0.6	1.0	1.4	0.5	0.9	1.3	0.4	0.7	1.1
		2	2	2	4	2	2	6	3	5
40.0	0.4	0.5	0.9	1.4	0.5	0.9	1.4	0.5	0.9	1.4
		4	2	2	4	2	2	4	2	2
40.0	0.6	0.5	0.9	1.3	0.5	0.9	1.3	0.5	0.8	1.2
		4	4	2	4	4	2	4	4	2
40.0	0.8	0.5	0.8	1.3	0.5	0.8	1.2	0.4	0.7	1.0
		4	4	2	4	4	4	1	1	4

BETA VALUES & SENSITIVITY CODES FOR TYPE 2 DEFECTS,
TOUGHNESS (CTOD)=0.050 MM

Table 7.24

COVS		SDA1			SDA2			SDA3		
	S/SY	G1	G2	G3	G1	G2	G3	G1	G2	G3
0.1	0.4	1.0	1.5	1.9	1.0	1.4	1.9	0.9	1.4	1.9
0.1	0.6	9 0.8	9 1.3	9 1.8	9 0.8	9 1.2	9 1.7	5 0.6	9 1.0	9 1.5
0.1	0.8	9 0.8	9 1.2	9 1.7	9 0.6	9 1.0	9 1.5	5 0.4	5 0.7	5 1.2
20.0	0.4	9 0.9	9 1.3	9 1.8	5 0.9	5 1.3	5 1.8	3 0.8	3 1.2	5 1.7
20.0	0.6	2 0.7	9 1.1	9 1.6	2 0.7	2 1.1	9 1.5	2 0.6	2 0.9	2 1.4
20.0	0.8	2 0.6	2 1.0	9 1.5	2 0.5	2 0.9	2 1.3	5 0.4	5 0.7	5 1.1
30.0	0.4	2 0.8	2 1.2	2 1.7	5 0.8	2 1.2	2 1.7	3 0.7	3 1.1	3 1.6
30.0	0.6	2 0.6	2 1.0	2 1.5	2 0.6	2 0.9	2 1.4	2 0.5	2 0.8	2 1.3
30.0	0.8	4 0.5	2 0.8	2 1.2	4 0.4	2 0.7	2 1.1	1 0.3	2 0.6	2 0.9
40.0	0.4	4 0.7	4 1.1	4 1.5	1 0.7	4 1.1	4 1.5	6 0.6	6 1.0	1 1.5
40.0	0.6	4 0.5	2 0.8	2 1.3	4 0.5	2 0.8	2 1.2	4 0.4	4 0.7	2 1.1
40.0	0.8	4 0.4	4 0.6	4 0.9	4 0.4	4 0.6	4 0.9	1 0.3	4 0.5	4 0.8
		4	7	7	1	1	7	1	1	1

BETA VALUES & SENSITIVITY CODES FOR TYPE 3 DEFECTS,
TOUGHNESS (CTOD)=0.050 MM

Table 7.25

COVS		SDA1			SDA2			SDA3		
	S/SY	G1	G2	G3	G1	G2	G3	G1	G2	G3
0.1	0.4	1.0	1.3	1.7	1.0	1.3	1.7	1.0	1.3	1.6
0.1	0.6	9 0.6	9 1.0	9 1.5	9 0.6	9 1.0	9 1.4	9 0.6	9 0.9	9 1.4
0.1	0.8	9 0.7	9 1.1	9 1.6	9 0.6	9 1.0	9 1.5	9 0.5	9 0.8	9 1.3
20.0	0.4	9 0.9	9 1.2	9 1.5	5 0.9	9 1.2	9 1.5	3 0.9	5 1.2	5 1.5
20.0	0.6	2 0.5	9 0.9	9 1.3	2 0.5	9 0.9	9 1.3	2 0.5	2 0.8	9 1.3
20.0	0.8	2 0.6	2 1.0	9 1.4	2 0.5	2 0.9	2 1.4	2 0.4	2 0.7	2 1.2
30.0	0.4	2 0.8	2 1.1	2 1.4	2 0.8	2 1.1	2 1.4	3 0.8	5 1.1	5 1.4
30.0	0.6	2 0.4	2 0.8	2 1.2	2 0.4	2 0.8	2 1.2	2 0.4	2 0.7	2 1.1
30.0	0.8	2 0.5	2 0.8	2 1.3	4 0.5	2 0.8	2 1.2	4 0.4	2 0.7	2 1.1
40.0	0.4	4 0.7	2 0.9	2 1.3	4 0.7	2 0.9	2 1.3	6 0.7	4 0.9	2 1.3
40.0	0.6	4 0.4	2 0.7	2 1.1	4 0.4	2 0.7	2 1.1	4 0.4	2 0.6	2 1.0
40.0	0.8	4 0.4	4 0.7	2 1.2	4 0.4	4 0.7	2 1.1	4 0.3	4 0.6	2 1.0
		4	4	4	4	4	4	1	1	4

BETA VALUES & SENSITIVITY CODES FOR TYPE 4 DEFECTS,
TOUGHNESS (CTOD)=0.050 MM

Table 7.26

COVS		SDA1			SDA2			SDA3		
	S/SY	G1	G2	G3	G1	G2	G3	G1	G2	G3
0.1	0.4	1.2	1.7	2.1	1.1	1.6	2.1	1.0	1.5	2.0
0.1	0.6	9 1.0	9 1.4	9 1.9	9 0.9	9 1.3	9 1.8	5 0.7	9 1.1	9 1.6
0.1	0.8	9 0.9	9 1.3	9 1.8	5 0.6	9 1.1	9 1.6	3 0.4	5 0.8	5 1.3
20.0	0.4	9 1.0	9 1.5	9 2.0	3 1.0	5 1.5	5 2.0	3 0.9	3 1.4	5 1.9
20.0	0.6	2 0.8	9 1.3	9 1.8	2 0.7	2 1.2	9 1.7	5 0.6	5 1.0	2 1.5
20.0	0.8	2 0.7	2 1.1	9 1.6	2 0.5	2 0.9	2 1.4	3 0.4	5 0.7	5 1.1
30.0	0.4	2 0.9	2 1.4	2 1.9	6 0.9	2 1.4	2 1.9	6 0.8	6 1.3	3 1.8
30.0	0.6	2 0.7	2 1.1	2 1.6	2 0.6	2 1.0	2 1.5	2 0.5	2 0.9	2 1.4
30.0	0.8	4 0.5	2 0.9	2 1.2	4 0.5	2 0.8	2 1.1	6 0.3	1 0.6	2 1.0
40.0	0.4	4 0.8	4 1.2	7 1.8	1 0.8	1 1.2	1 1.7	6 0.7	6 1.1	1 1.6
40.0	0.6	4 0.6	2 1.0	2 1.4	4 0.5	2 0.9	2 1.4	4 0.5	4 0.8	2 1.2
40.0	0.8	4 0.4	4 0.7	4 0.9	4 0.4	4 0.6	4 0.9	1 0.3	1 0.5	4 0.8
		4	7	7	1	1	7	6	1	1

BETA VALUES & SENSITIVITY CODES FOR TYPE 5 DEFECTS,
TOUGHNESS (CTOD)=0.050 MM

Table 7.27

COVS		SDA1			SDA2			SDA3		
	S/SY	G1	G2	G3	G1	G2	G3	G1	G2	G3
0.1	0.4	1.3	1.7	2.1	1.3	1.7	2.1	1.2	1.6	2.1
0.1	0.6	9 0.9	9 1.4	9 1.9	9 0.9	9 1.3	9 1.8	9 0.8	9 1.2	9 1.7
0.1	0.8	9 0.9	9 1.3	9 1.8	9 0.8	9 1.2	9 1.7	5 0.6	5 1.0	9 1.5
20.0	0.4	9 1.1	9 1.5	9 2.0	5 1.1	9 1.5	9 2.0	3 1.1	5 1.5	5 1.9
20.0	0.6	2 0.8	9 1.2	9 1.7	2 0.8	9 1.2	9 1.7	2 0.7	2 1.1	9 1.6
20.0	0.8	2 0.7	2 1.2	9 1.6	2 0.6	2 1.1	9 1.5	5 0.5	5 0.9	5 1.3
30.0	0.4	2 1.0	2 1.4	9 1.9	2 1.0	2 1.4	2 1.9	3 1.0	5 1.4	5 1.8
30.0	0.6	2 0.7	2 1.1	2 1.6	2 0.7	2 1.1	2 1.6	2 0.6	2 1.0	2 1.5
30.0	0.8	2 0.6	2 1.0	2 1.5	2 0.6	2 0.9	2 1.4	4 0.5	2 0.8	2 1.2
40.0	0.4	4 0.9	2 1.3	2 1.7	4 0.9	2 1.3	2 1.7	6 0.8	6 1.2	2 1.7
40.0	0.6	4 0.6	2 1.0	2 1.5	4 0.6	2 1.0	2 1.4	4 0.5	2 0.9	2 1.3
40.0	0.8	4 0.5	4 0.9	2 1.3	4 0.5	4 0.8	2 1.3	4 0.4	4 0.7	2 1.1
		4	4	4	4	4	4	1	1	4

BETA VALUES & SENSITIVITY CODES FOR TYPE 6 DEFECTS,
TOUGHNESS (CTOD)=0.050 MM

Table 7.28

COVS		SDA1			SDA2			SDA3		
	S/SY	G1	G2	G3	G1	G2	G3	G1	G2	G3
0.1	0.4	1.1	1.6	2.0	1.1	1.6	2.0	1.1	1.6	2.0
0.1	0.6	9 0.9	9 1.4	9 1.9	9 0.9	9 1.3	9 1.8	9 0.8	9 1.3	9 1.8
0.1	0.8	9 0.9	9 1.3	9 1.8	9 0.8	9 1.2	9 1.7	5 0.6	9 1.1	9 1.6
20.0	0.4	9 1.0	9 1.4	9 1.9	5 1.0	9 1.4	9 1.9	5 1.0	5 1.4	5 1.9
20.0	0.6	2 0.8	9 1.2	9 1.7	2 0.7	9 1.2	9 1.7	2 0.7	2 1.1	9 1.6
20.0	0.8	2 0.7	2 1.1	9 1.6	2 0.6	2 1.0	2 1.5	2 0.5	2 0.9	2 1.4
30.0	0.4	2 0.9	2 1.3	2 1.8	2 0.9	2 1.3	2 1.8	6 0.8	2 1.3	2 1.8
30.0	0.6	2 0.6	2 1.0	2 1.5	2 0.6	2 1.0	2 1.5	2 0.6	2 1.0	2 1.5
30.0	0.8	4 0.5	2 0.9	2 1.2	4 0.5	2 0.8	2 1.2	4 0.4	2 0.7	2 1.1
40.0	0.4	4 0.8	4 1.2	7 1.6	4 0.8	4 1.2	7 1.6	1 0.7	1 1.1	4 1.6
40.0	0.6	4 0.5	2 0.9	2 1.3	4 0.5	2 0.9	2 1.3	4 0.5	2 0.8	2 1.3
40.0	0.8	4 0.4 7	4 0.7 7	4 0.9 7	4 0.4 4	4 0.7 7	4 0.9 7	4 0.4 1	4 0.6 1	4 0.9 7

BETA VALUES & SENSITIVITY CODES FOR TYPE 7 DEFECTS,
TOUGHNESS (CTOD)=0.050 MM

Table 7.29

COVS		SDA1			SDA2			SDA3		
	S/SY	G1	G2	G3	G1	G2	G3	G1	G2	G3
0.1	0.4	1.4	1.8	2.1	1.4	1.8	2.1	1.4	1.7	2.1
		9	9	9	9	9	9	9	9	9
0.1	0.6	0.9	1.3	1.8	0.9	1.3	1.8	0.9	1.3	1.7
		9	9	9	9	9	9	9	9	9
0.1	0.8	0.8	1.2	1.7	0.8	1.2	1.7	0.7	1.1	1.6
		9	9	9	9	9	9	5	5	9
20.0	0.4	1.3	1.6	2.0	1.3	1.6	2.0	1.2	1.6	2.0
		2	9	9	2	9	9	2	9	9
20.0	0.6	0.8	1.2	1.6	0.8	1.2	1.6	0.7	1.1	1.6
		2	2	9	2	2	9	2	2	2
20.0	0.8	0.7	1.1	1.6	0.6	1.0	1.5	0.6	1.0	1.4
		2	2	9	2	2	2	2	2	2
30.0	0.4	1.1	1.5	1.9	1.1	1.5	1.9	1.1	1.5	1.9
		2	2	2	2	2	2	2	2	2
30.0	0.6	0.7	1.1	1.5	0.7	1.0	1.5	0.6	1.0	1.5
		2	2	2	2	2	2	2	2	2
30.0	0.8	0.6	0.9	1.4	0.5	0.9	1.4	0.5	0.8	1.3
		4	2	2	4	2	2	4	2	2
40.0	0.4	1.0	1.4	1.8	1.0	1.4	1.8	1.0	1.3	1.8
		4	2	2	4	2	2	4	2	2
40.0	0.6	0.6	0.9	1.4	0.6	0.9	1.4	0.6	0.9	1.3
		4	4	2	4	4	2	4	4	2
40.0	0.8	0.5	0.8	1.3	0.5	0.8	1.2	0.4	0.7	1.1
		4	4	4	4	4	4	4	4	4

BETA VALUES & SENSITIVITY CODES FOR TYPE 8 DEFECTS,
TOUGHNESS (CTOD)=0.050 MM

Table 7.30

COVS		SDA1			SDA2			SDA3		
	S/SY	D1	D2	D3	D1	D2	D3	D1	D2	D3
0.1	0.4	1.5	1.5	1.5	1.5	1.5	1.4	1.5	1.5	1.3
0.1	0.6	1.4	1.4	1.3	1.4	1.3	1.1	1.3	1.2	0.8
0.1	0.8	1.0	1.1	1.0	1.0	1.0	0.7	0.9	0.8	0.4
20.0	0.4	1.3	1.4	1.4	1.3	1.4	1.3	1.3	1.3	1.1
20.0	0.6	1.2	1.2	1.2	1.2	1.2	1.0	1.1	1.1	0.7
20.0	0.8	0.8	0.9	0.8	0.8	0.8	0.6	0.7	0.6	0.4
30.0	0.4	1.2	1.3	1.3	1.2	1.2	1.2	1.2	1.2	1.1
30.0	0.6	1.0	1.1	1.1	1.0	1.0	0.9	1.0	1.0	0.7
30.0	0.8	0.6	0.7	0.7	0.6	0.6	0.5	0.6	0.6	0.3
40.0	0.4	1.1	1.1	1.1	1.1	1.1	1.1	1.0	1.1	1.0
40.0	0.6	0.9	0.9	0.9	0.9	0.9	0.8	0.8	0.8	0.6
40.0	0.8	0.5	0.5	0.6	0.5	0.5	0.4	0.5	0.5	0.3

TARGET SAFETY INDICES FOR TYPE 1 DEFECTS

Table 7.31

COVS		SDA1			SDA2			SDA3		
	S/SY	D1	D2	D3	D1	D2	D3	D1	D2	D3
0.1	0.4	1.6	1.6	1.6	1.5	1.5	1.5	1.5	1.5	1.3
0.1	0.6	1.5	1.5	1.4	1.5	1.4	1.2	1.4	1.3	0.9
0.1	0.8	1.3	1.3	1.2	1.3	1.2	0.8	1.1	1.0	0.5
20.0	0.4	1.4	1.4	1.4	1.4	1.4	1.4	1.4	1.4	1.2
20.0	0.6	1.4	1.4	1.3	1.3	1.3	1.1	1.3	1.2	0.8
20.0	0.8	1.2	1.2	1.0	1.1	1.1	0.8	1.0	0.9	0.5
30.0	0.4	1.3	1.3	1.3	1.3	1.3	1.2	1.3	1.3	1.1
30.0	0.6	1.2	1.2	1.2	1.2	1.2	1.0	1.2	1.1	0.8
30.0	0.8	1.0	1.0	0.9	1.0	0.9	0.7	0.9	0.8	0.5
40.0	0.4	1.2	1.2	1.2	1.2	1.2	1.1	1.2	1.2	1.0
40.0	0.6	1.1	1.1	1.1	1.1	1.1	0.9	1.0	1.0	0.7
40.0	0.8	0.9	0.9	0.8	0.9	0.8	0.6	0.8	0.7	0.4

TARGET SAFETY INDICES FOR TYPE 2 DEFECTS

Table 7.32

COVS		SDA1			SDA2			SDA3		
	S/SY	D1	D2	D3	D1	D2	D3	D1	D2	D3
0.1	0.4	1.5	1.5	1.5	1.5	1.4	1.4	1.4	1.3	1.2
0.1	0.6	1.3	1.4	1.3	1.3	1.3	1.0	1.1	1.1	0.7
0.1	0.8	1.0	1.0	0.9	0.9	0.9	0.6	0.7	0.6	0.3
20.0	0.4	1.4	1.3	1.4	1.3	1.3	1.3	1.2	1.2	1.1
20.0	0.6	1.1	1.2	1.2	1.1	1.1	0.9	0.9	1.0	0.6
20.0	0.8	0.7	0.8	0.7	0.6	0.7	0.5	0.5	0.5	0.3
30.0	0.4	1.2	1.2	1.3	1.2	1.2	1.2	1.1	1.1	1.0
30.0	0.6	0.9	1.1	1.0	0.9	1.0	0.8	0.8	0.9	0.6
30.0	0.8	0.5	0.6	0.6	0.5	0.6	0.5	0.4	0.5	0.3
40.0	0.4	1.1	1.1	1.1	1.0	1.0	1.1	1.0	1.0	0.9
40.0	0.6	0.8	0.9	0.9	0.7	0.9	0.7	0.7	0.7	0.6
40.0	0.8	0.4	0.5	0.5	0.4	0.5	0.4	0.3	0.4	0.3

TARGET SAFETY INDICES FOR TYPE 3 DEFECTS

Table 7.33

COVS		SDA1			SDA2			SDA3		
	S/SY	D1	D2	D3	D1	D2	D3	D1	D2	D3
0.1	0.4	9.5	14.9	1.8	3.8	6.0	1.8	1.9	3.0	1.6
0.1	0.6	2.0	1.8	1.6	2.0	1.8	1.3	2.3	1.7	1.1
0.1	0.8	1.7	1.5	1.2	1.6	1.4	0.9	1.5	1.2	0.6
20.0	0.4	2.3	2.1	1.7	2.7	2.1	1.7	1.7	2.6	1.5
20.0	0.6	1.8	1.7	1.4	1.8	1.7	1.2	1.8	1.6	1.0
20.0	0.8	1.5	1.4	1.1	1.4	1.3	0.8	1.3	1.1	0.6
30.0	0.4	2.2	2.0	1.6	2.2	1.9	1.5	1.5	1.9	1.4
30.0	0.6	1.7	1.6	1.3	1.7	1.5	1.1	1.5	1.4	0.9
30.0	0.8	1.3	1.2	1.0	1.2	1.1	0.8	1.1	1.0	0.5
40.0	0.4	1.9	1.8	1.5	1.7	1.8	1.4	1.3	1.8	1.3
40.0	0.6	1.5	1.4	1.2	1.4	1.4	1.0	1.3	1.3	0.8
40.0	0.8	1.1	1.0	0.9	1.0	1.0	0.7	0.9	0.9	0.5

TARGET SAFETY INDICES FOR TYPE 4 DEFECTS

Table 7.34

COVS		SDA1			SDA2			SDA3		
	S/SY	D1	D2	D3	D1	D2	D3	D1	D2	D3
0.1	0.4	2.4	2.7	2.7	2.3	2.5	2.2	1.9	2.1	1.7
0.1	0.6	2.7	2.7	2.3	2.4	2.3	1.6	1.9	1.7	1.0
0.1	0.8	2.5	2.4	1.8	2.0	1.8	1.0	1.2	1.1	0.6
20.0	0.4	2.3	2.6	2.6	2.2	2.4	2.1	1.7	2.0	1.6
20.0	0.6	2.5	2.5	2.2	2.2	2.1	1.5	1.7	1.5	1.0
20.0	0.8	1.7	1.9	1.6	1.5	1.5	1.0	1.0	1.0	0.6
30.0	0.4	2.1	2.5	2.5	2.0	2.3	2.0	1.6	1.9	1.5
30.0	0.6	2.3	2.4	2.0	2.0	1.9	1.4	1.5	1.4	0.9
30.0	0.8	1.2	1.3	1.4	1.1	1.2	0.9	0.9	0.9	0.5
40.0	0.4	2.0	2.3	2.4	1.8	2.1	1.9	1.4	1.7	1.4
40.0	0.6	1.8	2.0	1.9	1.6	1.7	1.3	1.3	1.3	0.9
40.0	0.8	0.9	1.0	1.1	0.9	0.9	0.8	0.7	0.8	0.5

TARGET SAFETY INDICES FOR TYPE 5 DEFECTS

Table 7.35

COVS		SDA1			SDA2			SDA3		
	S/SY	D1	D2	D3	D1	D2	D3	D1	D2	D3
0.1	0.4	11.1	3.0	2.9	4.5	2.8	2.5	2.2	3.1	2.1
0.1	0.6	2.9	2.9	2.6	2.7	2.6	2.0	2.3	2.2	1.4
0.1	0.8	2.8	2.7	2.1	2.5	2.2	1.4	1.8	1.6	0.9
20.0	0.4	2.7	2.9	2.8	3.3	2.7	2.4	2.0	2.8	2.0
20.0	0.6	2.8	2.8	2.4	2.6	2.5	1.9	2.1	2.0	1.3
20.0	0.8	2.7	2.6	2.0	2.3	2.1	1.3	1.6	1.5	0.9
30.0	0.4	2.6	2.8	2.7	2.8	2.6	2.3	1.8	2.4	1.9
30.0	0.6	2.7	2.7	2.3	2.5	2.4	1.8	1.9	1.9	1.2
30.0	0.8	2.5	2.4	1.9	2.1	1.9	1.3	1.4	1.4	0.8
40.0	0.4	2.5	2.6	2.6	2.4	2.5	2.2	1.6	2.2	1.8
40.0	0.6	2.6	2.6	2.2	2.3	2.2	1.6	1.7	1.7	1.2
40.0	0.8	2.2	2.3	1.8	1.8	1.7	1.2	1.3	1.3	0.8

TARGET SAFETY INDICES FOR TYPE 6 DEFECTS

Table 7.36

SECTION 8

OPTIMISATION OF PARTIAL SAFETY FACTORS AND CODE FORMAT FOR DEFECT ASSESSMENT

8.1 Introduction

The move from safe to critical mathematical models in defect assessment comes at a time when limit state methods of design are replacing permissible stress methods. The move has provoked the need to evaluate safety margins in defect assessment and to prescribe the means by which these can be incorporated into the assessment equations. In Section 6 the safety margin and reliability for defect assessment were defined. Section 7 presented a method of ensuring ongoing safety by factoring defect size alone. The drawback of this method is that it involves calculation of a different safety factor for every defect encountered. In the present section a code format is presented whereby defects assessed using the assessment equations with the specified partial safety factors will have reliabilities close to the target value.

In order to determine a target reliability a set of assessment inputs (i.e. defect type, defect size, stress, toughness, etc.) was created and weighted according to what were considered to be typical values. The reliability of each member of the set was then calculated from the failure function expressing the difference between critical defect size and tolerable defect size according to the PD6493 design curve[1]. The target reliability was taken as the average of these. Using the same set, and on the assumption of an initial set of partial factors, reliabilities were calculated using a failure function expressing the difference between critical defect size and tolerable defect size according to the revised Level 2 assessment route based on the strip yield method[2]. An

optimum set of partial factors was found such that the spread of these reliabilities about the target was a minimum. Figures 8.1 presents a schematic flow chart showing the sequence of calculations.

The sensitivity of the optimised partial factors to the choice of weighting is investigated and found not to be excessive.

Attempts to calibrate partial factors to higher orders of reliability resulted in an unacceptably large scatter in failure probabilities. A means of reducing this and the implications for code application are discussed.

8.2 Code Format for Defect Assessment

The format presented below serves to introduce the three partial safety factors and indicates their positions in the assessment equations. The terms assessment flaw and limiting flaw are defined. When the Failure Assessment Diagram (FAD) is used attention is drawn to the need to calculate the fracture characterising parameters using the factored flaw size.

A flaw is acceptable if

$$a^* < a^*_{LIM} \qquad (8.1)$$

where

a^* is the assessment flaw given by

$$a^* = a_{NDT}\gamma_a \qquad (8.2)$$

a_{NDT} is the characteristic flaw dimension being either the half length of a through thickness flaw, height of a surface flaw or half-height of an embedded flaw determined by non-destructive testing.

γ_a is a partial factor on flaw size.

a^*_{LIM} is the limiting flaw for the same geometry and loading conditions as the flaw being assessed. In ductile materials a^*_{LIM} is determined by the interaction of LEFM and plastic collapse mechanisms and cannot be expressed in closed form. It is given by the value of a satisfying

$$\text{function}\ (\delta_r(\sigma\gamma_\sigma\ ,\ \tau/\gamma_\tau\ ,\ a\ ,\ \text{other factors})\ ,$$
$$S_r(\sigma\gamma_\sigma\ ,\ a\ ,\ \text{other factors})) = 0 \qquad (8.3)$$

where

δ_r is the ratio of applied crack-tip opening displacement to the fracture toughness and is a function of total remote stress σ, fracture toughness τ, characteristic defect dimension a, and other factors depending on geometry and type of loading.

γ_σ is a partial factor on stress

γ_τ is a partial factor on fracture toughness

S_r is the ratio of net stress on the intact ligament to the plastic collapse stress. It is a function of total remote stress σ, characteristic flaw size a, and other factors depending on geometry, type of loading and tensile material properties.

Alternatively a flaw may be considered acceptable if the point

$$(S_r(\sigma\gamma_\sigma\ ,\ a^*\ ,\ \text{other factors})\ ,\ \delta_r(\sigma\gamma_\sigma\ ,\ \tau/\gamma_\tau\ ,\ a^*\ ,\ \text{other factors}))$$

plotted on the (x , y) plane lies within the area bounded by the x- and y-axes and the curve:

$$y = \frac{x}{\sqrt{\left[\frac{8}{\pi^2} \ln \sec\left(\frac{\pi}{2} x\right)\right]}} \qquad 0 < x < 1.0 \qquad (8.4)$$

8.3 Set of Typical Assessments

The aim of creating a data set was to represent the ranges of typical values likely to be found in practice. Heed was also paid to the sensitivity of the failure probability to variable. Hence stress, which has a marked influence on assessment failure probability, is represented by three discrete values for the lower, middle and upper portions of the curve in Figure 8.2.

In contrast to bridge and offshore structure calibration studies in Sections 2 to 4 of this thesis the set comprised different degrees of uncertainty as well as different mean values of the input variables. It was felt this was a better representation of the wide range of applications for which a defect assessment code would be used. Random uncertainty (COV) in toughness was, however, taken as constant at 52% for COD toughness and 20% for K_{1C} toughness.

The set comprised all combinations of

σ/σ_y:	0.1, 0.5, 0.9
stress COV:	5%, 30%
toughness values:	0.05mm, 0.125mm, 3000Nm$^{-3/2}$
defect size standard deviations:	2mm, 5mm, 10mm
defect geometry:	through thickness, semi elliptical, semi circular
loading:	pure bending, pure tension.

The total number in the set was 3 x 2 x 3 x 3 x 3 x 2 = 324.

8.4 Weighting

8.4.1 Stress

The range of possible stresses up to yield was firstly discretised as shown in column 1 of Table 8.1. A basic weighting, having a slight concentration in the middle of the range was then assumed. Considerations of the graph of safety index vs. stress, see Figure 8.2, leads to a 3-range discretisation approximately modelling the low, middle and upper portions of the curve. The reduced ranges and their representative stress values are shown in columns 3 and 4 of Table 8.1. The final adjusted weighting was obtained by summing the basic weighting over reduced range and rounding.

8.4.2 Toughness

It was firstly assumed that COD toughness data would be used two-thirds of the time and K_{1C} data one-third. The COD and K_{1C} values were assumed to occur with a weighting shown in columns 3 and 4 of Table 8.2. The fifth column gives the value of the product weighting e.g. .67x.16 etc. The graph of safety index vs. COD toughness, see Figure 8.3, rises steeply from low toughness to a plateau from about δ_{mat} = 0.1 and above. Accordingly two values of COD toughness were selected to represent the two sections of the curve. The graph of safety index vs. K_{1C} toughness, on the other hand maintains a much flatter profile over the range of K_{1C} values considered. A single value was thus selected to represent the entire range. The reduced ranges and their representative values are shown in columns 6 and 7 of Table 8.2. The net weighting, obtained by summing the basic (product) weighting over the reduced range is shown in column 8. This final value was rounded in column 9.

8.4.3 Defect Geometry and Loading Type

Surface cracks were assumed to occur more often than through thickness cracks in the ratio of 6:4. Table 8.3 summarises the six basic types considered and the assumed weighting.

8.4.4 Stress Uncertainty

Two values of stress COV, viz 5% and 30% were selected to cover the wide range of structures to which the revised defect assessment procedure will be applied. The lower value corresponds to stresses determined accurately, e.g. by strain gauging, or when structural analysis is used to determine the effects of an accurately known load, e.g. dead load. The higher value corresponds to stresses determined by structural analysis when large uncertainties exist in both the magnitude of the loading source e.g. waves, wind and currents as well as in the modelling of the transfer of the load into the structure e.g. inertia and drag coefficients in Morrison's Equation.

Equal weighting has been assumed for COV.

8.4.5 Defect Sizing Uncertainty

Three values of standard deviation of the error in defect sizing were assumed viz. 2mm, 5mm and 10mm. Notwithstanding some well known gross underestimates of defect size (which can be considered as upper tail values) it is considered these values represent the range achievable using available NDT methods. Equal weighting was assumed for the three values.

8.4.6 Alternative Weightings

In order to investigate the effect of the choice of weighting on the optimised partial factors alternative weightings were selected by adding more weight at the least safe end of the variable range. The above weighting scheme, labelled A (normal), and the four alternative weightings labelled from B to E resulted in five data sets from which to calculate failure probabilities. The various values are summarised in Table 8.4. For any set only one of the alternatives B-E was used, e.g. for set B the alternative weighting for stress was combined with the weightings under A for all the other variables. The example under Table 8.4 gives the value of w_1 for the normal weighting.

The value of

$$\sum_{i=1}^{3\,2\,4} w_i = 1.0 \qquad (8.5)$$

was confirmed for each of the five sets.

8.5 Assessment Routes

Three routes defining tolerable defect size were used. The first corresponds to the current PD6493 design curve with inputs of mean values of stress and K_{1C}. For COD toughness a value corresponding to the minimum of 3 CTOD tests was used as input. As shown in Appendix B of Section 6 this corresponds to the mean value divided by $3^{1/\alpha}$ where α is the shape factor of the Weibull distribution. Alternatively the 23rd percentile of the Weibull distribution may be used.

The second route corresponds to Level 1 in the 8th revision of PD6493[2]. It is essentially the same as the design curve but additionally requires a plastic collapse check. Inputs are as for the design curve.

The third route corresponds to the Level 2 route in the 8th revision of PD6493. It embodies LEFM and plastic collapse considerations and is far less conservative in the treatment of through thickness stress distributions. The equations are critical unlike those for the design curve which encorporate variable safety factor of approximately 2.0. An amendment included in the 8th revision is a scaling factor on the stress intensity factor which is intended to model the non-linear redistribution of stress across the intact ligament. It applies when the ratio of defect area to total load bearing area including the defect, a_r, exceeds 10%. The value of the factor is $\surd\sec(\pi a_r)$. Since this has a singularity for $a_r = 0.5$ and cannot be evaluated for larger ratios the limiting defect size in any assessment has to be taken as that for which $a_r = 0.5$.

8.6 Evaluation of Partial Safety Factors

Values of γ_σ, γ_τ and γ_a were found such that the objective function

$$OF = \sum_{i=1}^{n} w_i \ (\log_{10} p_{fi} - \log_{10} p_{fT})^2 \qquad (8.6)$$

was a minimum. p_{fi} was the failure probability $(1 - \Phi(\beta_i))$ of the i^{th} member of the assessment set with tolerable flaw defined by the Level 2 route with optimum values of the partial factors. p_{fT} was the target value given by

$$p_{fT} = \sum_{i=1}^{n/2} 2w_i \ p_{fDCi} \qquad (8.7)$$

where p_{fDCi} is the failure probability of the i^{th} member when the Design Curve is used to define tolerable flaw size. For evaluation of target reliability, flaws under bending were omitted hence only half of the assessment set appears in the summation. The weighting was adjusted accordingly. This follows the recognition that flaws under bending are conservatively assessed by the Design Curve. Figure 8.1 presents the sequence of calculation. The method by which partial factors were reselected was based on conventional search by trial and error technique for minimisation of a function of severable variables. None of the short cuts used in optimisation elsewhere in this thesis could be employed because the form of the function does not permit any amalgamation of the partial factors. However knowledge of the behaviour of the function in the region of the minimum and the fact that accuracy of partial factors to one decimal place is sufficient for design code purposes enabled a purpose built minimisation scheme to be used. This commenced with initial selection of six values of the partial factors (two each for γ_σ, γ_τ and γ_a) and step length T = 0.1. Three evaluations of the objective function were made:

$$OF_1 = OF(x_1 - T,\ x_2, \ldots, x_6)$$
$$OF_2 = OF(x_1,\ x_2, \ldots, x_6)$$
$$OF_3 = OF(x_1 + T,\ x_2, \ldots, x_6)$$

The interim minimum point then became the point corresponding to the minimum of OF_1, OF_2 and OF_3. This was repeated for all six variables whereupon a new current point was established. This process was repeated from x_1 until old and new current points were invariant. This method was found to be more successful than one where each variable is followed down "vallies" to its minimum before moving onto the next variable. To prevent repeated

evaluations of the same point each new point was stored with its functional value. Before any new evaluation was made the store was searched. Further improvements were made in speed by curve fitting the relationship between reliability and global factor for each member of the set. A sample of the curves is presented in Figures 8.4 and 8.5. Each new set of values of partial factors was then converted into a single value of global factor from which, using the fitted polynomial coefficients, failure probability for each member was readily found.

Figures 8.6 to 8.10 illustrate the various stages of the optimisation procedure for the normal weighting. In Figures 8.6 to 8.9 the abscissae give the number of the combination in the data set. The set comprises 324 different combinations of stress level, stress COV, toughness, defect standard deviation and defect type. Numbers 1 to 108 refer to stress=$0.1\sigma_y$, 109 to 216 to stress=$0.5\sigma_y$ and 217 to 324 to stress=$0.9\sigma_y$. The figures show the distribution of $-\log_{10} p_{fi}$ about the target value for the Design Curve (Figs. 8.6 and 8.7) the Level 1 route (Fig. 8.8) and the Level 2 route used with optimised partial factors (Fig. 8.9). In Figure 8.10 the ranges of $-\log_{10} p_{fi}$ are compared for different assessment routes. This figure shows more clearly the benefits of optimisation in greatly reducing the variability of reliabilities about the target.

Table 8.5 gives details of the optimisation results for each of the five differently weighted assessment sets. The first column gives the label of the set from A (normal) to E and indicates which particular value of the input

parameter has been emphasised by weighting. The second column presents the values of:

$$p_{fT} = \sum_{i=1}^{3\,2\,4} w_i \; p_{fiDC} \qquad (8.8)$$

$$OF_T = \left(\sum_{1}^{3\,2\,4} w_i (\log_{10} p_{fiDC} - \log_{10} p_{fT})^2 \right)^{\frac{1}{2}} \qquad (8.9)$$

and

$$\Delta \log_{10} p_{fi} = \min_i(-\log_{10} p_{fiDC}) - \max_i(-\log_{10} p_{fiDC}) \qquad (8.10)$$

where p_{fiDC} is the failure probability of the i^{th} member of the set when the tolerable defect is determined using the Design Curve.

The third column presents the same data with the Level 2 approach used to determine tolerable defect sizes, i.e.

$$\bar{p}_f = \sum_{i=1}^{3\,2\,4} w_i \; p_{fiSY} \qquad (8.11)$$

$$DF = \left(\sum_{1}^{3\,2\,4} w_i (\log_{10} p_{fiSY} - \log_{10} p_{fT})^2 \right)^{\frac{1}{2}} \qquad (8.12)$$

$$\Delta \log_{10} p_f = \min_i(-\log_{10} p_{fiSY}) - \max_i(-\log_{10} p_{fiSY}) \qquad (8.13)$$

where p_{fiSY} is the failure probability of the i^{th} member of the set when the tolerable defect is determined using the Level 2 route based on the strip yield model. The fourth column presents the partial factors optimised to an accuracy

of one decimal place. The notation used is as follows:

$\gamma_{\sigma 30}$ partial factor on stress when stress COV = 30%

$\gamma_{\sigma 5}$ partial factor on stress when stress COV = 5%

$\gamma_{\tau K}$ partial factor on toughness when K_{IC} is used

$\gamma_{\tau \delta}$ partial factor on toughness when δ_{mat} is used

γ_{a5} partial factor on defect size when defect standard deviation is 5mm or less

γ_{a10} partial factor on defect size when defect standard deviation is 10mm

The second entry for each set presents the effects on p_f, OF and $\Delta \log_{10} p_{fi}$ when the values of partial factors are constrained not to be below 1.0.

Table 8.6 presents the results of optimisation to higher reliabilities.

8.7 Discussion

The object of providing a Code Format for defect assessment is primarily to indicate in a brief manner where the respective partial factors appear in the assessment equations. The use of functional notation is an efficient way to minimalize the presentation. It should be understood by all users that the exact form of the function will be presented, for each individual case, in the main part of the documents. Attempts to avoid using functional notation necessarily would involve complex algebraic expression with terms not directly relevant to the matter at hand and would result in a loss of clarity.

The naming of two distinct quantities: assessment flaw and limiting flaw is new to defect assessment but the parallels in ultimate strength viz. characteristic load and design resistance are well established. The distinction between the two is necessary when partial factors on flaw size are introduced. The modes of solution for the limiting flaw using the strip yield model affect the presentation of the Code Format. Consideration was given to expressing:

$$a^*_{LIM} = \text{function } (\sigma\gamma_\sigma,\ \tau/\gamma_\tau,\ \text{other factors}) \qquad (8.14)$$

but since it is not possible to write down this function fully with a^*_{LIM} appearing as the subject it was avoided.

The most redeeming feature of the strip yield model for engineers who are unable to implement computer solutions is that it allows the flaw to be assessed graphically. For this method of assessment the code format emphasises that the factored flaw size, the "assessment flaw", must be used to calculate the fracture parameters δ_r and S_r.

It was considered adequate to perform unconstrained minimisation of the object function. The additional constraint

$$\sum_{i=1}^{n} w_i\ p_{fi} = p_{fT} \qquad (8.15)$$

used in other parts of the thesis would add undue complexity in the present case which already has 6 degrees of freedom. For symetrically distributed p_{fi} the constraint is automatically satisfied. For the more probable case of non-symmetrically distributed p_{fi} the constraint is satisfied approximately as can be seen by comparing values of p_{fT} and $\bar{p}_f$ in Table 8.5.

Obviously the typical input values and levels of uncertainty for assessments will be different for each application. The range of values used is considered sufficient to cover values typical for offshore jackets. Since the ranges are large it is thought many other applications will be encompassed.

Loading has been assumed either pure tension or pure bending. Flaws under combined tension and bending in the Level 2 approach are dealt with by superposition of the effects of the individual components and no additional failure mechanism occurs merely as a result of the presence of two loading modes. Consequently it is considered that the omission of specific tension/bending ratios in the set cannot lead to significant deviations from the mean failure probability and thus cannot significantly effect the results.

Table 8.5 presents the optimisation results and confirms that despite large shift in the assumed weighting the partial safety factors remain only slightly affected. This is encouraging particularly for case B where stresses of $0.9\sigma_y$ were assumed to occur with a frequency of 80%. For case B the target failure probability is seen to increase to 0.433, by far the largest increase out of all the cases considered, yet the partial factors are seen to have only slightly redistributed themselves (i.e. little or no overall increase).

The optimised partial factor on COD toughness, $\gamma_{\tau\delta}$, has values below 1.0 for each case considered. This stems from the fact that it has already been assumed in the calculation of a_{SY} that the minimum toughness from three COD tests will be used. The toughness input to a_{SY} differs from the toughness input to a_{crit} by a factor of $3^{\frac{1}{2}} = 1.73$ (see Appendix B of Section 6). Optimised partial factors less than 1.0 point to the fact that the minimum of

three is a sufficient (if not slightly excessive) lower bound value when compared to the uncertainties in other variables. Obviously such negative values would be out of place in an assessment code. For case A only partial factors were adjusted manually to obtain a reduced range of $\Delta \log_{10} p_{fi}$. The price for moving away from optimum values is an increase in the value of the objective function though this is still well below the value in column 2 for design curve assessments. The mean failure probability has also moved coincidentally closer to the target value. This set of partial factors was the final recommendation for the revised defect assessment document.

In order to appreciate the values of partial safety factors it is useful to consider what overall, net or global safety factor is being applied. From LEFM considerations a crack is tolerable if:

$$\surd\delta_r < 1$$

for a through crack in tension this is

$$\frac{(\sigma\gamma_\sigma)^2 \pi a \gamma_a}{\sigma_y E \delta_{mat}/\gamma_\tau} < 1$$

$$a < \frac{\sigma_y E \delta_{mat}}{\sigma^2 \pi} \frac{1}{\gamma_\sigma^2 \gamma_a \gamma_\tau} \qquad (8.16)$$

Thus the global factor is $\gamma_\sigma^2 \gamma_a \gamma_\tau$. The global factor corresponding to the 'optimised' values in row 2 of Table 8.5 is between 1.10 and 1.32 depending upon the uncertainties in the input parameters. If mean rather than minimum-of-three toughness were to be used then the range is 1.91 to 2.3.

Considering the COD design curve incorporated a factor of 2.0 on LEFM based assessment at low stresses and used a toughness input which corresponded to an additional factor of $\sqrt{3}$ the total global factor was 3.46. The re-evaluated global factor thus represents a decrease in deterministic factor of safety of approximately one third.

The spread of reliabilities given by the value of $\Delta \log_{10} p_{fi}$ in Table 8.6 for target failure probabilities of 10^{-3} and 10^{-5} is unacceptably large for code use. The reasons for the spread can be seen from the safety index vs. safety factor relationships such as those shown in Figures 8.4 and 8.5. As the safety factor increases so the difference between minimum and maximum safety index increases rapidly.

One way in which greater consistency can be achieved at higher reliabilities is to eliminate certain members of the assessment set. The implications for code application where higher reliabilities are required is the outlawing of assessment inputs where accuracy cannot be guaranteed, i.e. no defects would be tolerated if the uncertainty in measuring stress, toughness or defect size is beyond specified limits. Table 8.6 accordingly presents optimised partial factors to two higher target reliabilities, viz. 0.001 and 0.00001, for the normal set A and a second set F in which stresses of $0.9\sigma_y$, stress COVs of 30%, COD toughness (COV of 50%) and defect standard deviations of 5mm and 10mm have all been eliminated. The weighting was adjusted accordingly so that $\Sigma\, w_i = 1$ was maintained. The spread of reliabilities, seen by comparing values of OF and $\Delta \log_{10} p_{fi}$, is much reduced for the limited set F.

8.8 Conclusions

1. In order to achieve a consistant level of reliability similar to that achieved using the PD6493 Design Curve the Level 2 route based on the modified strip yield model should be used with estimates of stress, toughness and defect size factored as follows:

stress factor	= 1.2 when the stress COV is 30% or less
	= 1.1 when the stress COV is 5% or less
toughness factor	= 1.0 when K_{1C} toughness is used or when the minimum-of-three estimate of COD toughness is used.
defect size factor	= 1.0 when the standard deviation in defect size is less than 5mm
	= 1.1 when the standard deviation in defect size is less than 10mm.

2. The optimised partial factors are reasonably insensitive to the choice of weighting function for values of total stress less than $0.9\sigma_y$.
3. Consistently higher reliabilities can be achieved using the safety factors in Table 8.6. In order to achieve consistency at higher reliabilities certain assessment combinations should not be permitted (i.e. tolerable defect size = zero).
4. Little additional safety is achieved by increasing the partial factors beyond $\gamma_{\sigma}{}^{2}\ \gamma_a\ \gamma_\tau = 5.0$.

8.9 References

1. British Standards PD6493: 1980 Guidance on some methods for the derivation of acceptable levels of defects in fusion welded joints, London, 1980.

2. PD6493 8th revision not published.

3. Plane, C.A. and Cowling, M.J., 'Reliability Study of Existing and Proposed Defect Assessment Procedures'. Methodology Working Group Report No. 4, February 1987.

Table 8.1 Stress Weighting

Stress (x y)	Basic Weighting	Reduced Range	Representative Value	Adjusted Weighting
.1	.2	.05 - .20	.10	.1
.3	.2			
.5	.3	.20 - .80	.50	.8
.7	.2			
.9	.1	.80 - 950	.90	.1

Table 8.2 Toughness Weighting

	Frequency of use	Toughness mm or $Nmm^{3/2}$	Basic W't'g	Product W't'g	Reduced Range	Repres'tiv Value	Weighting	Rounded Weighting
mat	.67	.025	.16	.1072	.01-.1	.050	.1072	.11
		.050	.20	.1340				
		.075	.16	.1072				
		.100	.16	.1072				
		.150	.16	.1072				
		.200	.16	.1072	.1-.2	.125	.5628	.56
K_{1C}	.33	1500	.16	.0528				
		2000	.20	.0660				
		2500	.16	.0528				
		3000	.16	.0528				
		3500	.16	.0528	1500-			
		4000	.16	.0528	4000	3000	.33	.33

Table 8.3 Defect Geometry and Loading

Type	Geometry	Loading	Weighting
1	TT	T	.2
2	TT	B	.2
3	S1	T	.15
4	S1	B	.15
7	S5	T	.15
8	S5	B	.15

TT through thickness
S1 surface crack a/2c = 0.1
S5 surface crack a/2c = 0.5

T uniform tension
B pure bending

Table 8.4 Summary of Weighting

Stress (x_y)			Toughness			Defect Types		Stress Uncertainty			Defect Size Uncertainty		
Value	wt. A	wt. B	Value	wt. A	wt. C	Type	wt.	COV%	wt. A	wt. D	Std. dev.	wt. A	wt. E
.1	.10	.10	.050	.11	.56	1	.20				2mm	.33	.15
						2	.20	5	.50	.3			
.5	.80	.10	.125	.56	.11	3	.15				5mm	.34	.15
						4	.15						
						7	.15	30	.50	.7			
.9	.10	.80	3000	.33	.33	8	.15				10mm	.33	.7

Example: combination 1, normal weighting, - stress = .1 y, toughness = .05mm, Type 1, stress COV = 5%
defect std. dev. = 2mm: w_1 = .10x.11x.20x.50x.33 = 0.000363

Col. 1	Col. 2			Col. 3			Col. 4					
Weighting	Tolerable defect from Design Code			Tolerable defect from Level 2			Optimised Partial Factors					
	p_{fT}	OF_T	$\Delta\log_{10}p_{fi}$	$\overline{p_f}$	OF	$\Delta\log_{10}p_f$	$\gamma_{\sigma 30}$	$\gamma_{\sigma 5}$	$\gamma_{\tau K}$	$\gamma_{\tau\delta}$	γ_{a5}	γ_{a10}
A:Normal (see	0.231	0.279	6.4×10^{-5}-1.1	0.196	0.0845	.45-1.12	1.2	1.1	1.1	0.9	1.1	1.1
A:Table 8.4)	-	-	-	0.241	0.139	.31-.79	1.2	1.1	1.0	1.0	1.0	1.1
B:high stresses	0.433	0.196	6.4×10^{-5}-1.1	0.210	0.0555	.27-.66	1.3	1.0	1.0	0.7	1.0	1.0
B:weighted	-	-	-	0.182	0.0899	.27-.91	1.3	1.0	1.0	1.0	1.0	1.0
C:low toughnesses	0.273	0.257	6.4×10^{-5}-1.1	0.267	0.0739	.30-.92	1.2	1.1	1.1	0.8	1.0	1.1
C:weighted	-	-	-	0.229	0.1080	.32-.92	1.2	1.1	1.1	1.0	1.0	1.1
D:large stress	0.265	0.260	6.4×10^{-5}-1.1	0.219	0.0630	.40-1.1	1.2	1.1	1.0	0.8	1.1	1.1
D:uncertainty	-	-	-	0.193	0.113	.40-1.1	1.2	1.1	1.0	1.0	1.1	1.1
E:large defect	0.267	0.255	6.4×10^{-5}-1.1	0.247	0.0686	.40-1.1	1.2	1.1	1.0	0.8	1.1	1.1
E:uncertainty	-	-	-	0.218	0.105	.40-1.1	1.2	1.1	1.0	1.0	1.1	1.1

Table 8.5 Comparison of PSFS for Different Weightings

Target p_f	Set	tolerable flaw defined by Level 2 $\overline{p_f}$	OF	$\log_{10} p_{fi}$	Optimised Partial Factors: $\gamma_{\sigma 30}$	$\gamma_{\sigma 5}$	$\gamma_{\tau K}$	$\gamma_{\tau \delta}$	γ_{a5}	γ_{a10}
0.001	A	0.0217	1.159	0.71-3.3	1.6	1.4	1.2	1.4	1.2	1.4
	F*	0.0008	0.394	2.77-4.31	-	1.4	1.2	-	1.3	-
0.00001	A	0.00068	1.45	1.96-16.5	2.4	2.0	1.3	2.6	1.7	1.8
	F*	0.0000078	0.782	4.03-6.61	-	1.6	1.4	-	1.3	-

* Set F consisted of σ/σ_y = 0.1, 0.5; stress COV = 5%, toughness = 3000Nmm$^{-3/2}$, defect standard deviation = 2mm

Table 8.6 Optimisation to Higher Target Reliabilities

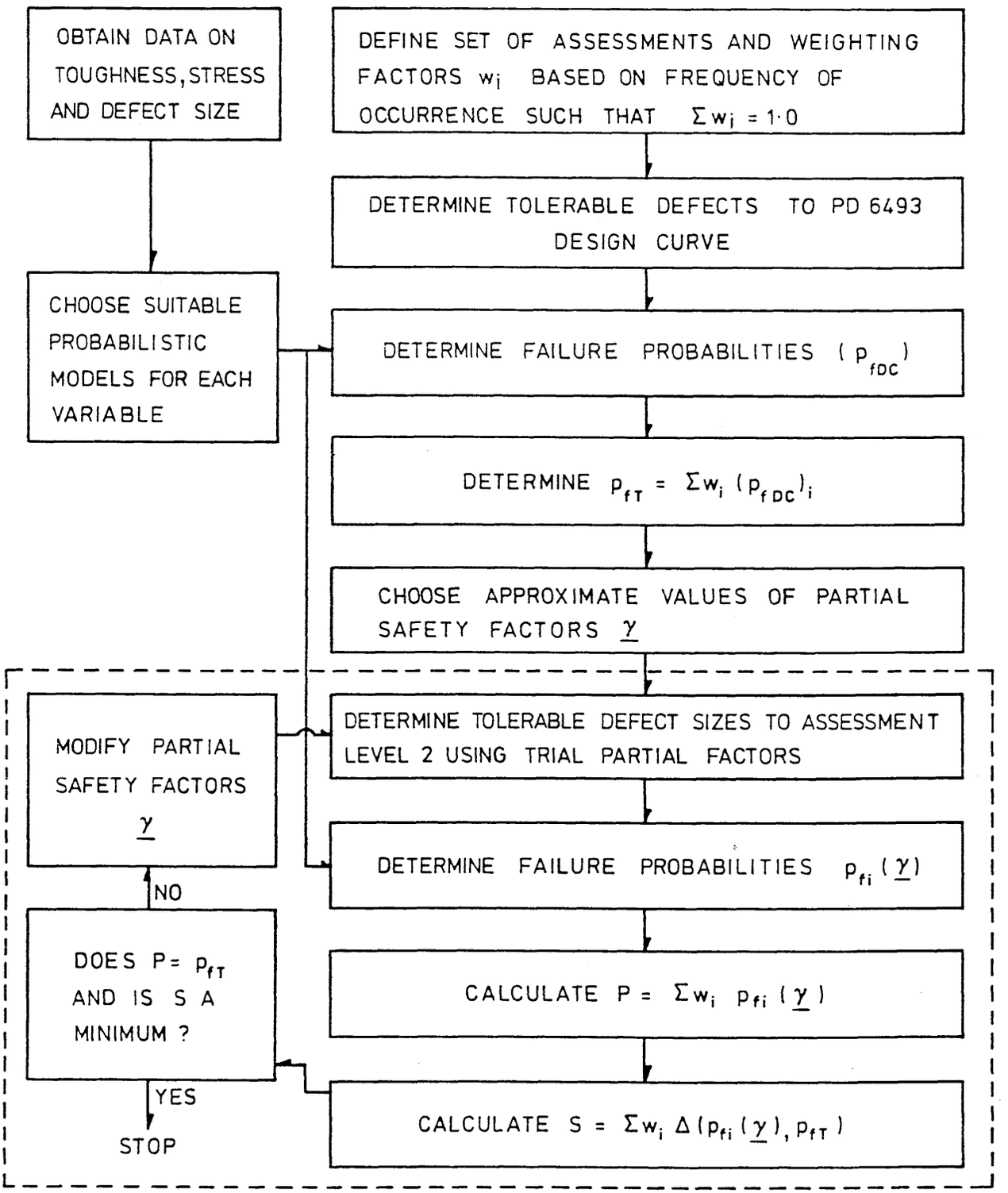

Fig. 8.1 Flow chart for Optimisation of Defect Assessment Partial Safety Factors

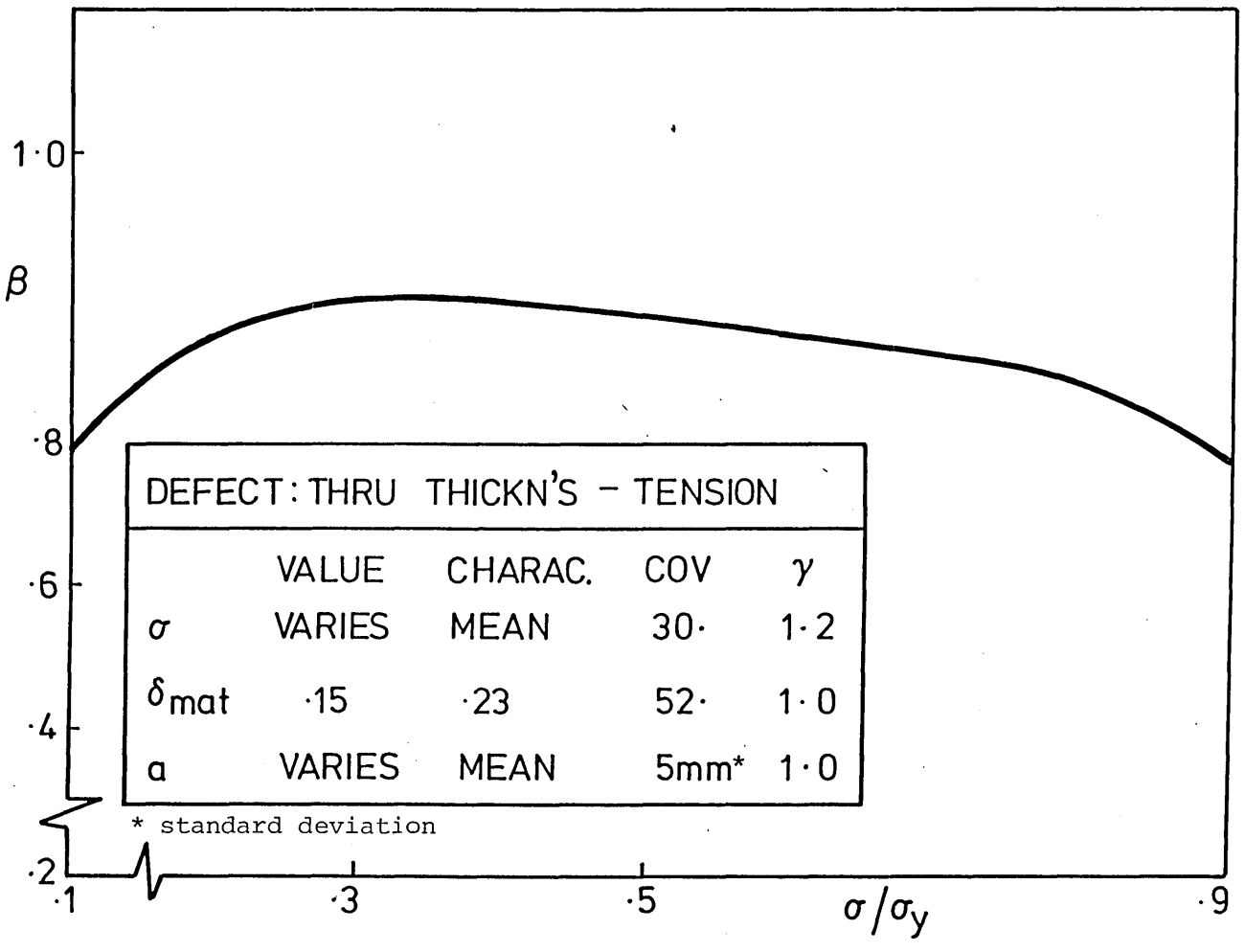

Fig. 8.2 SAFETY INDEX vs. STRESS RATIO for LEVEL 2 ROUTE.

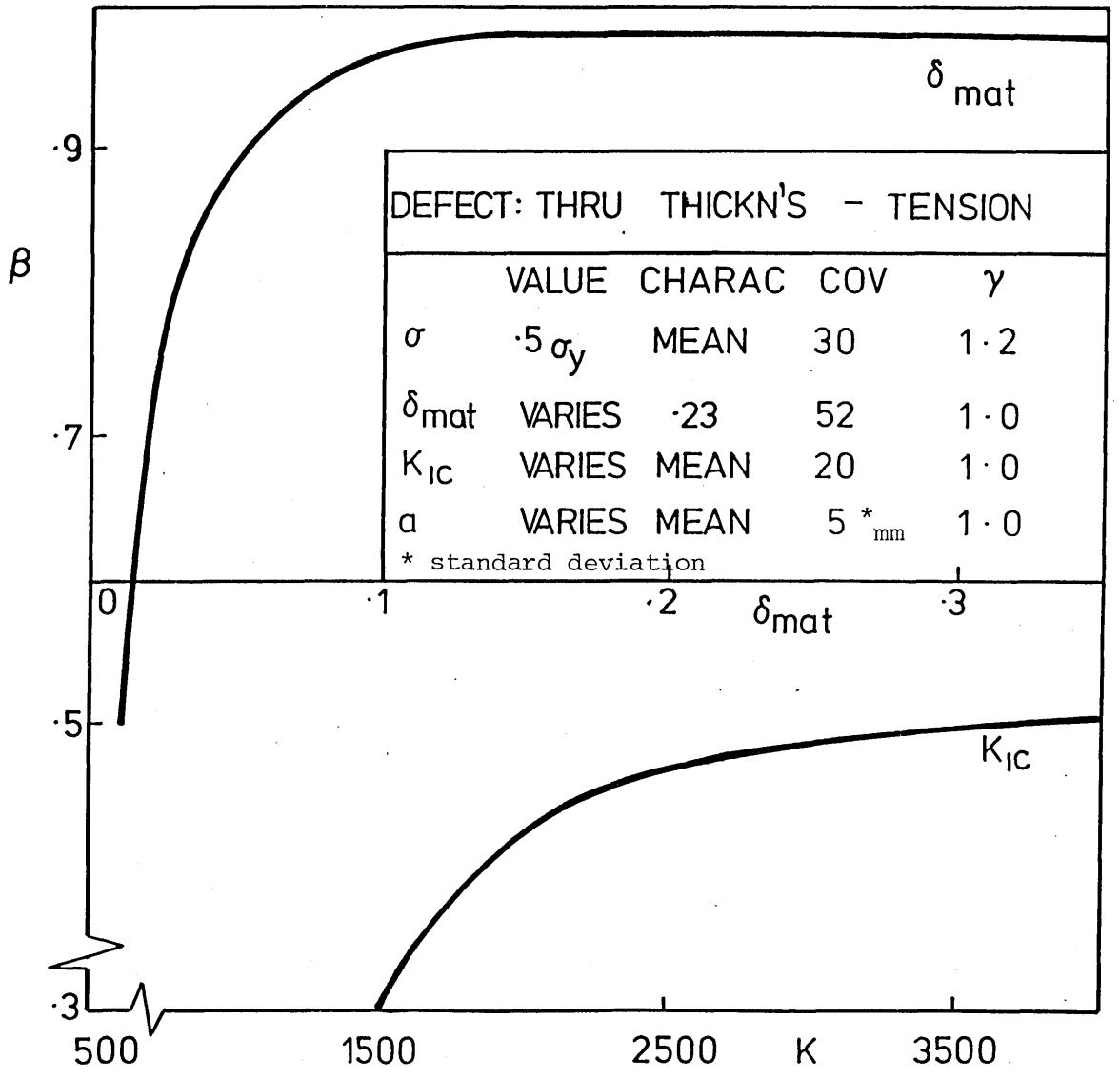

Fig. 8.3 SAFETY INDEX vs. CTOD and K_{IC} TOUGHNESS for LEVEL 2 ROUTE

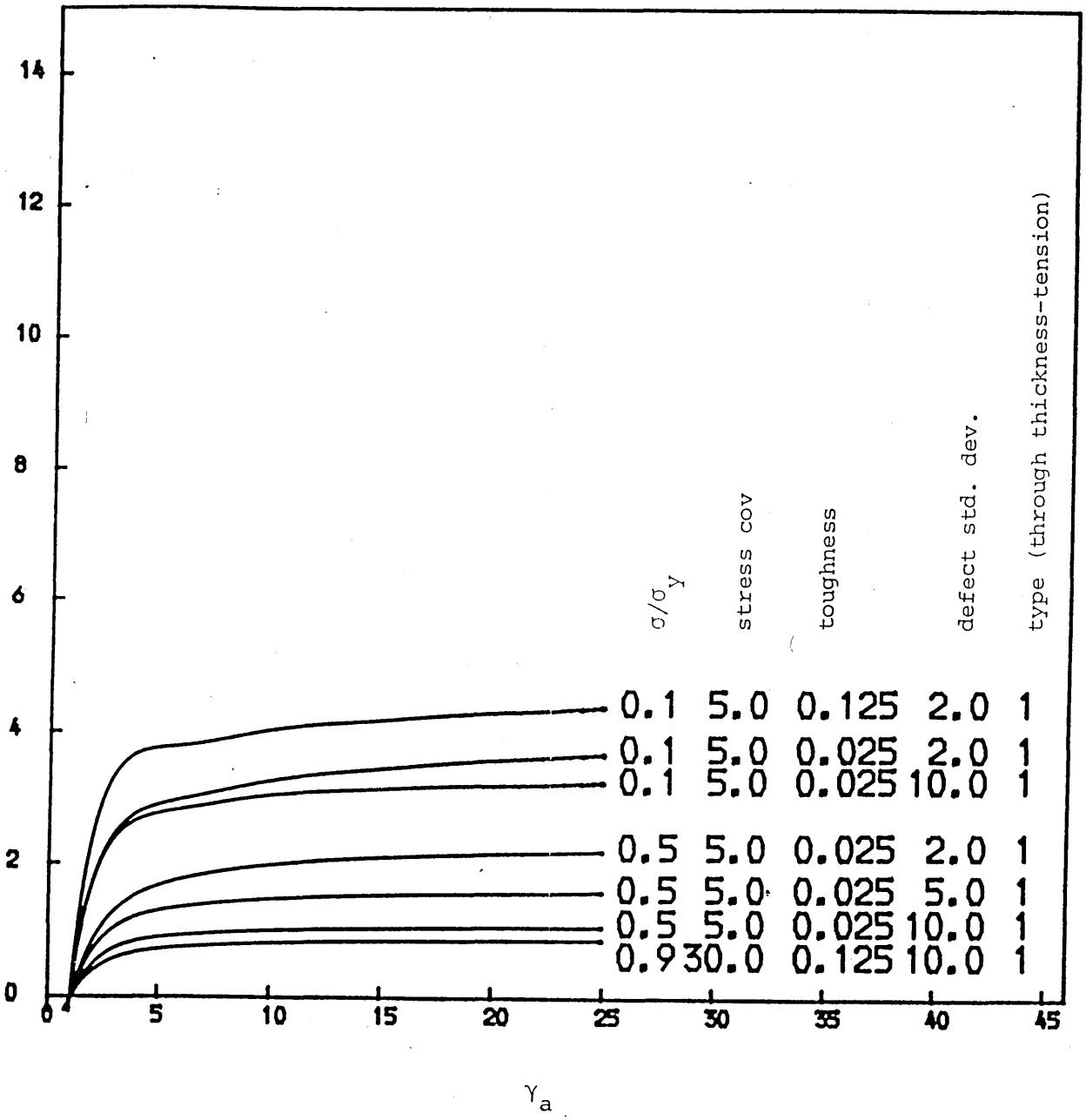

Fig. 8.4 Reliability vs. single safety factor on defect size - CTOD toughness

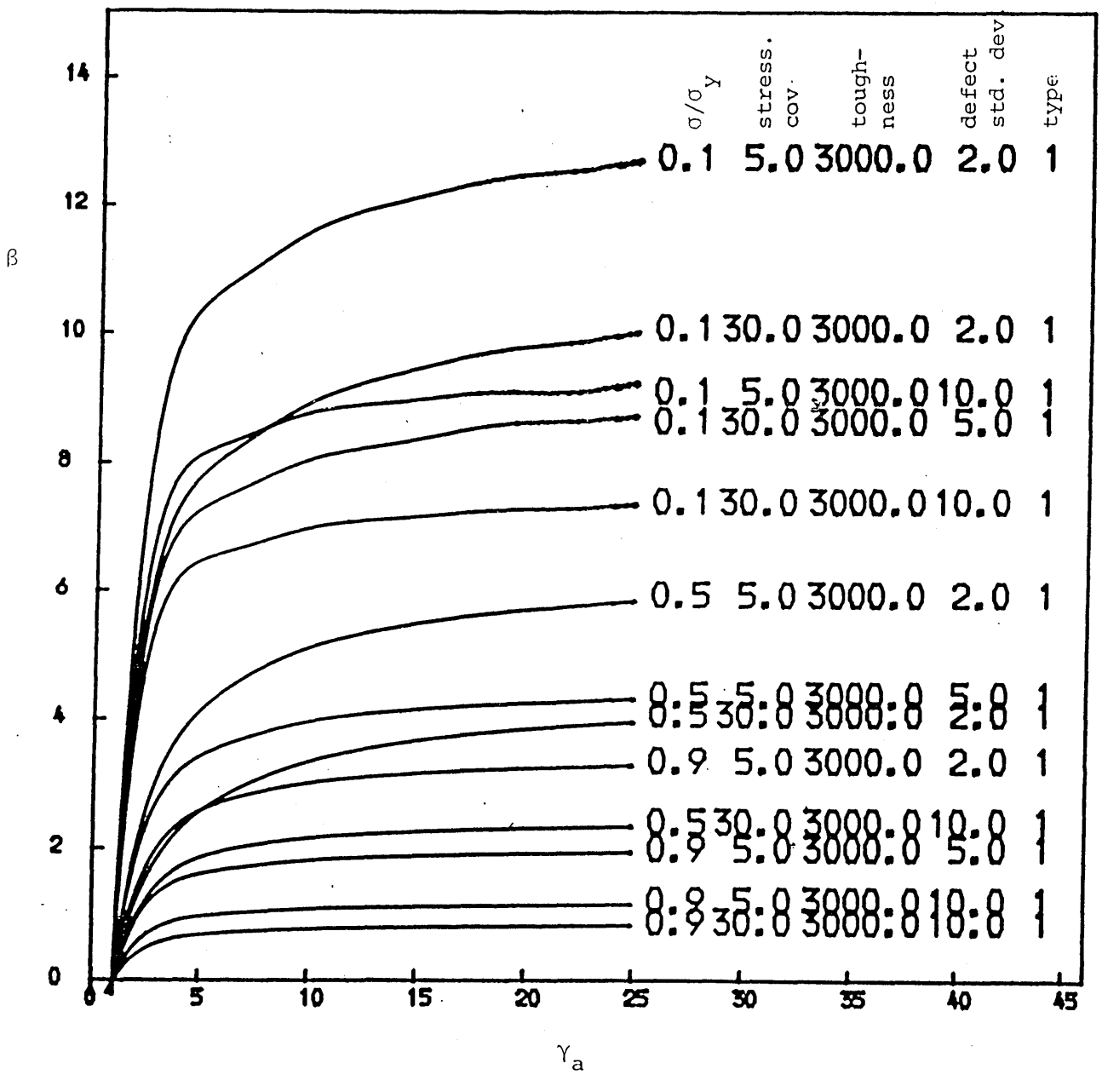

Fig. 8.5 Reliability vs. single safety factor on defect size - K_{1c} toughness

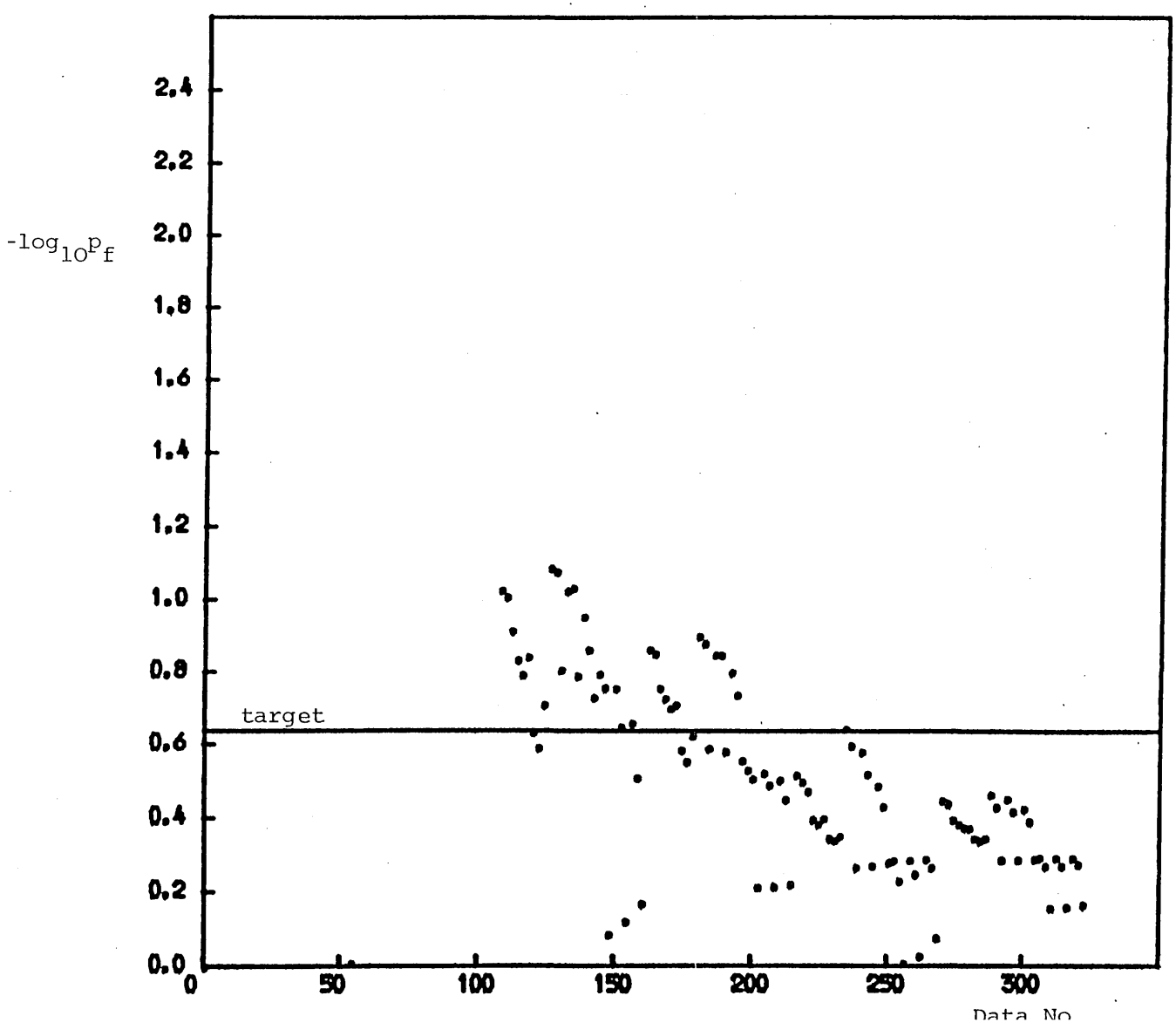

Fig. 8.6 Scatter of Reliabilities about target using Design Curve - tension cases only

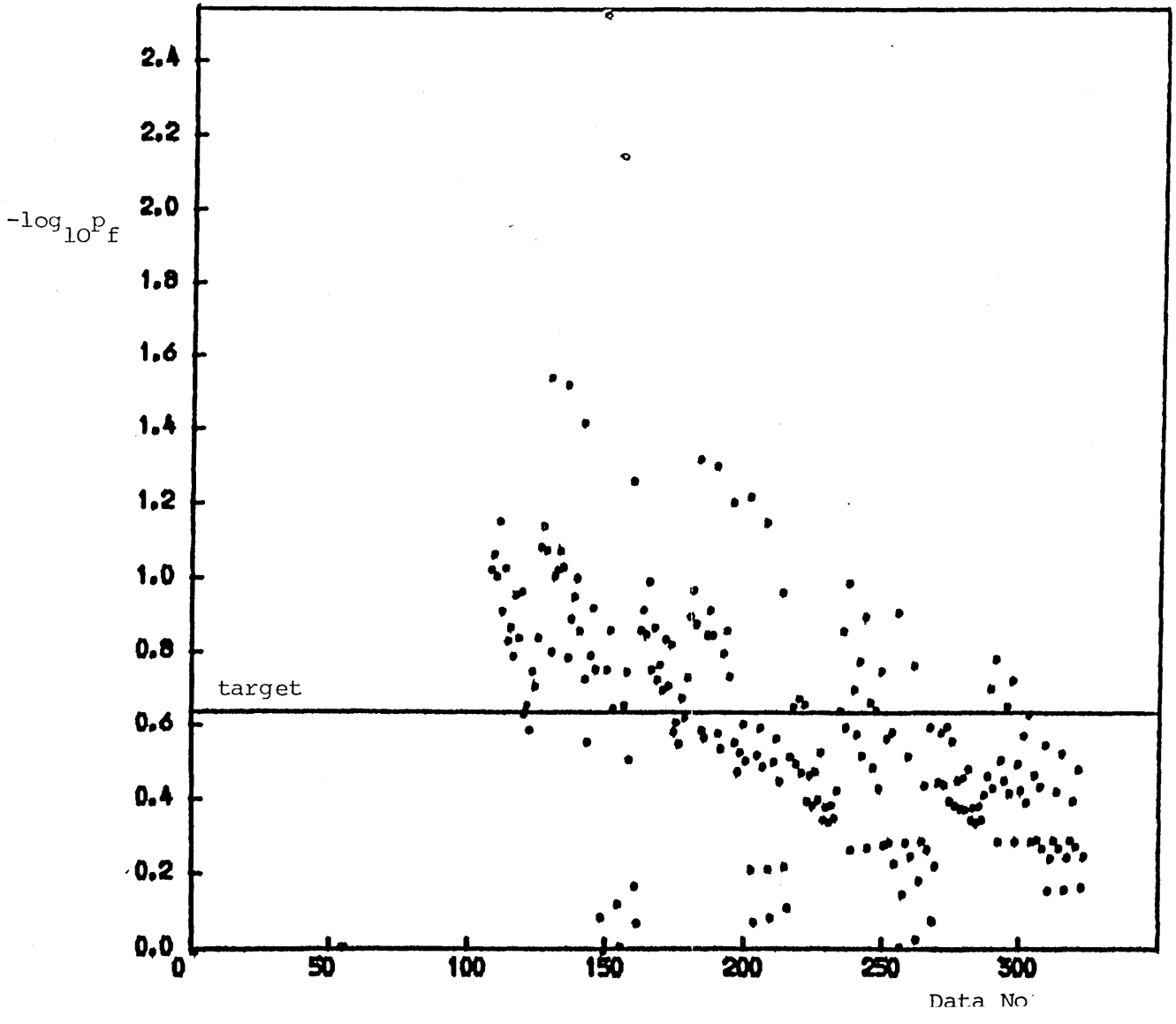

Fig.8.7 Scatter of Reliabilities about target using Design Curve - tension and bending cases

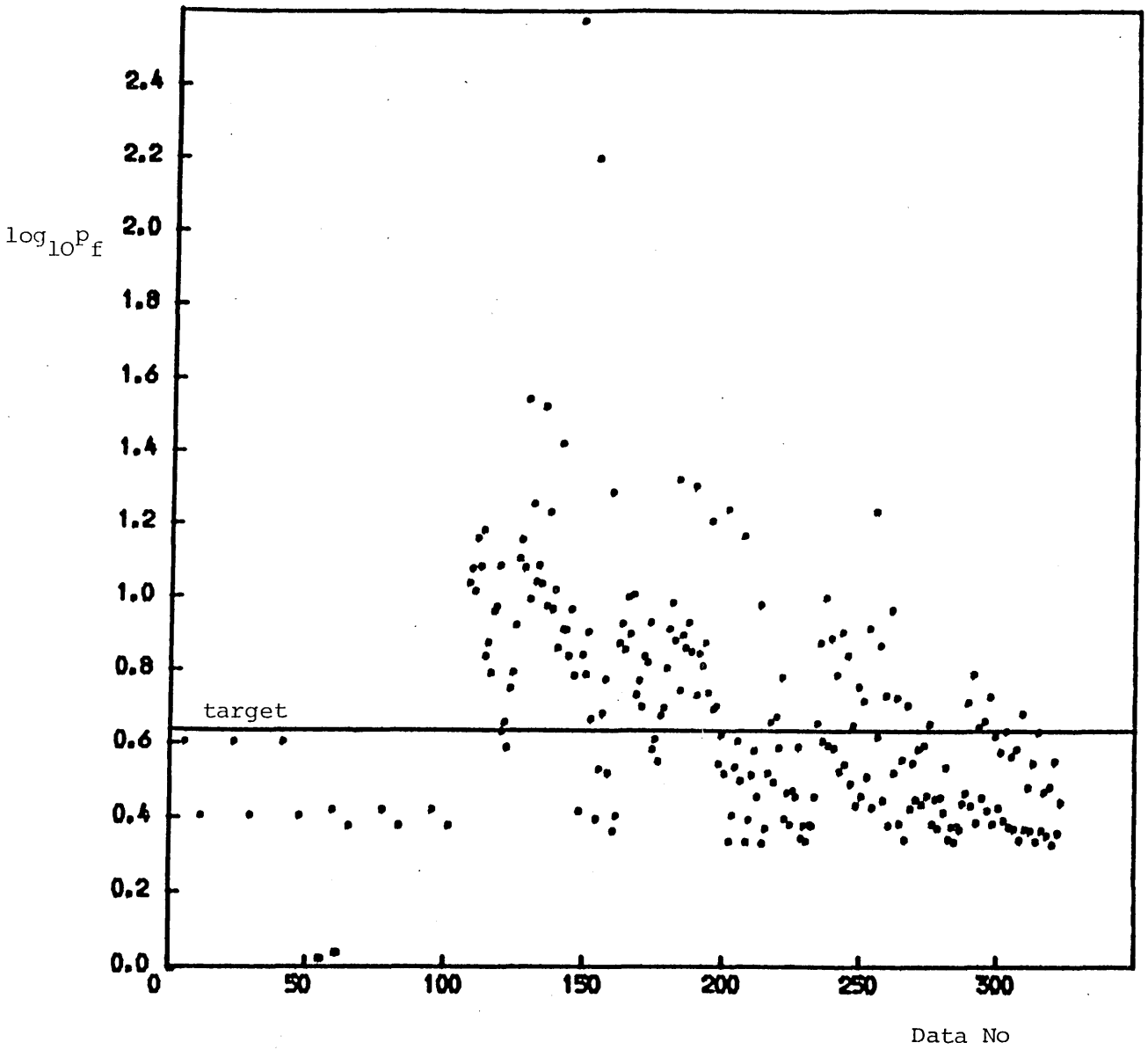

Fig. 8.8 Scatter of Reliabilities about target using Level 1 route

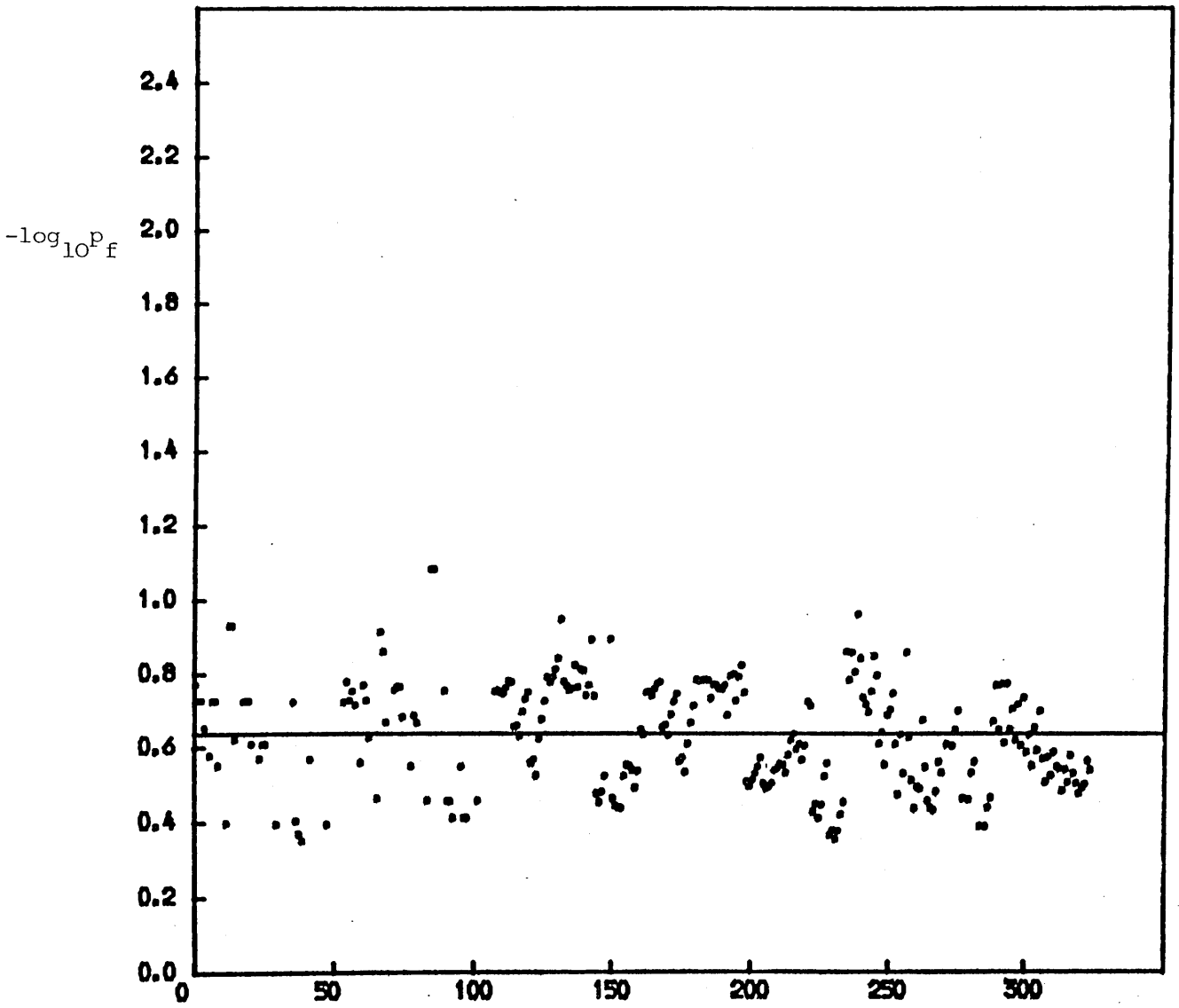

Fig. 8.9 Scatter of Reliabilities about target using Level 2 route with optimised partial factors.

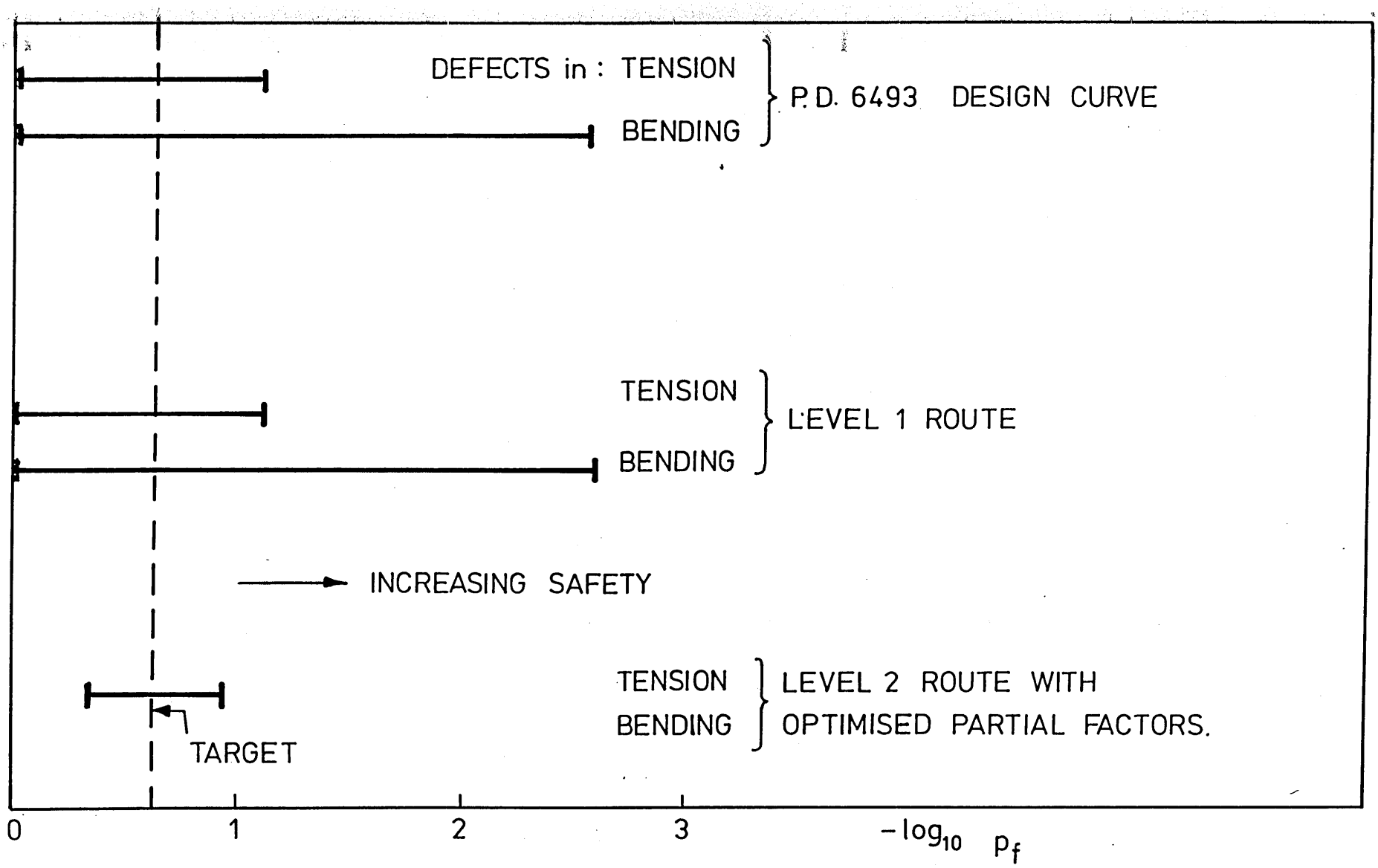

Fig. 8.10 COMPARISON of RELIABILITY RANGES for DIFFERENT ASSESSMENT ROUTES

SECTION 9

OVERALL CONCLUSIONS, RECOMMENDATIONS AND EXTENSIONS FOR DEFECT ASSESSMENT RELIABILITY ON OFFSHORE STRUCTURES

1. The methods presented in Sections 6, 7 and 8 for obtaining safety factors to use with critical defect assessment equations hinge to a large extent on a rational choice of target reliability. Since the bounds on reliability are substantially lower for fracture than for static collapse (as shown in both Sections 7 and 8) the choice cannot be made on the basis of comparisons with static collapse or upon adjustments to the static collapse value according to failure consequences and design life. The option taken in Sections 7 and 8 of determining a target on the basis of comparison with the PD6493 design curve is rational and has been shown to be practical.

2. Operators who have access to reliability analysis software will be able to use it with the failure function presented in Section 6 to obtain reliabilties directly. The advantage to operators is that they would be able to arrange known defects in order of declining failure probability and implement a repair program based on this. Reliability analysis of defect assessment methods based on hand calculation and/or graphical methods would provide all operators with a powerful maintenance tool.

3. For either of the methods presented the engineer is required to estimate the degree of variability in stress and defect sizing before selecting appropriate partial factors. For the present, such subjective judgements as 'high', 'medium' and 'low' variability would be appropriate for this

purpose. For a fixed design wave, large uncertainties enter the prediction of load effects on offshore structures at each of the following stages:

. prediction of water particle kinematics
. modelling of fluid-structure interaction
. estimation of residual stresses for as-welded joints
. prediction of stress concentration effects by parametric equations.

A detail affected by any of the above may be classified as 'high' stress variability and the partial safety factor according to a COV of 30% used. A PWHT detail affected mostly by dead loads with stress concentration effects calculated by finite element or similar methods may be classified as 'low' stress uncertainty and the partial factor according to stress COV=5% used. 'Medium' stress variability would describe a detail under predominantly dead loads but with stress concentration predicted by parametric equations. Linear interpolation between the stress partial factors for COVs of 30% and 5% would then be used.

To facilitate greater precision in both determination of stress partial factors and estimates of reliability it is proposed, as an extension of this study, to determine the contribution to stress variability made by each of the above-mentioned factors.

Since defect size is rarely a sensitive variable estimates of variability based on subjective judgements will suffice in almost every case.

4. Fracture, of course, is only one component of defect assessment and the fracture mechanics methods analysed herein ignore the potential of a defect to grow under fatigue loading. Consequently a study is underway to examine fatigue assessment methods from a reliability viewpoint.